UNIVERSITY OF ALBERTA

MAINTENANCE OF PEROXISOMES IN THE YEAST *YARROWIA LIPOLYTICA*

BY

JENNIFER JOY SMITH, B.SC. ©

A THESIS SUBMITTED TO THE FACULTY OF GRADUATE STUDIES AND RESEARCH IN PARTIAL FULFILMENT OF THE REQUIREMENTS FOR THE DEGREE OF DOCTOR OF PHILOSOPHY

DEPARTMENT OF CELL BIOLOGY

EDMONTON, ALBERTA

FALL 2000

National Library
of Canada

Acquisitions and
Bibliographic Services

395 Wellington Street
Ottawa ON K1A 0N4
Canada

Bibliothèque nationale
du Canada

Acquisitions et
services bibliographiques

395, rue Wellington
Ottawa ON K1A 0N4
Canada

Your file Votre référence

Our file Notre référence

The author has granted a non-exclusive licence allowing the National Library of Canada to reproduce, loan, distribute or sell copies of this thesis in microform, paper or electronic formats.

The author retains ownership of the copyright in this thesis. Neither the thesis nor substantial extracts from it may be printed or otherwise reproduced without the author's permission.

L'auteur a accordé une licence non exclusive permettant à la Bibliothèque nationale du Canada de reproduire, prêter, distribuer ou vendre des copies de cette thèse sous la forme de microfiche/film, de reproduction sur papier ou sur format électronique.

L'auteur conserve la propriété du droit d'auteur qui protège cette thèse. Ni la thèse ni des extraits substantiels de celle-ci ne doivent être imprimés ou autrement reproduits sans son autorisation.

0-612-59670-2

Canada

UNIVERSITY OF ALBERTA

LIBRARY RELEASE FORM

NAME OF AUTHOR:	Jennifer Joy Smith
TITLE OF THESIS:	Maintenance of Peroxisomes in the Yeast *Yarrowia lipolytica*
DEGREE:	Doctor of Philosophy
YEAR THIS DEGREE GRANTED:	2000

Permission is hereby granted to the University of Alberta Library to reproduce single copies of this thesis and to lend or sell such copies for private, scholarly or scientific research purposes only.

The author reserves all other publication and other rights in association with the copyright in the thesis, and except as herein before provided, neither the thesis nor any substantial portion thereof may be printed or otherwise reproduced in any material form whatever without the author's prior written permission.

Jennifer Smith

Jennifer J. Smith
602 Grace Street
Newmarket, Ontario
L3Y 2L1

July 25 2000
DATE

UNIVERSITY OF ALBERTA

FACULTY OF GRADUATE STUDIES AND RESEARCH

The undersigned certify that they have read, and recommend to the Faculty of Graduate Studies and Research for acceptance, a thesis entitled: **Maintenance of Peroxisomes in the Yeast *Yarrowia lipolytica***, submitted by Jennifer Joy Smith in partial fulfillment of the requirements for the degree of Doctor of Philosophy.

Richard A. Rachubinski, Ph.D.

Rick W. Wozniak, Ph.D.

JR Casey

Joseph R. Casey, Ph.D.

John D. Aitchison, Ph.D.

27 June 2000

Date

James M. Cregg, Ph.D.

ABSTRACT

Peroxisomes are organelles that perform several functions, including the β-oxidation of fatty acids. This thesis describes the identification and characterization of Pex8p and multifunctional enzyme type 2 (MFE2) of the yeast *Yarrowia lipolytica*, two proteins that each have a role in the maintenance of functional peroxisomes.

PEX8, the gene encoding Pex8p, was selected from a genomic library on the basis of its ability to functionally complement a mutant of peroxisome maintenance. Pex8p was shown to be membrane associated and intraperoxisomal, and to be necessary for the import of some matrix proteins into peroxisomes. Using a yeast two-hybrid system, Pex8p was found to interact with Pex20p, a primarily cytosolic protein that binds the β-oxidation enzyme thiolase in the cytosol and aids in targeting it to peroxisomes. A complex containing Pex8p and Pex20p was isolated by coimmunoprecipitation from a lysate of wild-type cells, confirming that the two proteins interact. Using an *in vitro* binding assay with recombinant proteins, the Pex8p-Pex20p interaction was shown to be specific, direct and autonomous. In cells lacking Pex8p, the majority of thiolase was found to be mislocalized to the cytosol, and Pex20p and a small amount of thiolase were found associated with the peroxisomal membrane. Together these data point to a direct role for Pex8p in Pex20p-dependent matrix protein import.

The *MFE2* gene encoding β-oxidation enzyme MFE2 was identified serendipitously. Peroxisomes of an *MFE2* deletion strain were observed to be larger and, depending on the growth condition, more or less abundant than peroxisomes of the wild-type strain under the same conditions, suggesting a role for yeast MFE2 in the regulation of peroxisome size and number. Cells lacking MFE2 contained higher amounts of β-

oxidation enzymes than did wild-type cells and increasing the level of thiolase in wild-type cells resulted in enlarged peroxisomes, suggesting that increased amounts of β-oxidation enzymes contribute to the enlarged peroxisomes in cells lacking MFE2. A noncatalytic version of MFE2 did not restore normal peroxisome morphology to cells of the *MFE2* deletion strain, demonstrating that their phenotype is not due to the absence of MFE2 but instead may be due to a nonfunctional β-oxidation pathway.

ACKNOWLEDGEMENTS

Foremost, I would like to thank Rick Rachubinski for allowing me to work with him and for his insight, encouragement and enthusiasm. He has provided an exciting research focus and high quality resources. In addition, he has given me the freedom to work independently and develop my own ideas. The environment he created has greatly contributed to my confidence and growth as a researcher.

I would like to recognize the contributions of my colleagues in the Rachubinski lab who have taught me and shared their ideas with me. In particular I wish to thank Gary Eitzen, Rachel Szilard, and Melchior Evers who were invaluable in making my project successful. In addition, I would like to express my appreciation to the students and faculty of other labs, including the members of my supervisory committee, who have contributed their advice and expertise. I am especially grateful to Rick Wozniak who was always very supportive and willing to share his time and thoughts with me.

To the Medical Research Council of Canada and the University of Alberta, I extend my appreciation for the financial support provided to me throughout my studies.

Finally, I am grateful to Marcello for his insightful suggestions and for his unwavering support and confidence in me.

TECHNICAL ACKNOWLEDGEMENTS

I would like to thank Eileen Recklow, Rick Poirier, Kris Decker-Eitzen, Rachel Oates, Gareth Lambkin and Hanna Króliczak for their excellent technical assistance and to acknowledge Honey Chan for preparing sections for electron microscopy.

I also wish to recognize those who contributed directly to this thesis through collaborative work. Trevor Brown and Gary Eitzen isolated a fragment of the *MFE2* gene, which was used to isolate the entire *MFE2* gene. Rachel Szilard constructed and isolated the *pex8-1* strain. Marcello Marelli complemented the *pex8-1* strain and performed a restriction map analysis of the *PEX8* gene.

These people were a pleasure to work with and are very much appreciated.

TABLE OF CONTENTS

CHAPTER 1 INTRODUCTION 1

1.1 Organelle maintenance 2
1.2 Peroxisomes and their functions 2
1.3 Peroxisomes and human health 5
1.4 Valuable experimental approaches to study peroxisome maintenance 7
  1.4.1 *In vitro* and *in vivo* import systems 7
  1.4.2 Mutants of genetically tractable systems 7
  1.4.3 Physical interactions amongst peroxins 10
1.5 Import of matrix proteins into peroxisomes 12
  1.5.1 Transporting proteins across cellular membranes 12
  1.5.2 General aspects of peroxisomal matrix protein import 14
  1.5.3 Targeting signals of peroxisomal matrix proteins 16
  1.5.4 Overview of peroxins involved in the import of matrix proteins 17
  1.5.5 Peroxins involved in matrix protein targeting 17
  1.5.6 Membrane-associated peroxins involved in matrix protein import 20
1.6 Integration of proteins into the peroxisomal membrane 22
  1.6.1 General aspects of peroxisomal membrane protein trafficking 22
  1.6.2 Targeting signals of peroxisomal membrane proteins 22
  1.6.3 Peroxins involved in peroxisomal membrane protein trafficking 23
  1.6.4 Involvement of the ER in peroxisomal membrane protein trafficking 23
1.7 Peroxisome size and number 24
  1.7.1 Formation of new peroxisomes 24
  1.7.2 Regulation of peroxisome size and number 26
1.8 Focus of this thesis 27

CHAPTER 2 MATERIALS AND METHODS 28

2.1 Materials 29
  2.1.1 List of chemicals and reagents 29
  2.1.2 List of enzymes 30
  2.1.3 Molecular size standards 31
  2.1.4 Multicomponent systems 31
  2.1.5 Radiochemicals and detection kits 31
  2.1.6 Plasmids 31
  2.1.7 Antibodies 32
  2.1.8 Oligonucleotides 33

2.1.9 Standard buffers and solutions 35

2.2 Microorganisms and culture conditions 35

2.2.1 Yeast strains and culture conditions 35
2.2.2 Bacterial strains and culture conditions 37
2.2.3 Mating of yeast 38

2.3 Introduction of DNA into microorganisms 38

2.3.1 Chemical transformation of *E. coli* 38
2.3.2 Electroporation of *E. coli* 39
2.3.3 Electroporation of *Y. lipolytica* 39

2.4 Isolation of DNA and RNA from microorganisms 40

2.4.1 Plasmid DNA isolation from bacteria 40
2.4.2 Chromosomal DNA isolation from yeast 41
2.4.3 Plasmid DNA isolation from yeast 42
2.4.4 RNA isolation from yeast 42

2.5 Standard DNA manipulations 42

2.5.1 Amplification of DNA by the polymerase chain reaction (PCR) 43
2.5.2 Restriction endonuclease digestion 43
2.5.3 Construction of blunt-ended DNA fragments 43
2.5.4 Dephosphorylation and phosphorylation of 5' ends 44
2.5.5 Separation of DNA fragments by agarose gel electrophoresis 44
2.5.6 Purification of DNA fragments from agarose gels 45
2.5.7 Purification and concentration of DNA from solution 45
2.5.8 Construction of hybrid DNA molecules by ligation 46
2.5.9 DNA mutagenesis 47

2.6 DNA and RNA analysis 47

2.6.1 DNA sequencing 47
2.6.2 Southern blot analysis 49
2.6.3 Colony lifts 49
2.6.4 Northern blot analysis 50
2.6.5 Labelling and hybridization of DNA 50

2.7 Protein analysis and manipulation 52

2.7.1 Precipitation of proteins 52
2.7.2 Determination of protein concentration 52
2.7.3 Electrophoretic separation of proteins 53
2.7.4 Detection of proteins by gel staining 53
2.7.5 Detection of proteins by immunoblotting 54
2.7.6 Protein sequencing 55

2.8 Subcellular fractionation of yeast 55

2.8.1 Preparation of whole cell lysates 55
2.8.2 Subcellular fractionation 56
2.8.3 Isolation of organelles by isopycnic centrifugation 57
2.8.4 Extraction and subfractionation of peroxisomes 57
2.8.5 Protease protection 58

2.9 Assays 59

2.9.1 Catalase 59
2.9.2 Fumarase 59
2.9.3 Alkaline phosphatase 59

2.10 Coimmunoprecipitation 60

2.11 Microscopy 61

2.11.1 Immunofluorescence microscopy 61
2.11.2 Electron microscopy 62
2.11.3 Morphometric analysis of peroxisomes 62

2.12 Isolation and sequencing of genes 63

2.12.1 Isolation and sequencing of *PEX8* 63
2.12.2 Isolation and sequencing of the *pex8-1* allele of *PEX8* 63
2.12.3 Isolation and sequencing of *MFE2* 64
2.12.4 Isolation and sequencing of *THFS* 65

2.13 Construction of plasmids for gene expression 66

2.13.1 Construction of a plasmid encoding epitope tagged MFE2 66
2.13.2 Construction of a plasmid encoding Myc-MFE2ΔAKL 67
2.13.3 Construction of a plasmid encoding Myc-MFE2ΔAΔB 68
2.13.4 Construction of a plasmid for overexpression of *POT1* gene encoding thiolase 69
2.13.5 Construction of a plasmid encoding Pex8p-HA^c 70

2.15 Construction of mutant strains of *Y. lipolytica* 71

2.15.1 Construction and isolation of *pex8-1* 71
2.15.2 Integrative disruption of *PEX8* 71
2.15.3 Integrative disruption of *MFE2* and *PEX5* 72
2.15.4 Construction of strains encoding Pex8p-HA^c and Pex8p-HA^i 73

2.16 Polyclonal antibody production 73

2.16.1 Production of antisera directed against Pex20p 75
2.16.2 Production of antisera directed against Pex1p 76
2.16.3 Production of antisera directed against Pex6p 76

2.17 Computer aided DNA and protein sequence analyses 77

2.18 *In vitro* binding assay 77

2.18.1 Construction of chimeric genes and isolation of recombinant proteins 77
2.18.2 *In vitro* binding assay with recombinant protein 78
2.18.3 *In vitro* binding assay with yeast lysate 79

2.19 Two-hybrid analysis 80

2.19.1 Construction of chimeric genes 80
2.19.2 Two-hybrid analysis 81

CHAPTER 3 PEX8P IS ASSOCIATED PERIPHERALLY WITH THE PEROXISOMAL MEMBRANE AND IS REQUIRED FOR MATRIX PROTEIN MPORT 82

3.1 Overview 83
3.2 The *pex8-1* mutant strain lacks normal peroxisomes 83
3.3 Isolation and characterization of the *PEX8* gene 84
3.4 Regulation of *PEX8* expression and Pex8p synthesis 92
3.5 Pex8p-HA^i is peripherally associated with the peroxisomal membrane 94
3.6 Mutations in *PEX8* affect the location of a subset of matrix proteins 98
3.7 Peroxisomal proteins found in the 20KgP of *pex8* mutant strains partially colocalize with marker proteins of other organelles 101
3.8 Analysis of the import defect of *pex8-KA* by immunofluorescence microscopy 104
3.9 Analysis of the *pex8-1* mutant allele of *PEX8* 104
3.10 Discussion 106
  3.10.1 Pex8p has a role in peroxisome maintenance 106
  3.10.2 Characteristics of *PEX8* and its encoded peroxin Pex8p 107
  3.10.3 Possible role for Pex8p in peroxisome maintenance 108

CHAPTER 4 ROLE OF PEX8P IN PEX20P-DEPENDENT THIOLASE IMPORT 110

4.1 Overview 111
4.2 Detection of physical interactions amongst peroxins 112
4.3 The interaction between Pex8p and Pex20p is direct and autonomous 116
4.4 Identification of p100, a second Pex20p-interacting protein 116
4.5 p100 is similar to C_1-tetrahydrofolate synthases of other organisms 119
4.6 Pex8p-HA^c and p100 coimmunoprecipitate with Pex20p 123
4.7 p100 does not have characteristics of a peroxisomal protein 124
4.8 Pex20p is not required for the targeting of Pex8p-HA^c to peroxisomes 128
4.9 Pex20p and a small amount of thiolase are peroxisome associated in cells of a *PEX8* disruption strain 128
4.10 Discussion 134
  4.10.1 Pex20p-dependent targeting and/or oligomerization of Pex8p 135
  4.10.2 A role for Pex8p in the Pex20p-dependent import of thiolase 136
  4.10.3 A role for Pex8p in the Pex5p-dependent import of PTS1-containing proteins 137
  4.10.4 Pex20p interacts with p100 138

CHAPTER 5 REGULATION OF PEROXISOME SIZE AND NUMBER BY FATTY ACID β-OXIDATION 139

5.1 Overview 140
5.2 Isolation and characterization of *Y. lipolytica MFE2* gene 140
5.3 Synthesis of MFE2 is induced by growth of *Y. lipolytica* on oleic acid medium 143
5.4 Peroxisomal localization of Myc-tagged MFE2 depends on Pex5p 146
5.5 MFE2 is targeted by a PTS1 and may be targeted as an oligomer 149
5.6 MFE2 may control peroxisome size and number of oleic acid-grown cells 150
5.7 MFE2 may control peroxisome size and number of acetate-grown cells 152
5.8 Enlarged peroxisomes are not caused by the absence of MFE2 protein 153
5.9 β-oxidation enzyme levels are increased in an *MFE2* deletion strain 157
5.10 Overproduction of β-oxidation enzyme results in enlarged peroxisomes 160
5.11 Discussion 162
  5.11.1 MFE2 protein of *Y. lipolytica* 162
  5.11.2 Lack of functional MFE2 affects peroxisome size and number 163
  5.11.3 What causes enlarged peroxisomes of the *MFE2* deletion strain? 163
  5.11.4 How does the deletion of *MFE2* affect peroxisome number? 164

CHAPTER 6 PERSPECTIVES 166

6.1 Synopsis, relevance and future directions of Pex8p analysis 167
  6.1.1 Pex8p is directly involved in matrix protein import 167
  6.1.2 Convergence of Pex20p- and Pex5p-dependent import 170
  6.1.3 Possible functions for Pex8p in matrix protein import 172
  6.1.4 Pex20p may enter peroxisomes with its cargo 173
  6.1.5 Identification of components of the translocation complex 174
6.2 Synopsis, relevance and future directions of MFE2 analysis 175
  6.2.1 Possible effects of growth medium on *pex* mutant phenotypes 176
  6.2.2 Possible effects of nonfunctional β-oxidation on pex mutant phenotypes 176

CHAPTER 7 REFERENCES 178

LIST OF TABLES

Table 1-1 Description of Peroxins 11

Table 2-1 Primary Antibodies 32
Table 2-2 Secondary Antibodies 33
Table 2-3 Oligonucleotides 33
Table 2-4 Standard Buffers and Solutions 35
Table 2-5 *Y. lipolytica* Strains 35
Table 2-6 Yeast Culture Media 36
Table 2-7 *E. coli* Strains 37
Table 2-8 Bacterial Culture Media 37
Table 2-9 Construction of Plasmids for the Yeast Two-Hybrid System 80

Table 5-1 Morphometric Analysis of Peroxisomes 150

LIST OF FIGURES

Figure 1-1 Peroxisomal β-oxidation 4
Figure 1-2 Physical interactions amongst peroxins 13
Figure 1-3 Model of peroxisomal matrix protein import 18

Figure 2-1 Mutagenesis by sequential PCR 48

Figure 3-1 Growth of various *Y. lipolytica* strains on oleic acid-containing medium 85
Figure 3-2 Ultrastructure of the wild-type strain *E122* and of the *pex8* mutant, and *PEX8* complemented strains 86
Figure 3-3 Complementing activity, restriction map and disruption strategy for the *PEX8* gene 88
Figure 3-4 Nucleotide sequence of *PEX8* and deduced amino acid sequence of Pex8p 89
Figure 3-5 Hydropathy analysis of Pex8p 90
Figure 3-6 Alignment of *Yl*Pex8p with other members of Pex8p family 91
Figure 3-7 Expression of Pex8p mRNA and synthesis of Pex8p-HA^{i} are induced by growth of *Y. lipolytica* in oleic acid-containing medium 93
Figure 3-8 Subcellular localization of Pex8p-HA^{i} 95
Figure 3-9 Peroxisomal matrix proteins are mislocalized to the 20KgS to various extents in *pex8* mutants 99
Figure 3-10 Sucrose density gradient analysis of 20KgPs from the wild-type strain and *pex8* mutant strains 103
Figure 3-11 Localization of peroxisomal proteins in a *PEX8* disruption strain by immunofluorescence microscopy 105

Figure 4-1 Identification of Pex1p-Pex6p and Pex8p-Pex5p interactions using the yeast two-hybrid system 113
Figure 4-2 Analysis of physical interaction between Pex8p and the amino terminus of Pex20p using the two-hybrid system 115
Figure 4-3 *In vitro* binding studies showing that the Pex8p-Pex20p interaction is direct and autonomous 117
Figure 4-4 Specific interaction of Pex8p-HA^{c} and a 100 kDa protein from a yeast lysate with the GST-Pex20p fusion 118

Figure 4-5 Nucleotide sequence of *THFS* and deduced amino acid sequence of p100 121
Figure 4-6 p100 is similar to C_1-THFSs of other organisms 122
Figure 4-7 Coimmunoprecipitation of Pex8p-HA^c and p100 with Pex20p 125
Figure 4-8 Localization of C_1-THFS in the wild-type and *PEX20* disruption strain 126
Figure 4-9 Subcellular localization of Pex8p-HA^c in wild-type and *pex20* mutant strains . 129
Figure 4-10 Pex20p is peroxisomal in cells of the *PEX8* disruption strain, *pex8-KA* 130
Figure 4-11 Pex20p and a small amount of thiolase are associated with the peroxisomal membrane in cells of a *PEX8* disruption strain 132

Figure 5-1 Characteristics of the *Y. lipolytica* MFE2 gene and its encoded protein, MFE2 142
Figure 5-2 Amino acid sequence alignment of MFE2 proteins of selected fungi 144
Figure 5-3 Growth of *Y. lipolytica* strains on oleic acid-containing medium 145
Figure 5-4 Synthesis of Myc-MFE2 is increased by growth of *Y. lipolytica* in oleic acid containing medium 147
Figure 5-5 Localization of Myc-MFE2 and Myc-MFE2ΔAKL in various strains 148
Figure 5-6 Peroxisomes are larger, more abundant and more variable in size in *mfe2-KO* cells than in wild-type cells 151
Figure 5-7 Peroxisomes of *mfe2-KO* cells are larger than those of wild-type cells when grown in acetate-containing medium 154
Figure 5-8 Expression of Myc-MFE2ΔAΔB does not restore growth on oleic acid medium to the *mfe2-KO* strain 155
Figure 5-9 Expression of Myc-MFE2ΔAΔB does not reverse the morphological defects of the *mfe2-KO* strain 158
Figure 5-10 Abundance of various peroxisomal matrix proteins and peroxins in wild-type and *mfe2-KO* cells under different growth conditions 159
Figure 5-11 Increased levels of the β-oxidation enzyme thiolase leads to enlarged peroxisomes 161

Figure 6-1 Revised diagram of physical interactions amongst peroxins 168
Figure 6-2 Revised model of peroxisomal matrix protein import 169
Figure 6-3 Alignment of the amino termini of Pex8p and Pex5p of *Y. lipolytica* 171

LIST OF SYMBOLS AND ABBREVIATIONS

20KgP	pellet resulting from a centrifugation at 20,000 x *g*
20KgS	supernatant resulting from a centrifugation at 20,000 x *g*
200KgP	pellet resulting from a centrifugation at 200,000 x *g*
200KgS	supernatant resulting from a cenrifugation at 200,000 x *g*
A	Ampere
AAA	ATPase associated with diverse cellular activities
ADP	adenosine diphosphate
ARF	ADP-ribosylation factor
ATP	adenosine triphoshpate
ATPase	adenosine triphosphatase
bp	base pair
BSA	bovine serum albumin
c	centi (x10^{-1})
C$_1$-THFS	C$_1$-tetrahydrofolate synthase
°C	degrees Celcius
CG	complementation group of human peroxisome biogenesis disorder
Ci	Curie
CoA	coenzyme A
cpm	counts per minute
d	day
D	dalton
DNA	deoxyribonucleic acid
DNase	deoxyribonuclease
dNTP	deoxyribonucleoside triphosphate
E.	*Escherichia*
ECL	Enhanced Chemilumenescence
ER	endoplasmic reticulum
F	farad
g	gram
g	gravitational force
GST	glutathione-S-transferase
H.	*Hansenula*
h	hour
HA	hemagglutinin
Hp	*Hansenula polymorpha*
HRP	horseradish peroxidase
IgG	immunoglobulin G
IPTG	isopropyl β-D-thiogalactoside
J	Joule
k	kilo (x10^{3})
L	litre
LC-MS/MS	capillary liquid chromatography tandem mass spectrometry
λ	wavelength
m	meter *or* milli (x10^{-3})

M	moles per litre
MBP	maltose binding protein
MFE	multifunctional β-oxidation enzyme
min	minute
mPTS	membrane protein peroxisomal targeting signal
mRNA	messenger RNA
μ	micro (x10^{-6})
n	nano (x10^{-9})
NCBI	National Centre for Biotechnology Information
NEM	N-ethylmaleimide
Ω	ohm
OD	optical density
ORF	open reading frame
P.	*Pichia*
PAGE	polyacrylamide gel electrophoresis
PCR	polymerase chain reaction
PBD	peroxisome biogenesis disorder
PEX#	wild-type gene encoding Pex#p
pex#	non-functional *PEX#* gene
Pex#p	peroxin # protein
pH	-log[H^+]
PM	peroxisomal membrane
PNS	post-nuclear supernatant
Pp	*Pichia pastoris*
PPAR	peroxisome proliferator-activated receptor
PTS	peroxisomal targeting signal
RNA	ribonucleic acid
RNase	ribonuclease
S.	*Saccharomyces*
Sc	*Saccharomyces cerevisiae*
SDS	sodium dodecyl sulphate
sec	second
SH3	Src homology-3
TCA	trichloroacetic acid
TPR	tetratricopeptide repeat
U	units of enzyme activity
v	volume
V	volt
w	weight
Y.	*Yarrowia*
Yl	*Yarrowia lipolytica*

CHAPTER 1

INTRODUCTION

1.1 Organelle maintenance

Eukaryotic cells contain distinct membrane-bound compartments that carry out different cellular processes. These compartments are called organelles and include peroxisomes, mitochondria, the nucleus, the endoplasmic reticulum (ER) and secretory organelles, lysosomes/vacuoles and chloroplasts. The maintenance of functional compartments is vital for the survival of eukaryotic organisms and requires that each organelle contain a specific complement of molecules (including enzymes, cofactors, structural proteins and lipids) and that these molecules be specifically organized both spatially and temporally. These requirements are dynamic and change in response to the needs of the cell (reviewed in Nunnari and Walter, 1996). Compartments are maintained by groups of interacting proteins that function in the transport of proteins into and out of organelles and in processes such as organelle fission, fusion, inheritance and degradation that control the number and size of organelles. This thesis focuses on some of the proteins involved in the maintenance of functional peroxisomes. This chapter introduces peroxisomes and their cellular functions, as well as our current understanding of the mechanisms of peroxisome maintenance.

1.2 Peroxisomes and their functions

Peroxisomes were first identified in mammalian kidney and liver cells as small, electron-dense vesicles bound by single membranes. As their name implies, peroxisomes were found to contain oxidative enzymes that generate, and catalase that decomposes, hydrogen peroxide (de Duve and Baudhuin, 1966). Peroxisomes belong to the microbody family of organelles, along with the glyoxysomes of plants and the glycosomes of trypanosomes. Organelles of this family contain enzymes involved in fatty acid β-oxidation and are found in virtually all eukaryotic cells (Borst, 1989; Kunau and Hartig, 1992; Subramani, 1993).

Peroxisomes are roughly spherical in shape and range in diameter from 0.1 to 1 µm, although there is evidence of a peroxisome reticulum in some rat and mouse cell types (Gorgas, 1984, 1985; Yamamoto and Fahimi, 1987). Peroxisomes contain a complete fatty acid β-oxidation pathway and catalase to degrade toxic hydrogen peroxide (Fig. 1-1; reviewed in Endrizzi et al., 1996; Hashimoto, 1999). Interestingly, peroxisomes also perform a variety of other functions depending on the organism, cell type and environmental conditions (reviewed in Kunau and Hartig, 1992; van den Bosch et al., 1992; Subramani, 1993). In fungi, peroxisomes have roles in the glyoxylate cycle, alcohol utilization and penicillin biosynthesis. In mammals, peroxisomes have roles in cholesterol and bile acid synthesis, prostaglandin metabolism and the biosynthesis of plasmalogens (ether phospholipids that protect the cell from oxidative damage).

In accordance with their functional diversity, the number, volume and protein composition of peroxisomes in a cell can change dramatically in response to environmental cues. In yeast, these cues include changes in carbon and nitrogen sources (Veenhuis and Harder, 1987; van der Klei and Veenhuis, 1997). In mammalian cells, these cues include a number of synthetic and naturally occurring compounds, including hypolipidemic and anti-inflammatory drugs, plasticizers and herbicides (van den Bosch et al., 1992; Reddy and Chu, 1996). Signals are transmitted to the proteins that maintain peroxisomes, at least in part, at the level of transcription through specific response

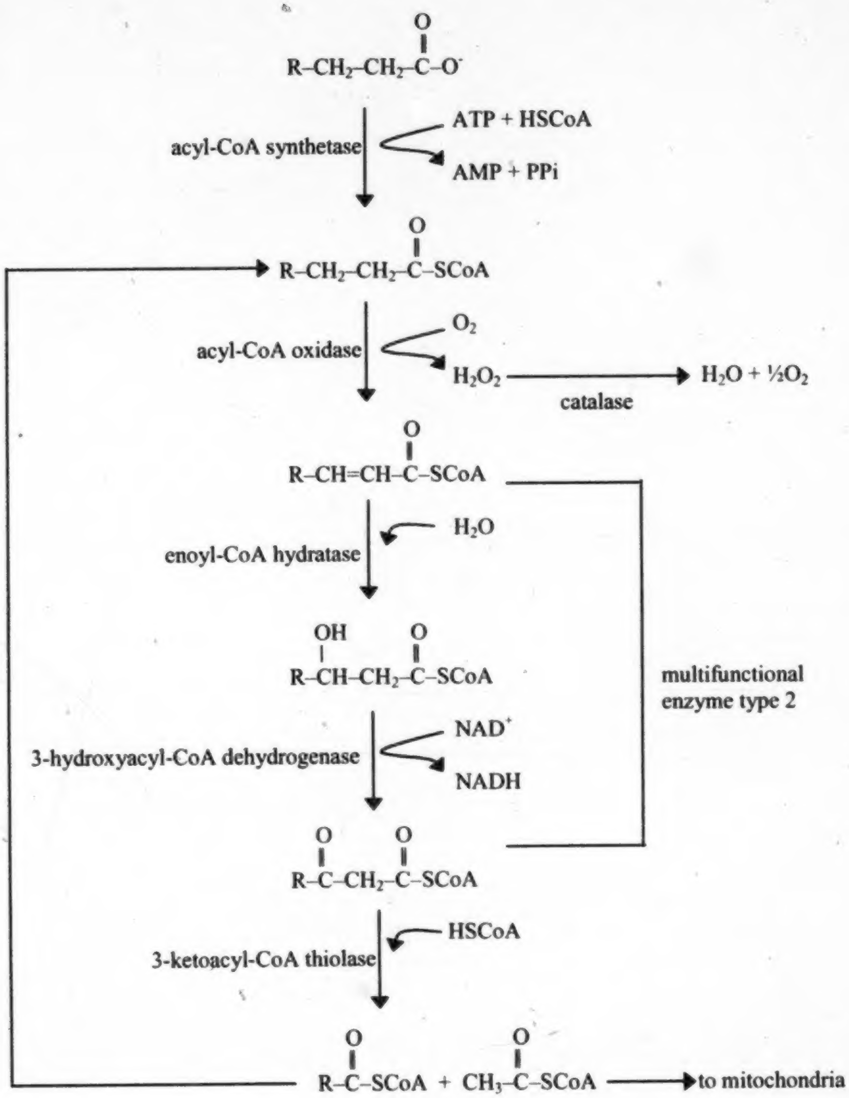
R–CH₂–CH₂–C(=O)–O⁻
acyl-CoA synthetase
ATP + HSCoA
AMP + PPi
R–CH₂–CH₂–C(=O)–SCoA
acyl-CoA oxidase
O₂
H₂O₂
catalase
H₂O + ½O₂
R–CH=CH–C(=O)–SCoA
enoyl-CoA hydratase
H₂O
R–CH(OH)–CH₂–C(=O)–SCoA
multifunctional enzyme type 2
3-hydroxyacyl-CoA dehydrogenase
NAD⁺
NADH
R–C(=O)–CH₂–C(=O)–SCoA
3-ketoacyl-CoA thiolase
HSCoA
R–C(=O)–SCoA + CH₃–C(=O)–SCoA
to mitochondria

Figure 1-1. Peroxisomal β-oxidation. Note that both enoyl-CoA hydration and 3-hydroxylacyl-CoA dehydrogenation are catalyzed by multifunctional enzyme type 2 (MFE2).

elements found upstream of certain genes encoding peroxisomal proteins (for examples, see Reddy and Chu, 1996; Karpichev and Small, 1998).

1.3 Peroxisomes and human health

The maintenance of functional peroxisomes is indispensable for normal human survival. This is demonstrated by a group of inherited peroxisomal diseases collectively called the peroxisome biogenesis disorders (PBDs) (reviewed in Lazarow and Moser, 1994; Moser and Moser, 1996; Wanders, 1999). These extremely severe diseases occur at a frequency of 1 in 25,000 to 1 in 50,000 live births (Lazarow and Moser, 1995) and most often cause fatality in early infancy. The symptoms of patients with these diseases are diverse and include severe mental retardation, defects in neuronal migration, renal and hepatic dysfunction, craniofacial abnormalities, and hypotonia.

A disease of this type, Zellweger syndrome, was first described in 1964. Nine years later, patients with this disease were found to have abnormal peroxisomes (Goldfischer et al., 1973), but because peroxisomes were thought at that time to only have a minor role in metabolism, this link was ignored. Attention was turned back to peroxisomes after it was discovered that peroxisomes are indispensable for the β-oxidation of very-long-chain fatty acids (Brown et al., 1982; Singh et al., 1984) and the biosynthesis of plasmalogens (Hajra et al., 1979; Heymans et al., 1983). The link between Zellweger syndrome and dysfunctional peroxisome maintenance was established by the discoveries that cells from patients with this disease contained peroxisomal "ghosts", structures that resembled peroxisomes but lacked matrix proteins (Wanders et al., 1985; Schram et al., 1986; Santos et al., 1988a, 1988b), and that these ghosts were the result of the inability of cells to import matrix proteins into peroxisomes (Walton et al., 1992; Wenland and Subramani, 1993). Over the years, many patients have been diagnosed with PBDs, and the diseases have been subdivided into different groups based on the nature and severity of the symptoms. PBDs now include Zellweger syndrome, infantile Refsum's disease, neonatal adrenoleukodystrophy and rhizomelic chondrodysplasia punctata. Using cell fusion complementation assays (Shimozawa et al., 1993), it has been determined that there are at least 13 complementation groups in the PBDs.

There are other peroxisomal disorders distinct from the PBDs that are caused by dysfunction of single metabolic enzymes rather than dysfunction of proteins involved in the maintenance of peroxisomes (reviewed in Moser and Moser, 1996; Wanders, 1999). These disorders include X-linked adrenoleukodystrophy (caused by the inactivity of a fatty acid transporter) and several diseases caused by inactive enzymes involved in fatty acid β-oxidation. Patients with these diseases have symptoms similar to those of patients with the PBDs, but they are usually less severe.

The study of peroxisomes contributes to our understanding of peroxisomal disorders and also to our understanding of other diseases (reviewed in Clarke et al., 1999). The study of peroxisome proliferation in mammalian cells led to the identification of a family of lipid-activated nuclear transcription factors called peroxisome proliferator-activated receptors (PPARs). PPARs regulate the expression of a wide variety of genes that encode proteins involved in lipid metabolism, cell differentiation and tumorigenesis. The study of peroxisomes and the agents that affect their proliferation may eventually contribute to the development of better treatments for diseases like diabetes, cancer and artherosclerosis.

1.4 Valuable experimental approaches to study peroxisome maintenance

Factors controlling peroxisome maintenance have been identified and characterized using a variety of experimental approaches. Three approaches that have contributed greatly to our understanding of peroxisome maintenance are outlined in this Section.

1.4.1 In vitro and in vivo import systems–One aspect of peroxisome maintenance is the import of proteins into peroxisomes. Some conditions of import have been elucidated by studying the *in vitro* import of proteins into yeast peroxisomes (Thieringer et al., 1991), rat peroxisomes (Imanaka et al., 1987) and plant glyoxysomes (Brickner et al., 1997; Brickner and Olsen, 1998; Crookes and Olsen, 1998; Pool et al., 1998). However, the results of *in vitro* studies of matrix protein import obtained in yeast and rat systems have been challenged, and these systems are therefore of limited use experimentally (reviewed in Subramani, 1993). Peroxisomal import has also been studied in semi-permeabilized (Rapp et al., 1993; Wendland and Subramani, 1993) and microinjected (Walton et al., 1992; Soto et al., 1993) mammalian cells. Although some of these systems have proven to be excellent models with which to study the requirements of peroxisomal import, they have not led to the identification of novel proteins necessary for this process.

1.4.2 Mutants of genetically tractable systems–Cells with gene defects are invaluable for elucidating the mechanisms of organelle maintenance, because the effects of mutant genes often provide "snapshots" of otherwise dynamic and often undetectable processes.

One caveat, however, is that mutations affecting organelle maintenance are often lethal, so the effects of these mutations must be conditional to facilitate analysis. Several methods have been developed for both yeast and mammalian cell systems to isolate and characterize mutants that are defective in peroxisome maintenance (reviewed in Fujiki, 1996; Subramani, 1998).

Cultured mammalian cells used to study peroxisome maintenance include skin fibroblasts from patients with PBDs (Santos et al., 1988b; Walton et al., 1992) and mutant Chinese hamster ovary (CHO) cells selected for their inability to synthesize plasmalogens (Zoeller and Raetz, 1986; Morand et al., 1990). These are good model systems, because although peroxisomes are essential for normal human development, mammalian peroxisomes are dispensable at the cellular level, so these peroxisome-deficient cells are easily maintained and studied. These systems are very useful for studying the effects of mutations on peroxisome maintenance but are not as useful for identifying the underlying defective genes. A method has been developed to determine the genetic bases of CHO mutant cells by transfecting the cells with library DNA and assaying for the complementation of plasmalogen deficiency (Tsukamoto et al., 1991), but few genes have been identified this way.

In 1989, the first screen was developed to identify mutants of peroxisome maintenance of the genetically tractable yeast *Saccharomyces cerevisiae* (Erdmann et al., 1989), marking the beginning of an explosive decade during which our understanding of this process has accelerated. This screen exploits the fact that yeast cells have a conditional requirement for peroxisomes. Unlike the peroxisomes of higher eukaryotes, peroxisomes of yeast are the only site of cellular fatty acid β-oxidation (Kunau et al., 1988); therefore, although yeast with nonfunctional peroxisomes can survive on most carbon sources, they cannot survive if fatty acids are the only carbon source available. Using this screen, mutant strains are first selected for their inability to utilize oleic acid as a sole carbon source. From this group, mutants with defects in peroxisome maintenance are selected by screening for strains with abnormal peroxisome morphology and/or mislocalized peroxisomal proteins. The conditional requirement yeast have for peroxisomes not only aids in identifying mutants, but also facilitates characterizing mutants for two reasons: 1) growth on medium requiring peroxisomes causes a considerable increase in peroxisome size and number (Veenhuis et al., 1987; Kunau et al., 1988), thus allowing for the isolation of large amounts of peroxisomal material and 2) defective genes can often be identified by transforming the mutant cells with a genomic DNA library and assaying for functional complementation of the conditional growth defects (Erdmann et al., 1991; Höhfeld et al., 1991).

This screen has since been used to isolate mutants of other yeasts using oleic acid or methanol (for methylotrophic yeast) as a carbon source. The screen was adapted for *Yarrowia lipolytica* (Nuttley et al., 1993), *Pichia pastoris* (Gould et al., 1992; Liu et al., 1992), and *Hansenula polymorpha* (Cregg et al., 1990). In addition, more direct screens have been developed that exploit the inability of some maintenance mutants to import matrix (van der Leij et al., 1992; Elgersma et al., 1993; Kalish et al., 1996; Johnson et al., 1999) or membrane (Snyder et al., 1999b) proteins into peroxisomes.

By producing and studying mutants, several genes necessary for peroxisome maintenance have been identified and their encoded proteins characterized. In 1996, a unified nomenclature was adopted to simplify and organize the large volume of data being produced (Distel et al. 1996). According to this nomenclature, mutants of peroxisome maintenance are called *pex* mutants, proteins involved in the maintenance of peroxisomes (excluding metabolic enzymes and transcription factors) are called peroxins, and the genes encoding peroxins are called *PEX* genes. Peroxins are numbered according to the order in which they are characterized, and those predicted to be orthologs (based on sequence and functional similarities) are assigned the same number. To differentiate *PEX* genes and peroxins of different organisms, one-letter abbreviations for genus and species are appended to the gene and protein names. To date, 23 peroxin families are known, most of which have been identified using yeast and CHO genetic screens. The evolutionary conservation of *PEX* genes has facilitated the identification of human orthologs of several peroxins. So far, the human orthologs of 13 peroxins have been identified, and the genetic basis of 10 of the 13 complementation groups of the PBDs have been determined. A brief description of the 23 peroxins and a list of the human orthologs identified are in Table 1-1.

1.4.3 Physical interactions amongst peroxins–Yeast two-hybrid studies (for examples, see Purdue et al., 1998; Girzalsky et al., 1999), coimmunoprecipitations (for examples, see Götte et al., 1998; Chang et al., 1999) and *in vitro* binding assays (for example, see Erdmann and Blobel, 1996) have been used to detect physical interactions amongst peroxins. These techniques are valuable, not only for elucidating the functions of peroxins, but also for identifying new peroxins, particularly those that contribute to, but are not necessary for, peroxisome maintenance. For example, two functionally redundant peroxins, Pex18p and Pex21p, have been identified via their interaction with Pex7p in a

Table 1-1. Description of Peroxins

Peroxin	Protein characteristics	Subcellular location	Human ortholog identified	PBD known
Pex1p	contains AAA ATPase domains; sequence is similar to NSF	cytosol; peripheral association with vesicles	+	+ (CG 1)
Pex2p	contains RING-finger motif	PM (integral)	+	+ (CG 10)
Pex3p	contains mPTS	PM (integral)	+	
Pex4p	ubiquitin conjugating enzyme	PM (peripheral, cytosolic face)		
Pex5p	sequence is similar to Pex20p; contains TPR repeats	PM; cytosol; peroxisomal matrix	+ +	+ (CG 2)
Pex6p	contains AAA ATPase domains; sequence is similar to NSF	cytosol; peripheral association with vesicles	+	+ (CG 4)
Pex7p	contains WD-40 repeats	PM; cytosol; peroxisomal matrix	+	+ (CG 11)
Pex8p	contains PTS1 and PTS2	PM (peripheral, matrix face); peroxisomal matrix		
Pex9p	contains cysteine-rich region	PM (integral)		
Pex10p	contains RING-finger motif	PM (integral)	+	+ (CG 5,7)
Pex11p	homodimerizes	PM (integral; peripheral, matrix face)	+ +	
Pex12p	contains RING-finger motif	PM (integral)	+	+ (CG 3)
Pex13p	contains SH3 domain	PM (integral)	+	+ (CG 13)
Pex14p	phosphorylated	PM (peripheral, cytosolic face)	+	
Pex15p	phosphorylated; contains mPTS	PM (integral)		
Pex16p	glycosylated in *Y. lipolytica*	PM (integral; peripheral, matrix face)	+	+ (CG 9)
Pex17p		PM (integral; peripheral, cytosolic face)		
Pex18p	sequence is similar to Pex21p	cytosol		
Pex19p	farnesylated	PM (peripheral, cytosolic face); cytosol	+	+ (CG 14)
Pex20p	sequence is similar to Pex5p	PM (peripheral, cytosolic face); cytosol		
Pex21p	sequence is similar to Pex18p	cytosol		
Pex22p		PM (integral)		
Pex23p		PM (integral)		

The number of plus signs denotes the number of human orthologs or PBD complementation groups that have been identified. Peroxins that have been identified in the yeast *Y. lipolytica* are *shaded*. Abbreviations used in this table: AAA, ATPases associated with diverse cellular activities; CG, complementation group; NSF, *N*-ethylmaleimide-sensitive factor; PBD peroxisome biogenesis disorder; PM, peroxisomal membrane; SH3, Src homology 3; TPR, tetratricopeptide repeat. For references and a detailed description of peroxins see text; Hettema et al., 1999; Subramani, 1998, except for Pex22p and Pex23p, see Koller et al., 1999 and Brown et al., 2000, respectively. For references of human orthologs, see Wanders, 1999, except for Pex11p, see Abe et al., 1998; Abe and Fujiki, 1998; Schrader et al., 1998 and for Pex16p, see Honsho et al., 1998; South and Gould, 1999. For PBD identification references, see Wanders, 1999, except for Pex13p, see Liu et al.,1999; Shimozawa et al., 1999, for Pex16p see Honsho et al., 1998; South and Gould, 1999, and for Pex19p see Matsuzono et al., 1999.

yeast two-hybrid system (Purdue et al., 1998). Because the absence of only one of these two peroxins does not greatly affect the maintenance of functional peroxisomes, they will not likely be identified using genetic screens like the ones described in Section 1.4.2.

All of the physical interactions amongst peroxins that have so far been identified are diagrammed in Figure 1-2. Interactions that are known to be direct are indicated by *solid* lines, and all other interactions are indicated by *dotted* lines. Recently, a comprehensive analysis was started to identify interacting proteins of *S. cerevisiae* on a large scale (Uetz et al., 2000). This will undoubtedly add to the lattice of characterized interactions.

Through the identification and characterization of peroxins using a variety of techniques, our understanding of peroxisome maintenance is becoming more clear. Most peroxins have been implicated in the import of matrix proteins into peroxisomes. Relatively few peroxins have been implicated in peroxisomal membrane protein import or processes such as peroxisome fission and fusion that control the size and number of peroxisomes. These aspects of maintenance and the peroxins that may be involved with each are discussed in the next three sections.

1.5 Import of matrix proteins into peroxisomes

1.5.1 Transporting proteins across cellular membranes–The mechanisms of transporting proteins across the bacterial inner membrane and the membranes of the ER, mitochondrion, chloroplast and nucleus have been studied extensively (reviewed in Nunnari and Walter, 1996; Schatz and Dobberstein, 1996). The following trends have

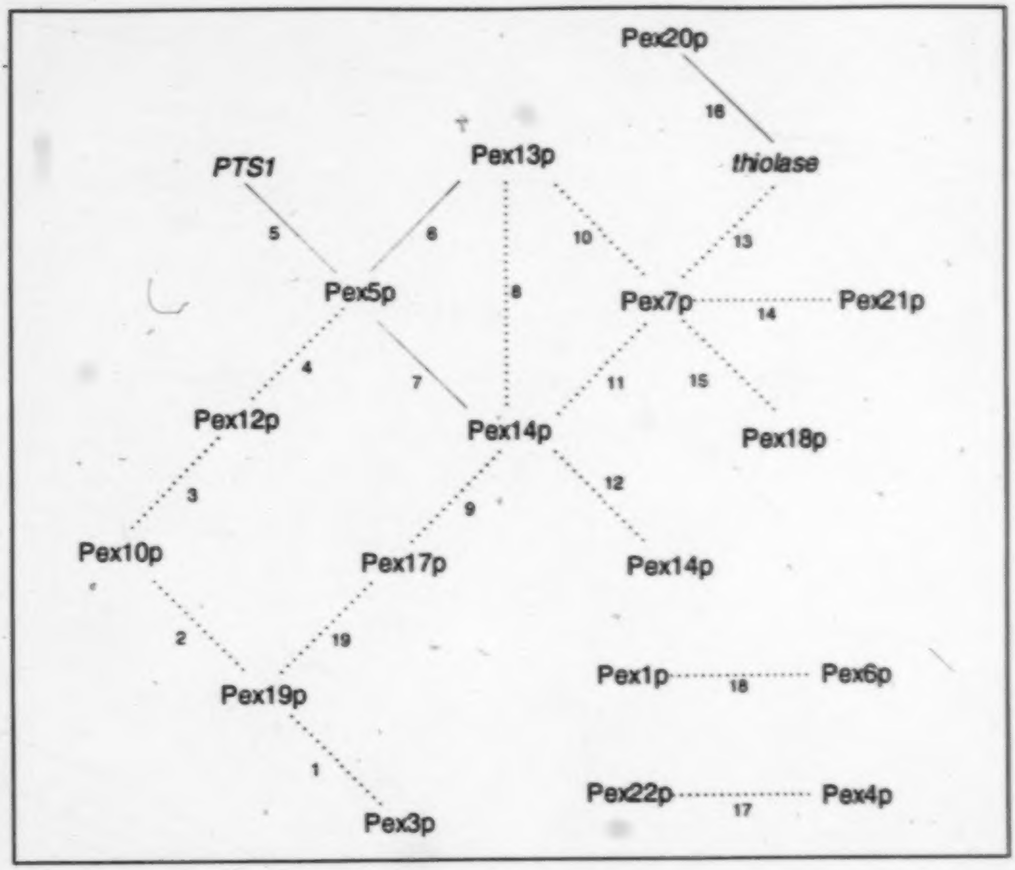
Pex20p
16
thiolase
PTS1
Pex13p
5
6
10
13
Pex5p
8
Pex7p
14
Pex21p
4
7
11
15
Pex12p
Pex14p
Pex18p
3
12
9
Pex10p
Pex17p
Pex14p
2
19
Pex1p
18
Pex6p
Pex19p
1
Pex22p
17
Pex4p
Pex3p

Figure 1-2. Physical interactions amongst peroxins. Interacting proteins that are not peroxins are *italicized*. Interactions that are direct (i.e., occur *in vitro* in the absence of proteins other than those in reticulocyte lysates) are represented by *solid lines*, all other interactions are represented by *dotted lines*. *1*, Götte et al., 1998; Snyder et al., 1999a. *2*, Snyder et al., 1999a. *3*, *4*, Chang et al., 1999. *5*, Dodt et al., 1995; Terlecky et al., 1995; Wiemer et al., 1995; Brocard et al., 1997; Kragler et al., 1998. *6*, Elgersma et al., 1996; Erdman and Blobel, 1996; Gould et al., 1996. *7*, Albertini et al., 1997; Brocard et al., 1997; Fransen et al., 1998; Schliebs et al., 1999; Shimizu, 1999; Will et al., 1999. *8*, Brocard et al., 1997; Albertini et al., 1997; Fransen et al., 1998. *9*, Huhse et al., 1998. *10*, Grizalsky, 1999. *11*, Brocard et al., 1997; Albertini et al., 1997; Shimizu, 1999. *12*, Brocard et al., 1997. *13*, Rehling et al., 1996; Zhang and Lazarow, 1996; Elgersma et al., 1998. *14*, *15*, Purdue et al., 1998. *16*, Titorenko et al., 1998. *17*, Koller et al., 1999. *18*, Faber et al., 1998; Geisbrecht et al. 1998; Tamura et al., 1998. *19*, Snyder et al., 1999b.

emerged: 1) Proteins to be transported have *cis*-acting targeting signals that direct them to a particular organelle (Blobel and Sabatini, 1971; Blobel and Dobberstein, 1975). Note that these targeting signals are distinct from other signals that may act as folding inhibitors or that are necessary for membrane translocation but not targeting. 2) Targeting signals are recognized by receptors that direct the proteins to the target organelle. Some receptors, including those for SRP-dependent translocation across the ER membrane (reviewed in Kalies and Hartmann, 1998), shuttle between the cytosol and the membrane of the target organelle. Other receptors, including those of mitochondria and chloroplasts (reviewed in Herrmann and Neupert, 2000; Chen and Schnell, 1999), do not shuttle and are located on the cytoplasmic face of the target membrane. Uniquely, receptors involved in transport across the nuclear membrane shuttle between the cytosol and the inside of the nucleus (Talcott and Moore, 1999). 3) In most cases, cargo proteins are transported across the membrane through heterooligomeric, gated transmembrane channels in a nucleoside triphosphate dependent manner.

Most translocation systems can only transport proteins that are at least partially unfolded (Eilers and Schatz, 1986; 1988). To aid in unfolding and refolding cargo proteins, cytosolic and intraorganellar chaperones are often involved (reviewed in Schatz and Dobberstein, 1996). Chaperones interact with nonnative conformations of cargo proteins. Often, their release is dependent on ATP or GTP and, as in the case of many cytosolic chaperones, is mediated by a cochaperone.

1.5.2 General aspects of peroxisomal matrix protein import–All matrix proteins that have been analyzed are synthesized on free polyribosomes and posttranslationally translocated into peroxisomes (Lazarow and Fujiki, 1985). Using the import systems described in Section 1.4.1, it has been determined that targeting matrix proteins to the peroxisomal membrane is dependent on a *cis*-acting targeting signal but independent of ATP, and that translocation across the membrane is dependent on membrane proteins and ATP hydrolysis, but is independent of a membrane potential.

Interestingly, unlike most other organelles, which import proteins in an unfolded conformation, yeast peroxisomes (Glover et al., 1994; McNew and Goodman, 1994) and plant glyoxysomes (Häusler et al., 1996; Lee et al., 1997) are capable of importing oligomeric protein complexes *in vivo* (reviewed in McNew and Goodman, 1996). Even folded proteins and 9-nm gold particles decorated with PTS1 sequences can be imported into the peroxisomes of human fibroblasts *in vivo* (Walton et al., 1995). One system capable of this type of transport is the nuclear pore; however, studies using freeze-fracture electron microscopy have failed to identify large protein complexes at the peroxisomal membrane similar to the nuclear pore complex (Kryvi et al., 1990). In addition, the peroxisomal membrane is not freely permeable to small molecules *in vivo* (van Roermund et al., 1995). In accordance with these data, it has been suggested that matrix proteins are transported into peroxisomes by engulfment by peroxisomal membranes that are subsequently dissolved (McNew and Goodman, 1996) rather than by translocation through a pore or channel. However, there is no evidence for this type of translocation, and the mechanism by which peroxisomes import large protein complexes remains to be elucidated.

Because peroxisomes are capable of importing oligomeric protein complexes, it is somewhat surprising that in both mammalian (Walton et al., 1994) and yeast (Hettema et al., 1998) cells, cytosolic chaperones have been shown to be involved in peroxisomal matrix protein import. The involvement of chaperones can be explained by the fact that not all peroxisomal proteins are imported as oligomers (Evers et al., 1994; 1996; Waterham et al., 1997). Alternatively, chaperones may be required for aspects of import other than the maintaining cargo in an unfolded conformation for transport. For example, chaperones may prevent irreversible aggregations or nonproductive interactions of cargo proteins before they reach the peroxisomal matrix, they may mediate conformational changes of import factors during translocation or they may mediate targeting signal recognition (reviewed in Hettema et al., 1999).

1.5.3 Targeting signals of peroxisomal matrix proteins–There are two well characterized *cis*-acting peroxisomal targeting signals (PTSs) that direct proteins to peroxisomes (reviewed in de Hoop and AB, 1992; Subramani, 1998; Hettema et al., 1999). PTS1, the most commonly used signal, is located at the extreme carboxyl terminus of proteins. It is a tripeptide of the sequence SKL or a conserved variant thereof conforming to the consensus sequence (S/A/C)-(K/R/H)-(L/M/I). This targeting signal is both necessary and sufficient to target reporter proteins to peroxisomes (Gould et al., 1989) and has been conserved throughout evolution (Gould et al., 1990a; 1990b; Keller et al., 1991). PTS2 is a nonapeptide conforming to the consensus sequence (R/K)-(L/V/I)-$(X)_5$-(H/Q)-(L/A) located near the amino terminus of some peroxisomal proteins. It is a less commonly used signal and most notably targets peroxisomal thiolase of many organisms from yeast to humans (for examples, see Swinkles, 1991; Glover et al., 1994b).

It is likely that other PTSs remain to be discovered, as some peroxisomal matrix proteins have neither a PTS1 nor a PTS2 motif. In addition, some proteins may have multiple redundant targeting signals, as several proteins that contain a PTS1 or a PTS2 motif also have an internal sequence capable of directing them to peroxisomes (Small et al., 1988; Kragler et al., 1993; Elgersma et al., 1995). However, because some proteins can be transported into peroxisomes as oligomers (Section 1.5.2), it is possible that these internal sequences may not be true targeting signals but rather domains that allow proteins to heterooligomerize with proteins that have PTSs (Rachubinski and Subramani, 1995; Elgersma and Tabak, 1996).

1.5.4 Overview of peroxins involved in the import of matrix proteins–There are several peroxins that, in addition to being necessary for matrix protein import, have characteristics that implicate their involvement directly in this process. These peroxins are organized into an import model diagrammed in Figure 1-3. This model incorporates the results of several groups (reviewed in Subramani, 1998; Hettema et al., 1999), including the physical interactions diagrammed in Figure 1-2. Some of these proteins are described in Sections 1.5.5 and 1.5.6.

1.5.5 Peroxins involved in matrix protein targeting–The PTS receptors Pex5p and Pex7p bind specifically to PTS1 and PTS2, respectively, and are necessary for targeting proteins containing these signals to peroxisomes (reviewed in Hettema et al., 1999). The subcellular locations of these receptors are a matter of debate (reviewed in Rachubinski and Subramani, 1995; Waterham and Cregg, 1997). As both receptors have been found

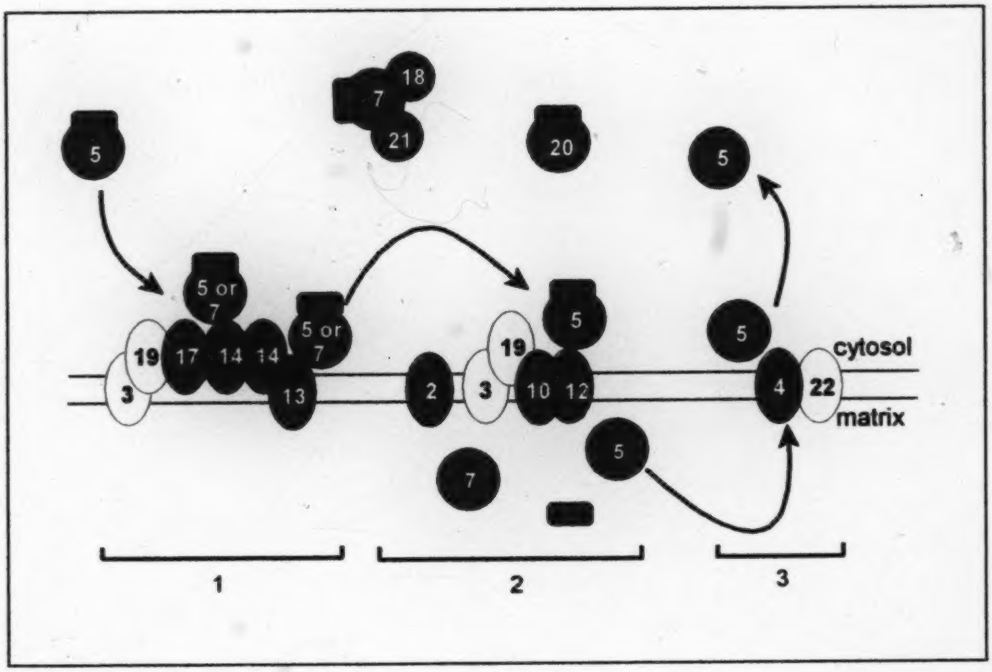

Figure 1-3. Model of peroxisomal matrix protein import. Cargo proteins are indicated by *rectangles*; peroxins involved in targeting are indicated by *circles*; membrane-bound peroxins involved in import are indicated by *ovals*; peroxins that interact with import components, but that have not been shown to have a direct role in import, are indicated in *white*. Physically interacting proteins are drawn connected. Peroxins in complex 1 have been implicated in the docking of targeting molecule, whereas those in complexes 2 and 3 are involved in aspects of import that occur after docking. Peroxins in complex 3 have been implicated in the recycling of targeting proteins. Aspects of import that have not yet been elucidated include where and how targeting proteins dissociate from their cargo and how proteins traverse the membrane.

in the cytosol, associated with the peroxisomal membrane and in the peroxisomal matrix, it has been suggested that they are mobile receptors that bind cargo proteins in the cytosol, dock at the peroxisomal membrane, enter the peroxisomes, release their cargo in the matrix, and recycle back to the cytosol (van der Klei et al., 1995; Dodt and Gould, 1996; Rehling et al., 1996; van der Klei and Veenhuis, 1996; Erdman et al., 1997). Consistent with this extended shuttle hypothesis, as it is known, a temporary block in peroxisomal import in mammalian cells causes cytoplasmic Pex5p to associate with peroxisomes, and release of the block causes Pex5p to recycle back to the cytoplasm (Dodt and Gould, 1996). Also in support of this hypothesis, many membrane-bound peroxins involved in import physically interact with Pex5p or Pex7p, whereas none have been found to interact directly with cargo (Fig. 1-3), suggesting that the receptors with cargo are passed to different components of the import apparatus. It should be noted that although these data provide evidence for the shuttling of targeting proteins between the cytosol and the peroxisomal membrane, they do not provide evidence for targeting proteins entering peroxisomes.

Recent evidence suggests that targeting of peroxisomal matrix proteins is more complex than outlined above. Firstly, targeting via the Pex7p-dependent pathway in *S. cerevisiae* requires both Pex18p and Pex21p. Evidence suggests that these peroxins bind to cargo-bound Pex7p in the cytosol and direct the receptor to peroxisomes (Purdue et al., 1998). Secondly, Pex5p may have a direct role in a PTS1-independent import mechanism in addition to its role in PTS1-dependent import. Evidence for this includes the fact that the targeting of a protein to peroxisomes via an internal targeting signal is dependent on Pex5p in *S. cerevisiae* (Elgersma et al., 1995). Also, the human (Dodt et al., 1995;

Fransen et al., 1995; Wiemer et al., 1995; Braverman et al., 1998), mouse (Braverman et al., 1998) and CHO (Otera et al., 1998) *PEX5* genes each encode two isoforms of Pex5p. One form is necessary for the import of PTS1-containing proteins, whereas the other is necessary for the import of both PTS1- and PTS2-containing proteins (Braverman et al., 1998; Otera et al., 1998). A similar targeting mechanism has been identified in the yeast *Y. lipolytica*. In this yeast, the PTS2 receptor Pex7p has not been identified, while interestingly, Pex20p, a peroxin with sequence similarity to Pex5p, interacts directly with thiolase in the cytosol and is necessary for its dimerization and peroxisomal targeting (Titorenko et al., 1998). *Y. lipolytica* thiolase (EMBL accession number X69988) contains a PTS2 and possibly a redundant internal targeting signal, but not a PTS1. Taken together, these results suggest that Pex5p and Pex5p-like peroxins are involved in a PTS1-independent targeting pathway.

1.5.6 Membrane-associated peroxins involved in matrix protein import–Pex14p and Pex13p are peripheral and integral peroxisomal membrane peroxins, respectively, that have been implicated in docking the targeting proteins Pex5p and Pex7p. The role of Pex13p and Pex14p in docking Pex5p and Pex7p has been suggested for three reasons: 1) In the absence of either Pex13p or Pex14p, PTS1- and PTS2-containing proteins are mislocalized (Elgersma et al., 1996; Erdmann and Blobel, 1996; Gould et al., 1996). 2) Pex14p and Pex13p interact with each other, and each interacts directly with both Pex5p and Pex7p (for references, see Fig. 1-2). In addition, it has recently been demonstrated that both Pex13p and Pex14p can interact with cargo-bound Pex5p (Urquhart et al., 2000). 3) In cells lacking Pex13p, much less Pex5p is associated with peroxisomal membranes than in wild-type cells (Gould et al., 1996).

Other peroxins that have been suggested to have direct roles in matrix protein import include *H. polymorpha* Pex4p (van der Klei et al., 1998) and human Pex2p, Pex10p and Pex12p (Dodt and Gould, 1996). Pex12p interacts with the PTS1 receptor Pex5p (Fig. 1-2), and in the absence of Pex2p or Pex12p, matrix proteins are mislocalized to the cytosol, and Pex5p accumulates on the cytosolic face of the peroxisomal membrane. In the absence of Pex4p or Pex10p, matrix proteins are mislocalized to the cytosol, and Pex5p accumulates inside peroxisomes. For these reasons, it has been suggested that these four proteins are involved in aspects of import that occur after docking. Interestingly, the import defect of cells lacking Pex4p can be complemented by the overproduction of Pex5p, suggesting that Pex4p may have a role in receptor recycling.

As Pex14p and Pex13p interact with each other and with both the PTS1 and PTS2 receptors (Fig. 1-2), it has been suggested that although PTS1- and PTS2-dependent targeting pathways are divergent, the docking and possibly translocation pathways are convergent (Albertini et al., 1997; Girzalsky et al., 1999). Consistent with this, in cells in which genes encoding other membrane-bound peroxins involved in import are disrupted or mutated, both PTS1- and PTS2-containing proteins are mislocalized to the cytosol (for examples, see Slawecki et al., 1995).

It should be noted that, although matrix protein import is the most intensively studied aspect of peroxisome maintenance, several important questions remain unanswered. For example, it has not yet been determined where or how targeting proteins are dissociated from their cargo, or how matrix proteins are transported across the membrane.

1.6 Integration of proteins into the peroxisomal membrane

1.6.1 General aspects of peroxisomal membrane protein trafficking–Several integral peroxisomal membrane proteins are translated on free cytoplasmic polyribosomes and posttranslationally inserted into the membranes of peroxisomes (Fujiki et al., 1984; Suzuki et al., 1987; Bodnar and Rachubinski, 1991). By studying both import into isolated rat liver peroxisomes (Distelkötter and Just, 1993; Imanaka et al., 1996; Pause et al., 1997) and into peroxisomes of permeabilized rat hepatocytes (Distelkötter and Just, 1993), it was determined that peroxisomal membrane protein import depends on cytosolic and peroxisome-associated factors but not on ATP or GTP hydrolysis. At least one targeting mechanism for peroxisomal membrane proteins has been conserved during evolution, as the integral peroxisomal membrane protein Pex2p of *Y. lipolytica* is localized to peroxisomes when synthesized in CHO cells (Eitzen et al., 1996).

1.6.2 Targeting signals of peroxisomal membrane proteins–The PTSs of integral membrane proteins are different from those of matrix proteins (reviewed in Subramani, 1993). Only one membrane PTS (mPTS) has been characterized. This signal conforms to the consensus sequence (F/L)-(L/I/V)-X-(R/K)-X-(K/R)-X-(K/R)-X-(L/I)(F/V/I/M)-$X_{8\text{-}9}$-(F/Y) (Elgersma et al., 1997; Soukupova et al., 1999). Sequences that match or closely resemble this sequence have been found within matrix-facing hydrophilic portions of several peroxisomal membrane proteins including *Candida boidinii* PMP47 (McCammon et al., 1994; Dyer et al., 1996), *H. polymorpha*, *P. pastoris*, and human Pex3p (Baerends et al., 1996; Wiemer et al., 1996; Kammerer et al., 1998; Soukupova et al., 1999), and *S. cerevisiae* Pex15p (Elgersma et al., 1997). Portions of proteins containing this signal have been shown to be necessary (Dyer et al., 1996) and sufficient (Baerends et al., 1996; Dyer et al., 1996; Wiemer et al., 1996; Kammerer et al., 1998) for peroxisomal targeting (reviewed in Subramani, 1998; Hettema et al., 1999). However, for at least Pex15p, peroxisomal targeting also requires a transmembrane domain (Elgersma et al., 1997).

1.6.3 Peroxins involved in peroxisomal membrane protein trafficking–Membrane protein import does not require the same group of peroxins as does matrix protein import, because several *pex* mutants have matrix protein import defects but do not appear to have membrane protein import defects (for examples, see Purdue and Lazarow, 1995; Tan et al., 1995; Erdmann and Blobel., 1996). It has been suggested that Pex16p (South and Gould, 1999), Pex3p (Höhfeld et al., 1991; Baerends et al., 1996; Wiemer et al., 1996), Pex17p (Snyder et al., 1999b) and, in some organisms, Pex19p (Götte et al., 1998; Matsuzono et al., 1999) are each involved in peroxisomal membrane protein import, as cells lacking any one of these peroxins mislocalize some peroxisomal membrane proteins to the cytosol, although a direct involvement of these peroxins in peroxisomal membrane protein import remains to be demonstrated.

1.6.4 Involvement of the ER in peroxisomal membrane protein trafficking–Three lines of evidence suggest that some membrane proteins reach peroxisomes via the ER (reviewed in Kunau and Erdman, 1988; Titorenko and Rachubinski, 1998a): 1) In cells of *H. polymorpha*, peroxisomal membrane proteins Pex3p and Pex14p associate with an ER-like compartment after treatment with brefeldin A (a fungal toxin that inhibits ARF1-COP1-mediated vesicular transport) (Salomons et al., 1997). 2) Overexpression studies demonstrate that peroxisomal membrane proteins *H. polymorpha* Pex3p (Baerends et al., 1996) and *S. cerevisiae* Pex15p (Elgersma et al., 1997) contain signals capable of directing them to the ER. It should be noted, however, that this localization might be nonspecific, as overproduced hydrophobic proteins are commonly mislocalized to the ER (Hettema et al., 1999; Stroobants et al., 1999). 3) Pex2p and Pex16p are *N*-glycosylated and may be targeted to peroxisomes via the ER in a Pex1p- and Pex6p-dependent manner in *Y. lipolytica* (Titorenko and Rachubinski, 1998b). However, interestingly, in mammalian cells, Pex16p does not traffic through the ER, Pex16p targeting is not dependent on Pex1p and peroxisomes can be formed in the presence of brefeldin A (South and Gould, 1999). As the targeting of Pex2p has been conserved between *Y. lipolytica* and mammalian cells (Eitzen et al., 1996), it will be interesting to see if the targeting of Pex2p involves the ER in mammalian cells.

1.7 Peroxisome size and number

1.7.1 Formation of new peroxisomes–New peroxisomes are formed to adapt to environmental changes. They may also be formed to pass peroxisomes on to progeny during cell division, or to replace old, nonfunctional peroxisomes. Whether new peroxisomes derive from preexisting peroxisomes or from a different vesicular compartment is a matter of debate.

The concept of peroxisomes arising by the growth and fission of preexisting peroxisomes is supported by characteristics of mammalian and yeast peroxins of the Pex11p family. Cells contain a few large peroxisomes in the absence of Pex11p (Erdman and Blobel, 1995; Marshall et al., 1995; Sakai et al., 1995) and several small peroxisomes when it is overproduced (Marshall et al., 1995; Schrader et al., 1998), suggesting the existence of a Pex11p-dependent mechanism of peroxisome fission. Recent evidence strongly suggests that in mammalian cells, Pex11p-dependent peroxisome fission involves ARF and coatomer (Passreiter et al., 1998), but, as peroxisome proliferation in mammalian cells is not inhibited by brefeldin A (South and Gould, 1999), this may not be the only mechanism for the formation of new peroxisomes.

The concept that peroxisomes can be formed in the absence of preexisting peroxisomes is also strongly supported. In mammalian and yeast cells, normal peroxisome morphology can be restored to *pex* mutants that do not have detectable peroxisomes (for examples, see Baerends et al., 1996; South and Gould., 1999) by introducing a wild-type copy of the defective gene. Evidence suggests that, at least in *Y. lipolytica* cells, this type of peroxisome formation can be mediated by the fusion of "preperoxisomal vesicles" in a Pex1p- and Pex6p-dependent manner (Titorenko et al., 2000).

Considering the evidence, perhaps peroxisomes can be derived from either source depending on the needs of the cell. For most purposes, peroxisomes may be preferentially formed by the seemingly more efficient process of fission of preexisting peroxisomes.

Consistent with this hypothesis, wild-type yeast cells contain peroxisomes under all growth conditions, even under conditions where they are not required. The production of peroxisomes from preperoxisomal vesicles, however, is most probably necessary under conditions in which existing peroxisomes are nonfunctional (for example, when a *pex* mutant is transformed with a wild-type copy of the defective gene).

It should be noted that although the formation of peroxisomes from preperoxisomal vesicles has been demonstrated, it has yet to be demonstrated that peroxisomes can be formed in the absence of some type of peroxisomal precursor. In fact, if this type of *de novo* formation is not possible, *pex* mutant strains truly lacking peroxisomes may not yet have been characterized, because characterization often begins with the identification of defective genes by functional complementation.

1.7.2 Regulation of peroxisome size and number–In addition to Pex11p (discussed in Section 1.7.1), peroxisomal membrane proteins Pex3p, Pex10p and Pex16p have been implicated in controlling peroxisome size and number. Peroxisome number is increased by overproduction of either Pex10p or Pex3p in *H. polymorpha* (Tan et al., 1995; Baerends et al., 1996), and peroxisome size is increased by overproduction of Pex16p in *Y. lipolytica* (Eitzen et al., 1997). In mammalian cells, there may also be metabolic control of peroxisome abundance and size. Cells of a patient with a specific deficiency in the β-oxidation enzyme acyl-CoA oxidase (Fig. 1-1) have enlarged peroxisomes that are heterogeneous in size (Poll-The et al., 1988). In addition, human cells lacking either acyl-CoA oxidase or MFE2 (Fig. 1-1) have a reduction in peroxisome abundance and an increase in peroxisome diameter compared to normal cells (Chang et al., 1999). The control of peroxisome size and number is not well understood, and the direct involvement of a protein, with the exception of Pex11p, in these processes has yet to be demonstrated.

1.8 Focus of this thesis

The use of the yeast *Y. lipolytica* as a model system for studying peroxisome maintenance was developed by the Rachubinski group in 1994. A massive proliferation of peroxisomes can be induced in these cells, thereby greatly facilitating peroxisomal analyses. To date, 11 peroxins have been identified using this model system (Table 1-1, *shaded* peroxins). This thesis focuses on the identification and characterization of two proteins of *Y. lipolytica* involved with peroxisome maintenance, Pex8p, a peroxin involved in matrix protein import, and multifunctional enzyme type 2 (MFE2), a metabolic enzyme that has a role in controlling peroxisome size and number.

CHAPTER 2

MATERIALS AND METHODS

2.1 Materials

2.1.1 List of chemicals and reagents

acrylamide	Gibco/BRL
acrylamide solution, ExplorER	J. T. Baker
acrylamide solution, Long Ranger	J. T. Baker
agar	Difco
agarose, electrophoresis grade	Gibco/BRL
agarose, NuSieve GTG	FMC BioProducts
agarose, SeaKem GTG	FMC BioProducts
albumin, bovine serum (BSA)	Roche
L-amino acids	Sigma
ammonium persulphate	BDH
ampicillin	Sigma
antipain	Roche
aprotinin	Roche
benzamidine hydrochloride	Sigma
Bio-Rad protein assay dye reagent	Bio-Rad
B-PER bacterial protein extraction reagent	Pierce
Brij-35 (polyoxyethylene 23-lauryl ether)	Sigma
bromophenol blue	BDH
CSM (complete supplement mixture)	BIO 101
Coomassie Brilliant Blue R-250	ICN
cytochrome *c*, horse heart	Sigma
DMF	dimethyl formamide
DNA, from salmon testes, sodium salt	Sigma
DTT (dithiothreitol)	ICN
EDTA (ethylenediaminetetraacetic acid)	Sigma
Ficoll	Amersham-Pharmacia
Freund's adjuvant (complete and incomplete)	Sigma
formamide	BDH
formaldehyde, 37% (v/v)	BDH
glutathione, reduced	Sigma
glutathione-sepharose	Amersham-Pharmacia
glycerol	BDH
HEPES (4-[2-hydroxyethyl]-1-piperazineethanesulphonic acid)	Roche
hydrogen peroxide solution, 30% (w/v)	Sigma
IPTG (isopropyl β-D-thiogalactopyranoside)	Vector Biosystems
leupeptin	Roche
L(-)malic acid (disodium salt)	Sigma
malt extract	Sigma
2-mercaptoethanol	BDH
MES (2-[N-morpholino]ethanesulphonic acid)	Sigma

N,N'-methylenebisacrylamide	Gibco/BRL
MOPS (3-[N-morpholino]propanesulphonic acid)	Sigma
p-nitrophenyl phosphate	Sigma
NP-40 (Nonidet P-40)	BDH
oleic acid	Fisher
Pefabloc SC	Roche
pepstatin A	Sigma
peptone	Difco
phenol, buffer-saturated	Gibco/BRL
PMSF (phenylmethylsulphonylfluoride)	Roche
poly *L*-lysine (solution of 1 mg/mL)	Sigma
polyvinylpyrrolidone	Sigma
Ponceau S	Sigma
protein A-Sepharose	Amersham-Pharmacia
Sephadex G-50	Amersham-Pharmacia
SDS (sodium dodecyl sulphate)	Sigma
sodium fluoride	Sigma
sodium sulphite	Sigma
sorbitol	BDH
TAAB 812 resin	Marivac
TCA (trichloroacetic acid)	BDH
TEMED (*N,N,N',N'*-tetramethylethylenediamine)	Gibco/BRL
Tris (tris[hydroxymethyl]aminomethane)	Roche
Triton X-100	Sigma
tryptone	Difco
Tween 20 (polyoxyethylenesorbitan monolaurate)	Sigma
Tween 40 (polyoxyethylenesorbitan monopalmitate)	Sigma
X-gal (5-bromo-4-chloro-3-indolyl-β-D-galactoside)	Vector Biosystems
xylene cyanole FF	Sigma
yeast extract	Difco
YNB (yeast nitrogen base without amino acids)	Difco

2.1.2 List of enzymes

CIP (calf intestinal alkaline phosphatase)	NEB
DNA ligase, T4	Gibco/BRL, NEB, Roche
DNA polymerase, T4	NEB
Klenow fragment of DNA polymerase I, *Escherichia coli*	NEB
polynucleotide kinase, T4	NEB
restriction endonucleases	NEB, Gibco/BRL, Roche, Promega
RNaseA (ribonuclease A), bovine pancreas	Sigma, Roche
Taq DNA polymerase, *Thermus aquaticus*	Roche
trypsin	Roche
Zymolyase 100T	ICN

2.1.3 Molecular size standards

1 kb DNA ladder (75-12,216 bp)	Gibco/BRL
25 bp DNA ladder (25-500 bp)	Gibco/BRL
prestained markers for SDS-PAGE (6.5, 16.5, 25, 32.5, 47.5, 62, 83, 175 kD)	NEB

2.1.4 Multicomponenet systems

BigDye Terminator Cycle Sequencing Ready Reaction Kit	ABI Prism
Matchmaker Two-Hybrid System	Clonetech
Protein Fusion and Purification System	NEB
QIAprep MiniPrep Kit	Qiagen
QIAquick Gel Extraction Kit	Qiagen
QIAquick PCR Purification Kit	Qiagen
Random Primed DNA Labelling Kit	Roche
Ready-To-Go PCR Beads	Amersham-Pharmacia
Re-Blot Western Blot Recycling Kit	Chemicon
Sequenase Version 1.0 DNA Sequencing Kit	USB
Sequenase Version 2.0 DNA Sequencing Kit	USB
TE Midi SELECT-D, G50 Columns	Eppendorf - 5 Prime

2.1.5 Radiochemicals and detection kits

α-[^{32}P]dATP, Redivue (3,000 Ci/mmol, 10 μCi/μL)	Amersham-Pharmacia
α-[^{32}P]dCTP, Redivue (3,000 Ci/mmol, 10 μCi/μL)	Amersham-Pharmacia
ECL Detection Kit for Immunoblotting	Amersham-Pharmacia
ECL Direct Nucleic Acid Labelling and Detection System	Amersham-Pharmacia
nitrocellulose	Schleicher & Schuell, Amersham-Pharmacia, Bio-Rad
X-ray film (BioMax MR, X-Omat AR and X-Omat X-K1)	Kodak

2.1.6 Plasmids

pBluescriptSKII(-)	Stratagene
pGEM7Zf (+)	Promega
pGEM5Zf (+)	Promega
pGEX-4T1	Amersham-Pharmacdia
pMAL-c2	NEB
pINA445 (*Y. lipolytica*/*E. coli* shuttle vector)[a]	Claude Gaillardin[b]

pINA443 (*Y. lipolytica*/*E. coli* shuttle vector) ....Claude Gaillardin (Nuttley et al., 1993)

[a] Contains *LEU2* gene for positive selection of yeast transformants and the *ARS68* gene for autonomous plasmid replication in yeast.
[b] Institut National Agronomique Paris-Grignon, Thiverval-Grignon, France.

2.1.7 Antibodies–The antibodies used in this study are described in Tables 2-1 and 2-2.

Table 2-1 Primary Antibodies

Antibody specificity	Type[a]	Name	Dilution[b]	Description
Y. lipolytica Pex1p	gp-pc	Pay41-N	1:5000	Section 2.17.2
Y. lipolytica Pex2p	gp-pc	Pay42-NN	1:1000	Eitzen et al., 1996
Y. lipolytica Pex2p	gp-pc	Pay5-NN	1:2000	Eitzen et al., 1996
Y. lipolytica Pex5p	gp-pc	N-3°	1:50,000	Szilard et al., 1995
Y. lipolytica Pex6p	gp-pc	P4-NN	1:5,000	Section 2.17.3
Y. lipolytica Pex16p	gp-pc	SOAP-2°	1:3,000	Eitzen et al., 1997
Y. lipolytica Pex19p	gp-pc	194-2°	1:10,000	Gareth Lambkin
Y. lipolytica Pex20p	rb-pc	H67-3T	1:1000	Section 2.17.1
Y. lipolytica Pex20p	gp-pc	N-1°	1:5,000	Section 2.17.1
Y. lipolytica isocitrate lyase	rb-pc	E405-1°	1:5,000	Eitzen et al., 1996
peptides with carboxyl-terminal SKL	rb-pc	16	1:1,000	Aitchison et al., 1992
Y. lipolytica Kar2p[c]	rb-pc	Kar2p	1:15,000	Titorenko et al., 1997
Y. lipolytica Aox5[d]	rb-pc	Aox5	1:5,000	Wang et al., 1999
S. cerevisiae Aox[e]	rb-pc	POX-N	1:1,000	Eitzen et al., 1996
Y. lipolytica thiolase	gp-pc	N-3°	1:100,000	Eitzen et al., 1996
S. cerevisiae cytoplasmic C_1-THFS[f]	rb-pc	611-FB	1:2,000	
S. cerevisiae malate synthase[g]	rb-pc	MLS	1:1,000	
9-amino-acid residue epitope of the influenza virus HA protein	m-mc	12CA5	1:1000	Berkeley Antibody Company
10 amino acid epitope of the human c-Myc protein	m-mc	9E10	1:1000	Santa Cruz Biotechnology

[a] gp, guinea pig; rb,rabbit; m, mouse; pc, polyclonal; mc, monoclonal.
[b] Dilutions are for Western blotting. For microscopy, antisera were at tenfold higher concentrations.
[c] A gift of David Ogrydziak (University of California, Davis, California).
[d] A gift of Jean-Marc Nicaud (Laboratoire de Génétique des Microorganismes, Thiverval-Grignon, France).
[e] A gift of Joel Goodman (University of Texas, Dallas, Texas). Antibodies recognize *Y. lipolytica* Aox1p.
[f] A gift of Dean R. Appling (University of Texas, Austin, Texas).
[g] A gift of Andreas Hartig (Institute of Biochemistry and Molecular Cell Biology, Vienna, Austria).

Table 2-2 Secondary Antibodies

Antibody	Type[a]	Source
horseradish peroxidase-conjugated anti-guinea pig IgG	gt	Sigma
horseradish peroxidase-conjugated anti-rabbit IgG	dk	Amersham-Pharmacia
horseradish peroxidase-conjugated anti-mouse IgG	dk	Amersham-Pharmacia
rhodamine-conjugated anti-mouse and anti-guinea pig IgG	dk	Jackson
fluorescein-conjugated anti-guinea pig and anti-rabbit IgG	dk	Jackson

[a] gt, goat; dk, donkey.

2.1.8 Oligonucleotides –Oligonucleotides were synthesized either at the DNA Sequencing Facility, Department of Biochemistry, University of Alberta or on an Oligo 1000M DNA Synthesizer (Beckman). Oligonucleotides used in this study are described in Table 2-3.

Table 2-3 Oligonucleotides

Name	Sequence [a, b, c]	Application
122-1	ATTGAATTCAATCATCTTCCACATTTCCAG	pGAD-P8ΔNC
122-2	ATTGAATTCATGAACAAGTATCTAGTGCCC	pGAD-PEX8/pGBT-PEX8
287	GCGAATTCATGACATCCAAGTCTGATTATTC	pMAL-PEX1
288	GCAAGCTTAACGCTTGTCCTCAGATTCGAT	pMAL-PEX1
290	GCAAGCTTCACTTCCCCATCCACACTTCCTC	pMAL-PEX20
336	ATTAGATCTTAATAACGTTCCATGCACTCG	pGAD-PEX8/pGBT-PEX8
337	ATTGGATCCTCATGTCTTCGGTTCTACGA	pGAD-PEX2/pGBT-PEX2
338	ACCAGATCTTTAATCTTTCATAAGCTGAAAG	pGAD-PEX2/pGBT-PEX2
339	ATTGAATTCATGTCGTTTATGAGAGGAGGA	pGAD-PEX5/pGBT-PEX5
340	ATTGGATCCCTAAAATTCAAACTCATTTCGG	pGAD-PEX5/pGBT-PEX5
341	ATTGAATTCATGACGATGAGCGCAAGGGTC	pGAD-PEX9/pGBT-PEX9
342	ATCAGATCTTCACATGTGTTTGCCTCCACAA	pGAD-PEX9/pGBT-PEX9
343	ATTGAATTCATGCCGTCGATCAGCCACAAA	pGAD-PEX6/pGBT-PEX6
344	ATTGAATTCTCATTTCTTGCCTCCCTCAAAT	pGAD-PEX6/pGBT-PEX6
394	GTAGAATTCATGACATCCAAGTCTGATTATTC	pGAD-PEX1/pGBT-PEX1
395	GTAGAATTCACATCATGCCAAGGTAGCCC	pGAD-PEX1/pGBT-PEX1
398	GTAGAATTCCACTCACTTCCCCATCCAC	pGAD-PEX20/pGBT-PEX20
399	GTAGAATTCATGGCATCTTGCGGACCTTC	pGAD-PEX20/pGBT-PEX20

414	GCGAATTCATGGCATCTTGCGGACCTC	pMAL-PEX20
424	GCGAATTCATGCCGTCGATCAGCCAC	pMAL-PEX6
425	GCAAGCTTAGATCTTGTCGGCGTATGC	PMAL-PEX6
548	GGTTTGTTACCGTTCTATTGTTCATGGTGTTGGGGTA	Pex8p-ΔPTS2
549	GTACCCCATTGAATTCATGAACAATAGAACGGTAACAAAC	Pex8p-ΔPTS2 /pGAD-P8ΔNC
564	GCCGAATTCAACCAAGACACACAAAAATG	*POX1*
565	GAAGGATCCGGCGGGGTTCTGCTCG	*POX1*
731	GGTTGTTCAGACCGCTA	*MFE2* sequencing
742	GGTGTTGAAGGCCTT	*MFE2* sequencing
760	GTTAGGAGATCTCCGTGGGAGTAGCCCACAG	*PEX8-HAc*
761	CCACGGAGATCTCCTAACGTTCCATGCACTCGAG	*PEX8-HAc*
901	AATGACCCTTGTTGCCCTCC	*MFE2* sequencing
909	CCAACAGTTGAACTTCGCC	*MFE2* sequencing
913	GCATTATCCATATCCGAGG	*MFE2* sequencing
921	TAATAGCGTCGACACCTCAATTGAGTTAGCAG	pΔMFE2
922	TGAGGTGTCGACGCTATTATCTGACCAAGTG	pΔMFE2
944	ATGTCTTACGTACTCTGGAGAACTAAGATACG	pMyc-MFE2
945	TCCAGAGTACGTAAGACATTGTGTGTGTGTGTTGAAT	pMyc-MFE2
953	CTTGGTCAGATAATAGCTTAATCCTTGGG	pMyc-MFE2ΔAKL
958	GAGCTCTTCCCCAAGGATTAAGCTATTAT	pMyc-MFE2ΔAKL
1001	AC(C/T)GT(A/G/C/T)GT(A/G/C/T)CA(C/T)TC(T/C)AA	*THFS*
1002	TC(A/G/C)GGGTT(G/A)GT(C/T)TT(G/A)TC	*THFS*
1009	GAAGGATCCGAGGCTATAATTACC	*ACT1*
1010	GAAGGATCCTCAACTGAACACAAC	*ACT1*
1011	ATTAAAATACGTAGTGTGGTGATTGCTGT	*ACT1*
1012	CCACACTACGTATTTTAATTTGTGTGGTTGTT	*ACT1*
1013	CAGGTTGTCATTGTCACT**A**G**T**GCCGGT	pMyc-MFE2(ΔAΔB)
1014	AATGCCAGCACCGGC**A**C**T**AGTGAC	pMyc-MFE2(ΔAΔB)
1015	AGGTCGTCATTGTTACC**A**GTGCCGG	pMyc-MFE2(ΔAΔB)
1016	ACCGCCACCGGCAC**T**GGTAACA	pMyc-MFE2(ΔAΔB)
RP	CAGGAAACAGCATGAC	pGEM7Zf(+)
UP	GTAAAACGACGGCCAGT	pGEM7Zf(+)

[a] Sequences are written 5' to 3'.

[b] Restriction endonuclease recognition sites are *underlined*. Sites were chosen based on the ability of the corresponding enzyme to cleave close to the ends of DNA fragments according to the NEB 1999 catalog.

[c] Site-directed mutations are indicated in **bold**.

***2.1.9 Standard buffers and solutions*–**Commonly used solutions are described below.

Table 2-4 Standard Buffers and Solutions

Solution	Composition	Reference
20 x Borate Buffer	0.4 M boric acid, 4 mM EDTA (pH 8.3)	Ausubel et al., 1989
50 x Denhardt's	1% Ficoll, 1% polyvinylpyrrolidone, 1% BSA	Maniatis et al., 1982
1 x protease inhibitor (PIN) cocktail	1 µg/mL each of leupeptin, pepstatin, aprotinin, antipain, 0.5 mM benzamidine hydrochloride, 5 mM NaF, 1 mM PMSF or 0.1-1 µg Pefabloc SC/mL	This study
20 x SSC	3 M NaCl, 0.3 M trisodium citrate (pH 7.0)	Maniatis et al., 1982
10 x TBE	0.89 M Tris-borate, 0.89 M boric acid, 0.02 M EDTA	Maniatis et al., 1982
TBST	20 mM Tris-HCl (pH 7.5), 150 mM NaCl, 0.05% (w/v) Tween 20	Huynh et al., 1985
TE	10 mM Tris-HCl (pH 7.0-8.0, as appropriate), 1 mM EDTA	Maniatis et al., 1982

2.2 Microorganisms and culture conditions

***2.2.1 Yeast strains and culture conditions*–**The *Y. lipolytica* strains used in this study are described in Table 2-5. Yeast culture media are described in Table 2-6. Growth of yeast was at 30°C. Cultures of 10 mL or less were grown in 16 x 150 mm glass tubes in a rotating wheel. Cultures greater than 10 mL were grown in flasks in a rotary shaker at 250 rpm. Culture volumes were approximately 20% of flask volumes. Strains and culture conditions for two-hybrid analysis were as described by the manufacturer (Clonetech).

Table 2-5 *Y. lipolytica* Strains

Strain	Genotype
E122[a]	*MATA ura3-302 leu2-270 lys8-11*
22301-3[a]	*MATB ura3-302 leu2-270 his1*

pex8-1	*MATA ura3-302 leu 2-270 lys8-11 pex8-1*
pex8-KA	*MATA ura3-302 leu2-270 lys8-11 pex8::URA3*
pex8-KB	*MATB ura3-302 leu2-270 his1 pex8::URA3*
PEX8-HA[i]	*MATA ura3-302 leu2-270 lys8-11 PEX8-HA*[i]
PEX8-HA[c]	*MATA ura3-302 leu2-270 lys8-11 PEX8-HA*[c]
D-8OB	*MATA/MATB ura3-302/ura3-302 leu2-270/leu2-270 lys8-11/+ his1/+ pex8-1/+*
D-8O8K	*MATA/MATB ura3-302/ura3-302 leu2-270/leu2-270 lys8-11/+ his1/+ pex8-1/pex8::URA3*
D-A8K	*MATA/MATB ura3-302/ura3-302 leu2-270/leu2-270 lys8-11/+ his1/+ pex8::URA3/+*
D-8KB	*MATA/MATB ura3-302/ura3-302 leu2-270/leu2-270 lys8-11/+ his1/+ pex8::URA3/+*
D-8K8K	*MATA/MATB ura3-302/ura3-302 leu2-270/leu2-270 lys8-11/+ his1/+ pex8::URA3/pex8::URA3*
D-AB	*MATA/MATB ura3-302/ura3-302 leu2-270/leu2-270 lys8-11/+ his1/+*
pex20KO[c]	*MATA ura3-302 leu2-270 lys8-11 pex20::URA3*
pex20-1[c]	*MATA ura3-302 leu2-270 lys8-11 pex20-1*
pex5-KO2[b]	*MATA ura3-302 leu2-270 lys8-11 pex5::URA3*
P16KO-6A[d]	*MATA ura3-302 leu2-270 lys8-11 ole-1*[e]
mfe2-KO	*MATA ura3-302 leu2-270 lys8-11 mfe2::URA3*

[a] A gift of Claude Gaillardin (Laboratoire de Génétique des Microorganismes, Thiverval-Grignon, France).
[b] Constructed by Rachel Szilard.
[c] Constructed by Vladimir Titorenko.
[d] Constructed by Gary Eitzen.
[e] Mutation at unknown locus that results in the inability to use oleic acid as a carbon source.

Table 2-6 Yeast Culture Media

Medium	Composition[a, b]	Reference
2 x CMA	1.34% YNB, 2 × CSM (minus leucine and uracil, as required), 2% sodium acetate	This study
2 x CMD	1.34% YNB, 2 × CSM (minus leucine and uracil, as required), 2% glucose	This study
2 x CMO	1.34% YNB, 2 × CSM (minus leucine and uracil, as required), 0.05% (w/v) Tween 40, 0.2% (w/v) oleic acid	This study
PSM	0.5% yeast extract, 0.5% $(NH_4)_2SO_4$, 0.2% KH_2PO_4, 2% glucose	Gaillardin et al., 1973
YEPA	1% yeast extract, 2% peptone, 2% sodium acetate	Brade, 1992
YEPD	1% yeast extract, 2% peptone, 2% glucose	Rose et al., 1988
YM	0.5% peptone, 0.3% yeast extract, 0.3% malt extract	Gaillardin et al., 1973
YNA[c]	0.67% YNB, 2% sodium acetate	Brade, 1992
YND[c]	0.67% YNB, 2% glucose	Rose et al., 1988

YNO[c]	0.67% YNB, 0.05% (w/v) Tween 40, 0.1% (w/v) oleic acid	Nuttley et al., 1993
YPBO	0.3% yeast extract, 0.5% peptone, 0.5% K_2HPO_4, 0.5% KH_2PO_4, 1% Brij 35, 1% (w/v) oleic acid	Kamiryo et al., 1982

[a] For solid media, agar was added to 2%.
[b] Glucose and oleic acid were added from stock solutions after autoclaving.
[c] Supplemented with leucine, uracil and lysine, each at 50 µg/mL, as required.

2.2.2 Bacterial strains and culture conditions*–*E. coli strains and culture media used in this study are described in Tables 2-7 and 2-8 respectively. Bacteria were grown at 37°C unless stated otherwise. Cultures of 5 mL or less were grown in culture tubes in a rotary shaker at ~180 rpm. Cultures greater than 5 mL were grown in flasks in a rotary shaker at 250 rpm. Culture volumes were approximately 20% of flask volumes.

Table 2-7 *E. coli* Strains

Strain	Genotype	Reference/source
DH5α	F$^-$ φ80d*lac*ZΔM15 Δ(*lac*ZYA-*arg*F)U169 *deo*R *rec*A1 *end*A1 *hsd*R17(r_K^-, m_K^+) *pho*A *sup*E44 λ$^-$ *thi*-1 *gyr*A96 *rel*A1	Gibco/BRL
TG1	K12Δ(*lac-pro*) *sup*E *thi hsd*D5/F' *tra*D36 *pro*A$^+$B$^+$ *lac*Iq *lacz*ΔM15	Amersham-Pharmacia
BRL-DE3	F$^-$ *omp*T *hsd*S$_B$(r_B^-, m_B^-) *gal dcm lon* (*srl-rec*A)*306::Tn10*(DE3)	Novagen

Table 2-8 Bacterial Culture Media

Medium	Composition	Reference
2 x YT[a]	1.6% tryptone, 1% yeast extract, 0.5% NaCl	Pharmacia GST Gene Fusion System Protocol, 2nd Edition
LB[a, b]	1% tryptone, 0.5% yeast extract, 1% NaCl (pH 7.5)	Maniatis et al., 1982
SOB	2% tryptone, 0.5% yeast extract, 10 mM NaCl, 2.5 mM KCl	Maniatis et al., 1982
SOC	SOB + (10 mM $MgCl_2$, 10 mM $MgSO_4$, 0.36% glucose)[c]	Maniatis et al., 1982

[a] Ampicillin was added to 100 µg/mL for plasmid selection, as necessary.
[b] For solid media, agar was added to 1.5%.
[c] Added after autoclaving.

2.2.3 Mating of yeast–Y. lipolytica strains were mated by the method of Gaillardin et al. (1973). Haploid strains of different mating types were grown separately at 30°C on YEPD agar overnight and then on PSM agar overnight. Strains were mixed on YM agar and incubated for four days at room temperature. Diploids were selected by restreaking yeast onto YND agar supplemented with the auxotrophic requirements of the diploid strain and selecting single colonies after three to four days of growth at 30°C.

2.3 Introduction of DNA into microorganisms

DNA was introduced into microorganisms via chemical transformation or electroporation, and transformants were identified by antibiotic selection. Electroporation was performed in microelectroporation chambers (width ~0.15 cm) using a Cell-Porator connected to a Voltage Booster (BRL).

2.3.1 Chemical transformation of E. coli–Plasmid DNA was introduced into transformation-competent DH5α cells (subcloning efficiency; Table 2.7) as described in a protocol from Gibco/BRL. Generally, 1 to 2 μL of a ligation reaction or 0.25 μg of plasmid DNA was added to 25 μL of cells. The mixture was incubated on ice for 30 min, subjected to heat shock at 37°C for 20 sec and then returned to ice for 2 min. 1 mL of LB (Table 2.8) was added, and the cells were incubated in a rotary shaker at 37°C for 45 min. Cells were spread onto LB agar plates containing ampicillin (Table 2.8) for antibiotic selection. When necessary, 75 μL of 2% X-gal in DMF was spread onto plates prior to the plating of cells. Plates were incubated at 37°C for ~16 h for colony formation.

2.3.2 Electroporation of E. coli–Electroporation was used for high efficiency transformation of DH5α cells with plasmid DNA. Cells were made electrocompetent following a method suggested by Gibco/BRL. Essentially, cells were grown overnight in 10 mL of SOB medium (Table 2.8). 0.5 mL of this overnight culture was added to 500 mL of SOB, and cells were grown to an OD_{600} (optical density at a wavelength [λ] of 600 nm) of 0.5. Cells were harvested by centrifugation at 2,600 x *g*, and washed twice with 500 mL of ice-cold 10% (v/v) glycerol. Cells were resuspended in a minimal amount of 10% (v/v) glycerol, aliquoted, frozen in a dry ice/ethanol bath and stored at -80°C. For transformation, 1 μL of a ligation reaction was added to 20 μL of cells, which were suspended between the bosses of an ice-cold electroporation chamber. Cells were subjected to electroporation with an electrical pulse of 395 V (amplified to ~2.4 kV) at a capacitance of 2 μF and a resistance of 4 kΩ. Cells were immediately added to 1 mL of SOC (Table 2.8), incubated in a rotary shaker at 37°C for 45 min and plated as described in Section 2.3.1.

2.3.3 Electroporation of Y. lipolytica–Yeast cells were made electrocompetent essentially following the method of Ausubel et al. (1989). Cells were grown overnight in 10 mL of YEPA (Table 2-6). 5 mL of culture was added to 50 mL of YEPA, and cells were grown to an OD_{600} of ~0.8. Cells were harvested by centrifugation, resuspended in TE (pH 7.5) (Table 2-4) containing 10 mM lithium acetate and incubated for 30 to 45 min at 30°C with gentle agitation. DTT was added to a final concentration of 20 mM, and the incubation was continued for an additional 15 min. Cells were harvested by centrifugation and washed successively with 50 mL each of room-temperature water, ice-cold water, and ice-cold 1 M sorbitol. Cells were resuspended in a minimal volume of 1 M sorbitol. 20 µL of cells was added to 1 µL of plasmid DNA, and the cells were suspended between the bosses of an ice-cold electroporation chamber. Cells were subjected to electroporation with an electrical pulse of 250 V (amplified to ~1.6 kV) at a capacitance of 2 µF and a resistance of 4 kΩ. Cells were immediately added to 100 µL of ice-cold 1 M sorbitol and plated onto YNA or YNO agar plates (Table 2-6). Plates were incubated at 30°C for 2 to 3 d for colony formation.

2.4 Isolation of DNA and RNA from microorganisms

2.4.1 Plasmid DNA isolation from bacteria–Single bacterial colonies were inoculated into 2 mL of LB (Table 2.8) containing ampicillin and grown overnight. Plasmid DNA was isolated from 1.5 mL of culture by the alkaline lysis method (Maniatis et al., 1982) or by using a QIAprep Miniprep Kit (Qiagen).

For the alkaline lysis method, cells were harvested by microcentrifugation and resuspended in 100 µL of 50 mM glucose, 25 mM Tris-HCl (pH 8.0), 10 mM EDTA. To denature DNA, samples were gently mixed by inversion with 200 µL of 0.2 M NaOH containing 1% SDS and incubated on ice for 5 min. To renature plasmid DNA and precipitate proteins, 150 µL of potassium acetate solution (3M K^+, 5M acetate) was added, and samples were incubated on ice for 5 min. The precipitate was pelleted by microcentrifugation for 5 min. Residual proteins were removed from the supernatant by extraction with phenol/chloroform/isoamyl alcohol (26:25:1), and DNA was precipitated by the addition of ethanol as described in Section 2.5.7. DNA was dissolved in 40 µL of TE (pH 8.0) (Table 2-4) containing 20 µg RNase A/mL.

Plasmid DNA isolation using the QIAprep Miniprep Kit was performed according to the manufacturer's instructions. This method employs essentially the same principles as the alkaline lysis method, except that after precipitation of proteins with potassium acetate solution, plasmid DNA is adsorbed onto a silica-gel membrane in a high-salt environment. Chaotropic salts are passed over the column to remove contaminating proteins, residual salts are removed, and plasmid DNA is eluted in 50 µL of 10 mM Tris-HCl (pH 7.5).

2.4.2 Chromosomal DNA isolation from yeast–Chromosomal DNA was isolated from yeast by a rapid isolation procedure (Ausubel et al., 1989). Yeast was grown overnight in 10 mL of YEPD. Cells were harvested by centrifugation and washed twice with 10 mL of water. Cells were transferred to a 1.5 mL microcentrifuge tube and washed once with breakage buffer (10 mM Tris-HCl (pH 8.0) 100 mM NaCl, 1 mM EDTA, 2% (w/v) Triton X-100, 1% SDS). Cells were mixed with 200 µL each of breakage buffer, glass beads and phenol/cholorform/isoamyl alcohol (25:24:1) and vortexed for 3 min at 4°C to simultaneously break yeast cells and separate nucleic acids from proteins. 200 µL of TE (pH 8.0) was added, tubes were vortexed briefly and the aqueous and organic layers were separated by centrifugation for 5 min. DNA was purified and precipitated from the aqueous solution as described in Section 2.5.7 and resuspended in 100 µL of TE (pH 8.0) containing 20 μg RNase A/mL. DNA was dissolved by heating at 37°C for 1 h, and DNA was quantified spectrophotometrically by measuring the optical density at a wavelength of 260 nm (OD_{260}) (1 OD_{260} = 50 μg DNA).

2.4.3 Plasmid DNA isolation from yeast–Recessive defects in genes of mutant yeast strains were rescued by complementation with a plasmid genomic library. To recover plasmids from complemented strains, the procedure described in Section 2.4.2 was used, except that yeast cells were grown in YND selective medium (Table 2-6) instead of YEPD, and isolated nucleic acids were dissolved in 20 μL of water instead of TE (pH 8.0). Isolated plasmid DNA was amplified by transformation of *E. coli* by electroporation (Section 2.3.2), followed by plasmid DNA isolation (Section 2.4.1).

2.4.4 RNA isolation from yeast–A modified version of the glass bead lysis method of Ausubel et al. (1989) was used to prepare RNA from yeast. This procedure is the same as that for DNA isolation (Section 2.4.2), except that the disruption buffer was 0.2 M Tris-HCl (pH 7.5) containing 0.5 M NaCl and 10 mM EDTA, TE (pH 8.0) was not added to samples after cell disruption and RNA was dissolved in 50 μL of water instead of TE (pH 8.0). RNA was quantified spectrophotometrically by measuring the OD_{260} (1 OD_{260} = 40 μg RNA/mL) and samples were stored at –80°C.

2.5 Standard DNA manipulations

Unless otherwise stated, reactions were in 1.5 mL microcentrifuge tubes, and microcentrifugation was done in an Eppendorf microcentrifuge at 16,000 x *g*.

2.5.1 Amplification of DNA by the polymerase chain reaction (PCR)–PCR was used either to introduce mutations or restriction endonuclease sites within a DNA molecule or to facilitate the construction of hybrid DNA molecules. PCR conditions (including primer design, cycling conditions and reaction components) were according to standard procedures (Innis and Gelfand, 1990; Saiki, 1990). Reactions were performed in 0.6 mL microcentrifuge tubes and typically contained 5 U of Taq DNA polymerase, 0.1 µg of template DNA, 20 to 100 pmol of each primer, 50 mM each of dATP, dCTP, dGTP and dTTP in 100 µL of reaction buffer. Alternatively, Ready-To-GO PCR beads were used according to the specifications of the manufacturer. Reactions were cycled in either a PHC-2 thermocycler (Techne) connected to a refrigerated circulating water bath (Neslab) or a Robocycler 40 (Stratagene) with a Hot Top attachment.

2.5.2 Restriction endonuclease digestion–DNA was digested according to the restriction enzyme manufacturers' instructions. For diagnostic and preparative digests, 0.5 to 1 µg and 2 to 3 µg of DNA, respectively, were digested respectively for 3 to16 h. Double digests were done according to the instructions supplied by NEB.

2.5.3 Construction of blunt-ended DNA fragments–The ends of DNA fragments with 5' overhangs were made blunt using the Klenow fragment of *E. coli* DNA polymerase I according to the instructions of the manufacturer. Reactions contained 2 to 3 µg of DNA, 5 U of enzyme, 33 µM of each dNTP and 1 x digestion buffer or 1 x DNA pol I buffer.

Reactions were incubated for 15 min at room temperature, and DNA fragments were analyzed by agarose gel electrophoresis (Section 2.5.5).

2.5.4 Dephosphorylation and phosphorylation of 5' ends–Prior to ligation, the 5' ends of linearized plasmid DNA molecules were usually dephosphorylated to prevent intramolecular ligations. Essentially, after plasmid digestion, reactions were mixed with 5 U of CIAP and incubated for 15 min at 37°C. Also prior to ligation, the 5' termini of DNA molecules amplified by PCR were phosphorylated. Essentially, reactions were mixed with 10 U of T4 polynucleotide kinase and ATP and PNK buffer (to 10 mM and 1 x respectively) and incubated at 37°C for 1 h. Dephosphorylation and phosphorylation reactions were terminated by agarose gel electrophoresis of the DNA fragments (Section 2.5.5).

2.5.5 Separation of DNA fragments by agarose gel electrophoresis– DNA fragments in solution were added to 0.2 volume of 6 x sample dye (30% glycerol (w/v), 0.25% bromophenol blue, 0.25% xylene cyanole) (Maniatis et al., 1982) and separated on agarose gels in 1 x TBE containing 0.5 µg ethidium bromide/mL. Fragments 100 bp in length or smaller were separated on 3% agarose gels consisting of 0.5% SeaKem Genetic Technology Grade (GTG) agarose and 2.5% NuSieve GTG agarose. Large DNA fragments were separated on 0.7 to 1.5% agarose gels. DNA was visualized using an Ultra-Violet Transilluminator Model 3-3006 (Photodyne).

2.5.6 Purification of DNA fragments from agarose gels–DNA fragments were isolated from agarose gels using a QIAQuick Gel Extraction Kit (Qiagen) according to the manufacturer's instructions. Essentially, the gel fragment containing the DNA of interest is dissolved, the DNA is adsorbed to a silica-gel surface, contaminants are removed by washing and the DNA is eluted in 30 µL of 10 mM Tris-HCl (pH 8.5).

Alternatively, DNA was isolated from agarose gels by electroelution using a unidirectional eluter (Model UEA, International Biotechnologies) according to the specifications of the manufacturer. Essentially, the eluter was filled with 0.5 x TBE, a gel fragment containing the DNA of interest was placed in the slot on the platform, and 80 µL of 7.5 M ammonium acetate containing 0.25% bromophenol blue was placed in the V-channel collection tube. DNA was transferred from the gel fragment to the salt solution by electrophoresis at 100 V for 15 to 45 min. 350 µL of the salt/DNA mixture was removed from the V-channel, the DNA was precipitated by the addition of ethanol and linear polyacrylamide (Section 2.5.7), and dissolved in 10 µL of water.

2.5.7 Purification and concentration of DNA from solution–The QIAquick PCR Purification Kit was used according to the specifications of Qiagen to concentrate DNA and remove contaminants (small olignucleotides, salt, dyes, ethidium bromide, triphosphates and protein). Essentially, DNA (100 bp to 10 kbp) is adsorbed to a silica-gel surface, contaminants are removed by washing, and DNA is eluted in 30 µL of Tris-HCl (pH 8.5).

Alternatively, DNA was purified by extraction against phenol/chloroform/isoamyl alcohol and precipitation with ethanol (Ausubel et al., 1989). Essentially, DNA in 0.1 to

0.4 mL of aqueous solution was vortexed with an equal volume of phenol/cholorform/isoamyl alcohol (25:24:1) for 10 sec, and the organic and aqueous phases were separated by microcentrifugation for 1 min. If a white precipitate was observed at the interface of the phases, the extraction was repeated. The aqueous layer was then extracted against an equal volume of choloform/isoamyl alcohol (24:1), and DNA was precipitated by adding 0.1 volume of 3 M NaCl and 2 to 2.5 volumes (calculated after salt addition) of ice-cold absolute ethanol and incubating at –20°C for 30 min. The precipitate was pelleted by microcentrifugation for 15 min, and salts were removed by washing the pellet in 70% ethanol. The pellet was dried in a rotary vacuum desicator and dissolved in a minimal volume of water or TE (pH 8.0). If the DNA solution contained a high concentration of salt (between 0.3 and 0.5 M), no additional salt was added to the precipitation reaction. Also, if the DNA concentration was very low, 5 µL of 0.25% linear polyacrylamide (Gaillard and Strauss, 1990) was added as a carrier molecule to the precipitation reaction.

2.5.8 Construction of hybrid DNA molecules by ligation**–**Circular hybrid DNA molecules capable of autonomous replication in bacteria were constructed using T4 DNA ligase. This enzyme catalyzes the formation of phosphodiester bonds between neighboring 3'-hydroxyl and 5'-phosphate groups in double-stranded DNA. DNA fragments to be ligated were usually obtained by restriction enzyme digestion (Section 2.5.2). Prior to ligation, the 5' ends of the plasmid DNA molecules were dephosphorylated to prevent intramolecular ligation and, if necessary, the 5' ends of the insert DNA fragments were phosphorylated (Section 2.5.4). Then, if necessary, DNA fragments were made blunt by filling in 5' overhangs (Section 2.5.3). DNA fragments to be ligated were purified by agarose gel electrophoresis (Sections 2.5.5 and 2.5.6), combined and treated with DNA ligase in the presence of 1 mM ATP and ligase buffer according to the instructions of the manufacturer. The molar ratio of plasmid to insert DNA molecules was typically between 1:3 and 1:5, and reactions were incubated at 16°C for 16 h for the ligation of blunt fragments or at room temperature for 3 to 16 h for all other ligations. 1 to 2 µL of ligation reaction was introduced into *E. coli* (Sections 2.3.1 and 2.3.2). Transformants were identified by antibiotic selection, and positives were identified by restriction digestion.

2.5.9 DNA Mutagenesis–Sequential PCR (Ausubel et al., 1989; Fig. 2-1) was used to introduce point mutations or endonuclease restriction sited in DNA. DNA fragments containing the mutation were excised by restriction endonuclease digestion and ligated into appropriate plasmids. Positives were identified by DNA sequencing.

2.6 DNA and RNA analysis

2.6.1 DNA sequencing–DNA sequencing was performed by the dideoxynucleotide chain-termination method (Sanger et al., 1977) using either fluorescently or radioactively labelled DNA.

To sequence radioactively labelled DNA, double-stranded plasmid templates were denatured by the method of Zhang et al. (1988). Essentially, 3 µg of plasmid DNA was denatured in 18 µL of 0.5 M NaOH containing 0.5 mM EDTA for 5 min at room temperature. Reactions were neutralized by adding ammonium acetate to 0.5 M in a final volume of 20 μL, and DNA was precipitated by addition of ethanol as described in Section 2.5.7. Sequencing reactions were performed using Sequenase DNA Sequencing Kits (Version 1.0 and 2.0) (USB) according to the manufacturer's instructions and α-[^{32}P]dATP as the label. Reaction products were separated on 5% ExplorER or 5% Long Ranger denaturing acrylamide gels. Gels were dried and exposed to BioMax or X-Omat AR film for 2 to 24 h.

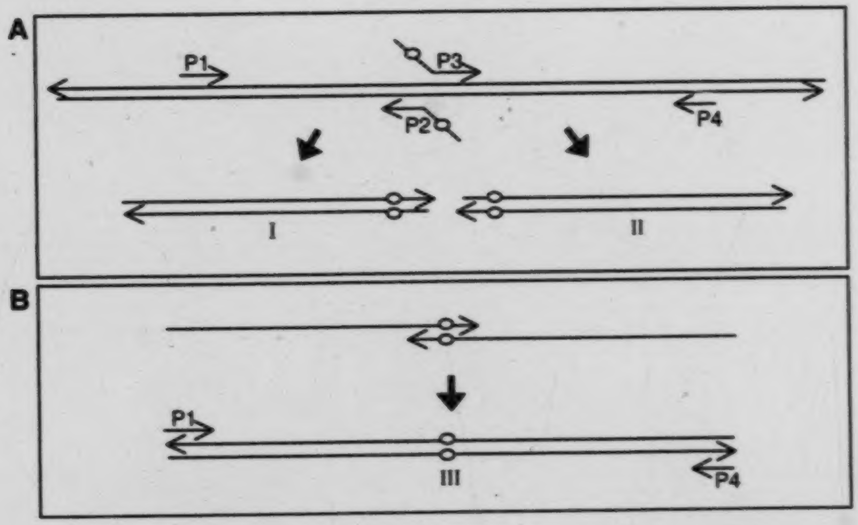

Figure 2-1. Mutagenesis by sequential PCR. Single-stranded DNA molecules are represented by *arrows* (5' is *tail* and 3' is *arrow head*). Mutations are indicated by *open circles*. (*A*) The sequences flanking the target site for mutagenesis were amplified from genomic DNA using oligonucleotides P1 and P2 for product I and P3 and P4 for product II. (*B*) Products I and II were used as templates for a second round of PCR. As P1 and P2 have complementary 5' ends and both contain the engineered mutation, single-stranded molecules of I and II anneal and extend by mutually primed synthesis to generate product III. Oligonucleotides P1 and P4 are added to this reaction to amplify product III.

To sequence fluorescently labelled DNA, sequencing reactions were performed on plasmid DNA using the BigDye Terminator Cycle Sequencing Ready Reaction Kit (ABI Prism) following the 0.5 x reaction protocol. Thermal cycle sequencing was performed in a RoboCycler 40 equipped with a Hot Top. Reactions consisted of 2 min denaturation at 96°C followed by 25 cycles of 96°C, 50°C and 60°C for 46 sec, 51 sec and 250 sec, respectively. Fluorescently labelled DNA was precipitated and analyzed by capillary electrophoresis in a 310 Genetic Analyzer (ABI Prism).

2.6.2 ***Southern blot analysis***–5 to 10 µg of yeast genomic DNA was digested with restriction endonucleases overnight, and fragments were separated on a horizontal agarose gel. The DNA was nicked by placing the gel on an ultra-violet light transilluminator for 5 min. DNA was denatured in situ by incubation of the gel in 1.5 M NaCl, 0.5 M NaOH for 30 min with shaking. The gel was then neutralized by incubation for 30 min in 3 M NaCl, 0.5 M Tris-HCl (pH 8.0) with shaking. DNA was transferred from the gel to nitrocellulose by capillary action in 5 x SSC overnight. The nitrocellulose was rinsed briefly in 5 x SSC, and exposed to 120,000 µJ/cm^2 of light in a UV Stratalinker 1800 (λ = 254 nm) (Stratagene) to immobilize the DNA. Blots were hybridized as described in Section 2.6.5.

2.6.3 ***Colony lifts***–This procedure was used to screen bacterially amplified plasmid DNA by hybridization to DNA probes and was done essentially according to method of Hanahan and Meselson (1980). Bacterial colonies containing plasmid DNA were lifted from agar plates onto nitrocellulose disks (82 mm) (Schleicher and Schuell). To disrupt the cells and denature DNA, disks were place colony side up in 1 mL puddles of 0.5 M NaOH (repeated once). The disks were then neutralized in 1 mL puddles of 0.5 M Tris-HCl (pH 7.5) (repeated once) and transferred to 1 mL puddles of 0.5 M Tris-HCl (pH 7.5) containing 1.5 M NaCl (repeated once). Bacterial debris was removed by washing disks briefly in 2 x SSC, and DNA was immobilized as described in Section 2.6.2 and hybridized as described in Section 2.6.5.

2.6.4 Northern blot analysis–The method of Ausubel et al. (1989) was used to separate RNA molecules and transfer them to nitrocellulose for subsequent hybridization analysis. Essentially, samples containing 5 to10 μg of total yeast RNA, 18% (v/v) formamide and 18% (v/v) formaldehyde in a final volume of 20 μL containing 2 x borate buffer (Table 2-4) were denatured by heating at 65°C for 5 min and then cooled on ice. 4 μL of 6 x DNA sample dye (Section 2.5.5) was added to samples, and RNA was separated by agarose gel electrophoresis in 1 x borate buffer (Table 2-4) containing 3.3% (v/v) formaldehyde as a denaturant. RNA was visualized by staining a portion of the gel in 1 x TBE containing 0.5 μg ethidium bromide/mL. The unstained gel was washed in water for 30 min and then in 10 x SSC for 45 min. RNA was transferred to nitrocellulose by capillary action in 20 x SSC overnight. RNA was immobilized on the nitrocellulose as described in Section 2.6.2 and hybridized with DNA probes as described in Section 2.6.5.

2.6.5 Labelling and hybridization of DNA–This technique was used to identify specific DNA and RNA molecules immobilized on nitrocellulose by Southern blotting, Northern blotting or colony lifts through their sequence complementary to radiolabelled or chemiluminescent DNA probes.

Probes were radiolabelled using a Random Primed DNA Labelling Kit (Roche) according to the manufacturer's instructions. Essentially, DNA fragments between 0.5 and 1.5 kbp in length were prepared by restriction enzyme digestion or by PCR amplification, purified from agarose gel and denatured by boiling. 10 ng of DNA was mixed with 50 μCi of α-[^{32}P]dATP (3,000 Ci/mmol), 1 U of the Klenow fragment of DNA polymerase I, 25 μM each of dCTP, dGTP, dTTP and reaction buffer containing random hexamers in a final volume of 20 μL and incubated at 37°C for 30 min. For colony lift analysis, 20 pmol of two specific primers and 1 x Klenow buffer (NEB) were substituted for reaction buffer for the generation of probes of greater specific activity. Labelled probes were separated from unincorporated nucleotides by chromatography on Sephadex-G50 spin columns (Maniatis et al., 1982) or TE Midi SELECT-D G50 columns. Radionucleotide incorporation was measured by liquid scintillation counting in a RackBeta 1209 scintillation counter (LKB). Nitrocellulose was incubated in hybridization buffer (1.25 x SSC, 0.16 x Denhardt's solution (Table 2-4), 4 μg sheared salmon testes DNA/mL, 0.01% SDS, 20 mM sodium phosphate (pH 7.0)) in heat-sealed pouches for 3 h at 65°C to reduce nonspecific hybridization. The buffer was discarded, and blots were incubated in hybridization buffer containing 5 to 10 x 10^{6} cpm of heat-denatured radiolabelled probe/mL and 30% (v/v) deionized formamide overnight at 42°C. Blots were washed four times for 15 min each at 55°C in 1 x SSC containing 0.1% SDS to remove unbound or weakly binding probe and exposed to X-Omat AR film (Kodak) for 1 to 5 d with an intensifying screen at –80°C.

The Enhanced Chemiluminescence (ECL) Direct Nucleic Acid Labelling and Detection System (Amersham/Pharmacia) was used according to the manufacturer's instructions to label and hybridize a chemiluminescent probe. This kit covalently links denatured DNA to positively charged complexes of peroxidase that are detected by ECL technology.

2.7 Protein analysis and manipulation

2.7.1 Precipitation of protein–To precipitate proteins from solution, trichloroacetic acid (TCA) was added to a final concentration of 10% (w/v), and samples were incubated on ice for 30 min. Precipitates were collected by centrifugation at 16,000 *g* for 30 min at 4°C. The resultant pellet was washed twice with 1 mL of 80% (v/v) ice-cold acetone and dried in a rotary vacuum desicator.

2.7.2 Determination of protein concentration–The concentration of protein in solution was determined by the method of Bradford (1976) using the Bio-Rad protein assay dye reagent. To create a standard curve, 1 mL of reagent was added to each of ten 100 µL aliquots of water containing from 0 to 20 µg of BSA. Samples were vortexed briefly and incubated at room temperature for 10 min. Absorbance at 595 nm was measured for each sample and plotted against protein concentration. Dilutions of samples to be assayed were prepared and measured in the same way as for standards and protein concentration was estimated from samples with absorbances in the linear range of the curve of standards.

To quantify proteins detected by immunoblotting, densitometry was performed with an Ultroscan XL laser densitometer (LKB). Quantification of densitometric signals was performed in the range in which the antigen concentration was linearly proportional to the densitometric signal.

2.7.3 Electrophoretic separation of proteins–Proteins were separated by sodium dodecyl sulphate-polyacrylamide gel electrophoresis (SDS-PAGE) by the method of Laemmli (1970) as described by Ausubel et al. (1989). Protein solutions were added to sample buffer to yield a final buffer concentration of 62.5 mM Tris-HCl (pH 6.8), 2% SDS, 10% sucrose, 10 mM DTT and 0.001% bromophenol blue. Samples were denatured by boiling for 5 min. Proteins were separated by electrophoresis on discontinuous slab gels. Stacking gels contained 3% acrylamide/*N*,*N'*-methylene-bis-acrylamide (30:0.8), 60 mM Tris-HCl (pH 6.8), 0.1% SDS, 0.1% (v/v) TEMED, 0.1% ammonium persulphate. Resolving gels contained between 7.5 and 15% acrylamide/*N*,N'-methylene-bis-acrylamide (30:0.8), 370 mM Tris-HCl (pH 8.8), 0.1% SDS, 0.1% (v/v) TEMED, 0.042% ammonium persulphate. Electrophoresis was in SDS-PAGE running buffer (50 mM Tris-HCl (pH 8.8), 0.4 M glycine, 0.1% SDS).

2.7.4 Detection of proteins by gel staining–Proteins in polyacrylamide gels were visualized by staining with 0.1% Coomassie Brilliant Blue R-250, 10% (v/v) acetic acid, 35% (v/v) methanol for 1 h. Unbound dye was removed by incubating gels in 10% (v/v) acetic acid, 35% (v/v) methanol. Gels were dried on a drier (Model 583, Bio-Rad).

2.7.5 Detection of proteins by immunoblotting–Proteins separated by SDS-PAGE were transferred to nitrocellulose for 3 h at 400 mA on ice or for 16 h at 100 mA at room temperature in transfer buffer (20 mM Tris base, 150 mM glycine, 20% (v/v) methanol) (Towbin et al., 1979; Burnette, 1981) in a Trans-Blot tank transfer system with plate electrodes (Bio-Rad). Proteins bound to nitrocellulose were visualized by staining with 0.1% Ponceau S in 1% TCA for 2 to 3 min and destaining in water. Specific proteins were detected on the nitrocellulose using an ECL Detection Kit (Amersham-Pharmacia) according to the manufacturer's instructions. In this system, proteins are indirectly labelled with horseradish peroxidase (HRP) and detected using ECL technology. To prevent non-specific binding of antibodies, blots were incubated with gentle agitation in blocking buffer (TBST (Table 2-4) containing either 1% skim milk powder or 1% BSA) for 1 h. Blots were then incubated for 1 h with primary antiserum in blocking buffer and then with the appropriate HRP-labelled secondary antibody in TBST for 30 min. After each antibody incubation, unbound antibodies were removed by washing blots three times for 10 min each in TBST. Antigen-antibody complexes were detected by incubating the blot with a 1:1 mixture of the two detection reagents and exposing the blot to X-Omat X-K1 film.

Blots could be reprobed using a Re-Blot Western blot recycling kit (Chemicon). Blots were rinsed with water, incubated with antibody stripping solution for 10 to 15 min, and washed three times in TBST for 5 min each. Proteins were then detected as described above.

2.7.6 Protein sequencing–Sequences of peptides derived from p100 (Section 4.4) were obtained by Micromass (Manchester, UK) as described below. A fragment of gel containing p100 was excised from a polyacrylamide gel stained with Coomassie Brilliant Blue R-250, cut into ~1 mm^3 pieces and digested in the gel with trypsin according to the procedure of Wilm et al. (1996). The gel fragment was destained by washing with 100 mM ammonium bicarbonate and acetonitrile. The peptide was then reduced with DTT, alkylated with iodoacetamide, washed and dehydrated. Tryptic fragments of p100 were obtained by digesting the peptide overnight in 10 • g trypsin/mL at room temperature. The tryptic peptides were eluted with 50 mM ammonium bicarbonate and acetonitrile, and reduced to dryness in a vacuum centrifuge. The tryptic peptides were solubilized in 0.2% formic acid and analyzed by capillary liquid chromatography tandem mass spectrometry (LC-MS/MS) using a quadrupole time-of-flight (Q-TOF) mass spectrometer. The MS/MS data for each peptide was processed using Max Ent 3 to produce an MS/MS spectrum on a singly charged scale with no isotope present. Amino acid sequences were then determined using MassSeq (Micromass), an automated Bayesian sequencing algorithm, and compared to protein sequences deposited in the National Centre for Biotechnology Information (NCBI) Protein Database (Section 2.17).

2.8 Subcellular fractionation of yeast

2.8.1 Preparation of whole cell lysates–Yeast lysates were prepared by glass bead disruption (adapted from Needleman and Tzagoloff, 1975). 200 μL of cells was pelleted from a freshly grown culture by centrifugation at 200 x g, washed three times with 10 mL of water and transferred to a 1.5 mL microcentrifuge tube. Cells were washed with 1 mL ice-cold disruption buffer (25 mM Tris-HCl (pH 7.5), 0.1 mM EDTA, 100 mM KCl, 1 mM DTT, 0.1 % (v/v) Triton X-100, 10% (w/v) glycerol) (adapted from Eitzen, 1997) containing 1 x PIN cocktail (Table 2-4) and resuspended in 200 µL of disruption buffer. A volume of glass beads was added to reach the bottom of the meniscus, and the mixture was vortexed at 4°C for 5 min to disrupt the cells. 100 µL of disruption buffer was added, and glass beads were pelleted by centrifugation for 20 sec. The lysate was recovered and clarified by microcentrifugation at 16,000 x *g* for 20 min at 4°C.

2.8.2 Subcellular fractionation–Yeast cells were fractionated into an organelle-enriched pellet (20KgP) and a cytosol-enriched supernatant (20KgS) essentially by the method of Aitchison et al. (1991) as described below. All solutions were ice-cold, and all centrifugations were performed at 4°C unless otherwise specified. Cells were harvested by centrifugation at 800 x *g* and washed three times with water at room temperature. Cells were resuspended in room temperature spheroplast solution (0.5 M KCl, 5 mM MOPS (pH 7.2), 10 mM sodium sulphite, 0.25 mg Zymolyase 100T/mL) at a concentration of 4 mL per g of wet cells and incubated with gentle agitation at 30°C for 30 min to convert cells to spheroplasts. Spheroplasts were harvested by centrifugation at 2,300 x *g* for 8 min at 4°C, gently resuspended in disruption buffer (5 mM MES (pH 5.5), 1 M sorbitol, 1 mM KCl, 0.5 mM EDTA, PINS (Table 2-4)) at a concentration of 3 mL per g of wet cells and transferred to a homogenization mortar. Spheroplasts were disrupted by ten strokes of a Teflon pestle driven at 1,000 rpm by a stirrer motor (Model 4376-00, Cole-Parmer). Cell debris, unbroken cells and nuclei were pelleted by centrifugation at 1,000 x *g* for 10 min. The postnuclear supernatant (PNS) was fractionated by centrifugation at 20,000 x *g* into a pellet (20KgP) enriched for heavy organelles (mostly peroxisomes and mitochondria) and a supernatant (20KgS) enriched for cytosol. For some experiments, the 20KgS fraction was subfractionated by the method of Titorenko et al. (1998). Essentially, the 20KgS was separated by centrifugation at 200,000 x *g* for 1 h into a pellet (200KgP) enriched for high-speed pelletable organelles and a supernatant (200KgS) highly enriched for cytosol .

2.8.3 Isolation of organelles by isopycnic centrifugation–Organelles of the 20KgP were separated by isopycnic centrifugation essentially by the method of Nuttley et al. (1990). The 20KgP fraction was resuspended in homogenization buffer, and a volume containing 3 mg of protein was loaded on top of a discontinuous sucrose gradient (4 mL of 25%, 7 mL of 35%, 14 mL of 42% and 7 mL of 53% (w/w) sucrose in 5 mM MES (pH 5.5)). Organelles were separated by centrifugation at 100,000 x *g* for 80 min at 4°C in a Beckman VTi50 rotor using a Beckman XL-70 Ultracentrifuge set at an acceleration rate of 2 and a deceleration rate of 9). Eighteen fractions of 2 mL each were collected from the bottom of the gradient.

2.8.4 Extraction and subfractionation of peroxisomes–Subfractionation and extraction of peroxisomes were performed by the methods of Goodman et al. (1990) and Fujiki et al. (1982) with modifications. For the analysis described in Chapter 3, peroxisomes purified by isopycnic density gradient centrifugation (~30 µg of protein) were lysed by incubation with ten volumes of ice-cold Ti8 buffer (10 mM Tris-HCl (pH 8.0), 5 mM

EDTA, 1 mM PMSF, 1 μg of leupeptin/mL, 1 μg of pepstatin/mL, 1 μg of aprotinin/mL) for 15 min with occasional agitation. Lysed peroxisomes were then separated by centrifugation at 200,000 x *g* for 1 h at 4°C into a membrane fraction (Ti8P) and a soluble fraction (Ti8S). The Ti8P was resuspended in ice-cold Ti8 buffer to a final protein concentration of 0.5 mg/mL. Half of the resuspension was incubated with 0.1 M Na_2CO_3 (pH 11.5) for 45 min with occasional gentle agitation and then separated by centrifugation at 200,000 x *g* for 1 h at 4°C into a supernatant (CO_3S) enriched for soluble proteins and a pellet (CO_3P) enriched for membrane proteins. For the analysis described in Chapter 4, the Ti8 extraction was the same as described above, except that the starting material was the 20KgP fraction (45 μg of protein), and incubation with Ti8 buffer was for 30 min.

2.8.5 Protease protection–Protease protection analysis was performed according to the method of Szilard et al. (1995) with modifications. For the analysis described in Chapter 3, peroxisomes (13 μg of protein) purified by sucrose density gradient centrifugation were incubated with increasing amounts of trypsin in the absence or presence of 0.5% (w/v) Triton X-100 on ice for 40 min. Reactions were terminated by TCA precipitation of proteins (Section 2.7.1). For the analysis described in Chapter 4, the same method was used except that the starting material was the 20KgP fraction (isolated in the absence of protease inhibitors), and reactions contained 60 μg of protein and 0.1% (w/v) Triton X-100.

2.9 Assays

2.9.1 Catalase–The *in vitro* measurement of the activity of the peroxisomal enzyme catalase was performed essentially according to the method of Lück (1963) by which the consumption of H_2O_2 by catalase is measured spectrophotometrically. Samples were made to a final concentration of 50 mM potassium phosphate (pH 7.5), 0.015% (w/v) H_2O_2 in 1 mL. The decrease in absorbance at 240 nm was measured for 120 sec at 10 sec intervals.

2.9.2 Fumarase–The *in vitro* measurement of the activity of the mitochondrial enzyme fumarase was performed essentially according to the method of Tolbert (1974) by which the conversion of the substrate L-malate to fumarate is measured spectrophotometrically. Samples were made to a final concentration of 50 mM potassium phosphate (pH 7.5), 15 mM L-malic acid in 1 mL. The increase in absorbance at 240 nm was measured for 60 sec at 5 sec intervals.

2.9.3 Alkaline phosphatase–The *in vitro* measurement of the activity of the vacuolar enzyme alkaline phosphatase was performed according to the method of Thieringer et al. (1991) by which the production of *p*-nitrophenol by the dephosphorylation of *p*-nitrophenyl phosphate is measured spectrophotometrically. Samples were made to 10 mM $MgCl_2$, 0.1% (w/v) Triton X-100, 6 mM *p*-nitrophenyl phosphate in a final volume of 0.5 mL and incubated for 2 to 3 h at 30°C. Reactions were stopped by adding an equal volume of 0.5 M glycine-Na_2CO_3 (pH 10) and the production of *p*-nitrophenol was measured at 400 nm. This assay was performed by Rachel K. Szilard.

2.10 Coimmunoprecipitation–Coimmunoprecipitation was performed by immunoaffinity chromatography using protein A-Sepharose CL-4B (Sigma). All steps were performed at 4°C unless otherwise specified. YPBO-grown *PEX8-HA*^{c} cells were collected by centrifugation, washed three times with water and once with RX buffer (20 mM HEPES-KOH (pH 6.8) 150 mM potassium acetate, 2 mM magnesium acetate, 0.5% (w/v) Triton-X 100, 0.1% (w/v) casaminoacids, PINS (Table 2-4)). Cells were resuspended in RX buffer and lysed using glass beads. The total cell lysate was clarified by centrifugation at 100,000 x *g* for 15 min at 4°C, diluted to a protein concentration of 10 mg/mL with RX buffer and divided into 500 µl aliquots. 4.5 µl of immune serum or 18 µl of preimmune serum (adjusted to obtain equal amounts of IgG molecules as judged by visualization of the heavy chain of IgG on immunoblots), was added to each of two aliquots and samples were tumbled end over end for 30 min. Protein A-Sepharose, pre-blocked in RX buffer containing 8% BSA for 1 hr, was pelleted by centrifugation and resuspended in RX buffer to a final concentration of 20% (v/v). 50 µl of the Protein A-Sepharose solution was added to each sample and the samples were tumbled end over end for 40 min. Antibody complexes were pelleted at 1,000 x *g* for 5 min and resuspended in 0.5 mL RX buffer. Samples were then applied to spin filters (filter frit is made of low-protein binding material that retains resin but allows contaminants to pass through) (CytoSignal), washed three times with RX buffer and eluted in SDS sample buffer at room temperature as instructed by the manufacturer. 20% of each eluate was separated by SDS-PAGE, along with 10 μg of protein of the cell lysate, and immunoblotted.

2.11 Microscopy

2.11.1 Immunofluorescence microscopy–Indirect immunofluorescence microscopy of yeast cells was performed according to the method of Pringle et al. (1991). Essentially, cells at the log phase of growth were fixed by adding formaldehyde to the culture medium to a concentration of 3.7% and incubating for 2 or 30 min, as indicated. Cells were collected by centrifugation and converted to spheroplasts by incubating with spheroplast solution (100 mM potassium phosphate (pH 7.5), 1.2 M sorbitol, 40 μg Zymolyase-100T/mL, 28 mM 2-mercaptoethanol) (1 mL per 100 μL of wet cells) for 30 min at 30°C with gentle rotation. Spheroplasts were spotted onto glass slides precoated with poly L-lysine and air-dried to completion. Slides were immersed in methanol for 6 min, then in acetone for 30 sec (each chilled to -20°C) to permeabilize the spheroplasts, and the slides were then air-dried to completion. The next three steps describing the immunodetection of specific proteins were performed in a dark humid box to prevent evaporation of solutions. Spheroplasts were incubated for 30 min in a drop of blocking solution (TBST containing 1% skim milk powder). Spheroplasts were next incubated with primary antiserum diluted in blocking solution for 1 h. Lastly, spheroplasts were incubated with secondary antibody conjugated to fluorescein or rhodamine diluted in blocking solution for 30 min. After the second and third steps, spheroplasts were washed ten times with TBST. The last wash was replaced by 10 μL of mounting medium (PBS containing 4% *n*-propyl gallate, 75% (w/v) glycerol), coverslips were placed over the cells, and the edges of the coverslips were sealed with nail polish. Cells were viewed on an Olympus BX50 microscope equipped for fluorescence. Images were captured using a Spot Cam digital fluorescence camera (Spot Diagnostic Instruments).

2.11.2 Electron microscopy–Cells were prepared for electron microscopy by Honey Chan. Whole cells were fixed in 1.5% $KMnO_4$ for 20 min at room temperature, dehydrated by successive incubations in increasing concentrations of ethanol, and embedded in TAAB 812 resin. Ultra-thin sections were cut using an Ultra-Cut E Microtome (Reichert-Jung) and examined in a Phillips 410 electron microscope.

2.11.3 Morphometric analysis of peroxisomes–Electron micrographs were enlarged to 16,620 × magnification on photographic paper. Images of cells were cut out and weighed, and the total cell area was calculated using standards (weights of pieces of photographic paper of known area). To quantify peroxisome size, the average peroxisome area was calculated. Essentially, peroxisome profiles were cut out and weighed, and the total peroxisome area was calculated and divided by the total number of peroxisomes counted. To quantify peroxisome number, the numerical density of peroxisomes (number of peroxisomes per μm^3 of cell volume) was calculated by the method of Weibe and Bolender (1973) for spherical organelles, as follows. First, the total number of peroxisome profiles was counted and reported as the number of peroxisomes per cell area assayed (N_A). Next, the peroxisome volume density (V_V) was calculated for each strain (total peroxisome area/total cell area assayed). Using the values V_V and N_A, the numerical density of peroxisomes was determined.

2.12 Isolation and sequencing of genes

2.12.1 Isolation and sequencing of PEX8–The *PEX8* gene was isolated from a library of *Y. lipolytica* genomic DNA in the autonomously replicating *E. coli* shuttle vector pINA445 by functional complementation of the *pex8-1* mutant strain by the method of Nuttley et al. (1993). The *pex8-1* strain was transformed with the library by electroporation (Section 2.3.3), and colonies that demonstrated both leucine prototrophy and reestablished growth on oleic acid (YNO agar) were selected. Complementing plasmids were recovered by transformation of *E. coli*, and one plasmid, pLD50, was chosen for further study.

Overlapping restriction endonuclease fragments of the *PEX8* gene were isolated from the complementing vector pLD50 and ligated into the vector pGEM5Zf(+) or pGEM7Zf(+). Both strands of the minimal complementing gene fragment were sequenced using radiolabelled DNA (Section 2.6.1). The sequence of the encoded protein, *Yl*Pex8p, was deduced from the gene nucleotide sequence and compared to protein sequences deposited in the NCBI Protein Database (Section 2.17).

2.12.2 Isolation and sequencing of the pex8-1 allele of PEX8–The *pex8-1* allele was isolated by DNA hybridization of colony lifts (Sections 2.6.3 and 2.6.5). To construct a library for colony hybridization, *Y. lipolytica* genomic DNA of the *pex8-1* strain was digested with *Hin*dIII and fractionated by size by agarose gel electrophoresis. DNA fragments between 5.5 and 6.5 kbp (the expected size range of the *pex8-1*-containing fragment) were ligated into *Hin*dIII-digested pGEM7zf(+). Colonies were probed with a 650-bp fragment of the *PEX8* gene that was excised from pLD50 by *Xho*I, gel purified and radiolabelled with α-[^{32}P]-dATP. One plasmid, pG7pex8-1, was isolated from a positively hybridizing colony. Both strands of the ~5-kbp insert were sequenced (Section 2.6.1), and the sequence was compared to that of *PEX8*.

2.12.3 Isolation and sequencing of MFE2–A fragment of the *MFE2* gene was isolated serendipitously by Gary A. Eitzen and Trevor W. Brown. Essentially, *P16KO-6A*, a *Y. lipolytica* strain containing a *PEX16::LEU2* disruption construct spuriously integrated into its genome, was selected on the basis of its inability to grow using oleic acid as a carbon source (performed by Gary A. Eitzen). A DNA fragment containing the disruption construct and flanking genomic DNA was recovered from this strain by DNA hybridization of colony lifts using a fragment of the *LEU2* gene as a probe and ligated into pGEM7Zf(+) to construct the plasmid, p6AD. By sequencing, a 1,146-bp fragment of the *MFE2* gene (nucleotides 1,090 to 2,235 where +1 is the 'A' nucleotide of the initiation codon) was identified within the disruption construct (performed by Trevor W. Brown).

To isolate the entire *MFE2* gene, *Y. lipolytica* genomic DNA of the wild-type strain *E122* was digested with *Eco*RI and fractionated by size. By PCR amplification of DNA fragments within each fraction using oligonucleotides 731 and 742 (Table 2-3), it was determined that fragments of DNA containing the *MFE2* gene were between 6 and 8 kbp in size. *Eco*RI-digested genomic DNA fragments of this size range were ligated into pGEM7Zf(+) to construct a library for colony hybridization. A fragment of the *MFE2* gene amplified by PCR from p6AD using oligonucleotides 731 and 742 was radiolabelled with α-[^{32}P]-dATP and used to probe this library. One plasmid, pG7MFE2, was isolated from a positively hybridizing colony, and both strands of the ~6.8-kbp insert were sequenced. The sequence of the MFE2 protein was deduced from the gene nucleotide sequence and compared to protein sequences of the NCBI Protein Database (Section 2.17).

To make an *MFE2* expression plasmid, pG7MFE2 was digested with *Sph*I, and the fragment containing the open reading frame (ORF) of the *MFE2* gene, as well as 1,066 bp and 426 bp of sequence upstream and downstream of the ORF, respectively, was ligated into the *E. coli/Y. lipolytica* shuttle vector pINA445 cut with *Sph*I to make the plasmid pMFE2 encoding MFE2.

2.12.4 Isolation and sequencing of THFS–An approximately 0.6-kbp fragment of *THFS*, the gene encoding p100, was amplified by PCR of genomic DNA isolated from the *Y. lipolytica* wild-type strain *E122* using the degenerate oligonucleotides 1001 and 1002 (Table 2-3). These oligonucleotides were designed from peptide sequences 2 and 4 (Fig. 4-6). The PCR product was used to isolate the entire *THFS* gene by colony hybridization, as described below. Genomic DNA was isolated from the *E122* strain, digested with *Eco*RI and fractionated by size. By PCR amplification of DNA fragments in each fraction using oligonucleotides 1001 and 1002 (Table 2-3), it was determined that the *THFS*-containing fragment was between 5 and 6 kbp in size. *Eco*RI-digested genomic DNA of this size range was ligated into pGEM7Zf(+), and transformants were probed by colony hybridization. The probe, the PCR-amplified 0.6 kbp fragment of the *THFS* gene, was radiolabelled using the Random Primed DNA Labelling Kit according to the manufacturer's instructions except that oligonucleotides 1001 and 1002 were used as primers instead of random hexamers. One plasmid, pG7THFS, was isolated from a positively hybridizing colony, and both strands of the approximately 5.5-kbp genomic insert were sequenced. The sequences of the encoded protein, C_1-THFS, were deduced from the gene nucleotide sequence and compared to protein sequences deposited in the NCBI Protein Database (Section 2.17).

2.13 Construction of plasmids for gene expression

2.13.1 Construction of a plasmid encoding epitope-tagged MFE2–A modified *MFE2* gene coding for a MFE2 protein tagged at its amino terminus was made by inserting a DNA fragment encoding three copies of the human c-Myc epitope (a gift of David Stewart, Department of Biochemistry, University of Alberta) in-frame at the 5' end of the *MFE2* ORF. First, a *Sna*BI site was introduced after the initiation codon of the *MFE2* gene using sequential PCR mutagenesis (Fig. 2-1). Essentially, the regions of the *MFE2* gene flanking the proposed *Sna*BI site were amplified from pG7MFE2 using oligonucleotides 909 and 945 for the 5' region and oligonucleotides 944 and UP for the 3' region (Table 2-3). The two products were used as templates for a second round of PCR with oligonucleotides 909 and UP. As oligonucleotides 944 and 945 have *Sna*BI recognition sequences and complementary 5' ends, the second round of PCR generated a single fragment containing both flanking regions of the *MFE2* gene with a *Sna*BI site between them. This product was digested with *Nco*I and *Eco*RV, and the fragment containing the PCR-generated *Sna*BI site was ligated into the corresponding sites of pG7MFE2. A fragment with *Hin*dII/*Xho*I termini encoding the peptide GEQKLISEEDLNGEQKLISEEDLNGEQKLISEEDLNG, which contains three repeats of the c-Myc epitope (underlined residues) (Kolodziej and Young, 1991), was made blunt with the Klenow fragment of DNA polymerase I and ligated in-frame into the *Sna*BI site to construct the plasmid pG7Myc-MFE2. This plasmid was digested with *Sph*I, and the fragment containing the modified *MFE2* gene, as well as 1,066 bp and 426 bp of sequence upstream and downstream of the *MFE2* gene, respectively, was ligated into *Sph*I-digested pINA445 to create the plasmid pMyc-MFE2 encoding Myc-MFE2. The region of pMyc-MFE2 that was amplified by PCR (between the *Nco*I and *Eco*RV sites) was determined to be correct by sequencing.

2.13.2 Construction of a plasmid encoding Myc-MFE2ΔAKL–Sequential PCR mutagenesis (Fig. 2-1) was used to generate a modified *MFE2* gene encoding Myc-MFE2 lacking its carboxyl-terminal tripeptide (Myc-MFE2ΔAKL). That portion of the *MFE2* gene 5' to the nucleotides encoding the carboxyl-terminal tripeptide of MFE2 was amplified from pG7Myc-MFE2 with oligonucleotides 909 and 953 (Table 2-3). The stop codon and downstream sequence of *MFE2* were amplified with oligonucleotides 958 and UP (Table 2-3). The two products were used as templates for a second round of PCR with oligonucleotides 909 and UP. As oligonucleotides 953 and 958 have complementary 5' ends, the second round of PCR generated a single fragment containing a modified *MFE2* gene encoding Myc-MFE2ΔAKL. This PCR product was digested with *Sph*I, and the fragment containing the modified *MFE2* ORF, as well as 1,066 bp and 426 bp of sequence upstream and downstream, respectively, of the *MFE2* gene, was ligated into the *Sph*I site of pINA445. The *MFE2* gene sequence upstream of the *Cla*I site was exchanged with the corresponding region of pMyc-MFE2 to construct pMyc-MFE2ΔAKL. The remainder of the *MFE2* gene was checked to be correct by sequencing.

2.13.3 Construction of a plasmid encoding Myc-MFE2ΔAΔB–Sequential PCR mutagenesis (Fig. 2-3) was used to generate a modified *MFE2* gene encoding Myc-MFE2ΔAΔB, a Myc-tagged version of MFE2 containing the mutations G16S and G324S. A portion of the *MFE2* gene 5' to the nucleotides encoding Gly16 was amplified from pG7Myc-MFE2 with oligonucleotides 1016 and 913 (Table 2-3). A portion of the MFE2 gene 3' to the nucleotides encoding Gly16 was amplified with oligonucleotides 1015 and 901 (Table 2-3). The two products were used as templates for a second round of PCR with oligonucleotides 901 and 913. As oligonucleotides 1015 and 1016 contain the G46A mutation and have complementary 5' ends, the second round of PCR generated a single fragment containing a modified *MFE2* gene encoding Myc-MFE2 containing the G16S mutation. A DNA fragment encoding MFE2 with the G324S mutation was made similarly, except that oligonucleotides 1013 and 1014 (containing the G1045A and the A1047T mutations) (Table 2-3) were used in place of oligonucleotides 1015 and 1016. The PCR product containing G46A was digested with *Eco*RV and *Nco*I and ligated into the corresponding sites of pG7Myc-MFE2 to yield the plasmid pG7Myc-MFE2ΔA. Next, the PCR product containing the G1045A and A1047T mutations was digested with *Eco*RV and *Afl*II and ligated into the corresponding sites of pG7Myc-MFE2ΔA to yield pG7Myc-MFE2ΔAΔB. pG7Myc-MFE2ΔAΔB was digested with *Sph*I, and the fragment containing the modified *MFE2* ORF, as well as 1,066 bp and 426 bp of sequence upstream and downstream of the *MFE2* gene, respectively, was ligated into the *Sph*I site of pINA445 to construct pMyc-MFE2ΔAΔB.

2.13.4 Construction of a plasmid for overexpression of the POT1 gene encoding thiolase–An overexpression cassette containing the promoter and terminator regions of the *ACT1* gene encoding *Y. lipolytica* actin was constructed using sequential PCR (Fig. 2-1). 645 bp upstream of the *ACT1* ORF was amplified from *Y. lipolytica* genomic DNA with oligonucleotides 1009 and 1012 (Table 2-3). 462 bp downstream of the *ACT1* ORF was amplified with oligonucleotides 1010 and 1011 (Table 2-3). The two products were used as templates for a second round of PCR with oligonucleotides 1009 and 1010. As oligonucleotides 1011 and 1012 have complementary 5' ends and contain *Sna*BI consensus sequences, the second round of PCR generated a single fragment containing the upstream and downstream regions of the *ACT1* gene separated by a *Sna*BI site. This PCR product was digested with *Bam*HI, and the cassette was ligated into the *Bam*HI site of pINA445 to make the plasmid pACT-OC. The *POT1* gene was amplified from *Y. lipolytica* genomic DNA using oligonucleotides 564 and 565 (Table 2-3), made blunt with the Klenow fragment of DNA polymerase I and ligated into the *Sna*BI site of pACT-OC in the correct orientation to make the plasmid pTHI-OV.

To quantify thiolase levels, *E122* cells transformed with either pTHI-OV or pINA445 were grown in YND medium overnight. Cells were harvested, and lysates were prepared. Equal amounts of protein at various dilutions from each strain were separated by SDS-PAGE, transferred to nitrocellulose and probed with either anti-thiolase or anti-Kar2p antibodies. The relative difference in the levels of thiolase in the pTHI-OV transformed strain versus the wild-type strain was determined by a comparison of the immunosignals for thiolase from different dilutions of lysate of each strain.

2.13.5 Construction of a plasmid encoding Pex8p-HA^c–A modified *PEX8* gene encoding Pex8p tagged at its carboxyl terminus was made by inserting a DNA fragment encoding two copies of the influenza virus HA epitope in-frame and downstream of the *PEX8* ORF as described below. A fragment containing the *PEX8* ORF flanked by 2.0 kbp and 1.2 kbp of genomic DNA at is 5' and 3' ends, respectively, was excised from pLD50 with *Hin*dIII and ligated into the *Hin*dIII site of pGEM7Zf(+) to make the plasmid pG7PEX8. Next, a *Bgl*II site was generated just upstream of the stop codon of *PEX8* using sequential PCR (Fig. 2-1). Essentially, two regions of the *PEX8* gene flanking the proposed *Bgl*II site were amplified from pG7PEX8 using oligonucleotides RP and 761 for the 5' region and oligonucleotides UP and 760 for the 3' region (Table 2-3). The two products were used as templates for a second round of PCR with oligonucleotides UP and RP. As oligonucleotides 760 and 761 have *Bgl*II recognition sequences and complementary 5' ends, the second round of PCR generated a single fragment containing *PEX8* with a *Bgl*II site just upstream of the stop codon. This product was digested with *Hin*dIII and ligated into pGEM7Zf(+) to construct the plasmid pG7-PEX8B. Next, a fragment with *Bam*HI/*Bgl*II termini, encoding the peptide DPLAMYPYDVPDYA AMYPYDVPDYAAMGKGE, which contains two repeats of the HA epitope (*underlined* residues) (Kolodziej and Young, 1991), was ligated in-frame into the *Bgl*II site of pG7PEX8B to construct the plasmid pG7PEX8-HA^{c}. The region of pG7PEX8-HA^{c} amplified by PCR was confirmed to be correct by sequencing.

To make a PEX8-HA^{c} expression plasmid, PEX8-HA^{c} was excised from pG7PEX8-HA^{c} with *Hin*dIII and ligated into the *Hin*dIII site of pINA445 to make the plasmid pPEX8-HA^{c} encoding Pex8p-HA^{c}. The *pex8-KA* disruption strain transformed with pPEX8-HA^{c} grew on oleic acid medium.

2.15 Construction of mutant strains of *Y. lipolytica*

2.15.1 Construction and isolation of pex8-1–Wild-type *Y. lipolytica E122* haploid cells were chemically mutagenized with 1-methyl-3-nitro-1-nitrosoguanidine, and the *pex8-1* strain was isolated by its inability to utilize oleic acid as the carbon source (Nuttley et al., 1993) (performed by Rachel K. Szilard).

2.15.2 Integrative disruption of PEX8–pLD50 was digested with *Sal*I to excise a fragment of 2.4 kbp encompassing 1.1 kbp of the ORF and 1.3 kbp of the 5' upstream region of the *PEX8* gene (see Fig. 3-3). A *Sal*I fragment of 1.7 kbp containing the *URA3* gene of *Y. lipolytica* was ligated into this site. This plasmid was digested with *Hin*dIII to release a 4.8-kbp fragment containing the *URA3* gene flanked at its 5' and 3' ends by 1.2 and 1.8 kbp of *Y. lipolytica* genomic DNA, respectively. This linear fragment was stably transformed into *Y. lipolytica* strains *E122* and *22301-3* by electroporation to replace the wild-type *PEX8* gene by homologous recombination. Strains that converted to uracil prototrophy and that were unable to use oleic acid as the carbon source were further characterized by Southern blotting. Two disruption strains, *pex8-KA* and *pex8-KB* in *E122* and *22301-3* backgrounds, respectively (Table 2-5), were chosen for further analysis.

2.15.3 Integrative disruption of MFE2 and PEX5–The flanking regions of the *MFE2* ORF were amplified from pG7MFE2 using oligonucleotides 909 and 921 for the 5' region and oligonucleotides 922 and UP for the 3' region (Table 2-3). The two products were used as templates for a second round of PCR using oligonucleotides 909 and UP. As oligonucleotides 922 and 921 have *Sal*I recognition sequences and complementary 5' ends, the second round of PCR generated a single fragment containing the *MFE2* flanking regions separated by a *Sal*I site. This PCR product was cut with *Sph*I, and the 1,467-bp fragment was ligated into the *Sph*I site of pGEM-7Zf(+). The *Y. lipolytica* *URA3* gene flanked by *Sal*I sites was then ligated into the unique *Sal*I site to construct the plasmid pΔMFE2. The *URA3* gene flanked by 1,019 bp and 426 bp of *MFE2* upstream and downstream regions, respectively, was excised from pΔMFE2 with *Sph*I, and the linear fragment was introduced into the wild-type strain *E122* by electroporation. Strains that converted to uracil prototrophy and that were unable to grow on oleic acid medium (YNO agar) were further characterized by Southern blotting. One strain, *mfe2-KO*, was confirmed to have the *MFE2* ORF replaced by *URA3*. The *PEX5* disruption strain, *pex5-KO2*, was constructed by Rachel K. Szilard as previously described (Szilard et al., 1995), except that the *URA3* gene was used in place of the *LEU2* gene.

***2.15.4 Construction of strains encoding Pex8p-HA*^{c} *and Pex8p-HA*^{i}**–To construct the strain *PEX8-HA*^{c}, a fragment containing the modified *PEX8* gene was excised from pG7PEX8-HA^{c} (Section 2.14.2) with *Hin*dIII and used to stably transform the *pex8-1* mutant strain (Table 2-5) at the *PEX8* locus. Transformants were selected for reestablished growth on oleic acid medium (YNO agar) and then characterized by Southern blotting and electron microscopy. One strain, *PEX8-HA*^{c}, having the correct genotype and wild-type morphology, was chosen for further study.

To construct the strain *PEX8-HA*^{i}, an *Xba*I/*Hin*dIII fragment containing the ORF of the *PEX8* gene flanked by ~0.8 and ~1.0 kbp of genomic DNA at its 5' and 3' ends, respectively, was ligated into the plasmid pGEM7Zf(+). A fragment with *Sal*I termini and encoding a peptide containing two repeats of the influenza virus HA epitope was ligated into the unique *Sal*I site in the *PEX8* gene between the codons for amino acids 365 (Val) and 366 (Asp). This construct was digested with *Xba*I and *Hin*dIII to release a fragment containing the modified *PEX8* gene. The fragment was used to stably transform the *pex8-1* mutant strain at the *PEX8* locus. Transformants able to use oleic acid as the carbon source were further characterized by Southern blotting and immunoblotting. One strain, *PEX8-HA*^{i}, having the tagged *PEX8* gene at the correct locus and synthesizing HA-tagged Pex8p (Pex8p-HA^{i}), was chosen for further study.

2.16 Polyclonal antibody production

Antibodies were raised in rabbit and guinea pig against protein fusions to maltose-binding protein (MBP) that were produced and purified as described below.

Gene fragments were ligated into pMAL-c2 in-frame and downstream of the *malE* ORF encoding MBP. The plasmids were transformed into *E. coli* DH5α or BRL-DE3 cells. Protein synthesis was induced by addition of 0.1 M IPTG. Cells were disrupted by 2.5 min sonication in 30 sec bursts using a Branson Sonifier 250 (duty 30%, output control 3). MBP protein fusions were purified on amylose resin columns in 20 mM Tris-HCl (pH 7.4) containing 200 mM NaCl, 1 mM EDTA, 1 mM DTT and 1 mM PMSF using the Protein Fusion and Purification System (NEB). Purified protein was quantified as described in Section 2.7.2.

Proteins were further purified by electrophoresis by the method of Harlow and Lane (1988). Essentially, proteins were separated on 10% SDS-polyacrylamide preparative gels. To visualize proteins, gels were stained for 10 to 15 min in 0.05% Coomassie Brilliant Blue R-250 in water and destained briefly in water. Gel fragments (3 cm x 0.5 cm) containing protein of the correct molecular mass were excised from the gel with a razor blade and placed in dialysis tubing with 10 mL of (0.2 M Tris-acetate (pH 7.4), 1% SDS, 10 mM DTT)/g of wet gel. Proteins were eluted from the gel by electrophoresis at 50 V overnight at 4°C in 500 mL of 50 mM Tris-HCl (pH 7.4), 0.1% SDS. Gel fragments were discarded, and the eluate was dialyzed against 4 L of 50 mM ammonium bicarbonate once at room temperature and three times at 4°C. The protein solution was then frozen and dried by lyophilization overnight. Protein was dissolved in a minimal volume of water. Protein was quantified by separating various dilutions of protein by SDS-PAGE (Section 2.7.3), staining with Coomassie Brilliant Blue R-250, and comparing the intensity of their staining with that of samples of protein of known concentration.

Rabbits and guinea pigs were immunized by the method of Harlow and Lane (1988). Protein samples were diluted to 500 µg/mL; SDS was added to a final concentration of 0.02% and half of each sample was boiled for 5 min. Boiled and unboiled fractions were combined immediately before immunization, mixed with an equal volume of Freund's complete or incomplete adjuvant for primary and subsequent injections, respectively, and sonicated briefly. 1 mL and 0.4 mL were injected into several subcutaneous sites of rabbits and guinea pigs, respectively, every six weeks. Bleeds were taken 10 d after each injection. Red blood cells were removed from serum by clotting blood at room temperature for 1 h and pelleting clots by centrifugation at 2,000 x *g* for 15 min at room temperature. Serum was stored in the presence of 1.5 mM sodium azide at –20°C. The presence of specific antibodies in serum was assessed by immunoblotting (Section 2.7.5).

2.16.1 Production of antisera directed against Pex20p–pMAL-PEX20, the plasmid encoding the MBP-Pex20p fusion protein, was constructed by Richard A. Rachubinski. Essentially, the entire ORF of *PEX20* was amplified by PCR from *E122* genomic DNA using oligonucleotides 414 and 290 (Table 2-3) containing *Eco*RI and *Hin*dIII recognition sequences, respectively. The PCR product was digested with *Eco*RI and *Hin*dIII and ligated into the corresponding sites of pMAL-c2 to construct the plasmid pMAL-PEX20.

Antibodies to MBP-Pex20p were elicited in rabbits (H67 and H68) and guinea pigs (56N and 56NN) as described in Section 2.17. Note that rabbits were injected once with MBP-Pex6p fusion protein (Section 2.17.3), but the sera do not recognize Pex6p by immunoblotting. All animals produced specific antibodies.

2.16.2 Production of antisera directed against Pex1p–pMAL-PEX1, the plasmid encoding the MBP-Pex1p fusion protein, was constructed by Richard A. Rachubinski. Essentially, the portion of *PEX1* encoding the amino-terminal 409 amino acid residues of Pex1p was amplified by PCR from *E122* genomic DNA using oligonucleotides 287 and 288 (Table 2-3) containing *Eco*RI and *Hin*dIII recognition sequences respectively. The PCR product was digested with *Eco*RI and *Hin*dIII and ligated into the corresponding sites of pMAL-c2 to construct the plasmid pMAL-PEX1. Antibodies to MBP-Pex1p were elicited in rabbits (H63 and H64) and guinea pigs (41NN and 41N) as described in Section 2.17. All animals produced specific antibodies.

2.16.3 Production of antisera directed against Pex6p–pMAL-PEX6, the plasmid encoding the MBP-Pex6p fusion protein was constructed by Rache K. Szilard. Essentially, the portion of *PEX6* encoding the amino-terminal 452 amino acid residues of Pex6p was amplified by PCR from plasmid pO1 (Nuttley et al., 1994) using oligonucleotides 424 and 425 (Table 2-3) containing *Eco*RI and *Hin*dIII recognition sequences, respectively. The PCR product was digested with *Eco*RI and *Hin*dIII and ligated into the corresponding sites of pMAL-c2 to construct the plasmid pMAL-PEX6. Antibodies to MBP-Pex6p were elicited in rabbits (H182 and H183) and guinea pigs (4N and 4NN) as described in Section 2.17. All animals except guinea pig 4N produced specific antibodies.

2.17 Computer-aided DNA and protein sequence analyses

Query protein sequences were compared to sequences deposited in the NCBI Protein Database using the BLAST algorithm (Altshul et al., 1990) via the network service (www.ncbi.nlm.nih.gov) of the NCBI. Protein sequences were aligned using the Clustal W algorithm of Omiga 1.1.3 (Oxford Molecular Group). Similarities between protein sequences were quantified using the structure genetics comparison matrix of the PC-GENE software package (IntelliGenetics) with an open gap cost of 4 and a unit gap cost of 4. PC-GENE software was used for all other DNA and protein sequence analyses.

2.18 *In vitro* binding assay

2.18.1 Construction of chimeric genes and isolation of recombinant proteins–Chimeric genes encoding MBP or glutathione-S transferase (GST) fusions were constructed as described below. The *PEX8* ORF was excised from pGAD-PEX8 (Table 2-9) with *Eco*RI and *Bgl*II and ligated into *Eco*RI/*Bam*HI-digested pBluescript SKII(+) to construct the plasmid pBS-PEX8. To construct plasmid pMAL-PEX8 encoding MBP-Pex8p, *PEX8* was excised from pBS-PEX8 with *Eco*RI and *Xba*I and inserted into pMAL-c2 digested with *Eco*RI and *Xba*I. To construct plasmid pGEX-PEX20 encoding GST-Pex20p, pGBT-PEX20 (Table 2-9) was digested with *Eco*RI and the *PEX20* ORF was ligated into *Eco*RI-digested pGEX-4T1.

Plasmids pGEX-4T1, pGEX-PEX20, pMAL-c2 and pMAL-PEX8 were introduced into the protease-deficient *E. coli* strain BLR (DE3). Induction and purification of GST fusion proteins were conducted according to the manufacturer's (Pharmacia Biotech) specifications with the following modifications. Expression of the chimeric genes was induced at 30°C with 1 mM IPTG for 2 h. Cells were lysed using B-PER reagent according to the manufacturer's instructions. Induction and purification of MBP fusion proteins was performed according to the manufacturer's specifications. All purified proteins were dialyzed against 20 mM HEPES-KOH (pH 6.8), 150 mM potassium acetate, 5 mM magnesium acetate, 1 mM EDTA, 20% (w/v) glycerol and stored at –70°C.

2.18.2 In vitro binding assay with recombinant proteins–The *in vitro* binding assay was performed using the recombinant proteins GST, GST-Pex20p, MBP and MBP-Pex8p purified as described above. Glutathione-Sepharose 4B was washed three times in RW buffer (20 mM HEPES-KOH (pH 6.8), 150 mM potassium acetate, 5 mM magnesium acetate, 0.1% Tween 20, 0.1% casaminoacids, PINS (Table 2-4)). GST or GST chimeras were tumbled end over end in batch with glutathione-Sepharose (2.5 µg of GST fusion protein and 5 µl of packed beads per reaction) in 0.5 mL of RW buffer for 20 min at room temperature. The beads were collected by centrifugation at 2,000 x *g* for 30 s and washed three times in 0.5 mL of RW buffer. Purified MBP or MBP fusion protein (5 µg in 100 µl of RW buffer) was added to the beads and the mixture was tumbled end over end for 30 min at room temperature. The beads were collected by centrifugation, and the supernatant was retained as the unbound fraction. The beads were resuspended in 0.5 mL RW buffer and applied to a spin filters (CytoSignal), washed three times with RW buffer and eluted in 50 µl of SDS sample buffer at room temperature, as instructed by the manufacturer. 50% of bound fractions and 25% of unbound fractions were run on 9% polyacrylamide gels, and protein was detected by staining gels with Coomassie Brilliant Blue R-250.

2.18.3 In vitro binding assay with yeast lysate–Aliquots of glutathione-Sepharose 4B (10 µl of packed beads per reaction) were washed four times with 1 mL of RX buffer (Section 2.10) and resuspended in 0.5 mL RX buffer. 3 µg of GST or GST-Pex20p was added, and reactions were tumbled end over end at room temperature for 80 min and then washed three times with 0.5 mL RX buffer. YPBO grown cells of the *PEX8-HA*^{c} strain were collected by centrifugation, washed three times with water, and once with RX buffer. Cells were disrupted by glass bead lysis in RX buffer. The lysate was clarified by centrifugation at 20,000 *g* in a microcentrifuge for 45 min at 4°C. 120 µl of the cleared supernatant (10 mg protein/mL) or RX buffer alone was tumbled end over end in batch with each of the glutathione-Sepharose-bound GST constructs for 2 h at 4°C. Beads were washed twice with 0.8 mL RX, applied to spin filters and washed four times with 0.5 mL RX. Bound proteins were eluted in 40 µl SDS sample buffer according to the manufacturer's instructions. Proteins in equal fractions of each sample were separated on 10% polyacrylamide gels and either stained with Coomassie Brilliant Blue R-250 or transferred to nitrocellulose and immunoblotted.

2.19 Two-hybrid analysis

2.19.1 Construction of chimeric genes–Chimeric genes were constructed by amplifying the ORFs of *PEX* genes by PCR from *Y. lipolytica* genomic DNA and ligating them in-frame and downstream of the DNA encoding the GAL4 transcription-activating domain (AD) and the GAL4 DNA-binding domain (DB) in plasmids pGAD424 and pGBT9, respectively, as described below in Table 2-9. Plasmid pGBT9-P8(1-366) encoding DB-Pex8p(1-366) was constructed by dropping out the *Sal*I fragment from pGBT9-PEX8 (Table 2-9). To construct pGAD-P8ΔNC encoding AD-Pex8p(12-644), a portion of the *PEX8* gene with flanking *Eco*RI sites was amplified from genomic DNA with oligonucleotides 122-1 and 549 (Table 2-3) and ligated into *Eco*RI-digested pGAD424. To construct plasmid pGAD-P8(12-370) encoding AD-Pex8p(12-370), pGAD-P8ΔNC was digested with *Eco*RI and *Bam*HI and the 1080-bp fragment was ligated into the corresponding sites of pGAD424. Plasmid pGAD-P8(164-644) encoding AD-Pex8p(164-644) was constructed by cutting pGAD-P8ΔNC with *Apo*I and *Eco*RI and ligating the 1442-bp fragment into *Eco*RI-digested pGAD424. Plasmid pGAD-P20(1-76) encoding AD-Pex20p(1-76) was constructed by dropping out the *Bal*I/*Sma*I fragment from pGBT-PEX20 (Table 2-9).

Table 2-9 Construction of Plasmids for the Yeast Two-Hybrid System

Construct	Gene[a]	Oligonucleotides used to PCR gene	Enzymes used to digest PCR products	Plasmid digest[b]
pGBT-PEX1	*PEX1*	394 and 395	*Eco*RI	*Eco*RI
pGAD-PEX1	*PEX1*	394 and 395	*Eco*RI	*Eco*RI
pGBT-PEX2	*PEX2*	337 and 338	*Bam*HI/*Bgl*II	*Bam*HI

pGAD-PEX2	*PEX2*	337 and 338	*Bam*HI/*Bgl*II	*Bam*HI/*Bgl*II
pGBT-PEX5	*PEX5*	339 and 340	*Eco*RI/*Bam*HI	*Eco*RI/*Bam*HI
pGAD-PEX5	*PEX5*	339 and 340	*Eco*RI/*Bam*HI	*Eco*RI/*Bam*HI
pGBT-PEX6	*PEX6*	343 and 344	*Eco*RI	*Eco*RI
pGAD-PEX6	*PEX6*	343 and 344	*Eco*RI	*Eco*RI
pGBT-PEX8[c]	*PEX8*	122-2 and 336	*Eco*RI/*Bgl*II	*Eco*RI/*Bam*HI
pGAD-PEX8[c]	*PEX8*	122-2 and 336	*Eco*RI/*Bgl*II	*Eco*RI/*Bgl*II
pGBT-PEX9	*PEX9*	341 and 342	*Eco*RI/*Bgl*II	*Eco*RI/*Bam*HI
pGAD-PEX9	*PEX9*	341 and 342	*Eco*RI/*Bgl*II	*Eco*RI/*Bam*HI
pGBT-PEX16	*PEX16*[d]	not applicable	not applicable	*Eco*RI
pGAD-PEX16	*PEX16*[d]	not applicable	not applicable	*Eco*RI
pGBT-PEX20[c]	*PEX20*	398 and 399	*Eco*RI	*Eco*RI
pGAD-PEX20[c]	*PEX20*	398 and 399	*Eco*RI	*Eco*RI

[a] Genes were amplified from *E122* genomic DNA.

[b] Plasmids are pGAD424 and pGBT9 for constructs beginning with pGAD and pGBT respectively.

[c] The entire ORF of *PEX* gene was confirmed to be correct by sequencing. For all other plasmids, only the sequence of the first 500 bp of the *PEX* gene was confirmed to be correct by sequenced.

[d] *PEX16* was not generated by PCR, instead it was removed from p16TH (Eitzen et al., 1997) with *Eco*RI.

2.19.2 Two-hybrid analysis**–**Cells of the yeast strain *SFY526* were simultaneously transformed with a pGBT9-derived plasmid and a pGAD424-derived plasmid. Transformants were grown on synthetic medium lacking tryptophan and leucine and tested for activation of the integrated *lacZ* construct using β-galactosidase filter and liquid assays. Both assays were performed according to the manufacturer's (Clonetech) instructions with the following exceptions. For liquid assays, yeast from 1 mL of culture was used instead of from 0.1 mL, and cells were broken by three freeze-thaw cycles at -70°C instead of by chemical lysis. For the filter assay, agar plates contained 100 μg adenine/mL to reduce the red color of the yeast.

CHAPTER 3

PEX8P IS ASSOCIATED PERIPHERALLY WITH THE PEROXISOMAL MEMBRANE AND IS REQUIRED FOR MATRIX PROTEIN IMPORT

A version of this chapter has previously been published as " The peroxin Pex17p of the yeast *Yarrowia lipolytica* is associated peripherally with the peroxisomal membrane and is required for the import of a subset of matrix proteins" (Jennifer J. Smith, Rachel K. Szilard, Marcello Marelli and Richard A. Rachubinski. 1997. *Mol. Cell. Biol.* 17:2511-2520). Reprinted with permission.

3.1 Overview

A genetic screen was used to identify mutants of peroxisome maintenance of the yeast *Y. lipolytica*. The mutant *pex8-1* was isolated on the basis of its inability to use oleic acid as a carbon source and its lack of normal peroxisome morphology. The growth defect of this strain was complemented with *PEX8*, a previously uncharacterized gene that encodes Pex8p, a protein of 671 amino acid residues that has sequence similarity to the three members of the Pex8p family of peroxins. Pex8p is peripherally associated with the matrix face of the peroxisomal membrane. Synthesis of Pex8p is low in cells grown in glucose-containing medium and increases after the cells are shifted to oleic acid-containing medium.

Pex8p proteins of other yeasts have been shown to be required for the import of matrix proteins into peroxisomes. Cells of *pex8-1* and *pex8-KA* (a *PEX8* gene disruption strain) fail to form normal peroxisomes but instead contain numerous large, multimembraned structures. The import of peroxisomal matrix proteins in these mutants is selectively impaired. The selectivity of import is not a function of the nature of the peroxisomal targeting signal as both PTS1- and PTS2-containing proteins are mislocalized. Taken together, these results point to a role for *Y. lipolytica* Pex8p (*Yl*Pex8p) in the import of a subset of matrix proteins into peroxisomes.

3.2 The *pex8-1* mutant strain lacks normal peroxisomes

A previously developed screen (Nuttley et al., 1993) was used to identify mutants of peroxisome maintenance of the yeast *Y. lipolytica*. The wild-type strain, *E122*, was mutagenized, and the *pex8-1* mutant strain was selected on the basis of its inability to grow on medium containing oleic acid as the sole carbon source (performed by Rachel Szilard) (Szilard, 2000) (for growth defect, see Fig. 3-1). Biochemical characterization demonstrated that the *pex8-1* mutant had deficiencies in the targeting and import of several peroxisomal matrix proteins (a detailed discussion follows), which conforms to the classical *pex* mutant phenotype.

The morphology of cells of the *pex8-1* strain after incubation in medium containing oleic acid was compared to that of cells of the wild-type *E122* strain by electron microscopy (Fig. 3-2, compare *B* to *A*). The *E122* strain showed several round peroxisomes surrounded by single membranes. Normal peroxisomes were absent in the *pex8-1* mutant strain. Instead, irregularly shaped structures surrounded by multiple membranes were observed.

3.3 Isolation and characterization of the *PEX8* gene

The *PEX8* gene was isolated by functional complementation of the *pex8-1* strain (performed in collaboration with Marcello Marelli). The mutant strain was transformed with a plasmid library of *Y. lipolytica* genomic DNA. Of approximately 10^5 transformants, ten grew on a medium containing oleic acid as the sole carbon source. Restriction enzyme analysis of the complementing plasmids revealed that each contained a set of common overlapping fragments. One plasmid, pLD50, was chosen for further study. Introduction of this plasmid into the *pex8-1* mutant strain rescued growth on oleic acid (Fig. 3-1, compare *PEX8* to *pex8-1*) and reestablished wild-type peroxisome morphology (Fig. 3-2 *C*). Further analysis of pLD50 revealed that its complementing activity was restricted to a 3.5-kbp fragment (Fig. 3-3). Sequencing within this minimal

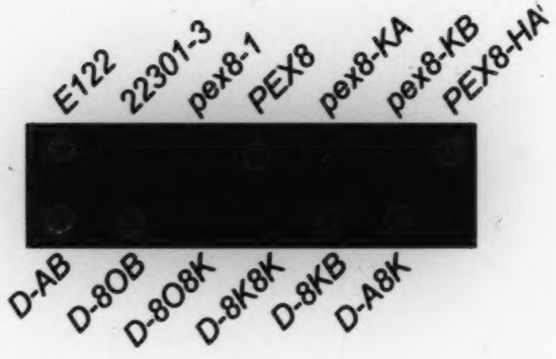

Figure 3-1. Growth of various *Y. lipolytica* strains on oleic acid-containing medium. Strains were spotted onto YNO agar supplemented with leucine, uracil, and lysine, each at 50 µg/mL, and incubated for 2 d at 30°C. The appearance of the complemented *PEX8* strain is compared to those of the wild-type strains *E122* and *22301-3*, the original *pex8-1* mutant, the *pex8-KA* and *pex8-KB* gene disruption strains and the *pex8-HA*^{i} strain synthesizing Pex8p-HA^i. Strain *22301-3* was not supplemented for its auxotrophic requirements. The appearances of diploid strains containing one (*D-8OB*, *D-8KB*, *D-A8K*) or two (*D-8K8K*, *D-8O8K*) mutant alleles of *PEX8* are compared to that of the wild-type diploid strain, *D-AB*. Growth on YNO requires one functional copy of the *PEX8* gene.

Figure 3-2. Ultrastructure of the wild-type strain *E122* and of the *pex8* mutant, and *PEX8* complemented strains. *E122* (*A*), *pex8-1* (*B*), *PEX8* (*C*), *pex8-KA* (*D* and *E*), and *PEX8-HA^{i}* (*F*) strains were grown for 10 h in YEPD medium (YND for the *PEX8* strain), transferred to YPBO medium (YNO for the *PEX8* strain), and grown for an additional 8 h. Cells were fixed in 1.5% $KMnO_4$ and processed for electron microscopy (performed by Honey Chan). *P*, peroxisome; *M*, mitochondrion; *N*, nucleus; *V*, vacuole. *Arrows*, multimembraned structures. *Bars*, 1μm.

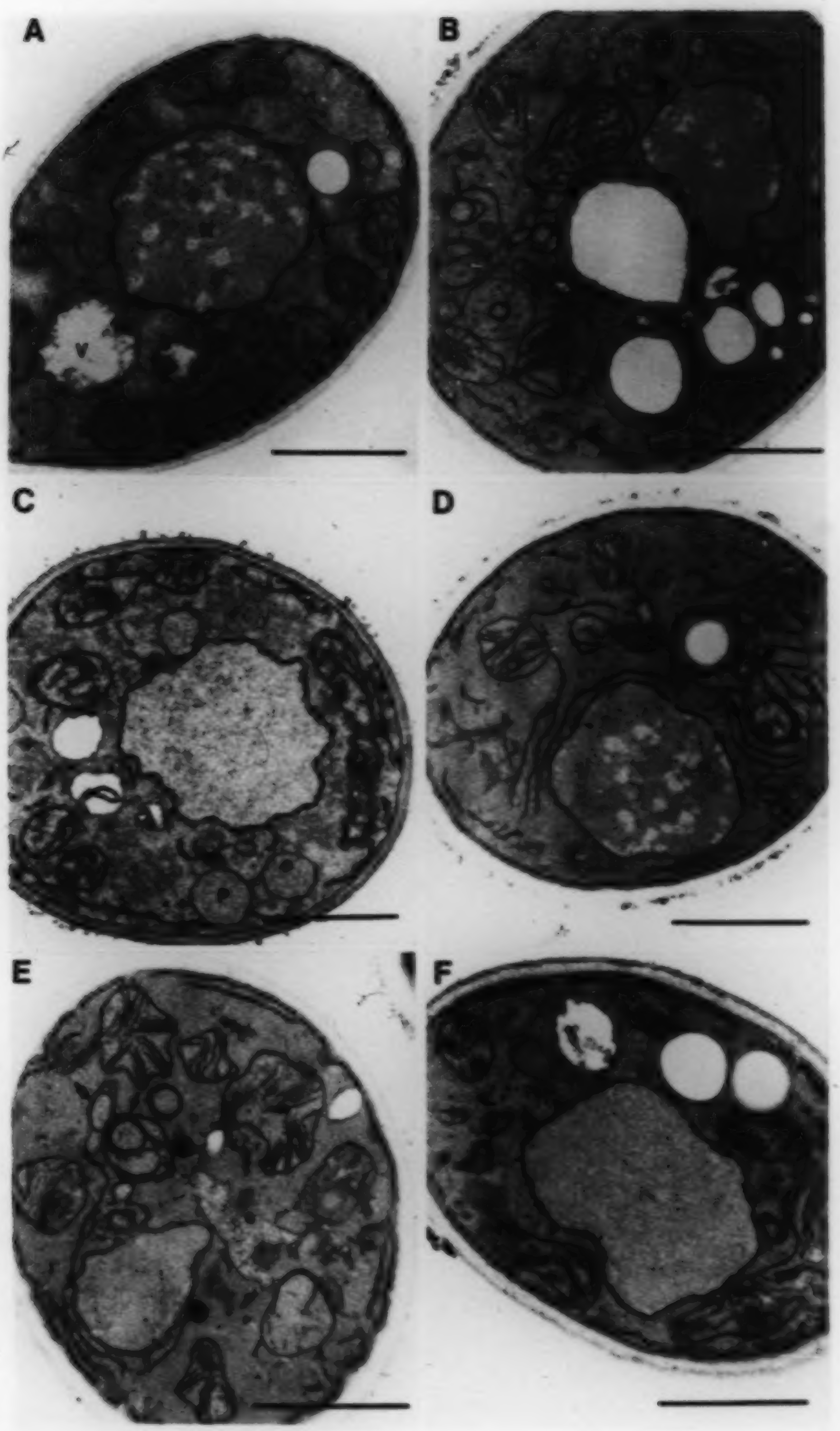
A
V
B
C
D
E
F

complementing fragment revealed a gene, termed *PEX8*, that encodes a protein of 671 amino-acid residues with a predicted molecular mass of 75,588 Da, termed Pex8p (Fig. 3-4). The upstream regulatory region of the *PEX8* gene contains the sequence CGGCTGTGA between nucleotides -117 and -109. This sequence closely resembles the consensus oleic acid-response element (C/T)GGTT(A/G)TT(C/A/G) of *Candida tropicalis* (Sloots et al., 1991) and fits the consensus oleic acid-response element CGGNNNTNA of *S. cerevisiae* (Filipits et al., 1993; Karpichev and Small, 1998), which are sequences often found upstream of genes encoding peroxisomal proteins.

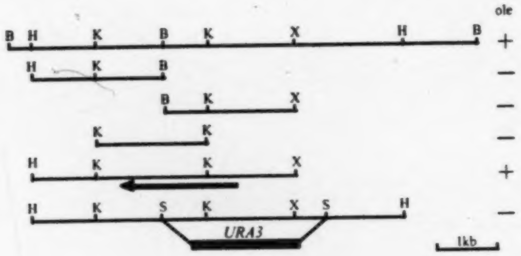

Figure 3-3. Complementing activity, restriction map, and disruption strategy for the *PEX8* gene. The top line represents the genomic insert in the original complementing vector, pLD50. The (+/-) symbols denote the ability (+) or inability (-) of an insert to confer growth on oleic acid to the *pex8-1* strain. The arrow shows the direction and position of the *PEX8* ORF. The site of integration of the *Y. lipolytica URA3* gene into the *PEX8* gene is shown in the bottom construct. *B*, *Bam*HI; *H*, *Hin*dIII; *K*, *Kpn*I; *S*, *Sal*I; *X*, *Xba*I.

Hydropathy analysis showed Pex8p to be hydrophobic overall and to contain three potential transmembrane domains (Figure 3-5). The sequence of Pex8p is similar to those of the Pex8p family of peroxins (Figure 3-6). The protein sequence is 19.9%

```
-291 CCGACAAAGACTTTGAAATCAATTCTTTTGATTCGATGGCAGACAACCCTGGTGGTCACCACCCTCCCGCCTGGTCATAGG
-210 CTACAGTAATCTCTTTGCTCTGGCTTACCGCGCTCAATCAAATGAGACCGAAAAGAGATGACCAGATGTGCTTGTGTGACT
-129 AAAATCCCCCAGCGGCTGTGAGTTCGATTCCCTCTCCGCCCACTTAAGGTATACTATGCACTCTAACATACCTCGGTTCCC
 -48 CGCATGTAACTTTCACGGACCTGCAACTCACAGAACTACCCCAACACCATGAACAAGTATCTAGTGCCCCCGCCCCAGGCC
                                                      M  N  K  Y  L  V  P  P  P  Q  A  11
  34 AATAGAACGGTAACAAACCTCGATCTGCTCATCAACAACCTCCGTGGCTCCTCTACGCCCGGAGCCGCAGAGGTCGATACC
      N  R  T  V  T  N  L  D  L  L  I  N  N  L  R  G  S  S  T  P  G  A  A  E  V  D  T  38
 115 AGGGATATCCTCCAACGAATCGTCTTTATTCTCCCTACCATCAAGAACCCTCTCAACCTCGATCTGGTGATCAAGGAGATT
      R  D  I  L  Q  R  I  V  F  I  L  P  T  I  K  N  P  L  N  L  D  L  V  I  K  E  I  65
 196 ATCAACTCGCCACGCCTGCTGCCGCCTCTCATTGATCTCCATGACTACCAACAGCTCACAGACGCCTTCAGAGCAACCATC
      I  N  S  P  R  L  L  P  P  L  I  D  L  H  D  Y  Q  Q  L  T  D  A  F  R  A  T  I  92
 277 AAAAGAAAGGCCCTCGTCACAGACCCCACCATCAGCTTCGAGGCTTGGCTGGAGACCTGCTTCCAGGTCATTACTCGATTC
      K  R  K  A  L  V  T  D  P  T  I  S  F  E  A  W  L  E  T  C  F  Q  V  I  T  R  F  119
 358 GCAGGACCGGGTTGGAAGAAGCTACCTCTTCTGGCAGGATTGATTCTCGCAGATTACGACATTTCAGCTGATGGACCGACA
      A  G  P  G  W  K  K  L  P  L  L  A  G  L  I  L  A  D  Y  D  I  S  A  D  G  P  T  146
 439 CTGGAACGAAAACCAGGTTTCCCGTCGAAACTCAAGCATCTGCTCAAGAGGGAATTTGTCACCACTTTTGACCAGTGTCTT
      L  E  R  K  P  G  F  P  S  K  L  K  H  L  L  K  R  E  F  V  T  T  F  D  Q  C  L  173
 520 TCTATCGACACCCGAAACCGAAGCGACGCCACAAAATGGGTACCTGTGCTTGCCTGCATTTCTATCGCACAGGTCTACTCG
      S  I  D  T  R  N  R  S  D  A  T  K  W  V  P  V  L  A  C  I  S  I  A  Q  V  Y  S  200
 601 CTGCTAGGTGACGTTGCTATCAACTACAGACGGTTCTTGCAGGTGGGTCTGGATCTCATCTTCTCAAACTACGGTTTGGAA
      L  L  G  D  V  A  I  N  Y  R  R  F  L  Q  V  G  L  D  L  I  F  S  N  Y  G  L  E  227
 682 ATGGGCACGGCTCTGGCAAGACTCCATGCTGAGTCCGGAGGCGACGCTACAACCGCCGGTGGACTCATCGGAAAGAAACTC
      M  G  T  A  L  A  R  L  H  A  E  S  G  G  D  A  T  T  A  G  G  L  I  G  K  K  L  254
 763 AAAGAACCCGTTGTGGCTCTACTCAACACTTTTGCACACATCGCATCCTCCTGCATCGTTCACGTGGATATCGACTACATT
      K  E  P  V  V  A  L  L  N  T  F  A  H  I  A  S  S  C  I  V  H  V  D  I  D  Y  I  281
 844 GACCGTATCCAGAACAAAATTATCCTAGTGTGTGAGAACCAGGCCGAGACCTGGAGAATCCTCACCATCGAAAGTCCAACT
      D  R  I  Q  N  K  I  I  L  V  C  E  N  Q  A  E  T  W  R  I  L  T  I  E  S  P  T  308
 925 GTCATGCACCACCAGGAGTCTGTTCAGTACCTCAAATGGGAGCTGTTCACCCTCTGTATCATTATGCAGGGAATTGCAAAC
      V  M  H  H  Q  E  S  V  Q  Y  L  K  W  E  L  F  T  L  C  I  I  M  Q  G  I  A  N  335
1006 ATGCTGCTCACACAAAAGATGAACCAGTTCATGTACCTGCAGCTGGCATACAAACAGCTTCAGGCACTCCACAGCATCTAT
      M  L  L  T  Q  K  M  N  Q  F  M  Y  L  Q  L  A  Y  K  Q  L  Q  A  L  H  S  I  Y  362
1087 TTCATTGTCGACCAAATGGGATCCCAGTTTGCTGCATATGACTACGTCTTCTTCTCAGCGATCGATGTCCTGTTGTCGGAG
      F  I  V  D  Q  M  G  S  Q  F  A  A  Y  D  Y  V  F  F  S  A  I  D  V  L  L  S  E  389
1168 TACGCTCCTTACATCAAGAACAGAGGCACCATCCCACCCAACAAGGAGTTTGTGGCCGAAAGACTGGCCGCGAATCTCGCT
      Y  A  P  Y  I  K  N  R  G  T  I  P  P  N  K  E  F  V  A  E  R  L  A  A  N  L  A  416
1249 GGAACTTCAAACGTGGGGAGTCATCTTCCTATTGATCGCTCTCGAGTTCTGTTCGCTCTCAACTACTACGAACAGCTTGTC
      G  T  S  N  V  G  S  H  L  P  I  D  R  S  R  V  L  F  A  L  N  Y  Y  E  Q  L  V  443
1330 ACCGTATGTCACGATAGCTGCGTAGAGACCATCATTTATCCCATGGCACGATCCTTCCTCTATCCCACAAGCGACATTCAG
      T  V  C  H  D  S  C  V  E  T  I  I  Y  P  M  A  R  S  F  L  Y  P  T  S  D  I  Q  470
1411 CAACTTAAACCGCTGGTGGAAGCTGCTCACTCCGTGATTCTGGCTGGCCTGGCAGTGCCTACCAACGCTGTTGTGAACGCT
      Q  L  K  P  L  V  E  A  A  H  S  V  I  L  A  G  L  A  V  P  T  N  A  V  V  N  A  497
1492 AAGCTCATCCCAGAGTACATGGGGGGAGTTCTTCCTTTGTTTCCGGGAGTGTTTTCATGGAACCAGTTCGTGTTGGCCATT
      K  L  I  P  E  Y  M  G  G  V  L  P  L  F  P  G  V  F  S  W  N  Q  F  V  L  A  I  524
1573 CAGTCCATCGTTAACACTGTCTCTCCTCCTTCTGAAGTGTTTAAAACCAACCAGAAGCTCTTCCGTCTTGTGTTGGATTCT
      Q  S  I  V  N  T  V  S  P  P  S  E  V  F  K  T  N  Q  K  L  F  R  L  V  L  D  S  551
1654 TTGATGAAAAAGTGCAGAGACACGCCCGTGGGCATTCCTGTGCCACACTCAGTCACAGTATCTCAGGAACAGGAAGACATT
      L  M  K  K  C  R  D  T  P  V  G  I  P  V  P  H  S  V  T  V  S  Q  E  Q  E  D  I  578
1735 CCTCCTACACAGCGAGCTGTGGTAATGCTGGCTCTCATCAACTCGCTGCCCTACGTTGATATCCGGTCTTTTGAGTTGTGG
      P  P  T  Q  R  A  V  V  M  L  A  L  I  N  S  L  P  Y  V  D  I  R  S  F  E  L  W  605
1816 CTGCAGGAGACGTGGAATATGATCGAGGCCACTCCCATGCTTGCCGAAAACGCCCCCAACAAGGAGCTTGCGCATGCCGAG
      L  Q  E  T  W  N  M  I  E  A  T  P  M  L  A  E  N  A  P  N  K  E  L  A  H  A  E  632
1897 CACGAGTTTCTGGTTCTGGAAATGTGGAAGATGATTTCCGGCAACATTGACCAGCGTCTCAATGATGTGGCCATTCGATGG
      H  E  F  L  V  L  E  M  W  K  M  I  S  G  N  I  D  Q  R  L  N  D  V  A  I  R  W  659
1978 TGGTACAAAAAGAATGCTCGAGTGCATGGAACGTTATAACCGTGGGAGTAGCCCACAGTTCACATAGAGTAAGATCACATA
      W  Y  K  K  N  A  R  V  H  G  T  L  -                                            671
2059 AAGTAACTCAACAGATTTCAGCAGATGAATGCAAAGAAGTCCCCGAGGAGTCGGACATATCGGTAAAGACGTTAAATGCGA
2140 GACATCTCGCGTCTCTGGCGTCTCCGCAAAAGTTTATTATCTGACATATATGTGGGTACCAGGTTGGTGTGTTAGTACCTG
```

Figure 3-4. Nucleotide sequence of *PEX8* and deduced amino acid sequence of Pex8p. A putative oleic acid-response element is *underlined*. These sequences have been submitted to GenBank with accession number U73028.

identical and 17.5% similar to that of *H. polymorpha* Pex8p, a 71-kDa protein localized to the peroxisomal matrix and having both PTS1 and PTS2 motifs (Waterham et al., 1994). It is 22.8% identical and 17.3% similar to *P. pastoris* Pex8p, an 81-kDa PTS1-containing protein peripherally associated with peroxisomal membranes (Liu et al., 1995). It also shows 18.5% identity and 16.5% similarity to an *S. cerevisiae* PTS1-containing protein of 68 kDa encoded by ORF YGR077c of chromosome VII (NCBI accession number Z72862). This protein was recently shown to belong to the Pex8p family of peroxins and to be associated with the matrix face of peroxisomal membranes (Rehling et al., 2000). Interestingly, unlike the other proteins of the Pex8p family, *Yl*Pex8p contains neither a PTS1 nor a PTS2 consensus sequence.

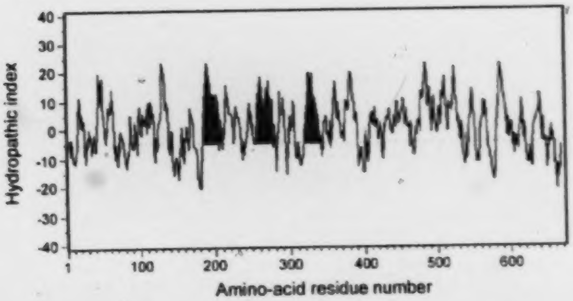

Figure 3-5. Hydropathy analysis of Pex8p. Hydropathy profile of Pex8p calculated according to Kyte and Doolittle (1982) with a window size of 9 amino-acid residues. Three sequences predicted to be membrane-spanning domains, calculated according to Klein et al. (1985), are highlighted in *black*.

The *PEX8* gene was disrupted in both the *E122* and *22301-3* wild-type strains by integration of the *Y. lipolytica URA3* gene (Fig. 3-3) to create the *pex8-KA* and *pex8-KB* strains, respectively (Table 2-5). These strains were unable to use oleic acid as a carbon source (Fig. 3-1) and had the same peroxisome morphology (Fig 3-2, compare *D* and *E* to

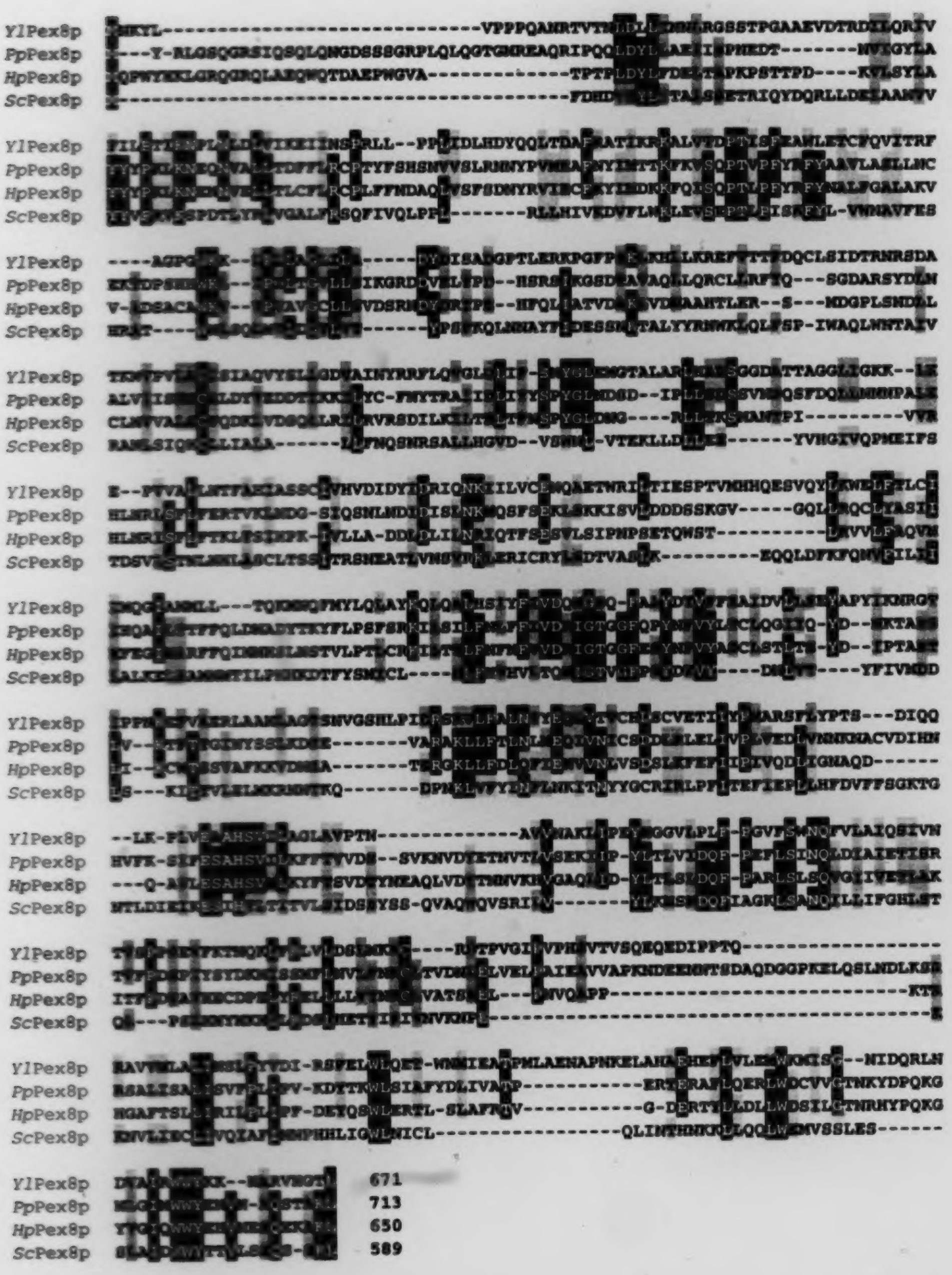
YlPex8p 46
PpPex8p 64
HpPex8p 58
ScPex8p 34
YlPex8p 119
PpPex8p 139
HpPex8p 133
ScPex8p 101
YlPex8p 183
PpPex8p 207
HpPex8p 198
ScPex8p 165
YlPex8p 255
PpPex8p 279
HpPex8p 260
ScPex8p 225
YlPex8p 328
PpPex8p 348
HpPex8p 323
ScPex8p 291
YlPex8p 399
PpPex8p 420
HpPex8p 395
ScPex8p 354
YlPex8p 471
PpPex8p 486
HpPex8p 455
ScPex8p 419
YlPex8p 529
PpPex8p 556
HpPex8p 524
ScPex8p 486
YlPex8p 582
PpPex8p 631
HpPex8p 569
ScPex8p 518
YlPex8p 653
PpPex8p 694
HpPex8p 630
ScPex8p 570
YlPex8p 671
PpPex8p 713
HpPex8p 650
ScPex8p 589

Figure 3-6. Alignment of *Yl*Pex8p with other members of the Pex8p family. Abbreviations: *Yl*, *Y. lipolytica*; *Pp*, *P. pastoris*; *Hp*, *H. polymorpha*; *Sc*, *S. cerevisiae*; *gray*, similar residues; *black*, identical residues. Sequences were aligned using ClustalW. Similarity rules: A=S=T; D=E; N=Q; R=K; I=L=M=V; F=Y=W.

B) and peroxisomal protein-targeting defects (described below) as those of the original *pex8-1* mutant strain. The diploid strains *D-8OB*, *D-A8K* and *D-8KB* (Table 2-5), obtained by crossing *pex8* mutant strains with wild-type strain *22301-3* or *E122*, were able to grow on oleic acid containing medium (Fig. 3-1), establishing that the *pex8-1* mutation and the *PEX8* gene disruption are recessive. The *D-8O8K* diploid strain (Table 2-5), obtained by crossing the *pex8-KB* disruption strain with the *pex8-1* mutant strain, was unable to use oleic acid as a carbon source (Fig. 3-1), confirming that the *pex8-1* mutation is allelic to *PEX8*.

3.4 Regulation of *PEX8* expression and Pex8p synthesis

To study the regulation of Pex8p synthesis, the levels of *PEX8* mRNA and Pex8p protein were analyzed in various strains after growth on oleic acid- or glucose-containing medium. For the analysis of *PEX8* mRNA, cells of *E122*, *pex8-KA* and *pex8-1* were grown in glucose-containing YEPD medium for 14 h and then transferred to oleic acid-containing YPBO medium to induce peroxisome proliferation. Growth in YPBO medium was continued for 8 h. RNA was extracted from cells immediately prior to the shift to YPBO medium (0 h) and at 1-h intervals after the shift. Northern blot analysis was performed with equal amounts of RNA from each time point (Fig. 3-7 *A*). mRNA encoding Pex8p derived from *E122* cells was barely detectable in extracts of cells at 0 h but was readily visible at 1 h after cells were shifted to YPBO medium. Pex8p mRNA continued at elevated levels until the final time point at 8 h. The level of mRNA encoding Pex8p was much lower than that of mRNA encoding thiolase, a peroxisomal matrix protein induced by growth in oleic acid. Pex8p mRNA levels in the *pex8-1* strain

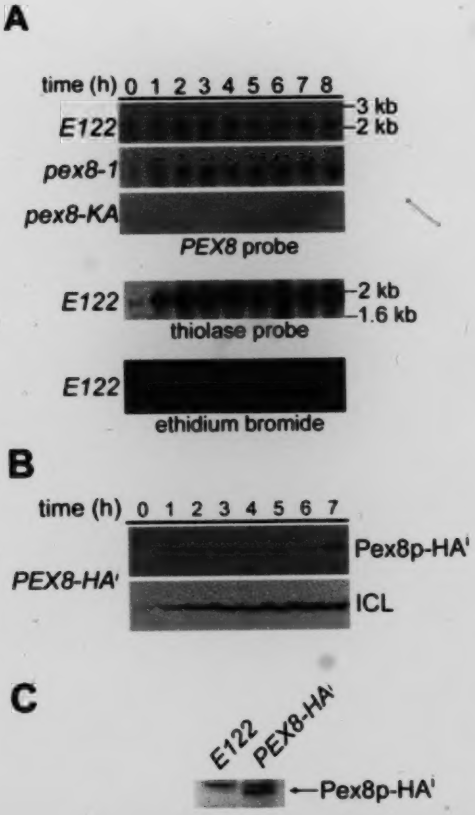
A
time (h) 0 1 2 3 4 5 6 7 8
E122
pex8-1
pex8-KA
3 kb
2 kb
PEX8 probe
E122
2 kb
1.6 kb
thiolase probe
E122
ethidium bromide
B
time (h) 0 1 2 3 4 5 6 7
PEX8-HA^{i}
Pex8p-HA^{i}
ICL
C
E122
PEX8-HA^{i}
Pex8p-HA^{i}

Figure 3-7. Expression of Pex8p mRNA and synthesis of Pex8p-HA^{i} are induced by growth of *Y. lipolytica* in oleic acid-containing medium. (A) Northern blot analysis of Pex8p mRNA. Total RNA was isolated from the wild-type strain *E122* and the mutant strains *PEX8-1* and *PEX8-KA* grown in YEPD medium (0 h) and at time points after transfer to YPBO medium (1-8 h). 10 µg of RNA from each time point was separated on a formaldehyde agarose gel and transferred to nitrocellulose. The loading of similar amounts of RNA was ensured by ethidium bromide staining (data for the wild-type *E122* strain; data for the mutant strains not shown). The blots were hybridized with radiolabelled probes specific for the *PEX8* gene and the gene encoding peroxisomal thiolase. Exposure time was 50 h for the Pex8p mRNA and 10 h for the thiolase mRNA. The numbers at right indicate the electrophoretic migrations of DNA markers (in kb). The numbers along the top indicate the time of oleic acid induction in hours. (B) Immunoblot analysis of Pex8p-HA^{i}. Total cell lysates were made from the *PEX8-HA^{i}* strain grown in YEPD (0 h) and at time points after transfer to YPBO. 40 µg of protein from each time point was subjected to electrophoresis on a 10% polyacrylamide gel in the presence of SDS and transferred to nitrocellulose for immunoblot analysis using anti-HA monoclonal antibodies (12CA5). The numbers along the top indicate the time of oleic acid induction in hours.

after the shift to YPBO medium were similar to those of the wild-type strain *E122*, suggesting that the mutation in the *pex8-1* strain does not affect transcription of the *PEX8* gene and does not cause the mRNA transcript to be unstable. As expected, no *PEX8* mRNA was detected in the *pex8-KA* disruption strain. These results suggest that the level of *PEX8* mRNA is coupled to peroxisomal induction.

The synthesis of Pex8p was analyzed by using the *PEX8-HA^i* strain, which synthesizes an HA epitope-tagged version of Pex8p (Pex8p-HA^i). This strain was able to use oleic acid as a carbon source (Fig. 3-1) and exhibited normal peroxisome morphology (Fig. 3-2 *F*). Immunoblotting with 12CA5 antibodies, which recognize the HA epitope, showed that Pex8p-HA^i was barely detectable in *PEX8-HA^i* cells grown in YEPD medium (Fig. 3-7 *B*) and could be seen only after extended exposure of the immunoblot (Fig. 3-7 *C*). The level of Pex8p-HA^i increased after the cells were shifted to YPBO medium, as did the level of the peroxisomal matrix protein, isocitrate lyase, but the levels of Pex8p-HA^i detected in lysates of each time point were more variable (Fig. 3-7 *B*).

3.5 Pex8p-HA^i is peripherally associated with the peroxisomal membrane

To examine the cellular distribution of Pex8p, subcellular fractionation was performed on *PEX8-HA^i* cells that were grown in oleic acid-containing medium for 8 h and fractions were analyzed. A postnuclear supernatant (PNS) was fractionated into a supernatant (20KgS) enriched for cytosol and a pellet (20KgP) enriched for peroxisomes and mitochondria. Immunoblot analysis showed Pex8p-HA^i to be localized primarily to the 20KgP fraction enriched for peroxisomes and mitochondria (Fig. 3-8 *A*). To determine if Pex8p was associated with peroxisomes, the organelles in the 20KgP

Figure 3-8. Subcellular localization of Pex8p-HA^{i}. (A) Immunoblot analysis with anti-HA monoclonal antibodies (12CA5) of PNS, 20KgS and 20KgP subcellular fractions (0.2% of the total volume of each) and of fractions of a sucrose density gradient (2% of the total volume of each). The distributions of the marker enzymes catalase (peroxisomes) and fumarase (mitochondria) in the gradient, as well as the sucrose density (g/cm^{3}) of fractions, are also presented. Pex8p-HA^{i} is enriched in those fractions enriched for catalase. (B) Immunoblot analysis of whole peroxisomes (PXM) and peroxisomal subfractions (Ti8S, Ti8P, CO$_3$S and CO$_3$P) of the *PEX8-HA*^{i} strain grown for 8 h in YPBO medium. Purified peroxisomes (30 µg of protein) were lysed with Ti8 buffer and subjected to centrifugation to yield a 245,000 x g_{max} supernatant (Ti8S) and pellet (Ti8P). CO$_3$S and CO$_3$P correspond to the 245,000 x g_{max} supernatant and pellet, respectively, recovered after treatment of Ti8P with 0.1 M Na$_2$CO$_3$ (pH 11.5). Blots were probed with antibodies to detect Pex8p-HA^{i} (12CA5), the peroxisomal integral membrane protein Pex2p, and the peroxisomal matrix protein thiolase. (C) Protease protection analysis. Whole peroxisomes (13 µg) isolated from the *PEX8-HA*^{i} strain were incubated with 1, 10, 20, or 40 µg of trypsin in the absence (-) or presence (+) of 0.5% (v/v) Triton X-100 for 40 min on ice. Samples were subjected to immunoblot analysis with anti-HA monoclonal antibodies (12CA5) to detect Pex8p-HA^{i} and with antibodies to the peroxisomal matrix protein isocitrate lyase (ICL).

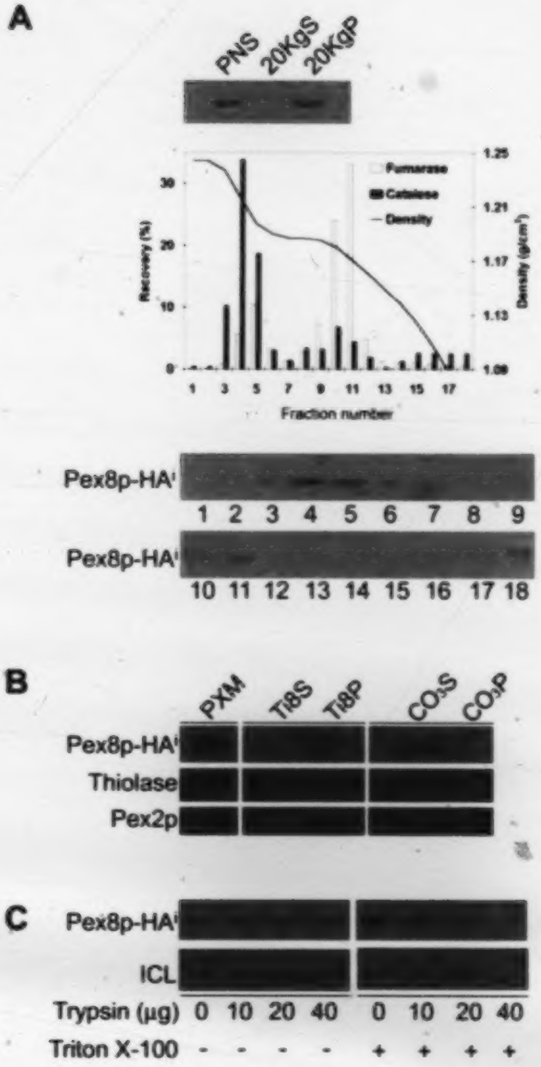
A
PNS
20KgS
20KgP
Fumarase
Catalase
Density
Recovery (%)
0
10
20
30
Density (g/cm³)
1.09
1.13
1.17
1.21
1.25
1
3
5
7
9
11
13
15
17
Fraction number
Pex8p-HA'
1 2 3 4 5 6 7 8 9
Pex8p-HA'
10 11 12 13 14 15 16 17 18
B
PXM
Ti8S
Ti8P
CO₃S
CO₃P
Pex8p-HA'
Thiolase
Pex2p
C
Pex8p-HA'
ICL
Trypsin (µg) 0 10 20 40 0 10 20 40
Triton X-100 - - - - + + + +

fraction were separated by isopycnic centrifugation on a discontinuous sucrose gradient, and fractions of equal volume were collected from the bottom of the gradient and analyzed (Fig. 3-8 *A*). The activity of the peroxisomal enzyme catalase peaked in fraction 4, whereas the activity of the mitochondrial enzyme fumarase peaked in fractions 9 and 10. Proteins in equal amounts of each fraction were separated by SDS-PAGE, and the location of Pex8p-HA^{i} in the gradient was determined by immunoblotting. Pex8p-HA^{i} cofractionated with the activity of catalase. To determine the subperoxisomal localization of Pex8p-HA^{i}, peroxisomes were extracted as described below and proteins in equal fractions of each extract were separated by SDS-PAGE and analyzed by immunoblotting. After an extraction of peroxisomes with Ti8 buffer followed by high-speed centrifugation, Pex8p-HA^{i} was found exclusively in the pellet fraction enriched for membranes, as was the peroxisomal integral membrane protein Pex2p, whereas the matrix protein thiolase was found in the supernatant (Fig. 3-8 *B*, lanes *Ti8P* and *Ti8S*). Treatment of the Ti8P fraction with 0.1 M Na_2CO_3 (pH 11.5), followed by high-speed centrifugation, liberated Pex8p-HA^{i} but not Pex2p from the pellet fraction (Fig. 3-8 *B*, compare lanes CO_3S and CO_3P), consistent with Pex8p-HA^{i} being associated with, but not integral to, the peroxisomal membrane.

A protease protection assay was performed with isolated peroxisomes to determine whether Pex8p-HA^{i} was preferentially associated with the matrix or cytosolic face of the peroxisomal membrane. Aliquots of peroxisomes were treated with increasing amounts of trypsin in the presence or absence of the nonionic detergent Triton X-100. Immunoblot analysis showed degradation of Pex8p-HA^{i} by trypsin in the presence, but not in the absence, of detergent, in a manner similar to that of the matrix protein isocitrate lyase (Fig. 3-8 *C*). The entire Pex8p-HA^i was protected from digestion by the peroxisomal membrane. These data suggest that Pex8p-HA^i is associated with the matrix face of the membrane; however, it is possible that Pex8p-HA^i is associated with the cytosolic surface of the peroxisomal membrane and that the addition of detergent exposes otherwise inaccessible trypsin sites.

3.6 Mutations in *PEX8* affect the localization of a subset of matrix proteins

To investigate the effects of mutation of the *PEX8* gene on peroxisomal matrix protein targeting, subcellular fractionation was performed on cells of the *E122*, *PEX8-HA^i*, *pex8-1*, and *pex8-KA* strains grown for 9 h in oleic acid-containing medium. A postnuclear supernatant (PNS) was isolated and separated by centrifugation at 20,000 x g_{max} to produce a pellet fraction (20KgP) enriched for organelles and a supernatant fraction (20KgS) enriched for cytosol. Equal portions of each fraction were analyzed both by immunoblotting and by measuring enzymatic activities. The levels of peroxisomal matrix proteins (i.e., malate synthase, acyl-CoA oxidase, a 62-kDa anti-SKL-reactive polypeptide, thiolase, isocitrate lyase, and catalase) in the PNS fraction of all four strains were analyzed. The levels of most of these proteins in the *pex8-1* and *pex8-KA* strains were unchanged from the levels in the wild-type strain, except for acyl-CoA oxidase, which was at levels 55% to 65% of that in the wild-type strain, and catalase, which was at levels approximately four times that found in the wild-type strain (Fig. 3-9 *A*). The reason for the highly elevated levels of catalase in the mutant strains is unknown.

The distributions of peroxisomal and mitochondrial proteins between the 20KgS and the 20KgP fractions for the various strains are illustrated in Fig. 3-9 *B* and *C*,

Figure 3-9. Peroxisomal matrix proteins are mislocalized to the 20KgS to varying extents in *pex8* mutants. Wild-type *E122* (*solid bar*), *PEX8* (*dark gray bar*), *PEX8-1* (*open bar*) and *PEX8-KA* (*light gray bar*) strains were grown in YPBO medium and subjected to subcellular fractionation. Malate synthase (MLS), acyl-CoA oxidase (AOX), a 62-kDa anti-SKL reactive polypeptide (SKL), thiolase (THI), and isocitrate lyase (ICL) were detected by immunoblot analysis with their respective antibodies. Immunoblots were quantified by densitometry (arbitrary units) in the range at which the antigen concentration was linearly proportional to the densitometric signal. The distributions of fumarase (FUM) and catalase (CAT) were determined from their enzymatic activities. (A) The total amount (activity) of proteins in the postnuclear supernatants (PNS) of the four strains expressed relative to the total amount (activity) of proteins in the wild-type strain *E122*, which is taken as 100%. (B) Recovery of proteins in the 20KgS. (C) Recovery of proteins in the 20KgP. For (B) and (C), recovery is reported as a percentage of the densitometric signal or enzymatic activity found in the PNS. Equal fractions of the 20KgS and 20KgP were analyzed for the distribution of matrix proteins. (D) Recovery of proteins in the 20KgPs of the *PEX8-1* and *PEX8-KA* mutant strains relative to their recovery in the 20KgP of the wild-type *E122* strain, which is taken as 100%.

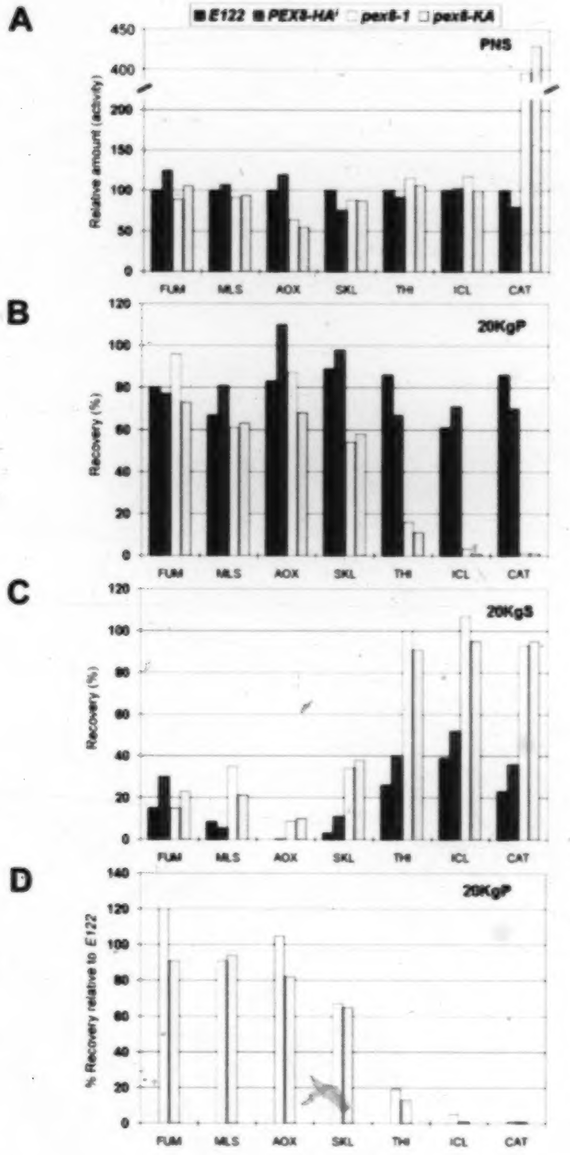
A
■ E122 ■ PEX8-HA' □ pex8-1 □ pex8-KA
PNS
Relative amount (activity)
0
50
100
150
200
400
450
FUM
MLS
AOX
SKL
THI
ICL
CAT
B
20KgP
Recovery (%)
0
20
40
60
80
100
120
FUM
MLS
AOX
SKL
THI
ICL
CAT
C
20KgS
Recovery (%)
0
20
40
60
80
100
120
FUM
MLS
AOX
SKL
THI
ICL
CAT
D
20KgP
% Recovery relative to E122
0
20
40
60
80
100
120
140
FUM
MLS
AOX
SKL
THI
ICL
CAT

respectively. In both the wild-type strain *E122* and the *PEX8-HA¹* strain, peroxisomal and mitochondrial proteins were associated primarily with the 20KgP. In the *pex8-1* and *pex8-KA* mutant strains, the mitochondrial marker enzyme fumarase was localized primarily to the 20KgP, as in the *E122* and *PEX8-HA¹* strains. However, the distributions of peroxisomal matrix proteins in the *pex8-1* and *pex8-KA* strains were different from those in *E122* (Fig 3-9 *D*). Although the mutant strains showed little impairment in their ability to target the matrix proteins malate synthase and acyl-CoA oxidase (both were imported at greater than 80% of the efficiency in wild-type cells), the targeting of other matrix proteins was affected to various greater degrees. A 62-kDa anti-SKL-reactive protein (a peroxisomal matrix protein) (Szilard et al., 1995) was mislocalized to the 20KgS to an intermediate extent (61% to 65% of the level in the 20KgP from the wild-type strain). Thiolase was more severely mislocalized to the 20KgS (less than 20% of the level in the 20KgP from the wild-type strain), whereas isocitrate lyase and catalase were almost exclusively mislocalized to the 20KgS (less than 5% of the levels in the 20KgP from the wild-type strain for each).

3.7 Peroxisomal proteins found in the 20KgPs of *pex8* mutant strains partially colocalize with marker proteins of other organelles

To determine if the peroxisomal marker proteins in the 20KgP fractions of *pex8* mutant cells are associated with peroxisomes, cells of oleic acid-grown *E122*, *pex8-1*, and *pex8-KA* strains were fractionated by isopycnic centrifugation on discontinuous sucrose gradients, and fractions were analyzed. The distributions of the mitochondrial marker fumarase, the peroxisomal marker catalase and the vacuolar marker alkaline phosphatase were determined by analyzing enzymatic activities in fractions derived from cells of *E122*, *pex8-1* and *pex8-KA* (Fig 3-10 *A*; -----, —o— and —•—, respectively). The distributions of the ER marker Kar2p and the peroxisomal markers thiolase and two anti-SKL-reactive polypeptides (the 62-kDa polypeptide and isocitrate lyase) were analyzed in fractions derived from cells of *E122* and *pex8-KA* by immunoblotting (Fig. 3-10 *B*). In the fractionation of the 20KgP derived from *E122* cells, the peroxisomal markers peaked in fraction 4 (density = 1.21 g/cm^3), the mitochondrial marker fumarase peaked in fraction 10 (density = 1.18 g/cm^3), whereas the ER marker Kar2p peaked in fraction 11 (density = 1.17 g/cm^3). Some trailing of Kar2p to both heavier and lighter fractions was evident. The vacuolar marker alkaline phosphatase showed a peak of activity in fraction 17 (density = 1.09 g/cm^3), with secondary peaks in fractions 4 and 10.

In the fractionation of the 20KgPs derived from *pex8-1* and *pex8-KA* cells, distributions of marker proteins were observed that were different from the wild-type distributions. All peroxisomal marker proteins colocalized and peaked in fraction 4, as for the wild-type strain. Even the small amounts of catalase and thiolase found in the 20KgPs of the *pex8* mutant strains (Fig. 3-9) peaked in fraction 4. Interestingly, fumarase and Kar2p also peaked in fraction 4 as well as in fractions 9 and 10. The presence of a large peak of alkaline phosphatase in fraction 4 from the *pex8-1* and *pex8-KA* mutant strains suggests that mutation of the *PEX8* gene may lead to increased autophagy. Colocalization of marker proteins of peroxisomes, mitochondria, and the ER in fraction 4 could result from the presence of elements of each of these organelles in autophagosomes, which may correspond to the multimembraned structures seen in electron micrographs of *pex8* mutant cells (Fig. 3-2 *B*, *D* and *E*).

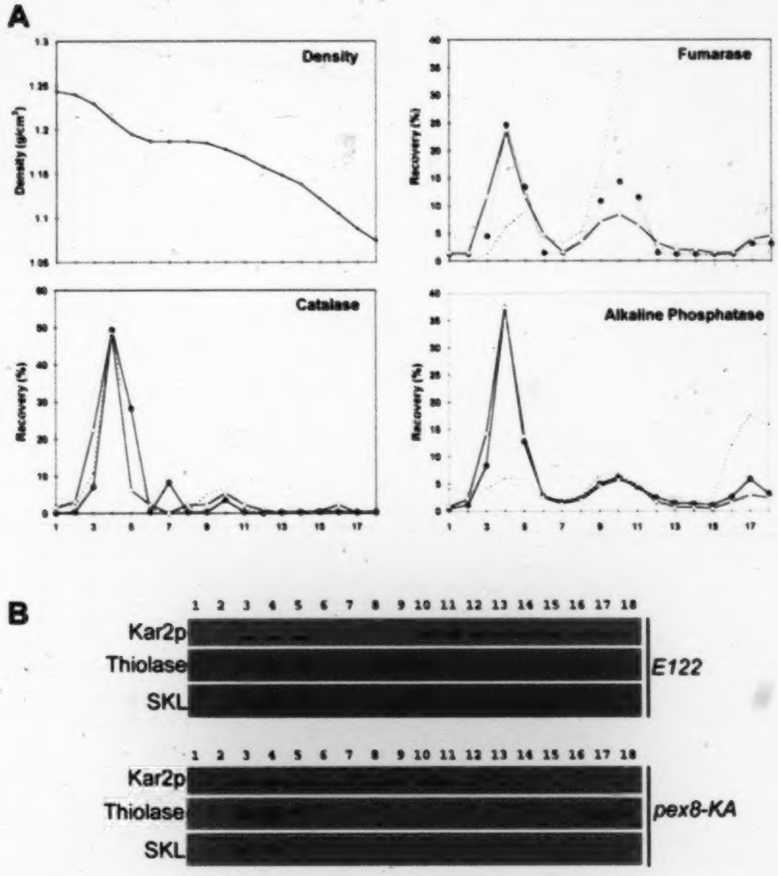

Figure 3-10. Sucrose density gradient analysis of 20KgPs from the wild-type strain and *pex8* mutant strains. 20KgPs (3 mg of protein each) isolated from the *E122*, *pex8-1*, and *pex8-KA* strains were subjected to sucrose density gradient centrifugation, and fractions were collected. Sucrose density (g/cm^3) and percent recovery of loaded protein and of enzymatic markers in gradient fractions for the strains *E122* (-----), *pex8-1* (—o—), and *pex8-KA* (—•—) are diagrammed. The distributions of fumarase, catalase and alkaline phosphatase were determined by analysis of enzymatic activities, and the distribution of Kar2p was determined by immunoblot analysis. Protein from equal volumes (1%) of each fraction was subjected to SDS-polyacrylamide gel electrophoresis, transferred to nitrocellulose and immunoblotted with antibodies to Kar2p, thiolase or the SKL carboxyl-terminal tripeptide (recognizing both isocitrate lyase and a 62-kDa peroxisomal matrix protein).

3.8 Analysis of the import defect of *pex8-KA* by immunofluorescence microscopy

We analyzed the distribution of peroxisomal proteins in *E122* and *pex8-KA* by double-labelling indirect immunofluorescence microscopy. Oleic acid-grown cells of *E122* and *pex8-KA* each transformed with pMyc-MFE2, encoding a Myc epitope-tagged version of the β-oxidation enzyme MFE2, were labelled indirectly with antibodies to thiolase and the Myc epitope (Fig. 3-11 *A*). Although thiolase and Myc-MFE2 colocalized in a punctate pattern of fluorescence characteristic of peroxisomal proteins in the wild-type *E122* cells, they showed a diffuse pattern of fluorescence characteristic of cytosolic proteins in the *pex8-KA* cells. Oleic acid-grown cells of the *E122* and *pex8-KA* strains were labelled indirectly with antibodies to the PTS1 tripeptide SKL, which recognize both isocitrate lyase and the 62-kDa anti-SKL-reactive protein, and to the integral peroxisomal membrane protein, Pex2p (Fig. 3-11 *B*). In the wild-type *E122* cells, both antibodies colocalized and had a punctate pattern of fluorescence characteristic of peroxisomal proteins. In the *pex8-KA* cells, Pex2p showed a punctate pattern of fluorescence whereas the anti-SKL-reactive proteins showed a more diffuse pattern of fluorescence that appeared to partially colocalize with the Pex2p pattern. These data indicate that Pex2p and a fraction the anti-SKL-reactive proteins may be peroxisomal in *pex8-KA* cells. Further evidence to support a peroxisomal localization of Pex2p in the *pex8-KA* strain is provided in Section 4.9.

3.9 Analysis of the *pex8-1* mutant allele of *PEX8*

To further characterize the *pex8-1* mutant strain, the *pex8-1* allele was isolated from a plasmid library of *pex8-1* genomic DNA by colony hybridization using a

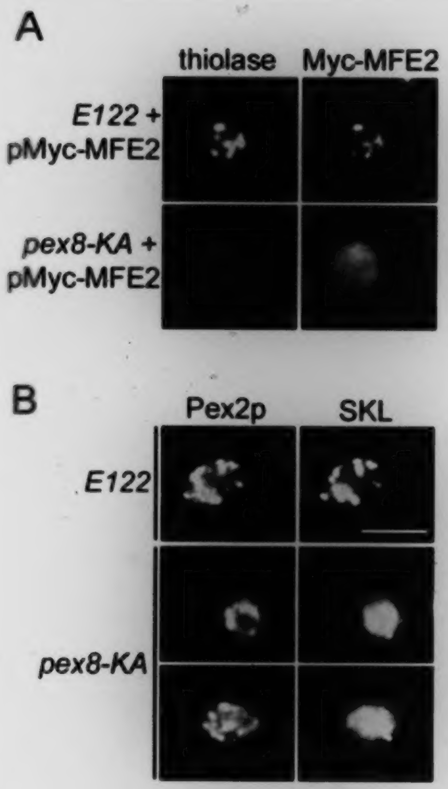

Figure 3-11. Localization of peroxisomal proteins in a *PEX8* disruption strain by immunofluorescence microscopy. (*A*) Strains *E122* and *pex8-KA* were transformed with the plasmid pMyc-MFE2, grown overnight in YND medium, and then grown for 10 h in YNO medium. Cells were fixed for 2 min in 3.7% formaldehyde and processed for double-labelling indirect immunofluorescence microscopy using guinea pig anti-thiolase (*left panels*) and mouse anti-c-Myc (*right panels*) antibodies. Guinea pig primary antibodies were detected with fluorescein-conjugated donkey anti-guinea pig IgG secondary antibodies, and mouse primary antibodies were detected with rhodamine-conjugated donkey anti-mouse IgG secondary antibodies. (*B*) Strains *E122* and *pex8-KA* were grown overnight in YEPD medium and then grown for 10 h in YPBO medium. Cells were fixed for 30 min in 3.7% formaldehyde and processed for double-labelling indirect immunofluorescence microscopy using guinea pig antibodies to the peroxisomal membrane protein Pex2p and rabbit antibodies to the carboxyl-terminal tripeptide SKL (recognizing both isocitrate lyase and a 62-kDa peroxisomal matrix protein). Guinea pig primary antibodies were detected with rhodamine-conjugated donkey anti-guinea pig IgG secondary antibodies, and rabbit primary antibodies were detected with fluorescein-conjugated donkey anti-rabbit IgG secondary antibodies. Bar = 10 μm.

radiolabelled probe specific for the *PEX8* gene. By sequencing the *pex8-1* allele, it was determined that it contains a single substitution mutation in the *PEX8* gene (A1924T), creating a premature stop codon. *pex8-1* encodes Pex8-1p, a version of Pex8p lacking its carboxyl-terminal 30 amino-acid residues.

3.10 Discussion

3.10.1 Pex8p has a role in peroxisome maintenance–In this chapter, the generation, isolation and characterization of *pex8* mutant strains of *Y. lipolytica* are described, as well as the identification and characterization of the *PEX8* gene, and its encoded peroxin, Pex8p.

Unlike the wild-type strain, *pex8* strains are unable to use oleic acid as a carbon source. Growth of *pex8* strains in oleic acid-containing media leads to the accumulation of structures surrounded by multiple membranes rather than to the formation of normal peroxisomes, which proliferate under these conditions in the wild-type strain. These results suggest that *pex8* mutant strains are defective in the maintenance of functional peroxisomes.

Results of the localization of peroxisomal marker proteins in wild-type cells and cells of the *pex8* mutant strains, both by subcellular fractionation analysis and by immunofluorescence microscopy, confirm that *pex8* mutant strains are defective in peroxisome maintenance. In cells of these strains, various peroxisomal membrane proteins are mislocalized, including catalase, isocitrate lyase, thiolase and MFE2, which are almost completely mislocalized, and a 62-kDa anti-SKL-reactive polypeptide, which is only partially mislocalized. This selective mislocalization does not appear to depend on the type of PTS found in a particular matrix protein. For example, thiolase, which contains a PTS2 (Berninger et al., 1993), and MFE2 and isocitrate lyase, which contain PTS1 sequences (Section 5.5 and Barth and Schueber, 1993, respectively), are mislocalized to the cytosol. Although various matrix proteins are mislocalized in *pex8* mutant strains, the location of an integral peroxisomal membrane protein, Pex2p, appears to be peroxisomal in the *PEX8* disruption strain, *pex8-KA*. Further evidence for the peroxisomal localization of Pex2p in *pex8-KA* is provided in Section 4.9.

Interestingly, mutation of the *PEX8* gene results in colocalization of marker proteins of the peroxisome, mitochondrion, ER and vacuole, as determined by subcellular fractionation and density gradient centrifugation analysis. This colocalization could result from increased autophagy in *pex8* mutant strains, with elements of peroxisomes, mitochondria and ER undergoing digestion together in autophagosomes, which may correspond to the multimembrane structures seen in electron micrographs of *pex8* cells.

3.10.2 Characteristics of PEX8 and its encoded peroxin Pex8p–The *Y. lipolytica PEX8* gene and its product Pex8p were characterized. Pex8p is a 671-amino acid protein with a predicted molecular mass of 75,588 Da. The *PEX8* gene contains a putative upstream oleic acid-response element and consistent with this, the synthesis of Pex8p-HA^{i}, an HA epitope-tagged version of the protein, was induced by growth of *Y. lipolytica* in oleic acid-containing medium. Although three possible transmembrane domains were identified in Pex8p by hydropathy plot anlysis, sodium carbonate extraction of a fraction from the *PEX8-HA*^{i} strain suggests that Pex8p is peripherally associated with the peroxisomal membrane. Protease protection analysis of fractions from this strain suggests that Pex8p is intraperoxisomal. Database searches revealed sequence similarity between Pex8p and proteins of the Pex8p family of peroxins (Fig. 3-5), which are defined as 71- to 81-kDa peroxisome-associated proteins containing PTS1 motifs (Distel et al., 1996). Interestingly, the carboxyl-terminal tripeptide of *Yl*Pex8p does not fit the consensus PTS1 sequence.

The *pex8-1* mutant gene encodes Pex8-1p, a truncated version of Pex8p missing 30 amino acid residues at its carboxyl terminus. As *pex8-1* mRNA is present at wild-type levels in cells of the *pex8-1* mutant strain (Fig. 3-7), Pex8-1p may also be present at wild-type levels in this strain. If this is the case, the carboxyl-terminal 30 amino-acid residues of Pex8p are important for its function.

3.10.3 Possible role for Pex8p in peroxisome maintenance–pex8 mutants of *Y. lipolytica* and of other yeasts (Waterham, 1994; Liu et al., 1995; Rehling et al., 2000) mislocalize a subset of matrix proteins to the cytosol. This phenotype suggests that Pex8p either has a direct role in matrix protein import or that it has a role in another aspect of maintenance that indirectly causes matrix proteins to be mislocalized. We suggest that Pex8p has a direct role in the import of matrix proteins for two reasons: 1) Peroxisomal matrix and membrane proteins are imported into peroxisomes by distinct pathways (Section 1.6.3; Erdman and Blobel, 1996; Gould et al., 1996). Therefore, if Pex8p is involved directly in matrix protein import, the localization of membrane proteins is expected to be unaffected. Integral peroxisomal membrane protein Pex2p appears to be peroxisomal in *Y. lipolytica pex8* mutants. In addition, it has recently been demonstrated that Pex11p and Pex14p, integral and peripheral peroxisomal membrane proteins, respectively, localize to structures characteristic of peroxisomes in an *S. cerevisiae PEX8* disruption strain (Rehling et al., 2000). 2) Cells of *pex* mutant strains that are specifically defective in matrix protein import characteristically contain large, often multimembraned, structures instead of normal peroxisomes (for example, see Szilard et al., 1995). In contrast, cells of *pex* mutant strains, whose matrix protein import defects are a consequence of other defects such as defects of membrane protein import or peroxisome fusion, typically contain very small vesicular structures (for example, see Nuttley et al., 1994). Cells of *pex8* mutant strains of *Y. lipolytica* and of other yeast strains contain peroxisomal remnants that are typical of strains defective specifically in matrix protein import.

In conclusion, these data point to a role for *Yl*Pex8p in the import of matrix proteins into peroxisomes. To further understand the function of Pex8p in peroxisome maintenance, a search for peroxins that physically interact with Pex8p was conducted. The results of this investigation and the characterization of one interaction are discussed in the next chapter.

CHAPTER 4

ROLE OF PEX8P IN PEX20P-DEPENDENT THIOLASE IMPORT

A version of this chapter entitled "Role of the peroxin Pex8p in Pex20p-dependent thiolase import into peroxisomes of the yeast *Yarrowia lipolytica*" (Jennifer J. Smith and Richard A. Rachubinski) has been submitted for publication to *The Journal of Biological Chemistry*.

4.1 Overview

This chapter describes the identification of physical interactions between *Y. lipolytica* Pex8p and Pex20p, Pex8p and Pex5p, and Pex1p and Pex6p using a yeast two-hybrid system and the characterization of the Pex8p-Pex20p interaction. The isolation of a complex containing Pex8p and Pex20p by coimmunoprecipitation from a lysate of wild-type cells confirms that these two proteins interact. The results of an *in vitro* binding study with recombinant proteins demonstrate that the Pex8p-Pex20p interaction is specific, direct and autonomous.

Pex20p is a primarily cytosolic peroxin that binds directly to the β-oxidation enzyme thiolase and is necessary for its dimerization and peroxisomal targeting (Titorenko et al., 1998). Detection of the Pex8p-Pex20p interaction may indicate that Pex20p targets Pex8p to peroxisomes, but Pex8p is not cytosolic in cells of a *PEX20* disruption strain, suggesting that this is not the case. An alternative possibility is that Pex8p is directly involved in the import of thiolase into peroxisomes. Consistent with this hypothesis, in cells of a *PEX8* disruption strain, thiolase is mostly cytosolic, and Pex20p and a small amount of thiolase are associated with the peroxisomal membrane and protected from proteases. These data point to a role for Pex8p in the import of thiolase after docking of the Pex20p-thiolase complex to the membrane and suggest that Pex20p accompanies thiolase into peroxisomes during import.

During the analysis of the Pex8p-Pex20p interaction, an interaction between Pex20p and a previously uncharacterized protein, p100 was identified. The sequence of p100 is very similar to C_1-tetrahydrofolate synthases (C_1-THFSs), enzymes involved in the biosynthesis of purines and amino acids.

4.2 Detection of physical interactions amongst peroxins

A limited two-hybrid screen (Fields and Song, 1989) was performed to identify physical interactions amongst *Y. lipolytica* peroxins Pex1p, Pex2p, Pex5p, Pex6p, Pex8p, Pex9p, Pex16p and Pex20p. Others have used this methodology successfully to detect interactions amongst peroxins (for examples, see Götte et al., 1998 and Erdmann and Blobel, 1996). Chimeric genes were constructed by ligating *Y. lipolytica PEX* genes in-frame and downstream of sequences encoding one of the two functional domains (AD or DB) of the GAL4 transcriptional activator. All possible combinations of plasmid pairs encoding AD and DB fusion proteins were transformed into the *S. cerevisiae* strain *SFY526*, and β-galactosidase filter detection assays were performed initially. Physical interaction between peroxins was expected to bring the two domains of the GAL4 transcriptional activator together and result in activation of transcription of the integrated *lacZ* construct resulting in detectable β-galactosidase activity in the form of blue coloration of the yeast colony in the presence of the substrate X-gal. Potential interactions were detected between Pex8p and Pex5p and between Pex1p and Pex6p using the filter assay.

To confirm the results of the filter assays, liquid β-galactosidase assays were performed. Cell lysates of strains synthesizing both Pex1p and Pex6p fusion proteins showed much greater β-galactosidase activity than lyastes of the control strains synthesizing either one or the other of the fusion proteins (Fig. 4-1 *A*), demonstrating that Pex1p and Pex6p interact physically. Lysates of strains synthesizing both Pex8p and Pex5p fusion proteins also showed very high β-galactosidase activity, but so did the

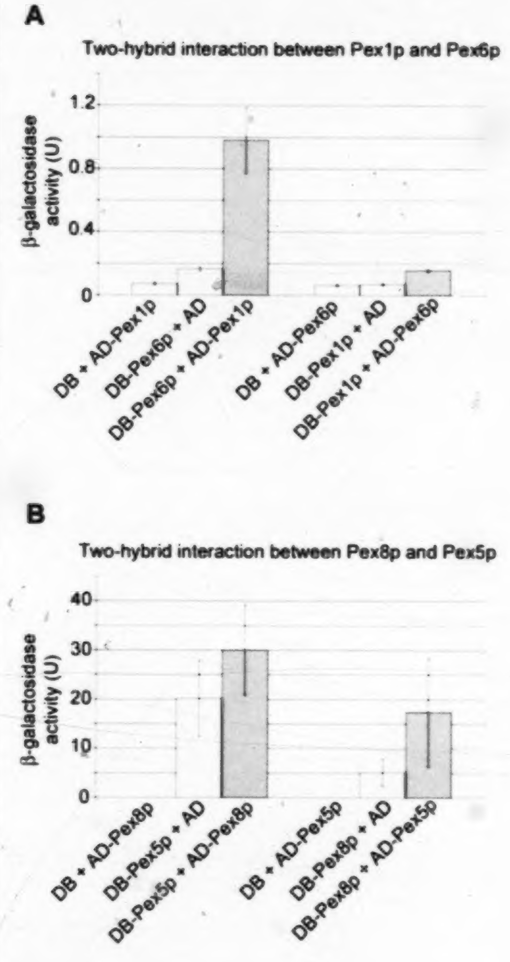

Figure 4-1. Identification of Pex1p-Pex6p and Pex8p-Pex5p interactions using the yeast two-hybrid system. A comparison of β-galactosidase activities of strains doubly transformed with plasmids encoding the fusion proteins labelled along the x-axis of each graph. β-galactosidase activity is measured in units (U) defined by the manufacturer (Clonetech). (*A*) Pex1p and Pex6p physically interact. Each column is a measure of the average β-galactosidase activity of at least three individual transformants. (*B*) Pex8p and Pex5p physically interact. Each column is a measure of the average β-galactosidase activity of at least six individual transformants. The levels of activity from strains synthesizing DB-Pex8p and AD-Pex5p, and DB-Pex5p and AD-Pex8p are significantly different from those of the control strains at confidence levels of 95% and 90%, respectively. Error bars represent standard deviations.

lysates of control strains synthesizing one or the other of the fusion proteins (Fig. 4-1 *B*). Using the Smith-Satterthwaite test for statistical significance (Devore, 1987), it was determined that the levels of β-galactosidase activity from strains synthesizing both DB-Pex8p and AD-Pex5p or both DB-Pex5 and AD-Pex8 were significantly higher than those of the corresponding control strains at confidence levels of 95% and 90%, respectively, suggesting that Pex8p and Pex5p physically interact.

Lysates of strains transformed with constructs encoding DB-Pex8p or DB-Pex20p showed high levels of β-galactosidase activity, making it difficult to identify an interaction between Pex20p and Pex8p. Therefore, a plasmid encoding DB-Pex20p(1-76), a fusion between the DB domain and the amino-terminal 76 amino-acid residues of Pex20p, was constructed. DB-Pex20p does not have intrinsic transcription activational activity. Lysates of strains synthesizing both AD-Pex8p and DB-Pex20p(1-76) showed significantly higher β-galactosidase activity than did lysates of control strains synthesizing one or the other of the fusion proteins (Fig. 4-2; compare *row 1* to *rows 5* and *6*), suggesting that Pex8p and Pex20p interact physically. To characterize this interaction further, fusions to smaller domains of Pex8p were assayed. DB-Pex20p(1-76) still interacted with AD-Pex8p(12-644), containing Pex8p truncated at both its amino and carboxyl termini, but did not interact with AD domain fusions to more extensive amino- or carboxyl-terminal truncations of Pex8p (Fig. 4-2, compare *row 2* to *rows 3* and *4*). Therefore, Pex8p physically interacts with the amino terminus of Pex20p, and the 11 amino-terminal and 27 carboxyl-terminal amino-acid residues of Pex8p are dispensable for the interaction.

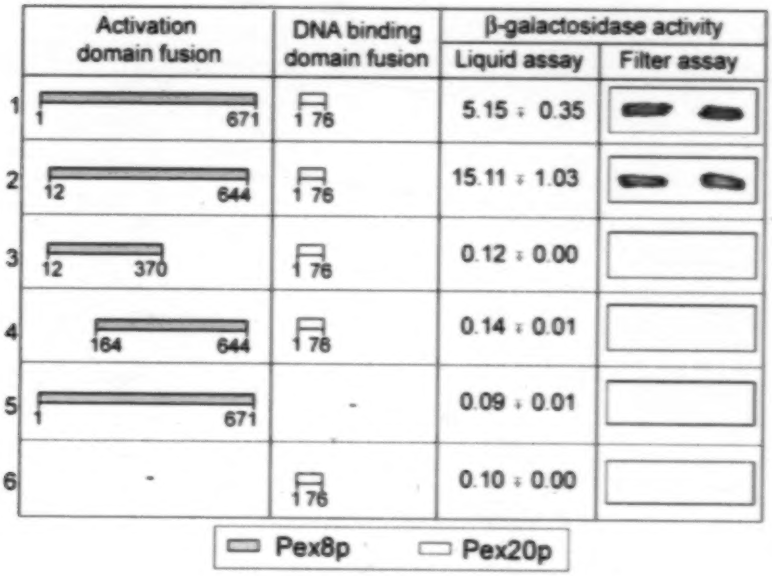

	Activation domain fusion	DNA binding domain fusion	β-galactosidase activity	
			Liquid assay	Filter assay
1	1 671	1 76	5.15 ± 0.35	
2	12 644	1 76	15.11 ± 1.03	
3	12 370	1 76	0.12 ± 0.00	
4	164 644	1 76	0.14 ± 0.01	
5	1 671	-	0.09 ± 0.01	
6	-	1 76	0.10 ± 0.00	

Pex8p
Pex20p

Figure 4-2. Analysis of physical interaction between Pex8p and the amino terminus of Pex20p using the yeast two-hybrid system. *SFY596* cells doubly transformed with chimeric genes encoding activation domain (*first column*) and DNA-binding domain (*second column*) fusion proteins were tested for β-galactosidase activity. The Pex8p and Pex20p portions of fusions are diagrammed as *shaded bars* and *open bars*, respectively, and numbers indicate the amino-acid residues at the amino and carboxyl termini. The activities obtained from the liquid assay (*third column*) are averages of the activities of three independent transformants ± standard deviations. For the filter assay, the color intensities of two representative independent transformants for each strain are shown (*last column*).

4.3 The interaction between Pex8p and Pex20p is direct and autonomous

Some interactions between peroxins that have been detected using the yeast two-hybrid system have been shown to be indirect (Huhse et al., 1998; Girzalsky et al., 1999). Therefore, it is possible that an endogenous *S. cerevisiae* protein may have bridged the observed interaction between Pex8p and Pex20p. To determine if the interaction between Pex8p and Pex20p is direct and autonomous, an *in vitro* binding assay was performed. The ORFs encoding Pex8p and Pex20p were fused to the 3' ends of DNA sequences encoding MBP and GST, respectively. The chimeric genes were expressed in *E. coli*, and fusion proteins were purified. GST and GST-Pex20p were immobilized on glutathione-Sepharose beads and tested for their ability to bind MBP or MBP-Pex8p. Proteins in bound and unbound fractions were separated by SDS-PAGE and visualized by staining with Coomassie Brilliant Blue (Fig. 4-3). MBP-Pex8p interacted with GST-Pex20p, whereas GST or MBP alone did not interact with MBP-Pex8p or GST-Pex20p, respectively. These data demonstrate that Pex8p interacts directly and autonomously with Pex20p.

4.4 Identification of p100, a second Pex20p-interacting protein

An *in vitro* binding experiment was performed to determine if GST-Pex20p could interact specifically with Pex8p tagged with the hemagglutinin epitope at its carboxyl terminus, Pex8p-HA^c, in a yeast lysate. GST and GST-Pex20p were immobilized on glutathione-Sepharose beads. A total cell lysate was prepared from *PEX8-HA^c*, a strain synthesizing Pex8p-HA^c, and incubated with immobilized GST or GST-Pex20p. The proteins bound to each column and the proteins of the total cell lysate were separated by

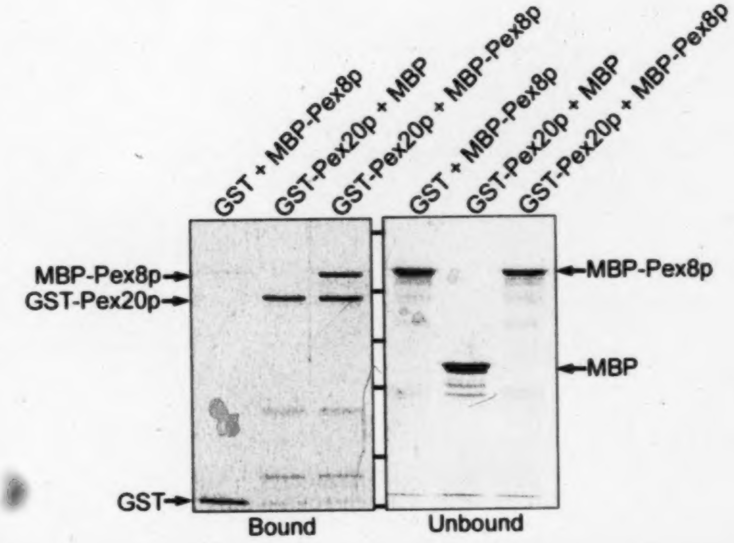
GST + MBP-Pex8p
GST-Pex20p + MBP
GST-Pex20p + MBP-Pex8p
GST + MBP-Pex8p
GST-Pex20p + MBP
GST-Pex20p + MBP-Pex8p
MBP-Pex8p
GST-Pex20p
GST
MBP-Pex8p
MBP
Bound
Unbound

Figure 4-3. ***In vitro* binding studies showing that the Pex8p-Pex20p interaction is direct and autonomous.** Genes encoding MBP, MBP-Pex8p, GST and GST-Pex20p were expressed in *E. coli*, and the proteins were purified. GST or GST-Pex20p were bound to glutathione Sepharose and then incubated with MBP or MBP-Pex8p as indicated at the *top* of each panel. 25% of bound (*left panel*) and 50% of unbound (*right panel*) fractions were separated on a 9% polyacrylamide gel and stained with Coomassie Brilliant Blue R-250. The migrations of molecular mass markers are marked between the panels. The markers are 175, 83, 62, 47.5, 32.5 and 25 kDa from *top* to *bottom*. MBP-Pex8p and GST-Pex20p interacted, whereas GST or MBP alone did not interact with MBP-Pex8p or GST-Pex20p, respectively.

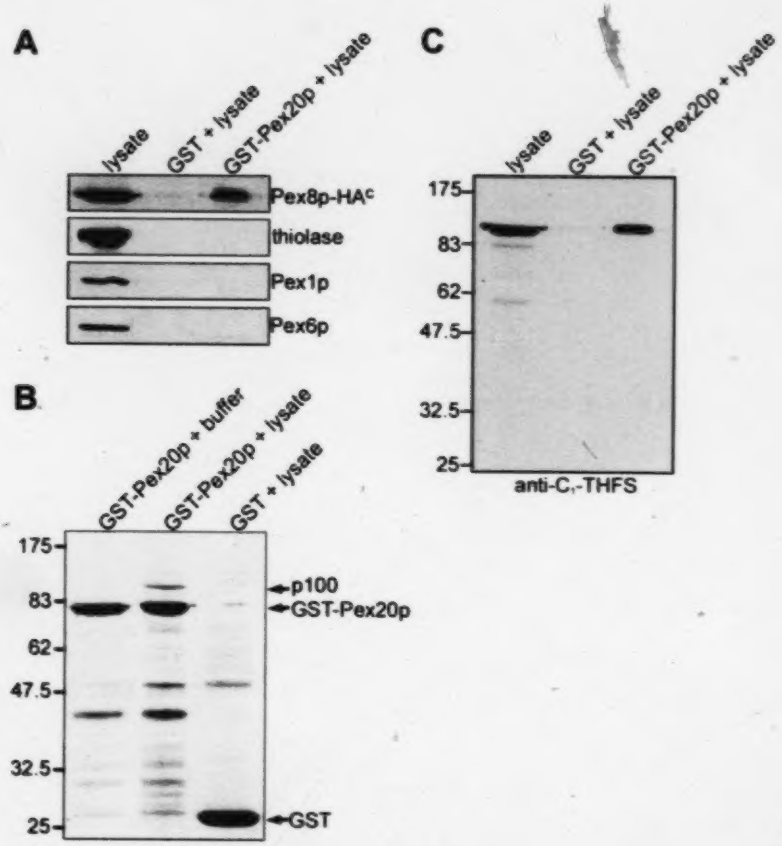
A
lysate
GST + lysate
GST-Pex20p + lysate
Pex8p-HA^c
thiolase
Pex1p
Pex6p
B
GST-Pex20p + buffer
GST-Pex20p + lysate
GST + lysate
175
83
62
47.5
32.5
25
p100
GST-Pex20p
GST
C
lysate
GST + lysate
GST-Pex20p + lysate
175
83
62
47.5
32.5
25
anti-C1-THFS

Figure 4-4. Specific interaction of Pex8p-HA^c and a 100-kDa protein from a yeast lysate with the GST-Pex20p fusion. Equal amounts of GST or GST-Pex20p were immobilized on glutathione Sepharose and incubated with a total cell lysate of the strain *PEX8-HA^c* or with buffer, as indicated at the *top* of each panel. Columns were washed, and bound proteins were eluted and separated by SDS-PAGE, along with a fraction of the total cell lysate. (*A*) Proteins were transferred to nitrocellulose and analyzed by immunoblotting. Blots were probed with various antisera, as indicated at *right*. Pex8p-HA^c specifically interacts with GST-Pex20p. (*B*) Proteins bound to each column were visualized by staining with Coomassie Brilliant Blue R-250. The migrations of the molecular mass markers (in kDa) are at *left*. p100, an ~100-kDa protein that bound specifically to GST-Pex20p is labelled at *right*. (*C*) Immunoblot showing p100 reacts with antiserum to cytosolic C_1-THFS of *S. cerevisiae*.

SDS-PAGE, transferred to nitrocellulose and analyzed by immunoblotting with various antibodies (Fig. 4-4 *A*). Pex8p-HA^c interacted specifically with GST-Pex20p, whereas the peroxins Pex1p and Pex6p did not. Interestingly, peroxisomal thiolase, which has been shown to interact with Pex20p (Titorenko et al., 1998), did not bind GST-Pex20p. Perhaps the interaction of GST-Pex20p with thiolase is hindered by the GST moiety.

To identify other proteins that are capable of physically interacting with Pex20p, the proteins bound to each column were separated by SDS-PAGE and stained (Fig. 4-4 *B*). Almost all bands detected in the fraction derived from GST-Pex20p incubated with the cell lysate were also detected in fractions derived from either GST-Pex20p incubated with buffer or GST incubated with the cell lysate. Therefore, most bands were either peptides derived from GST-Pex20p or proteins that nonspecifically interacted with the column material. Interestingly, one peptide of approximately 100 kDa, designated p100, bound to GST-Pex20p and not to GST alone. This band was not present in a fraction of GST-Pex20p that was not incubated with lysate.

4.5 p100 is similar to C_1-tetrahydrofolate synthases of other organisms

Sequences of tryptic fragments derived from p100 were obtained by Micromass (Manchester, United Kingdom). Essentially, p100 was excised from a gel stained with Coomassie Brilliant Blue R-250 and digested with trypsin. The tryptic fragments were analyzed by capillary liquid chromatography tandem mass spectrometry (LC-MS/MS) using a Q-TOF mass spectrometer, and several peptide sequences were obtained. The peptide sequences were compared to protein sequences deposited in the NCBI Protein Database. Excluding trypsin autolysis products and peptides derived from human keratin, nine peptides were sequenced. Seven of these were similar in sequence to portions of C_1-tetrahydrofolate synthases (C_1-THFSs) of *S. cerevisiae*, and the other two had no matches. C_1-THFSs are multifunctional enzymes that catalyze the interconversion of tetrahydrofolate between different oxidation states in both the cytosol and mitochondria. The products of this interconversion are involved in several metabolic processes including nucleic acid synthesis and the biosynthesis and conversions of amino acids (reviewed in Wagner, 1995).

The peptide sequences were used to isolate the gene encoding p100 by colony hybridization. Degenerate oligonucleotides 1001 and 1002 (Table 2-3), which were designed from two peptide sequences that were similar to C1-THFS, were used to amplify a DNA fragment from wild-type strain *E122* by PCR. This fragment was radiolabelled and used as a probe to isolate a larger genomic fragment from a *Y. lipolytica* genomic library by colony hybridization. Of the ~5,000 colonies screened, two were positives and the plasmids in each were shown to be identical by restriction mapping. Sequencing of the genomic insert revealed a potential ORF of 2813 bp encoding a protein of 937 amino-acid residues and having a molecular weight of 100,193 Da (Fig. 4-5). The ORF was designated THFS. A TATA box could not be found in the 426 bp of sequence upstream of the potential ORF. ‘A’ nucleotides are found at positions –1 and –3 upstream of the initiator ATG, a feature common to strongly expressed genes of *Y. lipolytica* (Barth and Gaillardin, 1997). A comparison of the protein sequence to those deposited in the NCBI Protein Database showed that the sequence of the encoded protein is similar to those of C_1-THFSs of other organisms. p100 is aligned with the two *S. cerevisiae* C_1-THFS isoforms, human C_1-THFS, and a potential isoform of human C_1-

```
 -179                                      gaattctgggcctactacgtagtctttgttacccctcactgctccgctgggccatattcattggtgtaatt
 -108  gtcacaccccacgttctccacattaactttagaggttattcttgtcaggttggtgaaggtcgatttcaggagctaaacatctttctttcctctacaactatccacaca
        M  A  S  I  I  D  G  N  S  I  A  K  N  I  R  E  R  L  H  T  E  I  A  D  V  Q  Q  T  N  P  R  F  Q  P  S  L     36
    1  atggcctccatcatcgacggcaattccattgccaaaaacatccgagaacggctgcacaccgaaatcgccgatgtgcaacagaccaacccccgattccagccctctctg
        V  I  I  Q  V  G  D  R  P  D  S  S  T  Y  V  R  M  K  L  K  A  A  D  E  A  A  I  K  C  E  L  K  K  L  D  E     72
  109  gtcatcatccaggtcggcgatcgacccgactcgtccacctacgtgcgaatgaagctcaaggccgcggacgaggccgccatcaagtgcgagctcaagaaactggacgag
        N  V  S  Q  H  E  L  L  R  E  I  T  E  L  N  E  D  P  S  V  D  G  V  L  V  Q  L  P  L  P  K  H  I  D  E  T    108
  217  aacgtgtcccagcacgagctgctgcgggagatcacccacctgaacgaggacccctccgtggacggtgttctggtccagctccctctgcccaagcacattgacgagacc
        T  I  T  N  A  V  A  A  D  K  D  V  D  G  F  G  P  L  N  I  G  E  L  A  K  R  G  G  N  P  S  F  V  A  C  T    144
  325  accatcaccaatgccgtcgccgccgacaaggacgttgatggcttcggtcctctcaacattggcgagctcgccaagcgaggtggaaacccttccttcgtcgcttgcacc
        P  K  G  V  M  E  L  L  K  V  A  G  I  D  V  A  G  K  T  A  V  V  L  G  R  S  D  I  V  G  A  P  V  S  Y  L    180
  433  cccaagggagtcatggagctgctcaaggttgccggcatcgatgttgctggcaagaccgctgttgttcttggccgatccgacattgtcggagcccccgtttcctatctg
        L  R  N  A  D  A  T  V  T  V  V  H  S  K  T  A  N  I  P  E  I  V  K  T  A  D  I  V  V  A  A  I  G  Q  P  G    216
  541  ctgcgaaacgctgacgctaccgtcactgtcgtgcactccaaaactgccaacatccccgagattgtcaagactgccgacattgttgtcgccgccattggccagcccggc
        F  V  K  G  E  W  L  K  P  G  A  V  V  I  D  V  G  T  N  Y  I  P  D  D  T  K  K  S  G  Q  R  L  V  G  D  V    252
  649  tttgtcaagggtgagtggctcaagcctggcgccgttgtcatcgacgtgggaaccaactacattcccgatgataccaagaagtctggccagcgacttgttggagatgtt
        D  F  E  S  A  K  N  V  A  S  H  I  T  P  V  P  G  G  V  G  P  M  T  V  A  M  L  L  D  N  V  V  L  S  A  K    288
  757  gactttgagtctgccaagaacgtagcctcccacatcacccccgtccccggaggagtgggtcccatgaccgtggccatgctgctggacaacgttgtgctctctgccaag
        R  Q  A  E  K  L  T  A  R  S  I  T  P  L  P  L  K  K  E  N  P  V  P  S  D  F  A  I  S  R  A  Q  E  P  K  H    324
  865  cgacaggccgagaagttgaccgctcgatccatcacccctctgcctcttaagaaggagaaccctgtgccctccgactttgccatttctcgagcccaagagcccaagcac
        I  T  E  V  A  A  E  I  G  V  L  P  S  E  L  E  P  Y  G  A  Y  K  A  K  V  Q  L  P  I  L  D  R  L  A  H  R    360
  973  atcaccgaggtggctgccgaaattggcgtgctgccctctgagctcgagccctacggagcctacaaggccaaggtccagctgcccattcttgaccgtctggcccaccga
        K  N  G  K  Y  V  L  V  T  G  I  T  P  T  P  L  G  E  G  K  S  T  T  T  I  G  L  V  Q  A  L  G  A  H  L  G    396
 1081  aagaacggaaagtacgttctagtcaccggaatcactcccacccctcttggagagggcaagtccaccaccaccattggtctggtgcaggctcttggtgcccatcttggt
        K  M  A  F  A  N  V  R  Q  P  S  M  G  P  T  F  G  I  K  G  G  A  A  G  G  G  Y  A  Q  V  I  P  M  D  E  F    432
 1189  aagatggcttttgccaacgtcagacagccctccatgggccctacctttggtattaagggaggagctgctggaggaggatacgcccaggttatccccatggatgagttc
        N  M  H  L  T  G  D  I  H  A  I  S  A  A  N  N  L  L  A  A  A  I  D  T  R  M  F  H  E  S  T  Q  K  D  A  A    468
 1297  aacatgcacctgaccggtgacattcacgccatttcagctgccaacaacctgcttgccgctgccattgacacccgaatgtttcatgagtctacccagaaggacgctgct
        L  Y  K  R  L  V  P  A  K  K  G  V  R  T  F  T  R  G  M  Q  T  R  L  K  K  L  G  I  D  K  T  N  P  D  D  L    504
 1405  ctttacaagcgtctggtgcctgccaagaagggcgttcgaaccttcactcgaggcatgcagacccgactcaagaagcttggtatcgacaagaccaaccccgacgatctg
        T  E  E  E  I  A  K  F  V  R  L  D  I  D  P  E  T  I  T  W  R  R  V  V  D  C  N  D  R  H  L  R  G  I  T  V    540
 1513  actgaggaggagattgccaagtttgtgcgtctcgacattgatcctgagaccatcacctggcgacgagtggtcgattgcaatgatcgacatctgcgaggtatcactgtt
        G  Q  A  P  T  E  K  G  R  T  R  E  T  G  F  D  I  S  V  A  S  E  C  M  A  I  L  A  L  A  N  D  L  E  D  M    576
 1621  ggacaggcccctaccgagaagggccgaacccgagagaccggctttgacatttccgtcgcctccgagtgtatggccattctggctcttgccaacgatctcgaggacatg
        R  E  R  L  G  N  M  V  I  G  S  S  K  N  G  D  P  V  T  C  D  D  I  G  A  G  G  A  L  T  A  L  M  K  D  A    612
 1729  cgagagcgacttggaaacatggtcattggttcttccaagaacggcgaccccgtcacttgtgacgatatcggtgctggtggtgctcttactgctctcatgaaggacgcc
        I  K  P  N  L  M  Q  T  L  E  G  T  P  V  F  V  H  A  G  P  F  A  N  I  S  I  G  A  N  S  V  L  A  D  K  M    648
 1837  atcaagcccaacctcatgcagactctggagggtacccccgtctttgtgcatgccggtcccttcgccaacatttccattggtgctaactccgtgctggccgacaagatg
        A  L  K  L  A  G  T  E  P  N  E  S  D  D  K  A  G  F  V  V  T  E  A  G  F  D  F  T  M  G  G  E  R  F  F  N    684
 1945  gctctcaagctggctggtaccgaacccaacgagtctgacgacaaggccggctttgtggtcaccgaggccggtttcgatttcaccatgggaggtgagcgattcttcaac
        I  K  C  R  S  S  G  L  A  P  D  V  V  V  I  V  A  T  V  R  A  L  K  S  H  G  G  G  P  E  V  K  A  G  A  P    720
 2053  atcaagtgccgatcttccggtctggctcctgacgttgttgtcattgtcgctaccgttcgagccctgaagtctcatggaggaggtcctgaggtcaaggccggtgctcct
        L  P  K  E  Y  T  E  E  N  V  E  L  L  R  E  G  C  K  N  L  G  K  H  I  E  N  A  R  Q  Y  G  L  P  V  V  V    756
 2161  ctccccaaggagtacaccgaggagaacgtggagctcctgcgagagggatgcaagaacctcggaaagcacattgagaacgcccgacagtacggtctgcccgtggttgtt
        A  I  N  E  F  V  S  D  T  A  A  E  H  D  V  I  R  E  E  A  L  K  Y  G  A  E  D  A  V  V  A  K  H  W  A  E    792
 2269  gccatcaacgagtttgtctccgataccgctgccgagcacgatgtcatccgagaggaggctcttaagtacggtgccgaggacgctgttgtcgccaagcactgggccgaa
        G  G  A  G  A  V  D  L  A  Q  A  V  V  D  A  S  N  K  I  D  K  D  F  K  L  L  Y  E  A  D  T  T  A  E  E  K    828
 2377  ggaggcgctggagccgtggatcttgcccaggccgtcgttgacgcctccaacaagatcgacaaggatttcaagctgctttacgaggccgacacaaccgctgaggagaag
        L  N  T  I  A  Q  K  M  Y  G  A  K  D  V  E  L  S  E  L  A  R  K  K  I  D  A  Y  T  K  Q  G  F  G  N  L  P    864
 2485  ctcaacaccattgcccagaagatgtacggcgccaaggacgtggagctttccgagctggcccgaaagaagattgacgcctacaccaagcagggcttcggcaacctgccc
        I  C  V  A  K  T  Q  Y  S  L  S  H  D  P  T  L  K  G  V  P  T  G  F  T  V  P  I  R  D  V  R  A  S  V  G  A    900
 2593  atctgtgtggccaagacccagtactctctttcccacgaccctactctcaagggagtgcccactggcttcactgtgcccattcgagatgttcgagcctctgttggtgct
        G  Y  L  Y  A  L  A  A  E  I  Q  T  I  P  G  L  P  T  H  C  G  F  M  N  V  E  V  N  D  K  G  E  I  E  G  L    936
 2701  ggctacctctacgctctggctgccgagatccagaccattcctggtctccccactcattgtggcttcatgaacgttgaggtcaacgacaagggcgagatcgagggtctt
        F  -                                                                                                           937
 2809  ttctaagaccgcagtgtgacaccacacgattaaattattcaactaagcatcctaccagttcaacacgtatataagaatgcacgccaaagcgcgacttgtgatatgacc
 2962  tgaatgaaatctgcttgtaatgtgttggggtgttcactatactctaatttgctattgctgtatttttggccgtatggcaacaccatgatgtagtgtttggatgctttt
 3025  agggatcatgaaaagtatatcgatcgattcagaatttcgcgctgattcgattgataccaaaatatcctcctggaatatattgtagcttaacctattgctgctcagtta
 3133  cattgatacttacggcgtggtgtcataccgcccgtatacctgtttcaaacagtagtcatggtctatgccggatcagggggaaataaccgacggactatacaactacaa
 3241  caaggagaaccgtttattgatgctatttccggatacgtataatccgtaagtacttctattcgtacttactgtataatgtataatgtacttgtaataaggtcatgtctc
 3349  gtatcgtatttctaggtttcttcactccatgtccaccccgaagttatttacagcatgttgcagcttcaggtgcatgagtggagatcgtcggatccggatgaatctgcg
```

Figure 4-5. Nucleotide sequence of *THFS* and deduced amino acid sequence of p100.

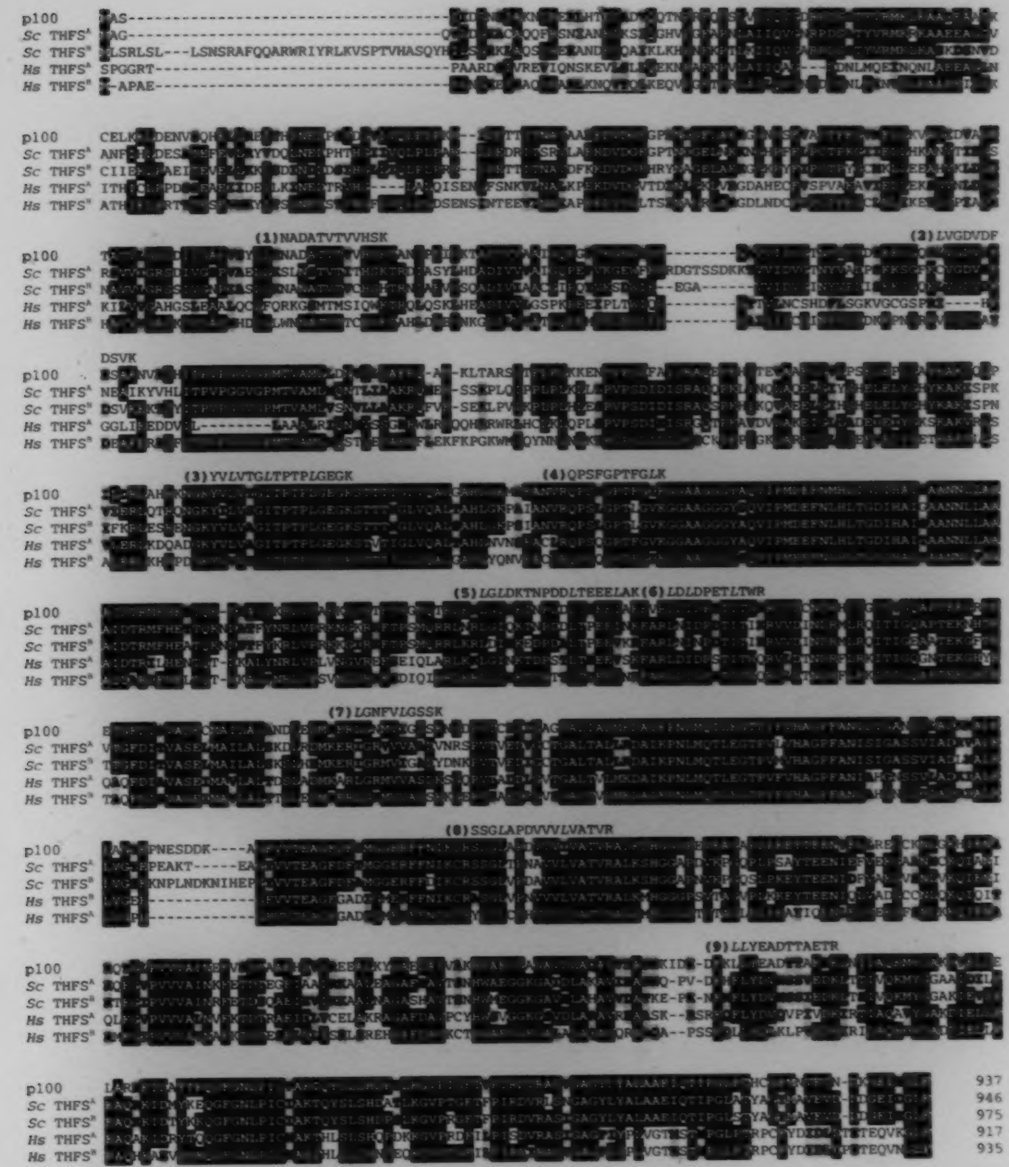
p100
Sc THFS^{A}
Sc THFS^{B}
Hs THFS^{A}
Hs THFS^{B}
(1) NADATVTVVHSK
(2) LVGDVDF
DSVK
(3) YVLVTGLTPTPLGEGK
(4) QPSFGPTFGLK
(5) LGLDKTNPDDLTEEELAK
(6) LDLDPETLTWR
(7) LGNFVLGSSK
(8) SSGLAPDVVVLVATVR
(9) LLYEADTTAETR
937
946
975
917
935

Figure 4-6. p100 is similar to C_1-THFSs of other organisms. p100 is aligned with the two *S. cerevisiae* C_1-THFS isoforms (*Sc* THFS^{A} and *Sc* THFS^{B}), human C_1-THFS (*Hs* THFS^{B}), and a potential second human isoform (*Hs* THFS^{A}). Identical and similar residues are shaded in *black* and *gray*, respectively. For similarity rules see the legend of Figure 3-6. A PTS2 consensus sequence near the amino terminus of *Hs* THFS^{B} is *underlined*. Sequences of *Sc* THFS^{A}, *Sc* THFS^{B}, *Hs* THFS^{A} and *Hs* THFS^{B} are available from EMBL/GenBank under accession numbers M12878, J03724, CAB55934 and A31903 (J04031), respectively. The peptide sequences obtained by LC-MS/MS of p100 tryptic fragments are printed above the p100 sequence. Leucine and isoleucine residues could not be differentiated and are designated as *L* in the tryptic fragment sequences.

THFS (Fig. 4-6). A mitochondrial targeting signal has been identified at the amino terminus of the *S. cerevisiae* isoform labelled THFS^B, and it has been proposed that this is the mitochondrial C_1-THFS (Shannon and Rabinowitz, 1988). Human C_1-THFS has not been localized, but, interestingly, it has a consensus PTS2 near its amino terminus (*underlined* amino-acid residues). The peptide sequences obtained using LC-MS/MS are shown as the top line of the alignment. All nine of the sequences are either identical or very similar to regions of the deduced protein sequence of p100.

To confirm the identity of p100, antiserum to the nonmitochondrial isoform of *S. cerevisiae* (*Sc* THFS^A in Fig. 4-6) was tested for its ability to recognize p100 in fractions of the *in vitro* binding assay described in Section 4.4. Equal portions of the yeast lysate fractions that bound to GST and GST-Pex20p and a fraction of the total cell lysate were separated by SDS-PAGE, transferred to nitrocellulose and immunoblotted with antiserum to C_1-THFS (Fig. 4-4 *C*). The antiserum recognized a single band of approximately 100 kDa in a fraction of the total cell lysate and in a fraction of GST-Pex20p incubated with lysate. This band was not recognized in a fraction of GST incubated with lysate. The reactive band was superimposable onto p100 visualized by Ponceau S staining of the nitrocellulose. These data confirm that the peptides sequenced were derived from p100 and that p100 has sequence similarity to C_1-THFSs of other organisms.

4.6 Pex8p-HA^c and p100 coimmunoprecipitate with Pex20p

To determine if Pex20p was capable of interacting with Pex8p-HA^c and p100 *in vivo*, Pex20p was immunoprecipitated under native conditions from a total lysate of cells grown in YPBO medium, and coimmunoprecipitating proteins were analyzed by SDS-

PAGE and immunoblotting with various antibodies (Fig. 4-7). Although all proteins tested were present in the total cell lysate, Pex8p-HA^c and p100 (recognized by antibodies to C_1-THFS) coimmunoprecipitated specifically with Pex20p but not with peroxisomal isocitrate lyase (ICL) or the peroxin Pex6p. These data suggest that Pex8p-HA^c and p100 interact with Pex20p *in vivo*. As previously reported (Titorenko et al., 1998), the precursor form of thiolase also specifically coimmunoprecipitated with Pex20p.

4.7 p100 does not have characteristics of a peroxisomal protein

The levels of many peroxisomal enzymes are high in yeast cells grown in the presence of oleic acid relative to those in cells grown in the presence of glucose (van der Klei and Veenhuis, 1997). To determine if p100 has this characteristic, wild-type cells were grown in the presence of glucose or oleic acid, cells were lysed and fractions of each lysate were separated by SDS-PAGE and analyzed by immunoblotting (Fig. 4-8 *A*). The levels of p100 were the same in lysates of glucose- and oleic acid-grown cells, as were the levels of the ER protein Kar2p.

To determine the subcellular location of p100 and to determine if Pex20p has a role in targeting p100, we localized p100 in the presence and absence of Pex20p. Cells of the wild-type strain *E122* and of the *PEX20* disruption strain *pex20KO* were fractionated. For each cell type, a postnuclear supernatant (PNS) was isolated and then separated into a fraction enriched for cytosol and high-speed pelletable organelles (20KgS) and a fraction enriched for peroxisomes and mitochondria (20KgP). The 20KgS fraction was further separated into a cytosolic fraction (200KgS) and a fraction enriched

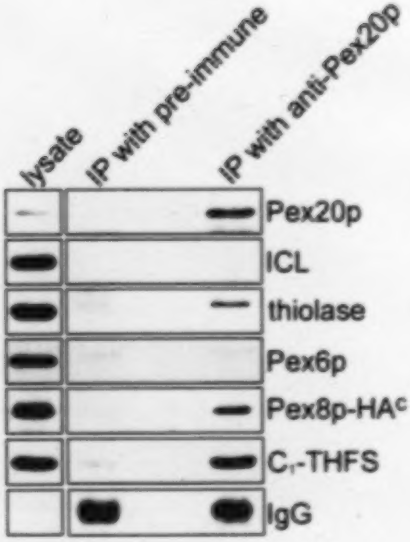
lysate
IP with pre-immune
IP with anti-Pex20p
Pex20p
ICL
thiolase
Pex6p
Pex8p-HA^c
C₁-THFS
IgG

Figure 4-7. Coimmunoprecipitation of Pex8p-HA^c and p100 with Pex20p. Pex20p was immunoprecipitated from total cell lysates of YPBO-grown *PEX8-HA^c* strain with antiserum to Pex20p or with preimmune serum. 10 µg of cell lysate and 20% of each immunoprecipitate were separated by SDS-PAGE and immunoblotted with various antisera (labelled at *right*). Although all proteins tested were present in the lysate, Pex8p-HA^c, unprocessed thiolase and p100 (recognized with antibodies to C_1-THFS) specifically coimmunoprecipitated with Pex20p, whereas peroxisomal isocitrate lyase (ICL) and the peroxin Pex6p did not. The bottom blot shows that each reaction contained approximately the same number of IgG heavy chain molecules.

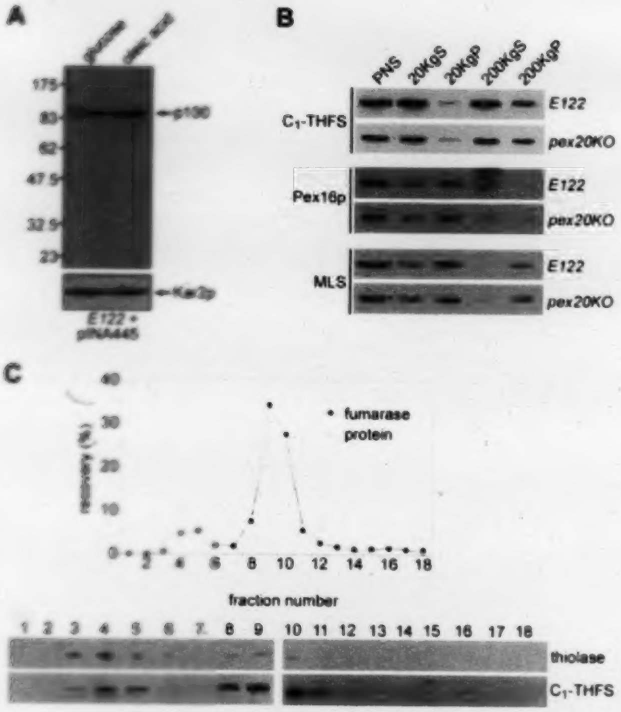

Figure 4-8. Localization of C_1-THFS in the wild-type and *PEX20* disruption strain. (*A*) Levels of C_1-THFS are the same in cells grown in glucose- and oleic acid-containing medium. Cells of the wild-type strain *E122* transformed with plasmid pINA445 were grown overnight in YND or YNO medium. Total cell lysates were prepared, and proteins were subjected to immunoblot analysis using antibodies to C_1-THFS (*top panel*) and Kar2p (*bottom panel*). The migrations of molecular mass standards (in kDa) are indicated at the left. (*B*) Immunoblot analysis of subcellular fractions of the wild-type strain *E122* and of the *PEX20* disruption strain *pex20KO*. The postnuclear supernatant (*PNS*) from each strain was separated into a fraction enriched for cytosol and high-speed pelletable organelles (*20KgS*) and a fraction enriched for peroxisomes and mitochondria (*20KgP*) fractions. The 20KgS fraction of each was separated into supernatant (*200KgS*) and pellet (*200KgP*). (*C*) Organelles of the 20KgP derived from wild-type cells were separated by sucrose density gradient centrifugation. Fractions were analyzed by measuring the enzymatic activity of the mitochondrial enzyme fumarase and by immunoblot analysis using antiserum to peroxisomal thiolase and to C_1-THFS.

for high-speed pelletable organelles (200KgP). All fractions were analyzed by immunoblotting (Fig. 4-8 *B*). p100 (recognized by antibodies to C_1-THFS) was primarily in fractions enriched for cytosol and high-speed pelletable organelles (20KgS, 200KgS and 200KgP), whereas the peroxisomal markers malate synthase and Pex16p were in the organelle-enriched fractions 20KgP and 200KgP in both strains. These data suggest that Pex20p is not necessary for the localization of p100 and that p100 is primarily cytosolic. To determine if the portion of p100 in the 20KgP fraction was associated with peroxisomes, organelles of this fraction were separated by isopycnic density gradient centrifugation, and fractions were analyzed by enzymatic analysis (mitochondrial fumarase) and by immunoblotting (p100 and peroxisomal thiolase) (Fig. 4-8 *C*). p100 (recognized by antibodies to C_1-THFS) colocalized with fumarase (in fractions 8 to 11) and not with thiolase (in fractions 3 to 5). Although a small fraction of p100 is present in fractions 4 and 5, a small amount of mitochondrial fumarase is also in these fractions, indicating that the presence of p100 in fractions 4 and 5 is likely due to contamination of the peroxisome fraction with mitochondrial proteins. These data suggest that the pelletable fraction of p100 is mitochondrial.

These data indicate that the level of p100 is not coupled to peroxisomal induction and that p100 is not peroxisomal, although, it is possible that the antibody used recognizes p100 as well as other isoforms of C_1-THFS in *Y. lipolytica*. In addition, it is also possible that the portion of p100 in the 200KgP fraction is associated with high-speed pelletable peroxisomes.

4.8 Pex20p is not required for the targeting of Pex8p-HA^c to peroxisomes

As Pex20p binds thiolase in the cytosol and is necessary for its targeting to peroxisomes (Titorenko et al., 1998), and because Pex20p interacts with Pex8p-HA^c, we investigated whether Pex20p might also bind Pex8p in the cytosol and act in targeting it to peroxisomes. To test this hypothesis, Pex8p-HA^c was localized by subcellular fractionation of cells of the wild-type strain *E122*, a *PEX20* disruption strain *pex20KO*, and a *PEX20* mutant strain *pex20-1* (Table 2-5), each transformed with the expression plasmid pPEX8-HA^c. For each strain, a PNS fraction was separated into 20KgS and 20KgP fractions and the 20KgS fraction was further separated into 200KgS and 200KgP fractions. Equal portions of each fraction were separated by SDS-PAGE and analyzed by immunoblotting (Fig. 4-9). Pex8p-HA^c was present in fractions enriched for peroxisomes and high-speed pelletable peroxisomes (20KgS, 20KgP and 200KgP) but not in the highly enriched cytosolic fraction (200KgS) of cells of all strains, suggesting that Pex20p is not required for the targeting of Pex8p to peroxisomes. As expected, thiolase was preferentially localized to peroxisome-enriched fractions of the wild-type strain and to cytosol-enriched fractions of cells of the *PEX20* mutant strains.

4.9 Pex20p and a small amount of thiolase are peroxisome associated in cells of a *PEX8* disruption strain

Interaction between Pex20p and Pex8p may occur at the level of the peroxisomal membrane during the targeting or import of thiolase. Consistent with this scenario, only a small fraction of thiolase is peroxisomal in a *PEX8* disruption strain (Sections 3.6 to 3.8). To further elucidate the role of Pex8p in the import of thiolase, the localization of Pex20p

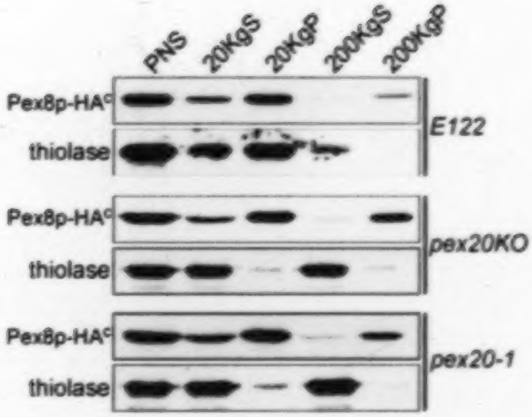
PNS
20KgS
20KgP
200KgS
200KgP
Pex8p-HA^c
thiolase
E122
Pex8p-HA^c
thiolase
pex20KO
Pex8p-HA^c
thiolase
pex20-1

Figure 4-9. Subcellular localization of Pex8p-HA^c in wild-type and *pex20* mutant strains. Immunoblot analysis of subcellular fractions of the wild-type strain *E122*, the *PEX20* disruption strain *pex20KO* and the original *PEX20* mutant strain *pex20-1*, each transformed with pPEX8-HA^c encoding Pex8p-HA^c. The postnuclear supernatant (*PNS*) fraction from each strain was separated into a fraction enriched for cytosol and high-speed pelletable organelles (*20KgS*) and a fraction enriched for peroxisomes and mitochondria (*20KgP*). The 20KgS fraction from each strain was separated into a high-speed supernatant (*200KgS*) and pellet (*200KgP*).

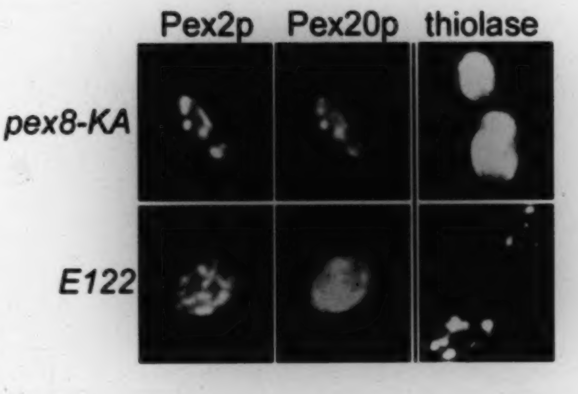

Figure 4-10. Pex20p is peroxisomal in cells of the *PEX8* disruption strain, *pex8-KA*. Strains *pex8-KA* (*top panels*) and *E122* (*bottom panels*) were grown overnight in YEPD medium and then transferred to YPBO medium and grown for 9 h. Cells of each strain were processed for immunofluorescence microscopy. Cells were either double labelled using guinea pig anti-Pex2p antibodies (*left panels*) and rabbit anti-Pex20p antibodies (*middle panels*) or labelled using guinea pig anti-thiolase antibodies (*right panels*). Guinea pig primary antibodies were detected with rhodamine-conjugated donkey anti-guinea pig IgG secondary antibodies, and rabbit primary antibodies were detected with fluorescein-conjugated donkey anti-rabbit IgG secondary antibodies. Pex20p colocalizes with peroxisomal membrane protein Pex2p in cells of *pex8-KA*, but has a diffuse cytosolic staining in wild-type cells. Thiolase, a peroxisomal matrix protein in wild-type cells, is cytosolic in cells of *pex8-KA*.

and the subperoxisomal localization of peroxisome-associated thiolase were determined in cells of the *PEX8* disruption strain, *pex8-KA* (Table 2-5). The localization of Pex20p was first analyzed by double-labelling immunofluorescence microscopy of YPBO-grown cells of wild-type strain *E122* and disruption strain *pex8-KA* (Fig. 4-10). In the wild-type cells, Pex20p had a diffuse localization characteristic of a cytosolic protein, whereas the peroxisomal membrane protein Pex2p had a punctate localization. This was expected as Pex20p is primarily cytosolic in this strain (Titorenko et al, 1998). Interestingly, in cells of *pex8-KA*, Pex20p colocalized with Pex2p to punctate structures characteristic of peroxisomes. As expected, peroxisomal thiolase had a diffuse localization in cells of the *pex8-KA* strain and a punctate localization characteristic of peroxisomes in cells of the wild-type strain. Therefore, whereas a very small fraction of Pex20p is peroxisomal in wild-type cells (Titorenko et al., 1998), a much larger fraction of Pex20p is associated with peroxisomes in cells devoid of Pex8p.

Pex20p and thiolase were also localized by subcellular fractionation of cells of the wild-type *E122* and *pex8-KA* strains. For each cell type, the PNS was separated into 20KgS and 20KgP fractions. Equal portions of each fraction were separated by SDS-PAGE and analyzed by immunoblotting (Fig. 4-11 *A*). As expected, Pex20p was found predominantly in the 20KgS fraction, whereas peroxisomal thiolase was found predominantly in the 20KgP fraction of cells of *E122*. In contrast, Pex20p was predominantly in the 20KgP fraction, whereas thiolase was primarily in the 20KgS fraction, of cells of *pex8-KA*. As expected, a small portion of thiolase was in the 20KgP fraction, as some thiolase is peroxisomal in *pex8-KA*. The results of subcellular fractionation are consistent with those of immunofluorescence analysis.

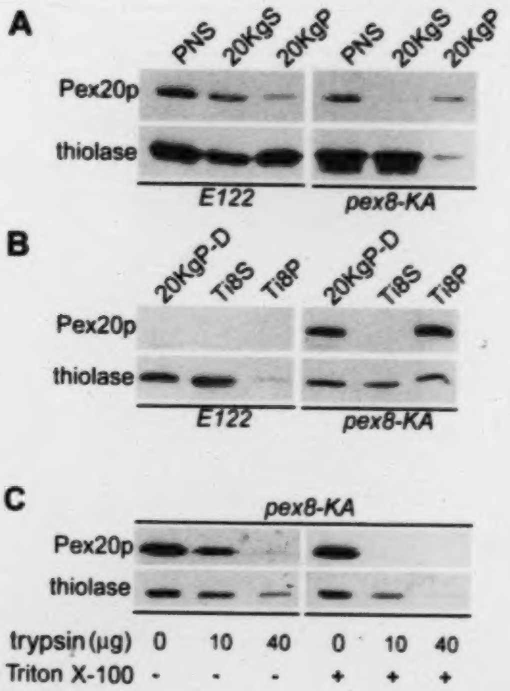
A
PNS
20KgS
20KgP
PNS
20KgS
20KgP
Pex20p
thiolase
E122
pex8-KA
B
20KgP-D
Ti8S
Ti8P
20KgP-D
Ti8S
Ti8P
Pex20p
thiolase
E122
pex8-KA
C
pex8-KA
Pex20p
thiolase
trypsin (μg) 0 10 40 0 10 40
Triton X-100 - - - + + +

Figure 4-11. Pex20p and a small amount of thiolase are associated with the peroxisomal membrane in cells of the *PEX8* disruption strain. (*A*) Immunoblot analysis of subcellular fractions of cells of wild-type strain *E122* and of *PEX8* disruption strain *pex8-KA*. For each, the postnuclear supernatant (*PNS*) fraction was separated into a supernatant enriched for cytosol and high-speed pelletable organelles (*20KgS*), and a pellet enriched for mitochondria and peroxisomes (*20KgP*). Proteins in equal portions of each fraction were separated by SDS-PAGE and immunoblotted with antibodies to Pex20p and thiolase. (*B*) Organelles in the 20KgP fraction were disrupted, and membranes were isolated by differential centrifugation. Proteins in equal fractions of the disrupted 20KgP fraction (*20KgP-D*), membrane pellet (*Ti8P*) and supernatant (*Ti8S*) were processed for immunoblotting as described in *A*. (*C*) Protease protection analysis. Organelles in the 20KgP fraction derived from cells of the *pex8-KA* strain were incubated with 0, 10, or 40 μg of trypsin in the absence (-) or presence (+) of 0.1% (v/v) Triton X-100 for 20 min on ice. Samples were immunoblotted with antisera to thiolase and Pex20p.

The subperoxisomal locations of Pex20p and thiolase in *pex8-KA* cells and in wildtype cells were now compared. Peroxisomes were disrupted by incubation of the 20KgP fraction in dilute Tris buffer. The disrupted 20KgP fraction (20KgP-D) was then separated by centrifugation into a pellet fraction (Ti8P) enriched for membranes and a supernatant fraction (Ti8S) enriched for soluble proteins. Proteins in equal portions of each fraction were separated by SDS-PAGE and analyzed by immunoblotting (Fig. 4-11 *B*). All detectable Pex20p and half of thiolase localized to the Ti8P fraction from *pex8-KA* cells. The conditions of the extraction were sufficient to release matrix proteins, as thiolase was almost completely extracted to the Ti8S fraction derived from wild-type cells after an identical incubation. Interestingly, Pex20p could not be detected in any wild-type subperoxisomal fraction, probably due to the extreme lability of Pex20p during extended subcellular fractionation analysis of wild-type cells.

The complete degradation of Pex20p in subperoxisomal fractions derived from wild-type cells and the absence of any extensive degradation of membrane-associated Pex20p in fractions derived from *pex8-KA* cells suggests that Pex20p is more resistant to the action of proteases in *pex8-KA* fractions. This resistance could be due to the fact that Pex20p is afforded enhanced protection from the action of proteases by the peroxsiomal membrane in fractions from *pex8-KA* cells. Alternatively, the increased protease resistance of Pex20p may be due to the possibility that during the course of fractionation, Pex20p remains associated with protective peroxisomal membranes in the absence of Pex8p but dissociates more readily from peroxisomal membranes of wild-type cells, facilitating its interaction with proteases.

To demonstrate that peroxisome-associated thiolase and Pex20p are protected from the action of proteases by the peroxisomal membrane in the absence of Pex8p, protease protection analysis was performed on the 20KgP fraction isolated from cells of the *pex8-KA* strain. Equal portions of the 20KgP fraction were incubated with increasing amounts of trypsin in the absence or presence of the nonionic detergent, Triton X-100. The proteins in equal portions of each reaction were separated by SDS-PAGE and analyzed by immunoblotting (Fig. 4-11 *C*). Both thiolase and Pex20p showed greater resistance to trypsin in the absence of detergent than in its presence. Therefore, thiolase and Pex20p associated with peroxisomes of *pex8-KA* may be afforded protection from the action of proteases by the peroxisomal membrane.

4.10 Discussion

Using the yeast two-hybrid system, an interaction between Pex8p and the amino terminus of Pex20p was identified. To confirm the Pex8p-Pex20p interaction, a complex containing Pex8p and Pex20p was isolated from a cell lysate by coimmunoprecipitation. The interaction was shown to be specific, direct and autonomous using *in vitro* binding studies with recombinant proteins. Although Pex20p and Pex8p are in different cellular compartments, there are at least two possible mechanisms for their interaction. One possibility is that Pex20p binds Pex8p in the cytosol and is necessary for its oligomerization and/or peroxisomal targeting. A second possibility is that Pex8p interacts with Pex20p at the peroxisomal membrane at a step in the import of thiolase into peroxisomes. To elucidate the mechanism of interaction of these two proteins, Pex8p and Pex20p were localized in cells of a *PEX20* and a *PEX8* disruption strain, respectively.

4.10.1 Pex20p-dependent targeting and/or oligomerization of Pex8p–The possibility of a Pex20p-dependent targeting and/or oligomerization of Pex8p is consistent with evidence that suggests Pex8p of *H. polymorpha* may be an oligomer (Waterham et al., 1994). It is also compatible with the fact that Pex8p is intraperoxisomal and, in most yeasts, contains a PTS1 motif (Liu et al., 1995) or both PTS1 and PTS2 motifs (Waterham et al., 1994; Rehling et al., 2000). As Pex8p shares the same types of PTS with peroxisomal metabolic enzymes, it is conceivable that it is also targeted to peroxisomes by the same peroxins involved in targeting these enzymes. Although this explanation is plausible, two lines of evidence suggest that Pex20p is not necessary for the targeting and/or oligomerization of Pex8p. Firstly, assuming that mislocalized or nonoligomerized Pex8p molecules are nonfunctional, if Pex20p were necessary for the oligomerization and/or the targeting of Pex8p, then a *PEX20* disruption strain should have a phenotype as severe as, or more severe than, a *PEX8* disruption strain. This is not the case, as several matrix proteins are mislocalized in *PEX8* disruption strains (Sections 3.6 and 3.8) (Waterham et al., 1994; Liu et al., 1995; Rehling et al., 2000), whereas only thiolase is mislocalized in a *PEX20* disruption strain (Titorenko et al., 1998). Secondly, an epitope-tagged version of Pex8p was present in fractions containing peroxisomes and mitochondria and not in cytosolic fractions derived from cells of a *PEX20* disruption strain and a *PEX20* mutant strain. Although these data strongly suggest that Pex20p is not necessary for the targeting and/or oligomerization of Pex8p, the possibility that two functionally redundant systems exist, one that requires Pex20p and one that does not, cannot be ruled out.

4.10.2 A role for Pex8p in the Pex20p-dependent import of thiolase–An alternative prospect is that Pex8p and Pex20p interact at the peroxisomal membrane as a step in the targeting or import of thiolase. This hypothesis is consistent with the fact that Pex8p is membrane-associated in three different systems including *Y. lipolytica* (Section 3.5) (Liu et al., 1995; Rehling et al., 2000) and with the fact that in cells of a *Y. lipolytica PEX8* disruption strain, thiolase is primarily cytosolic, and a small fraction is associated with peroxisomes (Sections 3.6 to 3.8).

The localization of Pex20p and thiolase in cells of a *PEX8* disruption strain point to a direct role for Pex8p in the Pex20p-dependent import of thiolase. While it has previously been shown that in wild-type cells a very small fraction of cellular Pex20p is associated with peroxisomes (Titorenko et al. 1998), a large fraction of Pex20p is associated with peroxisomal membranes in cells devoid of Pex8p relative to that in wild-type cells. Also, of the very small amount of peroxisomal thiolase in cells of a *PEX8* disruption strain, at least half of it is membrane-associated. These data point to a role for the Pex8p-Pex20p interaction in the import of thiolase at a stage later than docking of Pex20p-thiolase complexes at the membrane. The exact role of Pex8p in thiolase import has not been elucidated, but as Pex20p interacts with Pex8p in the absence of thiolase (or any other protein), it is tempting to speculate that Pex8p dissociates thiolase from Pex20p during translocation. Future experiments will be aimed at studying the interactions between Pex8p and thiolase-bound Pex20p.

Interestingly, membrane-associated Pex20p and thiolase in cells of the *PEX8* disruption strain are protected from proteases, whereas the membrane-associated fraction of Pex20p in wild-type cells is susceptible to proteases. These data suggest that although in wild-type cells peroxisomal Pex20p is associated with the matrix face of the membrane (Titorenko et al., 1998), in the absence of Pex8p, Pex20p and thiolase may be protected by the peroxisomal membrane or by other proteins. This, together with the fact that Pex20p interacts directly with an intraperoxisomal peroxin, suggests that Pex20p may enter peroxisomes with its cargo. This phenomenon may not be detectable in wild-type cells, because either the steady-state level of this population of Pex20p is very low or Pex20p may exit the channel during fractionation of wild-type cells.

4.10.3 A role for Pex8p in the Pex5p-dependent import of PTS1-containing proteins– In cells lacking Pex20p, thiolase is mislocalized to the cytosol, whereas in cells lacking Pex8p, several matrix proteins are mislocalized to the cytosol, including PTS1-containing proteins (Sections 3.6 to 3.8). One possible reason for this is more extensive mislocalization is that the Pex20p that is trapped in the peroxisomal membrane of cells of the *PEX8* disruption strain clogs the translocation apparatus. As it has been proposed that the PTS1- and PTS2-dependent import pathways are convergent (Albertini et al., 1997; Girzalsky et al., 1999), this obstruction may prevent PTS1-containing proteins from being translocated. Alternatively, Pex8p may be involved directly in both Pex5p- and Pex20p-dependent import. Our identification of an interaction between Pex8p and Pex5p in the yeast two-hybrid system is consistent with this scenario. In addition, it has recently been shown that Pex8p and Pex5p of *S. cerevisiae* interact, even in the absence of the PTS1 of Pex8p (Rehling et al., 2000). It has not yet been demonstrated that Pex8p and Pex5p interact directly, but as Pex20p and Pex5p have sequence similarity at their amino termini

(Titorenko et al., 1998) and Pex8p interacts directly with Pex20p, this is a possible mechanism of interaction.

4.10.4 Pex20p interacts with p100–During analysis of the Pex20p-Pex8p interaction, p100, a second Pex20p-interacting protein, was identified. p100 is very similar in sequence to C_1-THFS enzymes of other organisms. C_1-THFSs are multifunctional enzymes that catalyze the interconversion of tetrahydrofolate between different oxidation states in both the cytosol and mitochondria. The products of this interconversion are involved in several metabolic processes, including nucleic acid synthesis and the biosynthesis and conversions of amino acids (reviewed in Wagner, 1995). A mammalian isoform of C_1-THFS, which has not yet been localized, has a consensus PTS2 sequence at its amino terminus (Fig. 4-6). For this reason and because p100 and Pex20p interact, the possibility that p100 is a peroxisomal isoform of C_1-THFS was investigated. p100 was localized in both wild-type cells and cells devoid of Pex20p, and a peroxisomal localization was not detected. As C_1-THFS is a dimer (MacKenzie, 1984) and Pex20p is necessary for the dimerization of thiolase (Titorenko et al., 1998), it is possible that Pex20p plays a role in the dimerization of cytosolic C_1-THFS. It will be interesting to investigate this possibility in the future.

CHAPTER 5

REGULATION OF PEROXISOME SIZE AND NUMBER BY FATTY ACID β-OXIDATION

A version of this chapter has previously been published as "Regulation of peroxisome size and number by fatty acid β-oxidation in the yeast *Yarrowia lipolytica*" (Jennifer J. Smith, Trevor W. Brown, Gary A. Eitzen, and Richard A. Rachubinski. 2000. *J. Biol. Chem.* 275:20168-20178). Reprinted with permission.

5.1 Overview

The *Y. lipolytica MFE2* gene encodes the β-oxidation enzyme MFE2. MFE2 is peroxisomal in a wild-type strain but is cytosolic in a strain lacking the PTS1 receptor, Pex5p. MFE2 has a PTS1, Ala-Lys-Leu, that is essential for targeting to peroxisomes, but not in the presence of full-length MFE2. Therefore, MFE2 targeting is dependent on the PTS1 receptor, and MFE2 may be targeted as an oligomer.

Peroxisomes of an oleic acid-induced *MFE2* deletion strain, *mfe2-KO*, are larger and more abundant than those of the wild-type strain. Under growth conditions not requiring peroxisomes, peroxisomes of *mfe2-KO* are larger but less abundant than those of the wild-type strain. These results suggest a role for MFE2 in the regulation of peroxisome size and number. *mfe2-KO* cells contain higher amounts of β-oxidation enzymes than do wild-type cells. Increasing the level of the β-oxidation enzyme thiolase results in enlarged peroxisomes, suggesting that increased amounts of β-oxidation enzymes contribute to the enlarged peroxisomes in cells lacking MFE2. A nonfunctional version of MFE2 did not restore normal peroxisome morphology to *mfe2-KO* cells, indicating that their phenotype is not due to the absence of MFE2. These results implicate peroxisomal β-oxidation in the control of peroxisome size and number in yeast.

5.2 Isolation and characterization of the *Y. lipolytica MFE2* gene

Sequencing of a DNA fragment recovered from a *Y. lipolytica* strain that contained an incorrectly integrated *PEX16* disruption construct and which failed to grow on oleic acid-containing medium led to the identification of a 1,146-bp piece of the *MFE2* gene encoding peroxisomal β-oxidation MFE2 of *Y. lipolytica* (performed by Gary

A. Eitzen and Trevor W. Brown). This DNA sequence was used to make a probe to isolate the entire *Y. lipolytica MFE2* gene by colony hybridization. Three positively hybridizing colonies were identified out of 5,000 colonies screened, and the plasmids recovered from each positive colony were shown to be identical by restriction mapping. Sequencing demonstrated that the insert contained the entire *MFE2* ORF, as well as 3,474 bp and 426 bp upstream and downstream, respectively, of the ORF.

The *Y. lipolytica MFE2* gene and its encoded protein, MFE2, are shown in Figure 5-1. A putative TATA box, TATATAA, is found between nucleotides -124 and -118 (where +1 is the "A" nucleotide of the putative initiation codon of the *MFE2* gene). 'A' nucleotides are found at positions -1 and -3 upstream of the initiator ATG, a feature common to strongly expressed genes of *Y. lipolytica* (Barth and Gaillardin, 1997). The upstream regulatory region of the *MFE2* gene contains the sequence CGGTTATAA between nucleotides -459 and -467. This sequence closely resembles the consensus oleic acid-response element (C/T)GGTT(A/G)TT(C/A/G) of *C. tropicalis* (Sloots et al., 1991) and fits the consensus oleic acid-response element CGGNNNTNA of *S. cerevisiae* (Filipits et al., 1993; Karpichev and Small, 1998), which are sequences often found upstream of genes encoding peroxisomal proteins. The *MFE2* gene contains an intron. *Y. lipolytica* intron donor and branch sites (Barth and Gaillardin, 1997) were identified between nucleotides 172 and 178 and between nucleotides 234 and 245, respectively. The donor site GTGAGTA fits the consensus donor site GTGAGTPu, while the sequence AACTAACACCAG resembles very closely the consensus branch site (T/C)(A/G)CTAAC(N_{1-2})CAG. The *S. cerevisiae* transcription termination consensus sequence TAG…TA(T)GT…TTT located upstream of poly A addition sites (Zaret and

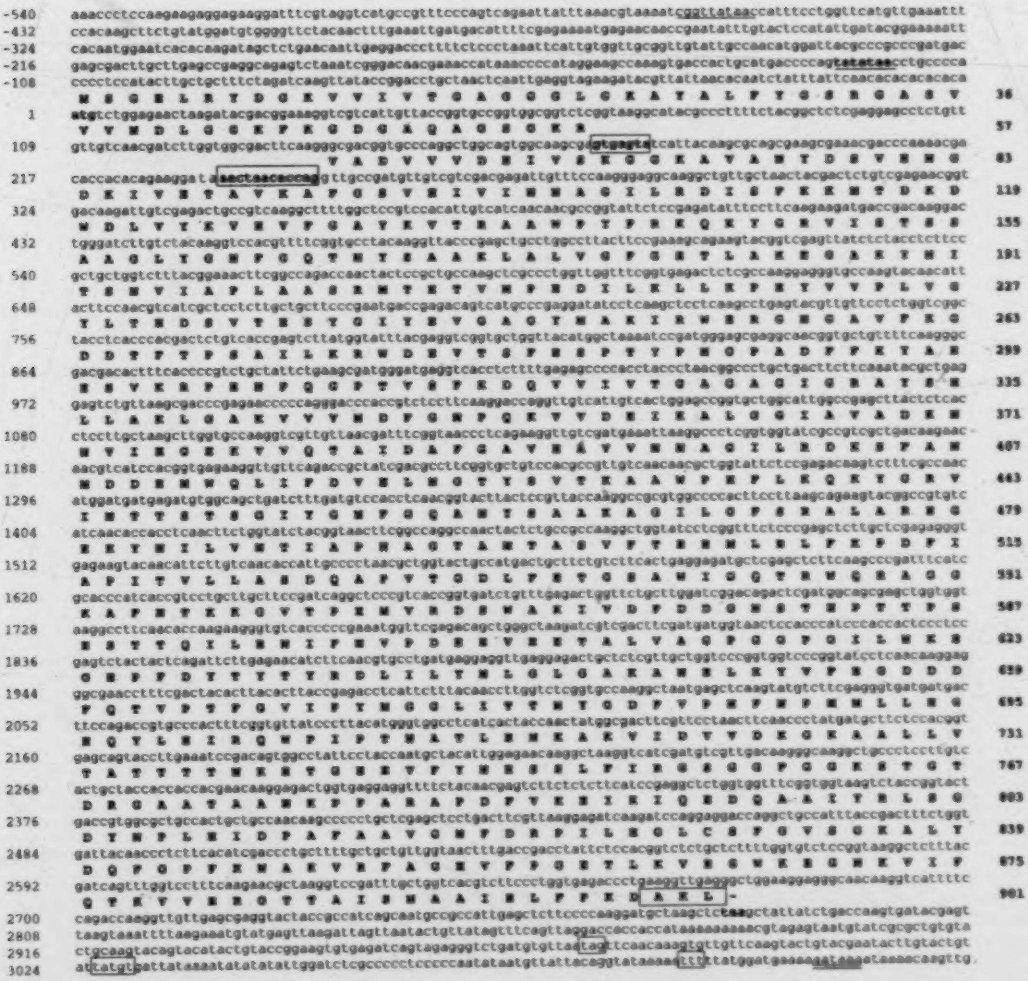

Figure 5-1. Characteristics of the *Y. lipolytica MFE2* gene and its encoded protein, MFE2. A putative TATA box is *boldface* and *underlined*. Putative transcription termination signals are *boxed*. A consensus polyadenylation signal is *doubly underlined*. Consensus intron donor and branch sites are *boldface* and *boxed*. A putative oleic acid-response element is *underlined*. A consensus PTS1 sequence in the MFE2 protein is *boxed* and *boldface*. These sequence data are available from EMBL/GenBank under accession number AF198225.

Sherman, 1982) is also a feature of *Y. lipolytica* genes (Barth and Gaillardin, 1997) and is found in the 3' untranslated region of the *MFE2* gene. A eukaryotic poly A addition signal, AATAAA (Proudfoot and Brownlee, 1976), is found between nucleotides 3113 and 3118.

MFE2 encodes MFE2, a protein that is 901 amino-acid residues in length and has a predicted molecular mass of 97,300 Da. A comparison of MFE2 to protein sequences deposited in the NCBI protein database showed that it has a high degree of similarity to peroxisomal MFE2 enzymes of other fungi (Fig. 5-2). The highest similarity is with *Neurospora crassa* MFE2, which shares 62% identical residues and 72% similar residues with *Y. lipolytica* MFE2. The carboxyl-terminal tripeptide Ala-Lys-Leu of *Y. lipolytica* MFE2 fits the PTS1 consensus sequence.

The entire *MFE2* ORF was deleted by integration of the *Y. lipolytica URA3* gene into the *E122* wild-type strain to create the strain *mfe2-KO*. The *mfe2-KO* strain grew well on media containing acetate (see Fig. 5-8 *C*) or glucose (data not shown), which do not require peroxisomal β-oxidation for their metabolism, but failed to grow on medium containing oleic acid as the carbon source (Fig. 5-3), which does require peroxisomal β-oxidation for its metabolism. Transformation of the *mfe2-KO* strain with the *MFE2* expression plasmid, pMFE2, led to the restoration of growth on oleic acid-containing medium (Fig. 5-3).

5.3 Synthesis of MFE2 is induced by growth of *Y. lipolytica* in oleic acid medium

Because a putative oleic acid-response element is present upstream of the *MFE2* gene, the effect of growth of *Y. lipolytica* in oleic acid medium on the synthesis of MFE2

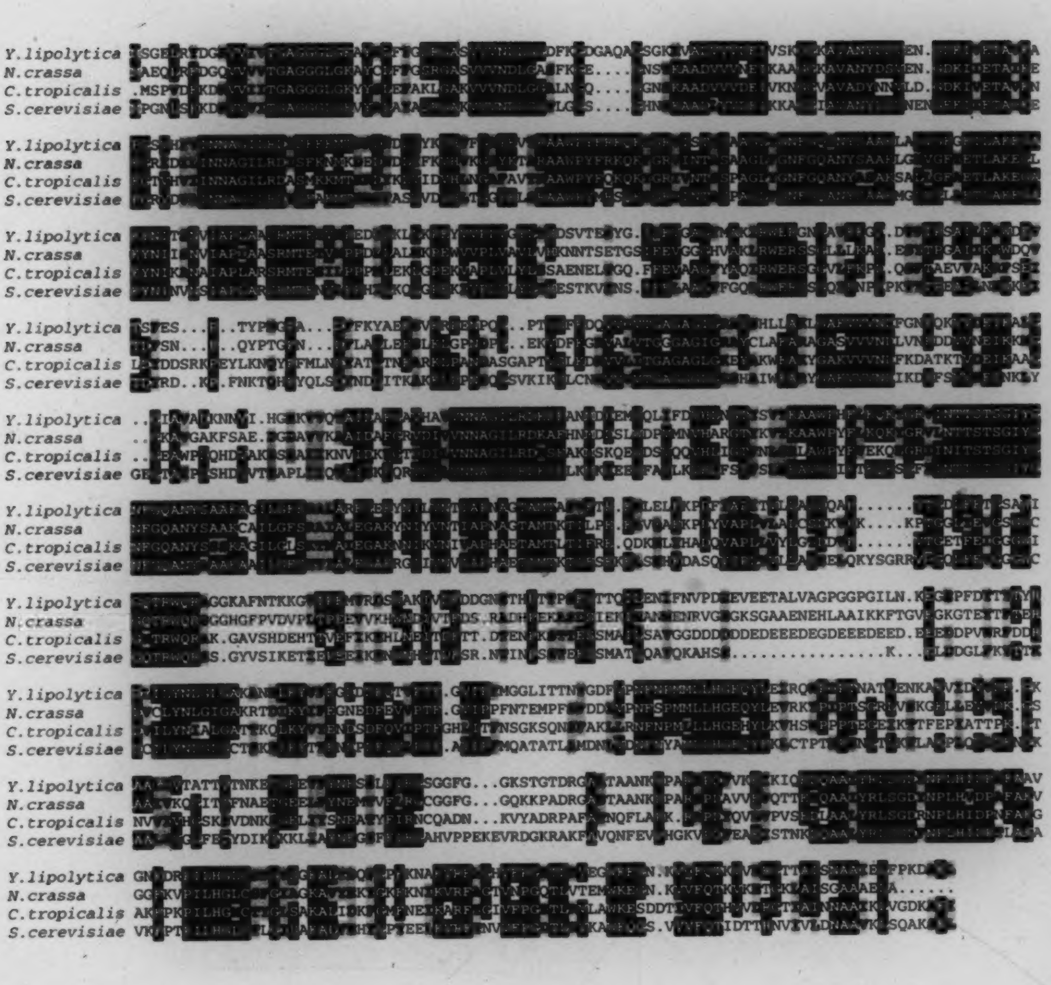
Y.lipolytica
N.crassa
C.tropicalis
S.cerevisiae

Figure 5-2. Amino acid sequence alignment of MFE2 proteins of selected fungi. Sequences were aligned using CLUSTAL W. Identical residues (*black*) or similar residues (*grey*) in three or more sequences are shaded. Similarity rule: A = S = T; D = E; N = Q; R = K; I = L = M = V; F = Y = W. The amino acid sequences of *N. crassa*, *C. tropicalis*, and *S. cerevisiae* MFE2 proteins have been deposited in GenBank with accession numbers X80052, X57854 and M86456, respectively.

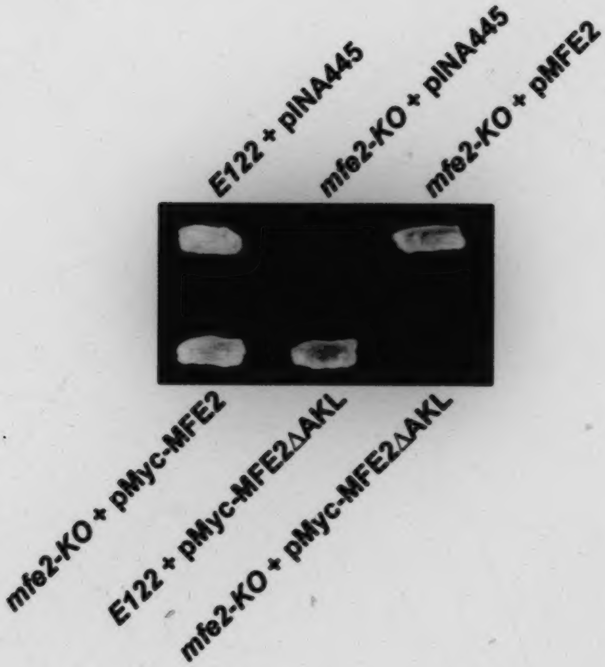
E122 + pINA445
mfe2-KO + pINA445
mfe2-KO + pMFE2
mfe2-KO + pMyc-MFE2
E122 + pMyc-MFE2ΔAKL
mfe2-KO + pMyc-MFE2ΔAKL

Figure 5-3. Growth of *Y. lipolytica* strains on oleic acid-containing medium. The wild-type strain *E122* and the deletion strain *mfe2-KO*, transformed with the plasmids indicated, were grown in YND medium overnight. Cells were harvested by centrifugation, washed, resuspended in water, spotted onto YNO agar plates and grown for 2 d.

was determined. To monitor the presence of MFE2, the *MFE2* gene was modified to encode Myc-MFE2, a version of the protein tagged at its amino terminus with the human c-Myc epitope. Cells of the *mfe2-KO* strain transformed with a plasmid encoding Myc-MFE2 were able to grow on oleic-acid medium (Fig. 5-3), indicating that Myc-MFE2 functions as does the wild-type MFE2 protein. Anti-c-Myc antibodies detected a protein in extracts of wild-type cells transformed with the plasmid pMyc-MFE2 encoding Myc-MFE2, but not in extracts of wild-type cells transformed with the parental plasmid pINA445 (Fig. 5-4). Myc-MFE2 was much more abundant in an extract of oleic acid-grown cells than in an extract of glucose-grown cells, while the levels of an ER protein, Kar2p, were unaffected by the composition of the growth medium (Fig. 5-4).

5.4 Peroxisomal localization of Myc-tagged MFE2 depends on Pex5p

Double-labelling, indirect immunofluorescence microscopy was performed on oleic acid-grown strains transformed with pMyc-MFE2 to determine the subcellular localization of MFE2. Myc-MFE2 had a punctate localization that was identical to that of the peroxisomal matrix enzyme thiolase in both wild-type cells and *mfe2-KO* cells (Fig. 5-5 *A*), indicating that Myc-MFE2 is peroxisomal. Because MFE2 shows a typical PTS1 motif, Ala-Lys-Leu, at its carboxyl terminus, Myc-MFE2 was localized in the strain *pex5-KO2*, which does not synthesize the PTS1 receptor. Myc-MFE2 gave a diffuse pattern of fluorescence characteristic of a cytosolic localization in the *pex5-KO2* strain, whereas thiolase, which is targeted by a PTS2-mediated pathway, still showed a punctate pattern of fluorescence characteristic of peroxisomes (Fig. 5-5 *B*). Therefore, Myc-MFE2 requires the PTS1 receptor for its targeting to peroxisomes.

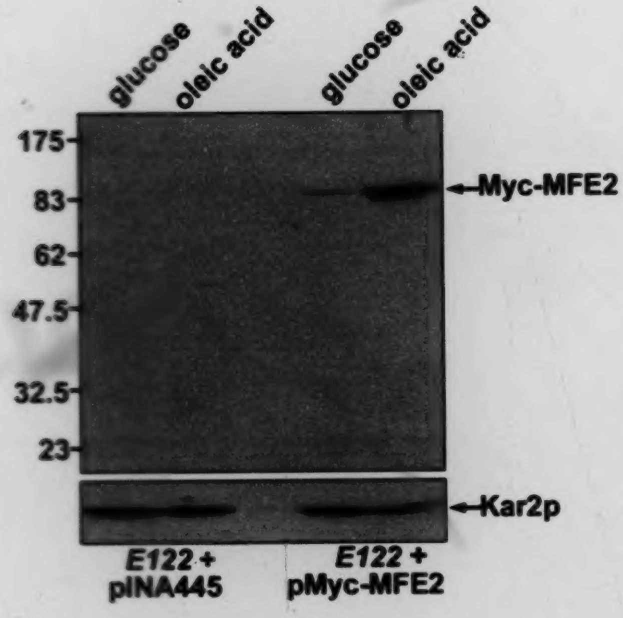
glucose
oleic acid
glucose
oleic acid
175
83
62
47.5
32.5
23
Myc-MFE2
Kar2p
E122 +
pINA445
E122 +
pMyc-MFE2

Figure 5-4. Synthesis of Myc-MFE2 is increased by growth of *Y. lipolytica* in oleic acid-containing medium. Cells of the wild-type strain *E122* transformed with either pMycMFE2 encoding Myc-MFE2 or the parental plasmid pINA445 were grown overnight in YND medium, harvested by centrifugation, transferred to fresh YND or YNO medium, and grown for an additional 9 h. Cells were harvested, and lysates were prepared by disruption with glass beads. Equal amounts of protein from each strain under each growth condition were separated by SDS-PAGE, transferred to nitrocellulose and probed with either anti-c-Myc antibodies (*top panel*) or anti-Kar2p antibodies (*bottom panel*). The numbers at left indicate the migrations of molecular mass standards (in kDa).

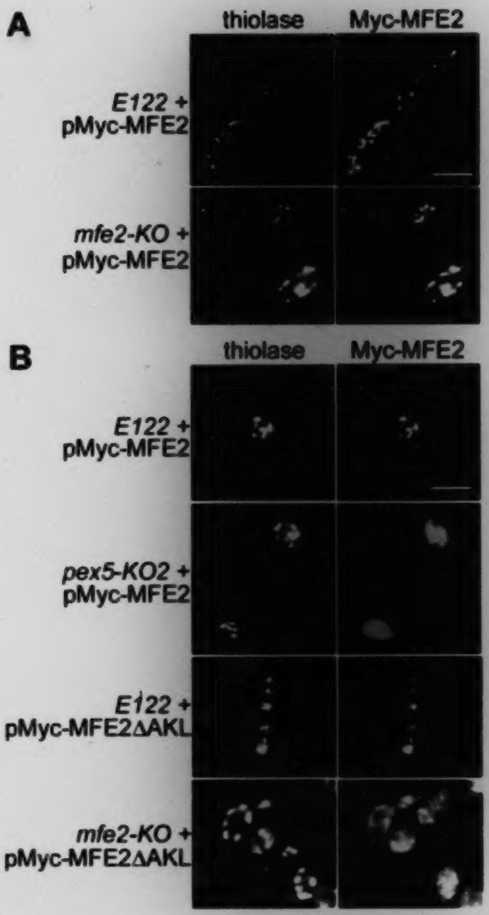
A
thiolase
Myc-MFE2
E122 +
pMyc-MFE2
mfe2-KO +
pMyc-MFE2
B
thiolase
Myc-MFE2
E122 +
pMyc-MFE2
pex5-KO2 +
pMyc-MFE2
E122 +
pMyc-MFE2ΔAKL
mfe2-KO +
pMyc-MFE2ΔAKL

Figure 5-5. Localization of Myc-MFE2 and Myc-MFE2ΔAKL in various strains. (*A*) Strains *E122* (*top panels*) and *mfe2-KO* (*bottom panels*) were transformed with pMyc-MFE2, grown overnight in YND medium, and then grown for 10 h in YNO medium. Cells were fixed for 30 min and processed for double-labelling immunofluorescence microscopy using guinea pig anti-thiolase (*left panels*) and mouse anti-c-Myc (*right panels*) antibodies. Guinea pig primary antibodies were detected with fluorescein-conjugated donkey anti-guinea pig IgG secondary antibodies, and mouse primary antibodies were detected with rhodamine-conjugated donkey anti-mouse IgG secondary antibodies. (*B*) Strains *E122*, *pex5-KO2* and *mfe2-KO* were transformed with either pMyc-MFE2ΔAKL or pMyc-MFE2, as indicated. Cells were grown and processed for immunofluorescence microscopy as described for *Panel A* except that cells were fixed for 2 min. Bar = 10 μm.

5.5 MFE2 is targeted by a PTS1 and may be targeted as an oligomer

The data presented above are consistent with the carboxyl-terminal tripeptide Ala-Lys-Leu of MFE2 acting as a PTS1. To test whether this tripeptide is a PTS1, a mutant *MFE2* gene encoding a carboxyl-terminally truncated, Myc-tagged version of MFE2, Myc-MFE2ΔAKL, was transformed into both the *mfe2-KO* and wild-type strains. The mutant *MFE2* gene was unable to rescue growth of *mfe2-KO* cells on oleic acid-containing medium (Fig. 5-3). To determine the localization of Myc-MFE2ΔAKL in both strains, double-labelling immunofluorescence microscopy was performed. In *mfe2-KO* cells, the truncated protein had a cytosolic localization, whereas thiolase had a punctate localization characteristic of peroxisomes (Fig. 5-5 *B*). These data indicate that the carboxyl-terminal Ala-Lys-Leu of MFE2 is a PTS1, as it is essential for the targeting of Myc-MFE2 to peroxisomes.

Next, Myc-MFE2ΔAKL was localized in wild-type cells. Interestingly, although Myc-MFE2ΔAKL showed a cytosolic localization in *mfe2-KO* cells, it showed a punctate pattern of distribution in wild-type cells that was identical to the distribution of peroxisomal thiolase (Fig. 5-5 *B*). These results are consistent with the import of MFE2 as an oligomer into peroxisomes. In a manner similar to what has been shown for the import of the thiolase dimer in *S. cerevisiae* (Glover et al., 1994), the carboxyl-terminally truncated form of Myc-MFE2 lacking its PTS1 may heterodimerize with full-length MFE2 encoded in the nucleus and then be targeted to the peroxisome by virtue of the PTS1 of the full-length MFE2. Although it is unknown whether *Y. lipolytica* MFE2 forms an oligomer, it is important to note that MFE2 of *S. cerevisiae* has been shown to form homodimers (Hiltunen et al., 1992).

5.6 MFE2 may control peroxisome size and number of oleic acid-grown cells

Previous evidence has suggested that human MFE2 has a role in controlling peroxisome abundance and size (Chang et al., 1999). Therefore, the effects of disrupting the *Y. lipolytica MFE2* gene on peroxisome morphology were investigated. Electron microscopy showed that the peroxisomes of *mfe2-KO* cells appeared more variable in size and more abundant than peroxisomes of wild-type cells (Fig. 5-6 *A*). Also, the peroxisomes of the mutant strain were often clustered, whereas the peroxisomes of the wild-type strain were usually well separated (Fig. 5-6 *A*). Morphometric analysis (Weibel and Bolender, 1973) showed that *mfe2-KO* cells had a numerical density of peroxisomes that was approximately 2.5 times that of wild-type cells (Table 5-1, compare *rows 1* and *2*).

Table 5-1. Morphometric Analysis of Peroxisomes

	Strain	Growth medium	Cell area assayed (μm^2)	Peroxisome count[a]	Numerical density of peroxisomes[b]	Average area of peroxisomes (μm^2)[c]
1	*E122*	YPBO	825	0.26	0.48	0.145 ± 0.057
2	*mfe2-KO*	YPBO	553	0.74	1.20	0.182 ± 0.109
3	*E122*	YEPA	725	0.11	0.38	0.075[d]
4	*mfe2-KO*	YEPA	880	0.09	0.19	0.243[d]
5	*mfe2-KO* + pMyc-MFE2	YNA	447	0.14	0.32	0.103[d]
6	*mfe2-KO* + pINA445	YNA	264	0.13	0.18	0.267[d]
7	*mfe2-KO* + pMyc-MFE2ΔAΔB	YNA	634	0.15	0.26	0.171[d]
8	*E122* + pINA445	YND	629	0.14	0.49	0.045[d]
9	*E122* + pTHI-OV	YND	475	0.21	0.51	0.087[d]

[a] Number of peroxisomes counted per μm^2 of cell area on micrographs.
[b] Number of peroxisomes per μm^3 of cell volume (Weibel and Bolender, 1973).
[c] Average area on micrographs.
[d] Standard error was not calculated as peroxisomes were not measured individually.

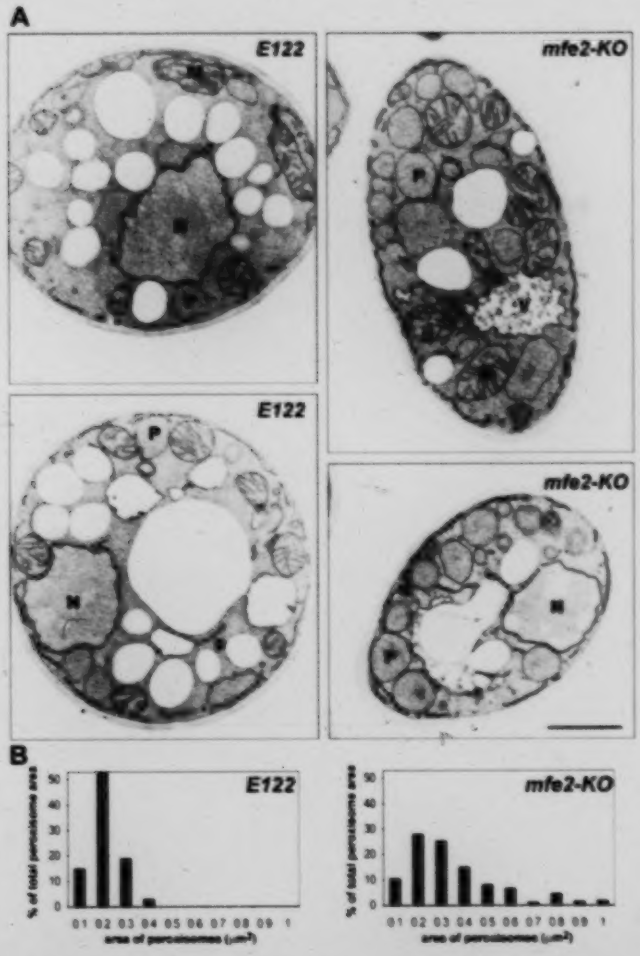
A
E122
M
N
mfe2-KO
P
V
M
E122
P
N
mfe2-KO
N
P
B
E122
% of total peroxisome area
0
10
20
30
40
50
01 02 03 04 05 06 07 08 09 1
area of peroxisomes (µm²)
mfe2-KO
% of total peroxisome area
0
10
20
30
40
50
01 02 03 04 05 06 07 08 09 1
area of peroxisomes (µm²)

Figure 5-6. Peroxisomes are larger, more abundant and more variable in size in *mfe2-KO* cells than in wild-type cells. (*A*) Ultrastructure of mutant *mfe2-KO* and wild-type *E122* cells. Cells were grown in YEPD medium overnight, transferred to YPBO medium, and grown in YPBO medium for 14 h. Cells were fixed and processed for electron microscopy. *P*, peroxisome; *M*, mitochondrion; *N*, nucleus; *V*, vacuole. *Bar* = 1 µm. (*B*) Morphometric analysis of oleic acid-grown *E122* (*left panel*) and *mfe2-KO* (*right panel*) cells. Electron micrographs encompassing 825 μm^2 of wild-type cell area and 553 μm^2 of *mfe2-KO* cell area were enlarged 16,620 × on photographic paper. Peroxisome profiles were cut out and weighed, and the total peroxisome area for each strain was calculated. Next, the areas of individual peroxisomes were calculated, and peroxisomes were separated into size categories. A histogram was generated for each strain depicting the percentage of total peroxisome area occupied by the peroxisomes of each category. The numbers along the x-axis are the maximum sizes of peroxisomes in each category (in μm^2).

Peroxisomes of the *mfe2-KO* strain were also much more variable in size than those of wild-type cells, with mutant cells having many peroxisomes greater than 0.4 μm^2 in area and wild-type cells having essentially no peroxisomes greater than 0.4 μm^2 in area (Fig. 5-6 *B*). In addition, the average area of *mfe2-KO* peroxisomes was significantly larger than the average area of *E122* peroxisomes (Table 5-1, compare *rows 1* and *2*). Using the large sample *z*-test, the average peroxisome area of *mfe2-KO* cells was found to be 1.26 ± 0.07 times larger than that of wild-type cells with a 95% confidence interval.

The fact that peroxisomes are more abundant in the *mfe2-KO* strain than in the wild-type strain was not obvious from immunofluorescence microscopy (Fig. 5-5 *B*). This apparent difference between electron microscopic and immunofluorescence microscopic analyses can be explained by the fact that peroxisomes of the deletion strain are often clustered (Fig. 5-6 *A*), and a cluster of peroxisomes can appear as one large peroxisome in immunofluorescence microscopy (Zhang et al., 1993).

5.7 MFE2 may control peroxisome size and number of acetate-grown cells

The morphological analysis of oleic acid-induced *mfe2-KO* cells suggested a dysregulation of peroxisome size and number in the absence of MFE2. To determine if this effect is coupled to peroxisomal induction, the morphology of *mfe2-KO* cells grown in medium containing acetate, a carbon source not requiring β-oxidation for its metabolism, was investigated. Peroxisomes of *mfe2-KO* cells grown in acetate were considerably larger than those of wild-type cells in electron micrographs (Fig. 5-7). Morphometric analysis of acetate-grown strains showed that the average area of peroxisomes of *mfe2-KO* cells was 3.2 times that of wild-type cells, whereas the number of peroxisomes counted per μm^2 of cell area was similar for both strains (Table 5-1, *rows 3* and *4*). However, a similar peroxisome count does not necessarily mean that the average number of peroxisomes per cell is the same for both strains, because the larger a peroxisome is, the greater the probability of observing it in any given micrograph (Weibel and Bolender, 1973). To estimate the peroxisome number for cells of each strain, the numerical density of peroxisomes, a value that takes into account peroxisome size (Weibel and Bolender, 1973), was calculated. This calculation showed that in contrast to what was observed for cells grown in oleic acid, *mfe2-KO* cells contained approximately half as many peroxisomes as did wild-type cells following growth in acetate (Table 5-1, *rows 3* and *4*).

5.8 Enlarged peroxisomes are not caused by the absence of MFE2 protein

To determine whether the enlarged peroxisomes present in *mfe2-KO* cells were caused by the absence of MFE2 protein or for another reason, such as the lack of a functional β-oxidation pathway, we determined whether a nonfunctional version of Myc-MFE2 could reverse the morphological defects of the *mfe2-KO* strain. *S. cerevisiae* MFE2 has two (3*R*)-hydroxyacyl-CoA dehydrogenase domains (*DA* and *DB* in Fig. 5-8 *A*) that are required for the β-oxidation of fatty acids (Qin et al., 1999). A form of MFE2 containing the mutations G16S and G329S in the nucleotide-binding sites of the two dehydrogenase domains has been shown to be nonfunctional in peroxisomal β-oxidation (Qin et al., 1999). Two consensus nucleotide-binding sites were identified in *Y. lipolytica* MFE2. An alignment of the *S. cerevisiae* and *Y. lipolytica* nucleotide-binding sites revealed that Gly-16 and Gly-324 of *Y. lipolytica* MFE2 correspond to Gly-16 and Gly-

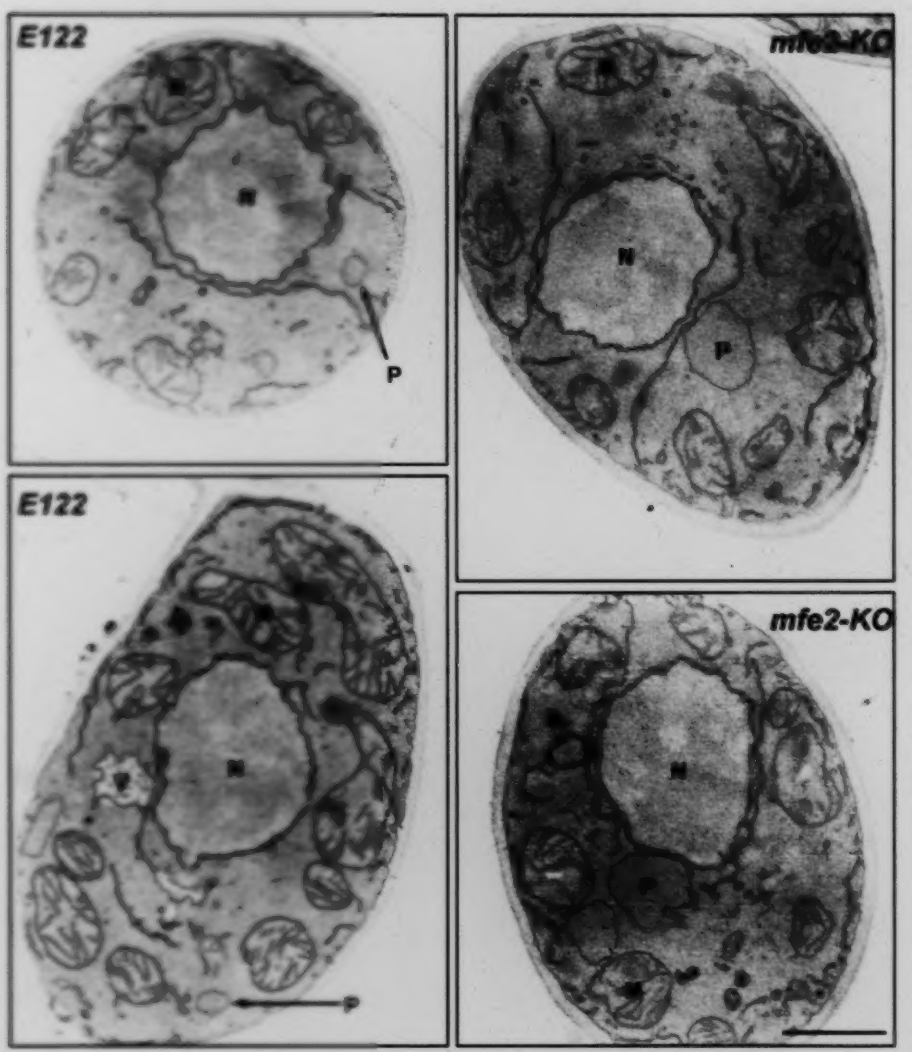

Figure 5-7. Peroxisomes of *mfe2-KO* cells are larger than those of wild-type cells when grown in acetate-containing medium. Ultrastructure of *mfe2-KO* and *E122* cells grown in acetate-containing YEPA medium for 24 h. Cells were fixed and processed for electron microscopy. *P*, peroxisome; *M*, mitochondrion; *N*, nucleus; *V*, vacuole. *Bar* = 1 µm.

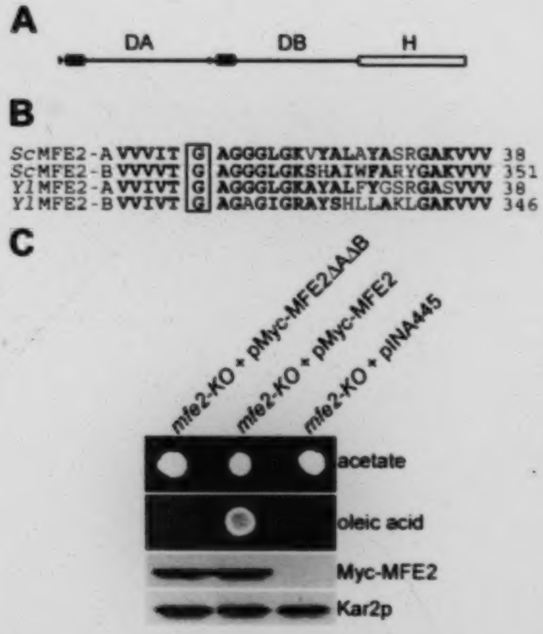
A
DA
DB
H
B
ScMFE2-A VVVIT G AGGGLGKVYALAYASRGAKVVV 38
ScMFE2-B VVVVT G AGGGLGKSHAIWFARYGAKVVV 351
YlMFE2-A VVIVT G AGGGLGKAYALFYGSRGASVVV 38
YlMFE2-B VVIVT G AGAGIGRAYSHLLAKLGAKVVV 346
C
mfe2-KO + pMyc-MFE2ΔAΔB
mfe2-KO + pMyc-MFE2
mfe2-KO + pINA445
acetate
oleic acid
Myc-MFE2
Kar2p

Figure 5-8. Expression of Myc-MFE2ΔAΔB does not restore growth on oleic acid medium to the *mfe2-KO* strain. (A) Domains of yeast MFE2. The two (3*R*)-hydroxyacyl-CoA dehydrogenase domains (*DA* and *DB*) are represented by *solid lines*. The 2-enoyl-CoA hydratase 2 domain (*H*) is represented by an *open box*. Nucleotide binding sites in the dehydrogenase domains are represented by *closed boxes*. (B) Sequence alignment of the nucleotide-binding sites of *S. cerevisiae* and *Y. lipolytica* MFE2 proteins. Residues identical or similar in three or more sequences are indicated in *boldface*. Similarity rules: A = S = T; D = E; N = Q; R = K; I = L = M = V; F = Y = W. Conserved glycine residues mutated in Myc-MFE2ΔAΔB are *boxed*. Residues are numbered at the right. (C) Growth characteristics and protein profiles of the *mfe2-KO* strain transformed with pMyc-MFE2ΔAΔB, pMyc-MFE2 or pINA445. Strains were grown as described in the legend to Figure 5-3 and spotted onto YNA agar (*top panel*) and YNO agar (*second panel from top*). Strains were also grown overnight in YND medium, transferred to YNO medium and grown for an additional 10 h in YNO medium. Cells were harvested, and lysates were prepared by disruption with glass beads. Equal amounts of protein from each strain were separated by SDS-PAGE, transferred to nitrocellulose and probed with either anti-c-Myc antibodies (*third panel from top*) or anti-Kar2p antibodies (*bottom panel*).

329 of *S. cerevisiae* MFE2, respectively (Fig. 5-8 *B*). The plasmid pMyc-MFE2ΔAΔB expressing Myc-MFE2ΔAΔB, which contains the mutations G16S and G324S, was constructed and transformed into *mfe2-KO* cells. The *mfe2-KO* strain transformed with pMyc-MFE2ΔAΔB, like the *mfe2-KO* strain transformed with the empty plasmid pINA445, was unable to grow on agar medium containing oleic acid as the carbon source, whereas the *mfe2-KO* strain transformed with a plasmid expressing Myc-MFE2 grew well on this medium (Fig. 5-8 *C*, *second panel*). All three strains grew well on agar medium containing acetate as the carbon source (Fig. 5-8 *C*, *top panel*). Myc-MFE2ΔAΔB and Myc-MFE were detected by immunoblot analysis of yeast lysates with anti-c-Myc antibodies. The levels of Myc-MFE2ΔAΔB and Myc-MFE2 were similar in the yeast lysates in which they were expressed (Fig. 5-8 *C*, *third panel*). The levels of the ER protein Kar2p were similar in the lysates of all three strains, confirming that equal amounts of total protein were analyzed (Fig. 5-8 *C*, *bottom panel*). Thus, Myc-MFE2ΔAΔB is unable to restore fatty acid β-oxidation activity to the *mfe2-KO* strain. When grown on acetate-containing medium, the *mfe2-KO* strain transformed with pMyc-MFE2ΔAΔB, like the *mfe2-KO* strain transformed with the empty plasmid pINA445, had peroxisomes larger than those of the *mfe2-KO* strain transformed with pMyc-MFE2, which encodes a functional version of MFE2 (Fig. 5-9). The average area of peroxisomes and the numerical density of peroxisomes were determined for each strain (Table 5-1, *rows 5-7*). Peroxisomes of the *mfe2-KO* strain synthesizing Myc-MFE2ΔAΔB were larger and less abundant than peroxisomes of the wild-type strain, but these effects were not as severe as those observed in the absence of MFE2. Because the *mfe2-KO* strain expressing normal levels of a nonfunctional form of Myc-MFE2 still had

abnormalities of peroxisome size and number, these abnormalities are not the result of the absence of MFE2 protein. These results instead point to a role for fatty acid β-oxidation in the regulation of peroxisome size and number.

5.9 β-Oxidation enzyme levels are increased in an *MFE2* deletion strain

An analysis of the levels of several peroxisomal proteins in total cell lysates of the *mfe2-KO* and wild-type strains grown in glucose-, oleic acid- or acetate-containing medium showed that two peroxisomal β-oxidation enzymes, thiolase and acyl-CoA oxidase 5 (one of five *Y. lipolytica* acyl-CoA oxidase isozymes (Wang et al., 1999)), were noticeably increased in *mfe2-KO* cells as compared to wild-type cells by growth in each carbon source (Fig. 5-10). The levels of two peroxisomal enzymes of the glyoxylate cycle, isocitrate lyase and malate synthase, appeared unchanged from the levels in wild-type cells or were marginally increased in *mfe2-KO* cells. The levels of three peroxins, Pex5p, Pex16p and Pex19p, were not increased in *mfe2-KO* cells compared to wild-type cells. In fact, all three peroxins appeared less abundant in the deletion strain than in the wild-type strain following growth in oleic acid-medium. This may be due to proteolytic degradation, because *mfe2-KO* cells cannot grow on oleic acid-medium and thus may contain more vacuoles and proteases than wild-type cells. The levels of the ER protein Kar2p were similar in lysates of each strain under all growth conditions, confirming that equal amounts of total protein were analyzed. These results demonstrate that *mfe2-KO* cells have an increased abundance of peroxisomal β-oxidation enzymes after growth in acetate- and oleic acid-containing media, the same growth conditions that result in enlarged peroxisomes in this strain. These results also demonstrate that *mfe2-KO* cells

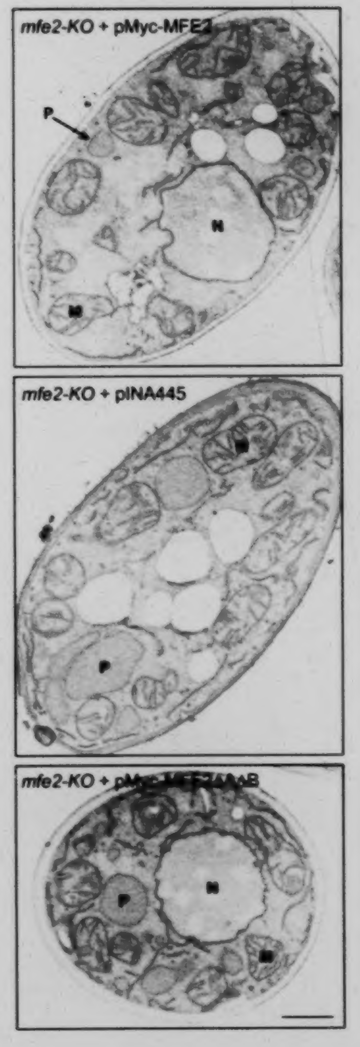
mfe2-KO + pMyc-MFE2
P
N
M
mfe2-KO + pINA445
M
P
mfe2-KO + pMyc-MFE2ΔAΔB
P
N
M

Figure 5-9. Expression of Myc-MFE2ΔAΔB does not reverse the morphological defects of the *mfe2-KO* strain. Cells of the *mfe2-KO* strain transformed with pMyc-MFE2ΔAΔB, pMyc-MFE2 or the parental plasmid pINA445 were grown overnight in YNA medium and processed for electron microscopy. *P*, peroxisome; *M*, mitochondrion; *N*, nucleus. *Bar* = 1 µm.

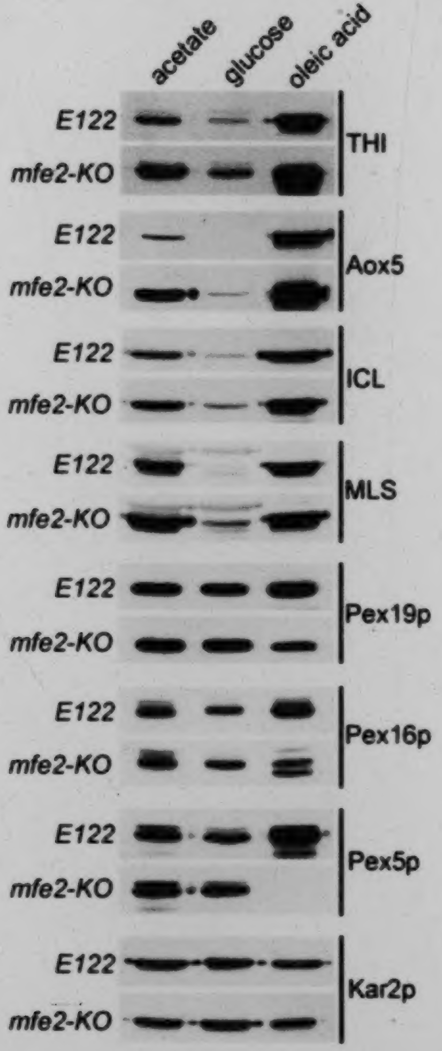
acetate
glucose
oleic acid
E122
mfe2-KO
THI
E122
mfe2-KO
Aox5
E122
mfe2-KO
ICL
E122
mfe2-KO
MLS
E122
mfe2-KO
Pex19p
E122
mfe2-KO
Pex16p
E122
mfe2-KO
Pex5p
E122
mfe2-KO
Kar2p

Figure 5-10. Abundance of various peroxisomal matrix proteins and peroxins in wild-type and *mfe2-KO* cells under different growth conditions. Wild-type *E122* and mutant *mfe2-KO* cells were grown in acetate-containing YEPA medium overnight, transferred to oleic acid-containing YPBO, glucose-containing YEPD or YEPA medium, and grown for an additional 14 h. Cells were lysed, and equal amounts of protein (25 µg) from lysates of cells from each growth condition (indicated at the *top*) were separated by SDS-PAGE and transferred to nitrocellulose. The nitrocellulose was probed with antibodies to the proteins indicated at the *right*. Immunodetection was by enhanced chemiluminescence. *THI*, thiolase; *Aox5*, acyl-CoA oxidase isozyme 5; *ICL*, isocitrate lyase; *MLS*, malate synthase.

have a decreased abundance of peroxins after growth in oleic acid-containing medium, but as the levels of peroxins in these cells is similar to those in wild-type cells after growth in acetate-containing medium, this phenotype is not coupled to peroxisome enlargement.

5.10 Overproduction of β-oxidation enzyme results in enlarged peroxisomes

It had been shown previously that increased amounts of peroxisomal matrix proteins lead to enlarged peroxisomes in cells of *S. cerevisiae* and the yeast *H. polymorpha* (Distel et al., 1988; Gödecke et al., 1989; Roggenkamp et al., 1989). Therefore, increased amounts of peroxisomal β-oxidation enzymes may contribute to peroxisome enlargement in *Y. lipolytica* cells. To investigate this possibility, *POT1*, the gene encoding peroxisomal thiolase, was overexpressed in wild-type cells and the effect of this overexpression on peroxisome size was analyzed. Peroxisome size was measured after growth of cells in glucose-containing medium, because the level of endogenous thiolase is very low under this condition (Fig. 5-10). Therefore, a high relative increase in the abundance of thiolase can be readily achieved by overexpression of its gene in wild-type cells grown in glucose. Also, because peroxisomes are normally very small in cells grown in glucose (Fig. 5-11 *B*, *top panel*), small changes in peroxisome size should be readily apparent.

After growth in glucose, wild-type cells transformed with pTHI-OV overexpressing *POT1* contained approximately 8-fold more thiolase than did wild-type cells transformed with the parental plasmid pINA445 (Fig. 5-11 *A*). This increase in the amount of thiolase led to peroxisomes in the pTHI-OV transformed strain (Fig. 5-11 *B*,

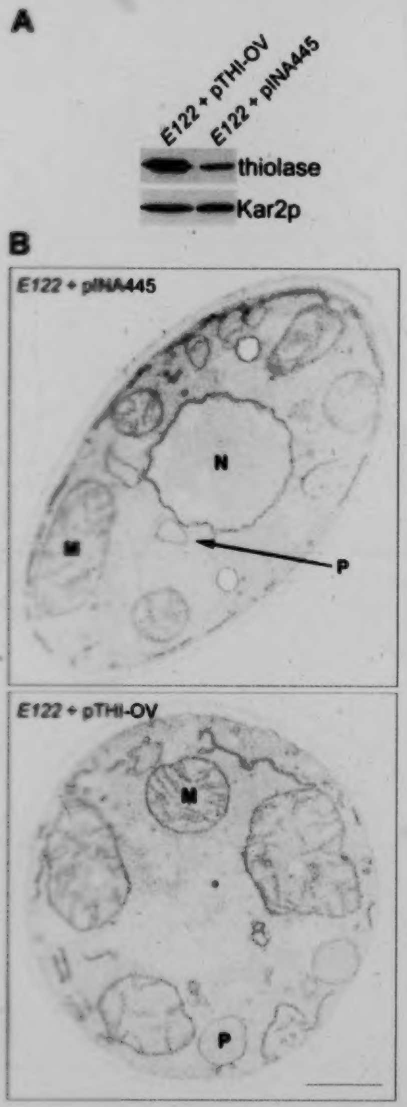
A
E122 + pTHI-OV
E122 + pINA445
thiolase
Kar2p
B
E122 + pINA445
N
M
P
E122 + pTHI-OV
M
P

Figure 5-11. Increased levels of the β-oxidation enzyme thiolase leads to enlarged peroxisomes. Wild-type *E122* cells transformed with either the *POT1* overexpression plasmid pTHI-OV or the parental plasmid pINA445 were grown in glucose-containing YND medium overnight. (A) Equal amounts of protein from cell lysates were separated by SDS-PAGE and transferred to nitrocellulose. The nitrocellulose was probed with antibodies to the proteins indicated at the *right*. (B) Cells were processed for electron microscopy. *P*, peroxisome; *M*, mitochondrion; *N*, nucleus. *Bar* = 1 μm.

bottom panel) that were noticeably larger than those of the pINA445 transformed strain (Fig. 5-11 *B*, *top panel*). The average area of peroxisomes was determined for both strains (Table 5-1, *rows 8* and *9*). Peroxisomes of the strain overexpressing *POT1* were almost twice as large as peroxisomes of the wild-type strain. These results suggest that an increase in abundance of peroxisomal β-oxidation enzymes in the *mfe2-KO* strain contributes to the enlarged peroxisomes seen in this strain.

5.11 Discussion

5.11.1 ***MFE2 protein of Y. lipolytica***–The *MFE2* gene of *Y. lipolytica* encodes MFE2, which shares a high degree of sequence similarity with MFE2 proteins from other fungi. *Y. lipolytica* cells devoid of MFE2 are unable to utilize oleic acid as a carbon source, as has been observed for *S. cerevisiae* (Qin et al., 1999). The *Y. lipolytica MFE2* gene contains a putative upstream oleic acid-response element, as do the genes of *S. cerevisiae* (Filipits et al., 1993; Karpichev and Small , 1998) and *C. tropicalis* (Sloots et al., 1991), and consistent with this, the synthesis of Myc-MFE2, a c-Myc epitope-tagged version of the protein, was induced by growth of *Y. lipolytica* on oleic acid-containing medium. *Y. lipolytica* MFE2 contains a PTS1, as do the MFE2 proteins of *C. tropicalis* and *S. cerevisiae*, and it is essential for targeting to peroxisomes. Similar to *S. cerevisiae* MFE2, which has been shown to form homodimers (Hiltunen et al., 1992), *Y. lipolytica* MFE2 may be targeted to peroxisomes as an oligomer.

5.11.2 ***Lack of functional MFE2 affects peroxisome size and number*–**As has recently been suggested for mammalian MFE2 (Chang et al., 1999), *Y. lipolytica* MFE2 appears to have a role in peroxisome maintenance. Cells of the deletion strain *mfe2-KO* grown in oleic acid contain more and larger peroxisomes than do wild-type cells grown under the same conditions. Also, peroxisomes of the *mfe2-KO* strain are more heterogeneous in size than those of wild-type cells and are often found in close proximity to one another. *mfe2-KO* cells grown in acetate, a carbon source not requiring peroxisomes for its metabolism, have larger peroxisomes than do identically grown wild-type cells, but only half as many. These data suggest that MFE2 contributes to the regulation of peroxisome size and number. The dysregulation in *mfe2-KO* cells is not due to the absence of MFE2 protein, as a nonfunctional form of MFE2 expressed at normal levels is unable to complement these morphological defect. Therefore, it appears that the inability of MFE2 to function in fatty acid β-oxidation affects peroxisome size and number.

5.11.3 ***What causes enlarged peroxisomes of the MFE2 deletion strain?*–**It has been shown previously that a high level of expression of genes encoding peroxisomal matrix enzymes in cells of *H. polymorpha* or *S. cerevisiae* leads to enlarged peroxisome (Distel et al., 1988; Gödecke et al., 1989; Roggenkamp et al., 1989). For this reason, the levels of various peroxisomal enzymes and peroxins in cells of the *mfe2-KO* strain were compared to those of wild-type cells. Although peroxins were less abundant in the *mfe2-KO* cells than in the wild-type cells after growth in oleic acid-containing medium, the levels were similar in both strains after growth on acetate-containing medium. Since *mfe2-KO* cells have enlarged peroxisomes after growth in either oleic acid- or acetate-containing medium, while the reduced levels of peroxins is specific to oleic acid-grown cells, the low abundance of these peroxins is not the basis of the morphological defect.

In contrast to other proteins analyzed, enzymes involved in β-oxidation were more abundant in the *mfe2-KO* cells than in wild-type cells after growth in oleic acid- or acetate-containing medium. It is therefore possible that the increased levels of β-oxidation proteins in *mfe2-KO* cells contribute to the enlarged peroxisomes observed in this strain. To investigate this possibility, the effects of thiolase overproduction were analyzed. The results of this analysis suggest that, while high amounts of β-oxidation enzymes do not contribute to the defect of peroxisome number in *mfe2-KO* cells, they may contribute to the enlargement of peroxisomes.

5.11.4 ***How does the deletion of MFE2 affect peroxisome number?***–Following growth in oleic acid, *mfe2-KO* cells have more peroxisomes than do wild-type cells. In contrast, *mfe2-KO* cells grown in acetate have fewer peroxisomes than do wild-type cells. A possible reason for this dichotomy is that the number of peroxisomes within a cell may be affected by the rate of cell division. It has been proposed that the number of peroxisomes in a cell is the result of both peroxisome accumulation due to proliferation and peroxisome loss due to cell division (Veenhuis and Goodman, 1990). In contrast to wild-type cells, cells of the *mfe2-KO* deletion strain cannot readily divide in oleic acid-containing medium, so few of their peroxisomes segregate to budding daughter cells. If peroxisomes continue to proliferate in *mfe2-KO* cells in the absence of cell division, possibly because of the presence of oleic acid, peroxisomes will accumulate in mother cells of the *mfe2-KO* strain, thereby effectively increasing the number of peroxisomes per cell. Consistent with this scenario, in acetate-containing medium, *mfe2-KO* cells divide at the rate of wild-type cells and do not have more peroxisomes than do wild-type cells. An alternative possibility for the increased number of peroxisomes in the oleic acid-grown *mfe2-KO* cells is that deletion of the *MFE2* gene causes an increased rate of peroxisome proliferation under this condition. However, how this would occur is not readily apparent.

It should be noted that although peroxisomes in the *mfe2-KO* strain are 2.5 times more abundant than, or half as abundant as, peroxisomes of the wild-type strain (depending on the growth condition), Chang et al. (Chang et al., 1999) observed that peroxisomes are 5-fold less abundant in human cells lacking MFE2 than in normal cells. One reason for the difference between yeast and human cells may be the method of analysis in that the human peroxisomes were observed using only immunofluorescence microscopy. If peroxisomes in the mutant human cells are clustered as they are in oleic acid-induced *mfe2-KO* cells, the number of peroxisomes may have been underestimated by using immunofluorescence microscopy. Alternatively, this difference in peroxisome number between yeast and human cells may indicate a difference in the mechanisms regulating peroxisome abundance in these two systems.

CHAPTER 6

PERSPECTIVES

6.1 Synopsis, relevance and future directions of Pex8p analysis

Both the diagram of physical interactions amongst peroxins and the matrix protein import model have been modified to include the data presented in Chapters 3 and 4 (Fig. 6-1 and Fig 6-2, respectively). The implications of these data and the modifications of the import model are discussed in Sections 6.1.1 to 6.1.5.

6.1.1 Pex8p is directly involved in matrix protein import –*Yl*Pex8p, a member of the Pex8p family of peroxins, was identified using the genetic screen outlined in Section 1.4.2. Two other members of this family are peroxisomal proteins that contain PTS1 (*P. pastoris* Pex8p) (Liu et al., 1995) or PTS1 and PTS2 (*H. polymorpha* Pex8p) (Waterham et al., 1994) motifs. Both are necessary for the peroxisomal localization of some matrix proteins, but it has not been demonstrated that either is directly involved in matrix protein import. This thesis describes the identification and characterization of the *PEX8* gene of *Y. lipolytica* and its encoded peroxin, Pex8p. *Yl*Pex8p is a membrane-associated, intraperoxisomal peroxin that is necessary for the import of PTS1- and PTS2-containing matrix proteins into peroxisomes, but which does not appear to be necessary for the targeting of peroxisomal membrane proteins or the biogenesis of peroxisomal membranes. *Yl*Pex8p interacts with the targeting peroxins Pex5p and Pex20p and has a role in Pex20p-dependent matrix protein import. Very recently, a fourth member of the Pex8p family of peroxins was identified in *S. cerevisiae* (*Sc*Pex8p) (Rehling et al., 2000). *Sc*Pex8p is also an intraperoxisomal, membrane-associated peroxin necessary for the peroxisomal localization of matrix proteins but not membrane proteins. Interestingly,

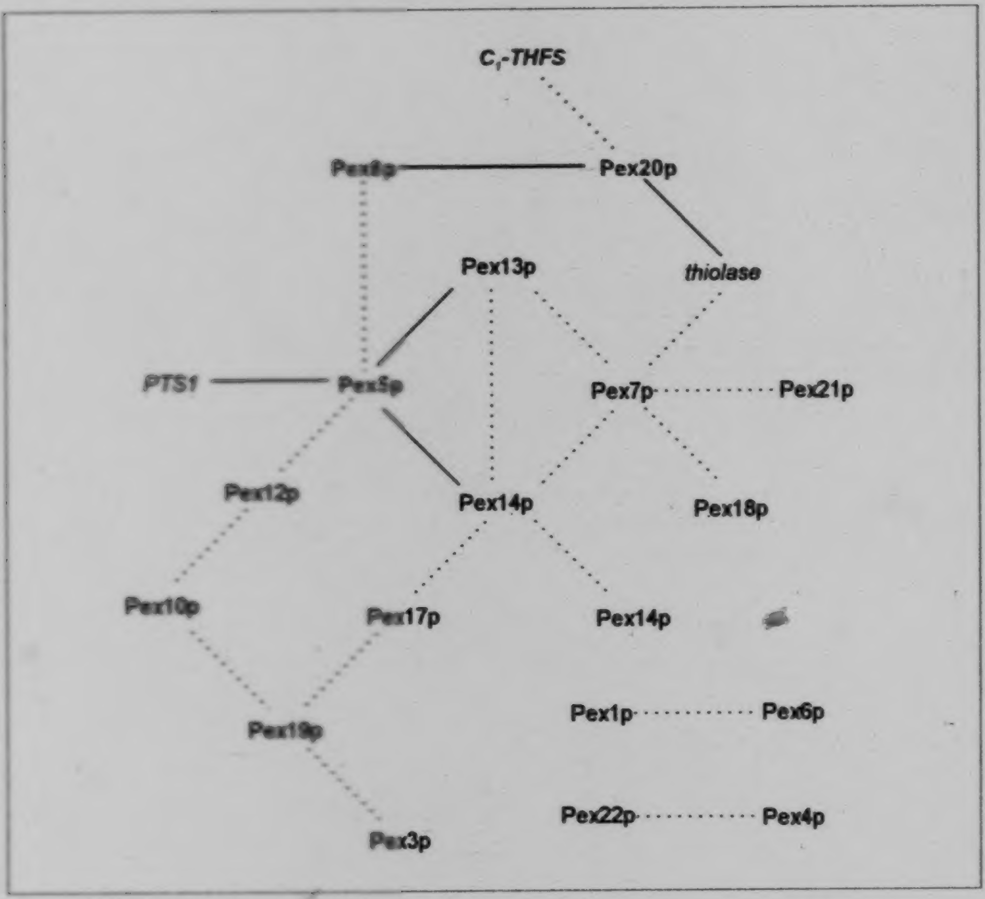
C_1-THFS
Pex8p
Pex20p
Pex13p
thiolase
PTS1
Pex5p
Pex7p
Pex21p
Pex12p
Pex14p
Pex18p
Pex10p
Pex17p
Pex14p
Pex19p
Pex1p
Pex6p
Pex22p
Pex4p
Pex3p

Figure 6-1. Revised diagram of physical interactions amongst peroxins. Interacting proteins that are not peroxins are indicated in *italics*. Interactions that have been demonstrated to be direct are represented by *solid* lines. All other interactions are represented by *dotted* lines. Novel interactions described in this thesis are represented by *grey* lines. Note that the indirect interaction between Pex8p and Pex5p was also recently identified in *S. cerevisiae* (Rehling et al., 2000). For references, see the legend to Figure 1-2.

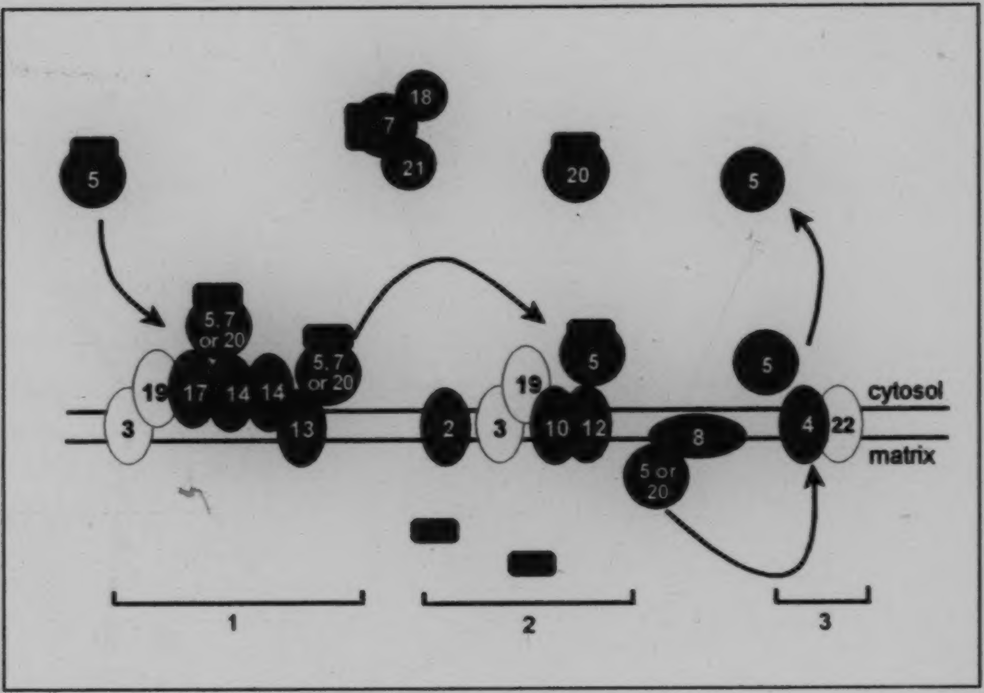

Figure 6-2. Revised model of peroxisomal matrix protein import. The import model presented in Figure 1-3 has been modified to incorporate the data presented here. Cargo proteins are indicated by *rectangles*; peroxins involved in targeting are indicated by *circles*; membrane-bound peroxins involved in import are indicated by *ovals*; peroxins that interact with import components, but which have not been shown to have a direct role in import, are indicated in *white*. Physically interacting proteins are drawn connected. Peroxins in complex 1 have been implicated in the docking of targeting proteins, whereas those in complexes 2 and 3 are involved in aspects of import that occur after docking. Peroxins in complex 3 have been implicated in the recycling of targeting proteins. Pex8p has been added as an intraperoxisomal component of the import apparatus that functions downstream of docking. The targeting protein Pex20p is now shown to dock at the same complex as other targeting proteins and to enter peroxisomes with its cargo. Possible roles of *Yl*Pex8p in the import of matrix proteins and the modifications that were made to the original model are discussed in Section 6.1.

this member of the Pex8p family interacts with Pex5p in the yeast two-hybrid system, suggesting that the function of *Yl*Pex8p may be conserved amongst yeasts.

6.1.2 Convergence of Pex20p- and Pex5p-dependent import–It has recently been demonstrated that *Sc*Pex8p interacts with the PTS1 receptor Pex5p and that the PTS1 of Pex8p is neither necessary for this interaction nor for the targeting of Pex8p to peroxisomes (Rehling et al., 2000). The authors suggested that *Sc*Pex8p might be involved in Pex5p-dependent matrix protein import. The data presented here demonstrate that *Yl*Pex8p interacts with both targeting peroxins Pex5p and Pex20p and point to a direct role for Pex8p in Pex20p-dependent import. Previous to these analyses, no peroxisomal membrane proteins involved in Pex20p-dependent import had been identified. Together these data indicate that, as has been suggested for Pex7p- and Pex5p-dependent import, Pex5p- and Pex20p-dependent import may converge at the peroxisomal membrane. Consistent with this possibility, the amino termini of peroxins of the Pex5p family have sequence similarity to the amino terminus of Pex20p (Titorenko et al., 1998) (for similarity to *Yl*Pex5p, see Fig. 6-3), and this domain of Pex5p interacts with membrane-bound import components Pex14p (Schliebs et al., 1999) and Pex13p (Urquhart et al., 2000). This similarity to Pex20p extends to two specific motifs implicated in Pex13p and Pex14p binding that are conserved amongst some members of the Pex5p family (Fig. 6-3, motifs marked with *chevrons* and *asterisks*, respectively). The first motif, PXXP, is an SH3-binding domain consensus sequence. As Pex5p interacts with the SH3 domain of Pex13p (Elgersma, 1996; Erdmann and Blobel, 1996; Gould et al., 1996), it has been suggested that this motif mediates the interaction between

Pex5p and Pex13p (Musacchio et al., 1994; Elgersma, 1996). The second motif, a pentapeptide of the consensus sequence WXXX(F/Y), is repeated several times within the amino-termini of Pex5p family members. Recent evidence suggests that these motifs are binding sites for the receptor docking protein Pex14p (Schliebs et al., 1999).

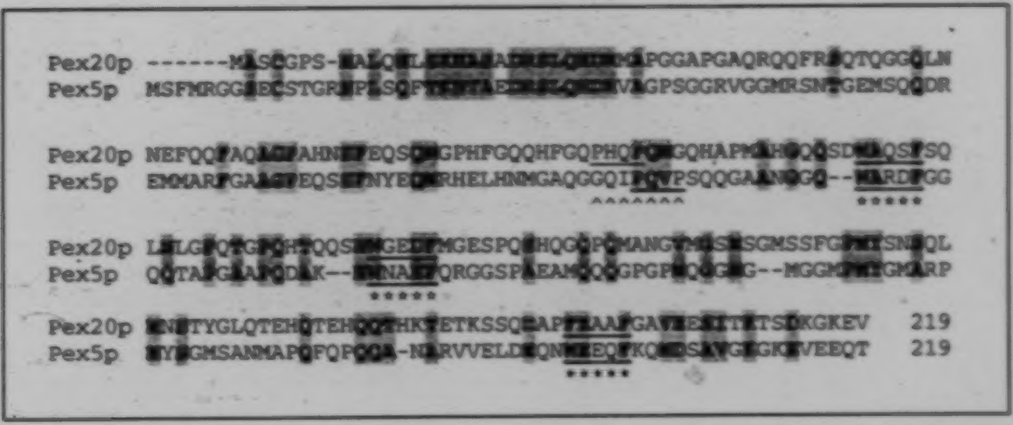

Figure 6-3. Alignment of the amino termini of Pex20p and Pex5p of *Y. lipolytica*. Potential Pex13p-binding PXXP motifs and potential Pex14p-binding WXXX(F/Y) motifs are indicated with *chevrons* and *asterisks*, respectively. Amino acid residues that are similar or identical are indicated in *boldface*. For similarity rules, see the legend to Figure 3-5.

Alternatively, the Pex20p-dependent import pathway may not converge with Pex5p- and Pex7p-dependent import systems. The interaction between Pex8p and the PTS1-receptor Pex5p may instead simply indicate that Pex5p is involved in the import of Pex8p. Consistent with this possibility, almost all peroxins of the Pex8p family have PTS1s. Although *Yl*Pex8p does not have a PTS1 and the peroxisomal targeting of *Sc*Pex8p is not dependent on its PTS1, they may be targeted by the aforementioned Pex5p-dependent, PTS1-independent pathway (Section 1.5.5) (Elgersma et al., 1995). The characterization of the Pex8p-Pex5p interaction and the identification of orthologs of

Pex14p and Pex13p in *Y. lipolytica* will help to determine if the Pex20p- and Pex5p-dependent import systems indeed converge at the peroxisomal membrane.

6.1.3 Possible functions for Pex8p in matrix protein import**–**Pex8p is not necessary for the peroxisomal docking of cargo-bound Pex20p, as Pex20p and a small amount of thiolase accumulate at the peroxisomal membrane in the absence of Pex8p. One possible role for Pex8p is that it pulls targeting peroxins complexed with cargo into peroxisomes through a transport channel. However, the fact that Pex8p can interact with Pex20p that is not bound to thiolase may indicate that Pex8p has a different role, such as to dissociate Pex20p from cargo or to recycle Pex20p back to the cytosol after dissociation. These possible roles are discussed below.

Pex8p may dissociate Pex20p from its cargo after import. Consistent with this proposed function, Pex8p is intraperoxisomal and interacts directly with Pex20p in the absence of thiolase (Section 4.3). To determine if Pex8p indeed has dissociative properties, an *in vitro* binding experiment could be performed to analyze the effect of Pex8p on thiolase-bound Pex20p. The speculation that Pex8p has dissociative properties, together with the possibility that Pex7p-, Pex5p- and Pex20p-dependent import may be convergent (Section 6.1.2), offers an explanation for the presence of PTS1 and PTS2 motifs within the structures of Pex8p family members. Perhaps these motifs facilitate the dissociation of PTS1- and PTS2-containing cargo from targeting peroxins Pex5p and Pex7p by competing with cargo proteins for binding sites on these peroxins. Although this is a tempting speculation, as mentioned previously it is also possible that some Pex8p peroxins have targeting signals because they are targeted by the same receptors that target soluble matrix proteins. A functional analysis of the PTSs of Pex8p peroxins may help to elucidate their exact roles; however, this analysis may be complicated by the fact that the function of Pex8p, at least in *S. cerevisiae*, is independent of its PTS1 (Rehling et al., 2000).

An alternative function for Pex8p that is also consistent with its intraperoxisomal localization and its ability to interact with Pex20p in the absence of thiolase is to recycle peroxins involved with targeting back to the cytosol. Recent data suggest that Pex5p is recycled (Dodt and Gould, 1996; van der Klei et al., 1998), and the inability to release Pex5p from the membrane for recycling does not clog the import apparatus (van der Klei et al., 1998). To investigate a possible role for Pex8p in Pex20p recycling, an overexpression study, similar to that used to investigate the role of Pex4p (van der Klei et al., 1998), could be performed. If Pex8p is involved in recycling Pex20p, then the overproduction of Pex20p in cells of a *pex8* mutant strain may complement their thiolase import defect.

6.1.4 Pex20p may enter peroxisomes with its cargo–For organelles like peroxisomes that do not have detectable pores in their membranes, targeting proteins are not commonly imported with their cargo. However, as peroxisomes seem to be capable of importing oligomerized protein complexes (discussed in Section 1.5.2), the idea of targeting peroxins entering peroxisomes with their cargo does not seem unlikely. The localization of Pex5p and Pex7p to both the cytosol and the inside of peroxisomes (reviewed in Rachubinski and Subramani, 1995) is suggestive of this; however, until now, no intraperoxisomal component of the import apparatus has been demonstrated to interact directly with peroxins involved in targeting.

The fact that Pex20p interacts directly with the intraperoxisomal peroxin Pex8p strongly suggests that Pex20p enters peroxisomes with thiolase during import. Consistent with this scenario, in the absence of Pex8p, Pex20p is protected in the peroxisomal membrane, suggesting that Pex20p is intraperoxisomal. Although this localization of Pex20p may only occur in the absence of Pex8p, it may also be a "snapshot" of the Pex20p-dependent translocation process. The intraperoxisomal localization of Pex20p was not detected in wild-type cells (Titorenko et al., 1998). Perhaps this is because Pex20p is exported too rapidly to be detected or because the steady-state level of intraperoxisomal Pex20p is very low.

6.1.5 Identification of components of the translocation complex–The mechanism by which proteins are translocated across the peroxisomal membrane is unknown. Matrix proteins may be imported through a proteinaceous channel, although no components of a translocation channel have been identified. Alternatively, proteins may be translocated by means of engulfment by the peroxisomal membrane, which is dissolved after entering the peroxisomal lumen (McNew and Goodman, 1994; 1996). Potential components of the translocation apparatus could possibly be identified by immunoprecipitating Pex20p from extracts of cells lacking Pex8p and characterizing coprecipitating proteins.

6.2 Synopsis, relevance and future directions of MFE2 analysis

Chapter 5 describes the identification and characterization of MFE2, a component of the peroxisomal β-oxidation pathway. Peroxisomes of a *Y. lipolytica MFE2* deletion strain are larger and, depending on the growth condition, more or less abundant than peroxisomes of the wild-type strain. Cells of the *MFE2* deletion strain contain higher amounts of β-oxidation enzymes than do wild-type cells. Increasing the level of thiolase in wild-type cells results in enlarged peroxisomes, suggesting that increased amounts of β-oxidation enzymes contribute to the enlarged peroxisomes in cells lacking MFE2. A nonfunctional version of MFE2 did not restore normal peroxisome morphology to these cells, suggesting that their phenotype is not due to the absence of MFE2, but instead may be due to a nonfunctional β-oxidation pathway. These results implicate peroxisomal β-oxidation in the control of peroxisome size and number in yeast.

To elucidate the mechanism of this control of peroxisome size and number, future experiments could include the identification and characterization of additional mutants of *Y. lipolytica* that contain enlarged peroxisomes or an increased number of peroxisomes. Mutant cells of this type could possibly be identified using a fluorescence-activated cell sorter (FACS)-based enrichment of mutagenized cells similar to that which was used to identify mutants defective in the targeting of membrane proteins to peroxisomes (Snyder et al., 1998b). If *MFE2* deletion cells synthesizing a thiolase-green fluorescent protein fusion have a useable FACS phenotype after growth on acetate- or oleic acid-containing medium, perhaps this analysis could be used to identify other mutants with enlarged or more numerous peroxisomes. The β-oxidation-mediated control of peroxisome size and number could also be studied using DNA microarray technology. If *S. cerevisiae* cells lacking MFE2 have the same phenotype as those of *Y. lipolytica*, the recognition of mRNAs that are up- or downregulated in cells of an *S. cerevisiae MFE2* deletion strain may lead to the identification of proteins involved in this mechanism.

6.2.1 Possible effects of growth medium on pex mutant phenotypes–Like cells of many *pex* mutant strains, cells of the *MFE2* deletion strain are unable to metabolize oleic acid but can metabolize both acetate and glucose. Cells of *pex* mutant strains are normally analyzed after growth on oleic acid-containing medium to obtain more peroxisomal material to facilitate analysis. The analysis of the *MFE2* deletion strain after growth on both oleic acid- and acetate-containing medium revealed characteristics that were specific to cells grown in the presence of oleic acid. Oleic acid-grown cells of the *MFE2* deletion strain had a greater number of peroxisomes and less abundant peroxins compared to identically-grown wild-type cells, whereas acetate-grown cells of this strain had fewer peroxisomes and equally abundant peroxins compared to identically grown wild-type cells. As discussed in Sections 5.11.3 and 5.11.4, this dichotomy may be a sign of the inability of this strain to metabolize oleic acid rather than of the function of MFE2. Therefore, for reasons such as possibly increased proteolytic degradation and the lack of cell division, the analysis of *pex* mutants after growth in media containing only oleic acid as a carbon source may be misleading. Perhaps analysis after growth in a medium that contains acetate as well as oleic acid would be more meaningful.

6.2.2 Possible effects of nonfunctional β-oxidation on pex mutant phenotypes–The function of a peroxin is often inferred from the phenotype of cells in which the gene encoding the peroxin is deleted or mutated. The data presented herein demonstrate that the lack of a β-oxidation protein and possibly the lack of β-oxidation affect both the abundance and size of peroxisomes in a given cell. Therefore, *pex* mutants that are defective in β-oxidation, such as mutants defective in matrix protein import, may have secondary abnormalities of peroxisome size and number that are not directly caused by the mutation. In fact it has been demonstrated that human cells lacking the PTS1 receptor Pex5p have fewer and larger peroxisomes than do wild-type cells (Chang et al., 1999). Therefore, the effects of nonfunctional β-oxidation should be considered when analyzing the phenotypes of *pex* mutants.

CHAPTER 7

REFERENCES

Abe I and Fujiki Y. 1998. cDNA cloning and characterization of a constitutively expressed isoform of the human peroxin Pex11p. *Biochem. Biophys. Res. Commun.* 252: 529-533.

Abe I, Okumoto K, Tamura S and Fujiki Y. 1998. Clofibrate-inducible, 28-kDa peroxisomal integral membrane protein is encoded by *PEX11*. *FEBS Lett.* 431: 468-472.

Aitchison JD, Murray WW and Rachubinski RA. 1991. The carboxyl-terminal tripeptide Ala-Lys-Ile is essential for targeting *Candida tropicalis* trifunctional enzyme to yeast peroxisomes. *J. Biol. Chem.* 266: 23197-23203.

Aitchison JD, Szilard RK, Nuttley WM and Rachubinski RA. 1992. Antibodies directed against a yeast carboxyl-terminal peroxisomal targeting signal specifically recognize peroxisomal proteins from various yeasts. *Yeast* 8: 721-734.

Albertini M, Rehling P, Erdmann R, Girzalsky W, Kiel JAKW, Veenhuis M and Kunau W-H. 1997. Pex14p, a peroxisomal membrane protein binding both receptors of the two PTS-dependent import pathways. *Cell* 89: 83-92.

Altshul SF, Gish W, Miller W, Myers EW and Lipman DJ. 1990. Basic local alignment search tool. *J. Mol. Biol.* 215: 403-410.

Ausubel FM, Brent R, Kingston RE, Moore DD, Seidman JG, Smith JA and Struhl K. 1989. *Current Protocols in Molecular Biology*. Greene Publishing Associates, New York, NY.

Baerends RJS, Rasmussen SW, Hilbrands RE, van der Heide M, Faber KN, Reuvekamp PTW, Kiel JAKW, Cregg JM, van der Klei IJ and Veenhuis M. 1996. The *Hansenula polymorpha PER9* gene encodes a peroxisomal membrane protein essential for peroxisome assembly and integrity. *J. Biol. Chem.* 271: 8887-8894.

Barth G and Scheuber T. 1993. Cloning of the isocitrate lyase gene (*ICL1*) from *Yarrowia lipolytica* and characterization of the deduced protein. *Mol. Gen. Genet.* 241: 422-430.

Barth G and Gaillardin C. 1997. Physiology and genetics of the dimorphic fungus *Yarrowia lipolytica*. *FEMS Microbiol. Rev.* 19: 219-237.

Berninger G, Schmidtchen R, Casel G, Knörr A, Rautenstrauss K, Kunau W-H and Schweizer E. 1993. Structure and metabolic control of the *Yarrowia lipolytica* peroxisomal 3-oxoacyl-CoA-thiolase gene. *Eur. J. Biochem.* 216: 607-613.

Blobel G and Dobberstein B. 1975. Transfer of proteins across membranes: presence of proteolytically processed and unprocessed nascent immunoglobulin light chains on membrane-bound ribosomes of murine myeloma. *J. Cell Biol.* 67: 835-851.

Blobel G and Sabatini DD. 1971. Ribosome-membrane interactions in eukaryotic cells. *In* Biomembranes. Vol. 2. Mason LA, editor. Plenum, New York, NY. pp. 193-195.

Bodnar AG and Rachubinski RA. 1991. Characterization of the integral membrane polypeptides of rat liver peroxisomes isolated from untreated and clofibrate-treated rats. *Biochem. Cell Biol.* 69: 499-508.

Borst P. 1989. Peroxisome biogenesis revisited. *Biochim. Biophys. Acta* 1008: 1-13.

Brade AM. 1992. Peroxisome assembly in *Yarrowia lipolytica*. M.Sc. Thesis, McMaster University, Hamilton, Ontario.

Bradford MM. 1976. A rapid and sensitive method for the quantitation of microgram quantities of protein using the principle of protein-dye binding. *Anal. Biochem.* 72: 248-254.

Braverman N, Dodt G, Gould SJ and Valle D. 1998. An isoform of Pex5p, the human PTS1 receptor, is required for the import of PTS2 proteins into peroxisomes. *Hum. Mol. Genet.* 7: 1195-1205.

Brickner DG and Olsen LJ. 1998. Nucleotide triphosphates are required for the transport of glycolate oxidase into peroxisomes. *Plant Physiol.* 116: 309-317.

Brickner DG, Harada JJ and Olsen LJ. 1997. Protein transport into higher plant peroxisomes. *Plant Physiol.* 113: 1213-1221.

Brocard C, Lametschwandtner G, Koudelka R and Hartig A. 1997. Pex14p is a member of the protein linkage map of Pex5p. *EMBO J.* 16: 5491-5500.

Brown FR, McAdams AJ, Cummins JW, Donkol R, Singh I, Moser AB and Moser HW. 1982. Cerebro-hepato-renal (Zellweger) syndrome and neonatal adrenoleukodystrophy: similarities in phenotype and accumulation of very long chain fatty acids. *Johns Hopkins Med. J.* 151: 344-351.

Brown TW, Titorenko VI and Rachubinski RA. 2000. Mutants of the *Yarrowia lipolytica PEX23* gene encoding an integral peroxisomal membrane protein mislocalize matrix proteins and accumulate vesicles containing peroxisomal matrix and membrane proteins. *Mol. Biol. Cell* 11: 141-152.

Burnette WN. 1981. "Western blotting": Electrophoretic transfer of proteins from sodium dodecyl sulfate-polyacrylamide gels to unmodified nitrocellulose and radiographic detection with antibody and radioiodinated protein A. *Anal. Biochem.* 112: 195-203.

Chang C-C, South S, Warren D, Jones J, Moser AB, Moser HW and Gould SJ. 1999. Metabolic control of peroxisome abundance. *J. Cell Sci.* 112: 1579-1590.

Chen X and Schnell DJ. 1999. Protein import into chloroplasts. *Trends Cell Biol.* 9: 222-227.

Clarke SD, Thuillier P, Baillie RA and Xiaoming S. 1999. Peroxisome proliferator-activated receptors: a family of lipid-activated transcription factors. *Am. J. Clin. Nutr.* 70: 566-571.

Cregg JM, van der Klei IJ, Sulter GJ, Veenhuis M and Harder W. 1990. Peroxisome-deficient mutants of *Hansenula polymorpha*. *Yeast* 6: 87-97.

Crookes WJ and Olsen LJ. 1998. The effects of chaperones and the influence of protein assembly on peroxisomal protein import. *J. Biol. Chem.* 273: 17236-17242.

de Duve C and Baudhuin P. 1966. Peroxisomes (microbodies and related particles). *Physiol. Rev.* 46: 323-357.

de Hoop MJ and AB G. 1992. Import of proteins into peroxisomes and other microbodies. *Biochem. J.* 286: 657-669.

Devore JL. 1987. Probability and statistics for engineering and the sciences. Wadsworth, Belmont, CA.

Diestelkötter P and Just WW. 1993. In vitro insertion of the 22-kD peroxisomal membrane protein into isolated rat liver peroxisomes. *J. Cell Biol.* 123: 1717-1725.

Distel B, Erdmann R, Gould SJ, Blobel G, Crane DI, Cregg JM, Dodt G, Fujiki Y, Goodman JM, Just WW, Kiel JAKW, Kunau W-H, Lazarow PB, Mannaerts GP, Moser HW, Osumi T, Rachubinski RA, Roscher A, Subramani S, Tabak HF, Tsukamoto T, Valle D, van der Klei IJ, van Veldhoven PP and Veenhuis M. 1996. A unified nomenclature for peroxisome biogenesis factors. *J. Cell Biol.* 135: 1-3.

Distel B, van der Ley I, Veenhuis M and Tabak HF. 1988. Alcohol oxidase expressed under nonmethylotrophic conditions is imported, assembled, and enzymatically active in peroxisomes of *Hansenula polymorpha*. *J. Cell Biol.* 107: 1669-1675.

Dodt G and Gould SJ. 1996. Multiple PEX genes are required for proper subcellular distribution and stability of Pex5p, the PTS1 receptor: evidence that PTS1 protein import is mediated by a cycling receptor. *J. Cell Biol.* 135: 1763-1774.

Dodt G, Braverman N, Wong C, Moser A, Moser HW, Watkins P, Valle D and Gould SJ. 1995. Mutations in the PTS1 receptor gene, *PXR1*, define complementation group 2 of the peroxisome biogenesis disorders. *Nature Genet.* 9: 115-125.

Dyer JM, McNew JA and Goodman JM. 1996. The sorting sequence of the peroxisomal integral membrane protein PMP47 is contained within a short hydrophilic loop. *J. Cell Biol.* 133: 269-280.

Eilers M and Schatz G. 1986. Binding of a specific ligand inhibits import of a purified precursor protein into mitochondria. *Nature* 322: 228-232.

Eilers M and Schatz G. 1988. Protein unfolding and the energetics of protein translocation across biological membranes. *Cell* 52: 481-483.

Eitzen GA. 1997. Peroxisome assembly in *Yarrowia lipolytica*. Ph.D. Thesis, University of Alberta, Edmonton, Alberta.

Eitzen GA, Aitchison JA, Szilard RK, Veenhuis M, Nuttley WM and Rachubinski RA. 1995. The *Yarrowia lipolytica* gene *PAY2* encodes a 42-kDa peroxisomal integral membrane protein essential for matrix protein import and peroxisome enlargement but not for peroxisome membrane proliferation. *J. Biol. Chem.* 270: 1429-1436.

Eitzen GA, Szilard RK and Rachubinski RA. 1997. Enlarged peroxisomes are present in oleic-acid grown *Yarrowia lipolytica* overexpressing the *PEX16* gene encoding an intraperoxisomal peripheral membrane protein. *J. Cell Biol.* 137: 1265-1278.

Eitzen GA, Titorenko VI, Smith JJ, Veenhuis M, Szilard RK and Rachubinski RA. 1996. The *Yarrowia lipolytica* gene *PAY5* encodes a peroxisomal integral membrane protein homologous to the mammalian peroxisome assembly factor PAF-1. *J. Biol. Chem.* 271: 20300-20306.

Elgersma Y and Tabak HF. 1996. Proteins involved in peroxisome biogenesis and functioning. *Biochim. Biophys. Acta* 1286: 269-283.

Elgersma Y, Elgersma-Hooisma M, Wenzel T, McCaffrey JM, Farquhar MG and Subramani S. 1998. A mobile PTS2 receptor for peroxisomal protein import in *Pichia pastoris*. *J. Cell Biol.* 140: 807-820.

Elgersma Y, Kwast L, Klein A, Voorn-Brouwer T, van den Berg M, Metzig B, America T, Tabak HF and Distel B. 1996. The SH3 domain of the *Saccharomyces cerevisiae* peroxisomal membrane protein Pex13p functions as a docking site for Pex5p, a mobile receptor for the import of PTS1-containing proteins. *J. Cell Biol.* 135: 97-109.

Elgersma Y, Kwast L, van den Berg M, Snyder WB, Distel B, Subramani S and Tabak HF. 1997. Overexpression of Pex15p, a phosphorylated peroxisomal integral membrane protein required for peroxisome assembly in *S. cerevisiae*, causes proliferation of the endoplasmic reticulum membrane. *EMBO J.* 16: 7326-7341.

Elgersma Y, van Roermund CWT, Wanders RJA and Tabak HF. 1995. Peroxisomal and mitochondrial carnitine acetyltransferases of *Saccharomyces cerevisiae* are encoded by a single gene. *EMBO J.* 14: 3472-3479.

Elgersma Y, van den Berg M, Tabak HF and Distel B. 1993. An efficient positive selection procedure for the isolation of peroxisomal assembly mutants of *Saccharomyces cerevisiae*. *Genetics* 135: 731-740.

Endrizzi A, Pagot Y, Le Clainche A, Nicaud J-M and Belin J-M. 1996. Production of lactones and peroxisomal β-oxidation in yeasts. *Crit. Rev. Biotechnol.* 16: 301-329.

Erdmann R and Blobel G. 1995. Giant peroxisomes in oleic acid-induced *Saccharomyces cerevisiae* lacking the peroxisomal membrane protein Pmp27p. *J. Cell Biol.* 128: 509-523.

Erdmann R and Blobel G. 1996. Identification of Pex13p, a peroxisomal membrane receptor for the PTS1 recognition factor. *J. Cell Biol.* 135: 111-121.

Erdmann R, Veenhuis M and Kunau W-H. 1997. Peroxisomes: Organelles at the crossroads. *Trends Cell Biol.* 7: 400-407.

Erdmann R, Veenhuis M, Mertens D and Kunau W-H. 1989. Isolation of peroxisome-deficient mutants of *Saccharomyces cerevisiae*. *Proc. Natl. Acad. Sci. USA* 86: 5419-5423.

Erdmann R, Wiebel FF, Flessau A, Rytka J, Beyer A, Frölich K-U and Kunau W-H. 1991. *PAS1*, a yeast gene required for peroxisome biogenesis, encodes a member of a novel family of putative ATPases. *Cell* 64: 499-510.

Evers ME, Titorenko VI, Harder W, van der Klei IJ and Veenhuis M. 1996. Flavin adenine dinucleotide binding is a crucial step in alcohol oxidase assembly in the yeast *Hansenula polymorpha*. *Yeast* 12: 917-923.

Evers ME, Titorenko VI, van der Klei IJ, Harder A and Veenhuis M. 1994. Assembly of alcohol oxidase in peroxisomes of the yeast *Hansenula polymorpha* requires the cofactor flavin adenine dinucleotide. *Mol. Biol. Cell* 5: 829-837.

Faber KN, Heyman JA and Subramani S. 1998. Two AAA family peroxins, PpPex1p and PpPex6p, interact with each other in an ATP-dependent manner and are associated with different subcellular membranous structures distinct from peroxisomes. *Mol. Cell. Biol.* 18: 936-943.

Fields S and Song OK. 1989. A novel genetic system to detect protein-protein interactions. *Nature* 340: 245-246.

Filipits M, Simon MM, Rapatz W, Hamilton B and Ruis H. 1993. A *Saccharomyces cerevisiae* upstream activating sequence mediates induction of peroxisome proliferation by fatty acids. *Gene* 132: 49-55.

Fransen M, Brees C, Baumgart E, Vanhooren JC, Baes M, Mannaerts GP and van Veldhoven PP. 1995. Identification and characterization of the putative human peroxisomal C-terminal targeting signal receptor. *J. Biol. Chem.* 270: 7731-7736.

Fransen M, Terlecky SR and Subramani S. 1998. Identification of a human PTS1 receptor docking protein directly required for peroxisomal protein import. *Proc. Natl. Acad. Sci. USA* 95: 8087-8092.

Fujiki Y, Hubbard AL, Fowler S and Lazarow PB. 1982. Isolation of intracellular membranes by means of sodium carbonate treatment: application to endoplasmic reticulum. *J. Cell Biol.* 93: 97-102.

Fujiki Y, Rachubinski RA and Lazarow PB. 1984. Synthesis of a major integral membrane polypeptide of rat liver peroxisomes on free polysomes. *Proc. Natl. Acad. Sci. USA* 81: 7127-7131.

Fujiki Y. 1996. Approaches to studies on peroxisome biogenesis and human peroxisome-deficient disorders. *Ann. N. Y. Acad. Sci.* 804: 491-501.

Gaillard C and Strauss F. 1990. Ethanol precipitation of DNA with linear polyacrylamide as a carrier. *Nucleic Acids Res.* 18: 378.

Gaillardin CM, Charoy V and Heslot H. 1973. A study of copulation, sporulation and meiotic segregation in *Candida lipolytica*. *Arch. Mikrobiol.* 92: 69-83.

Geisbrecht BV, Collins CS, Reuber BE and Gould SJ. 1998. Disruption of a PEX1-PEX6 interaction is the most common cause of the neurological disorders Zellweger syndrome, neonatal adrenoleukodystrophy, and infantile Refsum's disease. *Proc. Natl. Acad. Sci. USA* 95: 8630-8635.

Girzalsky W, Rehling P, Stein K, Kipper J, Blank L, Kunau W-H and Erdmann R. 1999. Involvement of Pex13p in Pex14p localization and peroxisomal targeting signal 2-dependent protein import into peroxisomes. *J. Cell Biol.* 144: 1151-1162.

Gleeson MA and Sudbery PE. 1988. Genetic analysis in the methylotrophic yeast *Hansenula polymorpha*. *Yeast* 4:293-303.

Glover JR, Andrews DW and Rachubinski RA. 1994a. *Saccharomyces cerevisiae* peroxisomal thiolase is imported as a dimer. *Proc. Natl. Acad. Sci. USA* 91: 10541-10545.

Glover JR, Andrews DW, Subramani S and Rachubinski RA. 1994b. Mutagenesis of the amino targeting signal of *Saccharomyces cerevisiae* 3-ketoacyl-CoA thiolase reveals conserved amino acids required for import into peroxisomes *in vivo*. *J. Biol. Chem.* 269: 7558-7563.

Gödecke A, Veenhuis M, Roggenkamp R, Janowicz ZA and Hollenberg CP. 1989. Biosynthesis of the peroxisomal dihydroxyacetone synthase from *Hansenula polymorpha* in *Saccharomyces cerevisiae* induces growth but not proliferation of peroxisomes. *Curr. Genet.* 16: 13-20.

Goldfischer S, Moore CL, Johnson AB, Spiro AJ, Valsamis MP, Wisniewski HK, Ritch RH, Noron WT, Rapin I and Gartner LM. 1973. Peroxisomal and mitochondrial defects in the cerebro-hepato-renal syndrome. *Science* 182: 62-64.

Goodman JM, Trapp SB, Hwang H and Veenhuis M. 1990. Peroxisomes induced in *Candida boidinii* by methanol, oleic acid and *D*-alanine vary in metabolic function but share common integral membrane proteins. *J. Cell Sci.* 97: 193-204.

Gorgas K. 1984. Peroxisomes in sebaceous glands V. Complex peroxisomes in the mouse preputial gland: serial sectioning and three-dimensional reconstruction studies. *Anat. Embryol.* 169: 261-270.

Gorgas K. 1985. Serial section analysis of mouse hepatic peroxisomes. *Anat. Embryol.* 172: 21-32.

Götte K, Girzalsky W, Linkert M, Baumgart E, Kammerer S, Kunau W-H and Erdmann R. 1998. Pex19p, a farnesylated protein essential for peroxisome biogenesis. *Mol. Cell. Biol.* 18: 616-628.

Gould SJ, Kalish JE, Morrell JC, Bjorkman J, Urquhart AJ and Crane DI. 1996. Pex13p is an SH3 protein of the peroxisome membrane and a docking factor for the predominantly cytoplasmic PTS1 receptor. *J. Cell Biol.* 135: 85-95.

Gould SJ, Keller G-A, Hosken N, Wilkinson J and Subramani S. 1989. A conserved tripeptide sorts proteins to peroxisomes. *J. Cell Biol.* 108: 1657-1664.

Gould SJ, Keller G-A, Schneider M, Howell SH, Garrard LJ, Goodman JM, Distel B, Tabak H and Subramani S. 1990a. Peroxisomal protein import is conserved between yeast, plants, insects and mammals. *EMBO J.* 9: 85-90.

Gould SJ, Krisans S, Keller G-A and Subramani S. 1990b. Antibodies directed against the peroxisomal targeting signal of firefly luciferase recognize multiple mammalian peroxisomal proteins. *J. Cell Biol.* 110: 27-34.

Gould SJ, McCollum D, Spong AP, Heyman JA and Subramani S. 1992. Development of the yeast *Pichia pastoris* as a model organism for a genetic and molecular analysis of peroxisome assembly. *Yeast* 8: 613-628.

Hajra AK, Burke CL and Jones CL. 1979. Subcellular localization of acyl coenzyme A: dihydroxyacetone phosphate acyltransferase in rat liver peroxisomes (microbodies). *J. Biol. Chem.* 254: 10896-10900.

Hanahan D and Meselson M. 1980. Plasmid screening at high colony density. *Gene* 1: 63-67.

Harlow E and Lane D. 1988. Antibodies: A Laboratory Manual. Cold Spring Harbor Laboratory, Cold Spring Harbor, NY. pp. 63, 70.

Hashimoto T. 1999. Peroxisomal β-oxidation enzymes. *Neurochem. Res.* 24: 551-563.

Häusler T, Stierhof Y-D, Wirtz E and Clayton C. 1996. Import of a DHFR hybrid protein into glyoxysomes in vivo is not inhibited by the folate-analogue aminopterin. *J. Cell Biol.* 132: 311-324.

Herrmann JM and Neupert W. 2000. Protein transport into mitochondria. *Curr. Opin. Microbiol.* 2: 210-214.

Hettema EH, Distel B and Tabak HF. 1999. Import of proteins into peroxisomes. *Biochim. Biophys. Acta* 1451: 17-34.

Hettema EH, Ruigrok CCM, Groot Koerkamp M, van den Berg M, Tabak HF, Distel B and Braakman I. 1998. The cytosolic DnaJ-like protein Djp1p is involved specifically in peroxisomal protein import. *J. Cell Biol.* 27: 421-434.

Heymans HAS, Schutgens RBH, Tan R, van den Bosch H and Borst P. 1983. Severe plasmalogen deficiency in tissues of infants without peroxisomes (Zellweger syndrome). *Nature* 306: 69-70.

Hiltunen JK, Wenzel B, Beyer A, Erdmann R, Fosså A and Kunau W-H. 1992. Peroxisomal multifunctional β-oxidation protein of *Saccharomyces cerevisiae*. *J. Biol. Chem.* 267: 6646-6653.

Höhfeld J, Veenhuis M and Kunau W-H. 1991. *PAS3*, a *Saccharomyces cerevisiae* gene encoding a peroxisomal integral membrane protein essential for peroxisome biogenesis. *J. Cell Biol.* 114: 1167-1178.

Honsho M, Tamura S, Shimozawa N, Suzuki Y, Kondo N and Fujiki Y. 1998. Mutation in *PEX16* is causal in the peroxisome-deficient Zellweger syndrome complementation group D. *Am. J. Hum. Genet.* 63: 1622-1630.

Huhse B, Rehling P, Albertini M, Blank L, Meller K and Kunau W-H. 1999. Pex17p of *Saccharomyces cerevisiae* is a novel peroxin and component of the peroxisomal protein translocation machinery. *J. Cell Biol.* 140: 49-60.

Huynh TV, Young RA and Davis RW. 1985. *In* DNA Cloning: A Practical Approach. Vol. 1. Glover DM, editor. IRL Press, Oxford.

Imanaka T, Shiina Y, Takano T, Hashimoto T and Osumi T. 1996. Insertion of the 70-kDa peroxisomal membrane protein into peroxisomal membranes in vivo and in vitro. *J. Biol. Chem.* 271: 3706-3713.

Imanaka T, Small GM and Lazarow PB. 1987. Translocation of acyl-CoA oxidase into peroxisomes requires ATP hydrolysis but not a membrane potential. *J. Cell Biol.* 105: 2915-2922.

Innis MA and Gelfand DH. 1990. Optimization of PCRs. *In* PCR Protocols: A Guide to Methods and Applications. Innis MA, Gelfand DH, Sninsky JJ and White TJ, editors. Academic Press, San Diego, CA. pp. 3-12.

Johnson MA, Waterham HR, Ksheminska GP, Fayura LR, Cereghino JL, Stasyk OV, Veenhuis M, Kulachkovsky AR, Sibirny AA and Cregg JM. 1999. Positive selection of novel peroxisome biogenesis-defective mutants of the yeast *Pichia pastoris*. *Genetics* 151: 1379-1391.

Kalies K-U and Hartmann E. 1998. Protein translocation into the endoplasmic reticulum (ER): two similar routes with different modes. *Eur. J. Biochem.* 254: 1-5.

Kalish JE, Keller G-A, Morrell JC, Mihalik SJ, Smith B, Cregg JM and Gould SJ. 1996. Characterization of a novel component of the peroxisomal import apparatus using fluorescent peroxisomal proteins. *EMBO J.* 15: 3275-3285.

Kamiryo T, Abe M, Okazaki K, Kato S and Shimamoto N. 1982. Absence of DNA in peroxisomes of *Candida tropicalis*. *J. Bacteriol.* 152: 269-274.

Kammerer S, Holzinger A, Welsch U and Roscher AA. 1998. Cloning and characterization of the gene encoding the human peroxisome assembly protein Pex3p. *FEBS Lett.* 429: 53-60.

Karpichev IV and Small GM. 1998. Global regulatory functions of Oaf1p and Pip2p (Oaf2p) transcription factors that regulate genes encoding peroxisomal proteins in *Saccharomyces cerevisiae*. *Mol. Cell. Biol.* 18: 6560-6570.

Keller G-A, Krisans S, Gould SJ, Sommer JM, Wang CC, Schliebs W, Kunau W, Brody S and Subramani S. 1991. Evolutionary conservation of a microbody targeting signal that targets proteins to peroxisomes, glyoxysomes and glycosomes. *J. Cell Biol.* 114: 893-904.

Klein P, Kanehisa M and De Lisi C. 1985. The detection and classification of membane-spanning proteins. *Biochim. Biophys. Acta* 815: 468-476.

Koller A, Snyder WB, Faber KN, Wenzel TJ, Rangell L, Keller G-A and Subramani S. 1999. Pex22p of *Pichia pastoris*, essential for peroxisomal matrix protein import, anchors the ubiquitin-conjugating enzyme, Pex4p, on the peroxisomal membrane. *J. Cell Biol.* 146: 99-112.

Kolodziej PA and Young RA. 1991. Epitope tagging and protein surveillance. *Methods Enzymol.* 194: 508-519.

Kragler F, Lametschwandtner G, Christmann J, Harting A and Harada JJ. 1998. Identification and analysis of the plant peroxisomal targeting signal 1 receptor NtPEX5. *Proc. Natl. Acad. Sci. USA* 95: 13336-13341.

Kragler F, Langeder A, Raupachova J, Binder M and Hartig A. 1993. Two independent peroxisomal targeting signals in catalase A of *Saccharomyces cerevisiae*. *J. Cell Biol.* 120: 665-673.

Kryvi H, Kvannes J and Flatmark T. 1990. Freeze-fracture study of rat liver peroxisomes: evidence for an induction of intramembrane particles by agents stimulating peroxisomal proliferation. *Eur. J. Cell Biol.* 53: 227-233.

Kunau W-H and Erdmann R. 1998. Peroxisome biogenesis: back to the endoplasmic reticulum? *Curr. Biol.* 8: 299-302.

Kunau W-H and Hartig A. 1992. Peroxisome biogenesis in *Saccharomyces cerevisiae*. *Antonie van Leeuwenhoek J. Microbiol. Serol.* 62: 63-78.

Kunau W-H, Bühne S, de la Garza M, Kionka C, Mateblowski M, Schultz-Borchard U and Thieringer R. 1988. Comparative enzymology of β-oxidation. *Biochem. Soc. Trans.* 16: 418-420.

Kyte J and Doolittle RF. 1982. A simple method for displaying the hydropathic character of a protein. *J. Mol. Biol.* 157: 105-132.

Laemmli UK. 1970. Cleavage of structural proteins during the assembly of the head of bacteriophage T4. *Nature* 227: 680-685.

Lazarow PB and Fujiki Y. 1985. Biogenesis of peroxisomes. *Annu. Rev. Cell Biol.* 1: 489-530.

Lazarow PB and Moser HW. 1994. Disorders of peroxisome biogenesis. *In* The Metabolic and Molecular Bases of Inherited Disease. Scriver CR, Beaudet AL, Sly WS and Valle D, editors. McGraw-Hill, New York, NY. pp. 2287-2324.

Lee MS, Mullen RT and Trelease RN. 1997. Oilseed isocitrate lyases lacking their essential type 1 peroxisomal targeting signal are piggybacked to glyoxysomes. *Plant Cell* 9: 185-197.

Liu H, Tan X, Russell KA, Veenhuis M and Cregg JM. 1995. *PER3*, a gene required for peroxisome biogenesis in *Pichia pastoris*, encodes a peroxisomal membrane protein involved in protein import. *J. Biol. Chem.* 270: 10940-10951.

Liu H, Tan X, Veenhuis M, McCollum D and Cregg JM. 1992. An efficient screen for peroxisome-deficient mutants of *Pichia pastoris*. *J. Bacteriol.* 174: 4943-4951.

Liu Y, Björkman J, Urquhart A, Wanders RJA, Crane DI and Gould SJ. 1999. *PEX13* is mutated in complementation group 13 of the peroxisome-biogenesis disorders. *Am. J. Hum. Genet.* 65: 621-634.

Lück H. 1963. Catalase. *In* Methods of Enzymatic Analysis. Bergmeyer H-U, editor. Academic Press, New York, NY. pp. 885-888.

MacKenzie RE. 1984. Biogenesis and interconversion of substituted tetrahydrofolates. *In* Folates and Pterins. Vol. 1. Blakley RL and Benkovic SJ, editors. Wiley, New York, NY. pp. 255-306.

Maniatis T, Fritsch EF and Sambrook J. 1982. Molecular Cloning: A Laboratory Manual. Cold Spring Harbor Laboratory, Cold Spring Harbor, NY.

Marshall PA, Krimkevich YI, Lark RH, Dyer JM, Veenhuis M and Goodman JM. 1995. Pmp27 promotes peroxisomal proliferation. *J. Cell Biol.* 129: 345-355.

Matsuzono Y, Kinoshita N, Tamura S, Shimozawa N, Hamasaki M, Ghaedi K, Wanders RJA, Suzuki Y, Kondo N and Fujiki Y. 1999. Human *PEX19*: cDNA cloning by functional complementation, mutation analysis in a patient with Zellweger syndrome, and potential role in peroxisomal membrane assembly. *Proc. Natl. Acad. Sci.* 96: 2116-2121.

McCammon MT, McNew JA, Willy PJ and Goodman JM. 1994. An internal region of the peroxisomal membrane protein PMP47 is essential for sorting to peroxisomes. *J. Cell Biol.* 124: 915-925.

McNew JA and Goodman JM. 1994. An oligomeric protein is imported into peroxisomes in vivo. *J. Cell Biol.* 127: 1245-1257.

McNew JA and Goodman JM. 1996. The targeting and assembly of peroxisomal proteins: some old rules do not apply. *Trends Biochem. Sci.* 21: 54-58.

Morand OH, Allen LA, Zoeller RA and Raetz CR. 1990. A rapid selection for animal cell mutants with defective peroxisomes. *Biochim. Biophys. Acta* 1034: 132-141.

Moser HW and Moser AB. 1996. Peroxisomal disorders: overview. *Ann. N. Y. Acad. Sci.* 804: 427-441.

Musacchio A, Saraste M and Wilmanns M. 1994. High-resolution crystal structures of tyrosine kinase SH3 domains complexed with proline-rich peptides. *Nature Struct. Biol.* 1: 546-551.

Needleman RB and Tzagoloff A. 1975. Breakage of yeast: a simple method for processing multiple samples. *Anal. Biochem.* 64: 545-549.

Nunnari J and Walter P. 1996. Regulation of organelle biogenesis. *Cell* 84: 389-394.

Nuttley WM, Bodnar AG, Mangroo D and Rachubinski RA. 1990. Isolation and characterization of membranes from oleic acid-induced peroxisomes of *Candida tropicalis*. *J. Cell Sci.* 95: 463-470.

Nuttley WM, Brade AM, Eitzen GA, Veenhuis M, Aitchison JD, Szilard RK, Glover JR and Rachubinski RA. 1994. *PAY4*, a gene required for peroxisome assembly in the yeast *Yarrowia lipolytica*, encodes a novel member of a family of putative ATPases. *J. Biol. Chem.* 269: 556-566.

Nuttley WM, Brade AM, Gaillardin C, Eitzen GA, Glover JR, Aitchison JD and Rachubinski RA. 1993. Rapid identification and characterization of peroxisome assembly mutants in *Yarrowia lipolytica*. *Yeast* 9: 507-517.

Otera H, Okumoto K, Takeishi K, Ikoma Y, Matsuda E, Nishimura M, Tsukamoto T, Osumi T, Ohashi K, Higuchi O and Fujiki Y. 1998. Peroxisome targeting signal type 1 (PTS1) receptor is involved in import of both PTS1 and PTS2: studies with *PEX5*-defective CHO cell mutants. *Mol. Cell. Biol.* 18: 388-399.

Passreiter M, Anton M, Lay D, Frank R, Harter C, Wieland FT, Gorgas K and Just WW. 1998. Peroxisome biogenesis: involvement of ARF and coatomer. *J. Cell. Biol.* 141: 373-383.

Pause B, Diestelkötter P, Heid H and Just WW. 1997. Cytosolic factors mediate protein insertion into the peroxisomal membrane. *FEBS Lett.* 414: 95-98.

Poll-The BT, Roels F, Ogier H, Scotto J, Vamecq J, Schutgens RBH, Wanders, RJA, van Roermund CWT, van Wijland MJA, Schram AW, Tager JM and Saudubray J-M. 1988. A new peroxisomal disorder with enlarged peroxisomes and a specific deficiency of acyl-CoA oxidase (pseudo-neonatal adrenoleukodystrophy). *Am. J. Hum. Genet.* 42: 422-434.

Pool MR, López-Huertas E and Baker A. 1998. Characterization of intermediates in the process of plant peroxisomal import. *EMBO J.* 17: 6854-6862.

Pringle JR, Adams AEM, Drubin DG and Haarer BK. 1991. Immunofluorescence methods for yeast. *Methods Enzymol.* 194: 565-602.

Proudfoot NJ and Brownlee GG. 1976. 3' non-coding region sequences in eukaryotic messenger RNA. *Nature* 263: 211-214.

Purdue PE and Lazarow PB. 1995. Identification of peroxisomal membrane ghosts with an epitope-tagged integral membrane protein in yeast mutants lacking peroxisomes. *Yeast* 11: 1045-1060.

Purdue PE, Yang X and Lazarow PB. 1998. Pex18p and Pex21p, a novel pair of related peroxins essential for peroxisomal targeting by the PTS2 pathway. *J. Cell Biol.* 143: 1859-1869.

Qin Y-M, Marttila MS, Haapalainen AM, Siivari KM, Glumoff T and Hiltunen JK. 1999. Yeast peroxisomal multifunctional enzyme: (3*R*)-hydroxyacyl-CoA dehydrogenase domains A and B are required for optimal growth on oleic acid. *J. Biol. Chem.* 274: 28619-28625.

Rachubinski RA and Subramani S. 1995. How proteins penetrate peroxisomes. *Cell* 83: 525-528.

Rapp S, Soto U and Just WW. 1993. Import of firefly luciferase into peroxisomes of permeabilized Chinese hamster ovary cells: a model system to study peroxisomal protein import in vitro. *Exp. Cell Res.* 205: 59-65.

Reddy JK and Chu R. 1996. Peroxisome proliferator-induced pleiotropic responses: pursuit of a phenomenon. *Ann. N. Y. Acad. Sci.* 804: 176-201.

Rehling P, Marzioch M, Niesen F, Wittke E, Veenhuis M and Kunau W-H. 1996. The import receptor for the peroxisomal targeting signal 2 (PTS2) in *Saccharomyces cerevisiae* is encoded by the *PAS7* gene. *EMBO J.* 15: 2901-2913.

Rehling P, Skaletz-Rorowski A, Girzalsky W, Voorn-Brouwer T, Franse MM, Distel B, Veenhuis M, Kunau W-H and Erdmann R. 2000. Pex8p, an intraperoxisomal peroxin of *S. cerevisiae* required for protein transport into peroxisomes binds the PTS1 receptor Pex5p. *J. Biol. Chem.* 275: 3593-3602.

Roggenkamp R, Didion T and Kowallik KV. 1989. Formation of irregular giant peroxisomes by overproduction of the crystalloid core protein methanol oxidase in the methylotrophic yeast *Hansenula polymorpha*. *Mol. Cell Biol.* 9: 988-994.

Rose MD, Winston F and Heiter P. 1988. Laboratory Course Manual for Methods in Yeast Genetics. Cold Spring Harbor Laboratory, Cold Spring Harbor, NY.

Saiki RK. 1990. Amplification of genomic DNA. *In* PCR Protocols: A Guide to Methods and Applications. Innis MA, Gelfand DH, Sninsky JJ and White TJ, editors. Academic Press, San Diego, CA. pp. 13-21.

Sakai Y, Marshall PA, Saiganji A, Takabe K, Saiki H, Kato N and Goodman JM. 1995. The *Candida boidinii* peroxisomal membrane protein Pmp30 has a role in peroxisome proliferation and is functionally homologous to Pmp27 from *Saccharomyces cerevisiae*. *J. Bacteriol.* 177: 6773-6781.

Salomons FA, van der Klei IJ, Kram AM, Harder W and Veenhuis M. 1997. Brefeldin A interferes with peroxisomal protein sorting in the yeast *Hansenula polymorpha*. *FEBS Lett.* 411: 133-139.

Sanger F, Niklen S and Coulson AR. 1977. DNA sequencing with chain-terminating inhibitors. *Proc. Natl. Acad. Sci. USA* 74: 5463-5467.

Santos MJ, Imanaka T, Shio H and Lazarow PB. 1988a. Peroxisomal integral membrane proteins in control and Zellweger fibroblasts. *J. Biol. Chem.* 263: 10502-10509.

Santos MJ, Imanaka T, Shio H, Small GM and Lazarow PB. 1988b. Peroxisomal membrane ghosts in Zellweger syndrome – aberrant organelle assembly. *Science* 239: 1536-1538.

Schatz G and Dobberstein B. 1996. Common principles of protein translocation across membranes. *Science* 271: 1519-1526.

Schliebs W, Saidowsky J, Agianian B, Dodt G, Herberg FW and Kunau W-H. 1999. Recombinant human peroxisomal targeting receptor PEX5. Structural basis for interaction of PEX5 with PEX14. *J. Biol. Chem.* 274: 5666-5673.

Schrader M, Reuber BE, Morrell JC, Jimenez-Sanchez G, Obie C, Stroh TA, Valle D, Schroer TA and Gould SJ. 1998. Expression of *PEX11β* mediates peroxisome proliferation in the absence of extracellular stimuli. *J. Biol. Chem.* 273: 29607-29614.

Schram AW, Strijland A, Hashimoto T, Wanders RJA, Schutgens RBH, van den Bosch H and Tager JM. 1986. Biosynthesis and maturation of peroxisomal β-oxidation enzymes in fibroblasts in relation to the Zellweger syndrome and infantile Refsum's disease. *Proc. Natl. Acad. Sci. USA* 83: 6156-6158.

Shannon, KW and Rabinowitz, JC. 1988. Isolation and characterization of the *Saccharomyces cerevisiae MIS1* gene encoding mitochondrial C_1-tetrahydrofolate synthase. *J. Biol. Chem.* 263: 7717-7725.

Shimizu N, Itoh R, Hirono Y, Otera H, Ghaedi K, Tateishi K, Tamura S, Okumoto K, Harano T, Mukai S and Fujiki Y. 1999. The peroxin Pex14p. cDNA cloning by functional complementation on a Chinese hamster ovary cell mutant, characterization, and functional analysis. *J. Biol. Chem.* 274: 12593-12604.

Shimozawa N, Suzuki Y, Zhang Z, Imamura A, Toyama R, Mukai S, Fujiki Y, Tsukamoto T, Osumi T, Orii T, Wanders RJ and Kondo N. 1999. Nonsense and temperature-sensitive mutations in *PEX13* are the cause of complementation group H of peroxisome biogenesis disorders. *Hum. Mol. Genet.* 8: 1077-1083.

Shimozawa N, Suzuki Y, Orii T, Moser A, Moser HW and Wanders RJA. 1993. Standardization of complementation grouping of peroxisome-deficient disorders and the second Zellweger patient with peroxisomal assembly factor-1 (PAF-1) defect. *Am. J. Hum. Genet.* 52: 843-844.

Slawecki M, Dodt G, Steinberg S, Moser AB, Moser HW and Gould SJ. 1995. Identification of three distinct peroxisomal protein import defects in patients with peroxisomal biogenesis disorders. *J. Cell Sci.* 108: 1817-1829.

Singh I, Moser AE, Goldfischer S and Moser HW. 1984. Lignoceric acid is oxidized in the peroxisome: implications for the Zellweger cerebro-hepato-renal syndrome and adrenoleukodystrophy. *Proc. Natl. Acad. Sci. USA* 81: 4203-4207.

Sloots JA, Aitchison JD and Rachubinski RA. 1991. Glucose-responsive and oleic acid-responsive elements in the gene encoding the peroxisomal trifunctional enzyme of *Candida tropicalis*. *Gene* 105: 129-134.

Small GM, Szabo LJ and Lazarow PB. 1988. Acyl-CoA oxidase contains two targeting sequences each of which can mediate protein import into peroxisomes. *EMBO J.* 7: 1167-1173.

Smith JJ, Szilard RK, Marelli M and Rachubinski RA. 1997. The peroxin Pex17p of the yeast *Yarrowia lipolytica* is associated peripherally with the peroxisomal membrane and is required for the import of a subset of matrix proteins. *Mol. Cell. Biol.* 17: 2511-2520.

Smith JJ, Brown TW, Eitzen GA and Rachubinski RA. 2000. Regulation of peroxisome size and number by fatty acid β-oxidation in the yeast *Yarrowia lipolytica*. *J. Biol. Chem.* 275: 20168-20178.

Snyder WB, Faber KN, Wenzel TJ, Koller A, Lüers GH, Rangell L, Keller G-A and Subramani S. 1999a. Pex19p interacts with Pex3p and Pex10p and is essential for peroxisome biogenesis in *Pichia pastoris*. *Mol. Biol. Cell* 10: 1745-1761.

Snyder WB, Koller A, Choy AJ, Johnson MA, Cregg JM, Rangell L, Keller G-A and Subramani S. 1999b. Pex17p is required for import of both peroxisome membrane and lumenal proteins and interacts with Pex19p and the peroxisome targeting signal-receptor docking complex in *Pichia pastoris*. *Mol. Biol. Cell* 10: 4005-4019.

Soto U, Pepperkok R, Ansorge W and Just WW. 1993. Import of firefly luciferase into mammalian peroxisomes in vivo requires nucleoside triphosphates. *Exp. Cell Res.* 205: 66-75.

Soukupova M, Sprenger C, Gorgas K, Kunau W-H and Dodt G. 1999. Identification and characterization of the human peroxin PEX3. *Eur. J. Cell Biol.* 78: 357-374.

South ST and Gould SJ. 1999. Peroxisome synthesis in the absence of preexisting peroxisomes. *J. Cell Biol.* 144: 255-266.

Stroobants AK, Hettema EH, van den Berg M and Tabak HF. 1999. Enlargement of the endoplasmic reticulum membrane in *Saccharomyces cerevisiae* is not necessarily linked to the unfolded protein response via Ire1p. *FEBS Lett.* 453: 210-214.

Subramani S. 1998. Components involved in peroxisome import, biogenesis, proliferation, turnover and movement. *Physiol. Rev.* 78: 171-188.

Subramani S. 1993. Protein import into peroxisomes and biogenesis of the organelle. *Annu. Rev. Cell Biol.* 9: 445-478.

Suzuki Y, Orii T, Takiguchi M, Mori M, Hijikata M and Hashimoto T. 1987. Biosynthesis of membrane polypeptides of rat liver peroxisomes. *J. Biochem.* 101: 491-496.

Swinkels BW, Gould SJ, Bodnar AG, Rachubinski RA and Subramani S. 1991. A novel, cleavable peroxisomal targeting signal at the amino-terminus of the rat 3-ketoacyl-CoA thiolase. *EMBO J.* 10: 3255-3262.

Szilard RK, Titorenko VI, Veenhuis M and Rachubinski RA. 1995. Pay32p of the yeast *Yarrowia lipolytica* is an intraperoxisomal component of the matrix protein translocation machinery. *J. Cell Biol.* 131: 1453-1469.

Szilard RK. 2000. Identification and characterization of *Yl*Pex5p, a component of the peroxisomal translocation machinery of *Yarrowia lipolytica*. Ph.D. Thesis, University of Alberta, Edmonton, Alberta.

Talcott B and Moore MS. 1999. Getting across the nuclear pore complex. *Trends Cell Biol.* 9: 312-318.

Tamura S, Shimozawa N, Suzuki Y, Tsukamoto T, Osumi T and Fujiki Y. 1998. A cytoplasmic AAA family peroxin, Pex1p, interacts with Pex6p. *Biochem. Biophys. Res. Commun.* 245: 883-886.

Tan X, Waterham HR, Veenhuis M and Cregg JM. 1995. The *Hansenula polymorpha PER8* gene encodes a novel peroxisomal integral membrane protein involved in proliferation. *J. Cell Biol.* 128: 307-319.

Terlecky SR, Nuttley WM, McCollum D, Sock E and Subramani S. 1995. The *Pichia pastoris* peroxisomal protein PAS8p is the receptor for the C-terminal tripeptide peroxisomal targeting signal. *EMBO J.* 14: 3627-3634.

Thieringer R, Shio H, Han Y, Cohen G and Lazarow PB. 1991. Peroxisomes in *Saccharomyces cerevisiae*: immunofluorescence analysis and import of catalase A into isolated peroxisomes. *Mol. Cell. Biol.* 11: 10-522.

Titorenko VI, Chan H and Rachubinski RA. 2000. Fusion of small peroxisomal vesicles in vitro reconstructs an early step in the in vivo multistep peroxisome assembly pathway of *Yarrowia lipolytica*. *J. Cell Biol.* 148: 29-43.

Titorenko VI and Rachubinski RA. 1998a. The endoplasmic reticulum plays an essential role in peroxisome biogenesis. *Trends Biochem. Sci.* 23: 231-233.

Titorenko VI and Rachubinski RA. 1998b. Mutants of the yeast *Yarrowia lipolytica* defective in protein exit from the endoplasmic reticulum are also defective in peroxisome biogenesis. *Mol. Cell. Biol.* 18: 2789-2803.

Titorenko VI, Smith JJ, Szilard RK and Rachubinski RA. 1998. Pex20p of the yeast *Yarrowia lipolytica* is required for the oligomerization of thiolase in the cytosol and for its targeting to the peroxisome. *J. Cell Biol.* 142: 403-420.

Titorenko VI, Ogrydziak DM and Rachubinski RA. 1997. Four distinct secretory pathways serve protein secretion, cell surface growth, and peroxisome biogenesis in the yeast *Yarrowia lipolytica*. *Mol. Cell. Biol.* 17: 5210-5226.

Tolbert NE. 1974. Isolation of subcellular organelles of metabolism on isopycnic sucrose gradients. *Methods Enzymol.* 31: 734-746.

Towbin H, Staehelin T and Gordon J. 1979. Electrophoretic transfer of proteins from polyacrylamide gels to nitrocellulose sheets: procedure and some applications. *Proc. Natl. Acad. Sci. USA* 76: 4350-4354.

Tsukamoto T, Miura S and Fujiki Y. 1991. Restoration by a 35K membrane protein of peroxisome assembly in a peroxisome-deficient mammalian cell mutant. *Nature* 350: 77-81.

Uetz P, Glot L, Cagney G, Mansfield TA, Judson RS, Knight JR, Lockshon D, Narayan V, Srinivasan M, Pochart P, Qureshi-Emill A, Li Y, Godwin B, Conover D, Kaibfleish T, Vijayadamodar G, Yang M, Johnston M, Fields S and Rothberg JM. 2000. A comprehensive analysis of protein-protein interactions in *Saccharomyces cerevisiae*. *Nature* 403: 623-627.

Urquhart AJ, Kennedy D, Gould SJ and Crane DI. 2000. Interaction of Pex5p, the type 1 peroxisome targeting signal receptor, with the peroxisomal membrane proteins Pex14p and Pex13p. *J. Biol. Chem.* 275: 4127-4136.

van den Bosch H, Schutgens RBH, Wanders RJA and Tager JM. 1992. Biochemistry of peroxisomes. *Annu. Rev. Biochem.* 61: 157-197.

van der Klei IJ and Veenhuis M. 1996. Peroxisome biogenesis in the yeast *Hansenula polymorpha*: A structural and functional analysis. *Ann. N. Y. Acad. Sci.* 804: 47-59.

van der Klei IJ and Veenhuis M. 1997. Yeast peroxisomes: function and biogenesis of a versatile cell organelle. *Trends Microbiol.* 5: 502-509.

van der Klei IJ, Hilbrands RE, Kiel JAKW, Rasmussen SW, Cregg JM and Veenhuis M. 1998. The ubiquitin-conjugating enzyme Pex4p of *Hansenula polymorpha* is required for efficient functioning of the PTS1 import machinery. *EMBO J.* 17: 3608-3618.

van der Klei IJ, Hilbrands RE, Swaving GJ, Waterham HR, Vrieling EG, Titorenko VI, Cregg JM, Harder W and Veenhuis M. 1995. The *Hansenula polymorpha PER3* gene is essential for the import of PTS1 proteins into the peroxisomal matrix. *J. Biol. Chem.* 270: 17229-17236.

van der Leij I, van den Berg M, Boot R, Franse M, Distel B and Tabak HF. 1992. Isolation of peroxisome assembly mutants from *Saccharomyces cerevisiae* with different morphologies using a novel positive selection procedure. *J. Cell Biol.* 119: 153-162.

van Roermund CWT, Elgersma Y, Singh N, Wanders RJA and Tabak HF. 1995. The membrane of peroxisomes in *Saccharomyces cerevisiae* is impermeable to NAD(H) and acetyl-CoA under *in vivo* conditions. *EMBO J.* 14: 3480-3486.

Veenhuis M and Goodman JM. 1990. Peroxisomal assembly: membrane proliferation precedes the induction of the abundant matrix proteins in the methylotrophic yeast *Candida boidinii*. *J. Cell Sci.* 96: 583-590.

Veenhuis M and Harder W. 1987. Metabolic significance and biogenesis of microbodies in yeasts. *In* Peroxisomes in Biology and Medicine. Fahimi HD and Sies H, editors. Springer-Verlag, Berlin. pp. 436-458.

Veenhuis M, Mateblowski M, Kunau W-H and Harder W. 1987. Proliferation of microbodies in *Saccharomyces cerevisiae*. *Yeast* 3: 77-84.

Wagner C. 1995. Biochemical role of folate in cellular metabolism. *In* Folate in Health and Disease. Bailey LB, editor. Marcel Dekker, New York, NY.

Walton PA, Gould SJ, Feramisco JR and Subramani S. 1992. Transport of microinjected proteins into peroxisomes of mammalian cells: inability of Zellweger cell lines to import proteins with the SKL tripeptide peroxisomal targeting signal. *Mol. Cell. Biol.* 12: 531-541.

Walton PA, Hill PE and Subramani S. 1995. Import of stably folded proteins into peroxisomes. *Mol. Biol. Cell* 6: 675-683.

Walton PA, Wendland M, Subramani S, Rachubinski RA and Welch WJ. 1994. Involvement of 70-kd heat-shock proteins in peroxisomal import. *J. Cell Biol.* 125: 1037-1046.

Wanders RJA, Schutgens RBH and Tager JM. 1985. Peroxisomal matrix enzymes in Zellweger syndrome: activity and subcellular localization in liver. *J. Inher. Metab. Dis.* 8 Suppl. 2: 151-152.

Wanders RJA. 1999. Peroxisomal disorders: clinical, biochemical and molecular aspects. *Neurochem. Res.* 24: 565-580.

Wang HJ, Le Dall M-T, Waché Y, Laroche C, Belin J-M, Gaillardin C and Nicaud J-M. 1999. Evaluation of acyl coenzyme A oxidase (Aox) isoenzyme function in the n-alkane-assimilating yeast *Yarrowia lipolytica*. *J. Bacteriol.* 181: 5140-5148.

Waterham HR and Cregg JM. 1997. Peroxisome biogenesis. *BioEssays* 19: 57-66.

Waterham HR, Russel KA, de Vries Y and Cregg JM. 1997. peroxisomal targeting, import, and assembly of alcohol oxidase in *Pichia pastoris*. *J. Cell Biol.* 139: 1419-1431.

Waterham HR, Titorenko VI, Haima P, Cregg JM, Harder W and Veenhuis M. 1994. The *Hansenula polymorpha PER1* gene is essential for peroxisome biogenesis and encodes a peroxisomal matrix protein with both carboxy- and amino-terminal targeting signals. *J. Cell Biol.* 127: 737-749.

Weibel ER and Bolender P. 1973. Stereological techniques for electron microscopic morphometry. *In* Principles and Techniques of Electron Microscopy. Vol. 3. Hayat MA, editor. Van Nostrand Reinhold, New York, NY. pp. 237-296.

Wendland M and Subramani S. 1993. Cytosol-dependent peroxisomal protein import in a permeabilized cell system. *J. Cell. Biol.* 120: 675-685.

Wiemer EAC, Lüers GH, Faber KN, Wenzel T, Veenhuis M and Subramani S. 1996. Isolation and characterization of Pas2p, a peroxisomal membrane protein essential for peroxisome biogenesis in the methylotrophic yeast *Pichia pastoris*. *J. Biol. Chem.* 271: 18973-18980.

Wiemer EAC, Nuttley WM, Bertolaet BL, Li X, Francke U, Wheelock MJ, Anne UK, Johnson KR and Subramani S. 1995. Human peroxisomal targeting signal-1 receptor restores peroxisomal protein import in cells from patients with fatal peroxisomal disorders. *J. Cell Biol.* 130: 51-65.

Will GK, Soukupova M, Hong X, Erdmann KS, Kiel JAKW, Dodt G, Kunau W-H and Erdmann R. 1999. Identification and characterization of the human orthologue of yeast Pex14p. *Mol. Cell. Biol.* 19: 2265-2277.

Wilm M, Shevchenko A, Houthaeve T, Breit S, Schweigerer L, Fotsis T and Mann M. 1996. Femtomole sequencing of proteins from polyacrylamide gels by nano-electrospray mass spectrometry. *Nature* 379: 466-469.

Yamamoto K and Fahimi HD. 1987. Three-dimensional reconstruction of a peroxisomal reticulum in regenerating rat liver: evidence of interconnections between heterogeneous segments. *J. Cell Biol.* 105: 713-722.

Zaret KS and Sherman F. 1982. DNA sequence required for efficient transcription termination in yeast. *Cell* 28: 563-573

Zhang H, Scholl R, Browse J and Somerville C. 1988. Double stranded DNA sequencing as a choice for DNA sequencing. *Nucleic Acids Res.* 16: 220.

Zhang JW, Han Y and Lazarow PB. 1993. Novel peroxisome clustering mutants and peroxisome biogenesis mutants of *Saccharomyces cerevisiae*. *J. Cell Biol.* 123: 1133-1147.

Zhang JW and Lazarow PB. 1996. Peb1p (Pas7p) is an intraperoxisomal receptor for the NH_2-terminal, type 2, peroxisomal targeting sequence of thiolase: Peb1p itself is targeted to peroxisomes by an NH_2-terminal peptide. *J. Cell Biol.* 132: 325-334.

Zhang JW, Han Y and Lazarow PB. 1993. Novel peroxisome clustering mutants and peroxisome biogenesis mutants of *Saccharomyces Cerevisiae*. *J. Cell Biol.* 123: 133-1147.

Zoeller RA and Raetz CRH. 1986. Isolation of animal cell mutants deficient in plasmalogen biosynthesis and peroxisome assembly. *Proc. Natl. Acad. Sci. USA* 83: 5170-5174.